Design features determining the sensitivity of wetting front detectors for managing irrigation water in the root zone

by

Goitom Teklay Adhanom

Submitted in partial fulfilment of the requirement for the degree PhD (Agronomy) in the faculty of Natural and Agricultural Sciences
University of Pretoria
Pretoria

Supervisor: **Professor JG Annandale**

Co-supervisors: **Professor RJ Stirzaker**

Professor SA Lorentz

Professor MJ Steyn

July 2014

CONTENTS

LIST OF FIGURES

LIST OF TABLES

ACKNOWLEDGEMENTS

Thanks to God, the merciful and passionate for giving me the strength and wisdom to step in the excellent world of science. To be able to step strong in this way, I have also been supported and supervised by several people to whom I would like to express my deepest gratitude.

I take this opportunity with much pleasure to thank to all my supervisors who have helped me through the course of my journey towards producing this valuable thesis.

I gratefully thank to Prof John Annandale for the opportunity he gave me to join his team in the first place to pursue my PhD study. I would also thank Prof Annandale for giving me the opportunity to attend several conferences and workshops, thorough which I was exposed to many of the issues and challenges facing the South African irrigation industry and other parts of the world as well.

I am deeply indebted to my supervisor Prof Richard Stirzaker whose help, quick and stimulating suggestions and encouragement through e-mail and in person over the years helped me a lot during the research and writing-up of this thesis. Prof Stirzaker's involvement as a supervisor had a massive influence on this thesis. I would like to thank Prof Stirzaker for helping me to structure the thesis, helping me through many difficult issues and for his extensive and clear feedback during the write-up phase. I would like to thank him for giving me more insights apart from the subject of my research, which I am sure, will be useful in different stages of my life.

Prof Simon Lorentz assisted me with many aspects of my thesis for which I am grateful, but I would especially like to thank him for guiding me in the laboratory measurements of the hydraulic properties of wick materials. I also thank Prof Simon Lorentz for assisting me in the work related to Hydrus-2D model.

I would like to thank Prof Martin Steyn for assisting me in securing the financial support provided by the National Research Fund. I also would like to thank him for his useful comments on chapters two and three of this thesis.

I would like to thank the Water Research Commission (WRC)-South Africa and the Commonwealth Scientific and Industrial Research Organization (CSIRO)-Australia for funding or supporting this research.

It was an honour to be a member of Australia's Cooperative Research Centre for Irrigation Futures (CRC IF). The CRF IF has given me the opportunity to visit CSIRO-Australia for three months and I thank them for sponsoring the visit, which became a reality in 2008.

Finally, this thesis would not have been possible without the confidence, endurance, prayer and support of my family. I wish to thank my sister Ghenet and my brother Amanuel for their support, understanding and patience especially toward the end of my study.

DECLARATION

I, Goitom Teklay Adhanom, hereby declare that this dissertation for the degree PhD (Agronomy) at the University of Pretoria is my own work and has never been submitted by myself at any other University. The research work reported is the result of my own investigation, except where acknowledged.

GT ADHANOM

JULY 2014

Design features determining the sensitivity of wetting front detectors for managing irrigation water in the root zone

by

Goitom Teklay Adhanom

Supervisor: Professor JG Annandale

Co-supervisors: Professor RJ Stirzaker

Professor SA Lorentz

Professor MJ Steyn

Degree: PhD (Agronomy)

ABSTRACT

Current irrigation scheduling technologies are limited to refilling the root zone based on measured or predicted amount of water stored within the root zone. This needs measurement of soil-water status and specifying soil field capacity that make this approach expensive and challenging. The FullStop^{TM} wetting front detector (FS) was specifically developed to be a simple and affordable technology to help farmers manage water, nutrients and salts in the root zone. This device responds to a strong wetting front, but research has shown it is less sensitive to weak redistributing wetting fronts, and this may compromise its efficacy in certain situations. The objectives of this study were to recommend a modified version of the FS that responds to weak redistributing wetting fronts and to develop guidelines for the deployment of these detectors to schedule irrigation.

The research described herein comprises of two phases: the first phase focused on literature review, field evaluation of wetting front detector of varying sensitivities (WFD) and laboratory measurements of hydraulic properties of soil and wick materials. The second phase validates the HYDRUS-2D/3D for the development of guidelines on how to use WFD to schedule irrigation. The first phase includes: i) a literature review on passive lysimetry that relates design features to the sensitivity of WFD and how prototypes of WFD operate; ii) hydraulic characterization of soil and wick materials to describe the functioning of the different WFD designs; iii) an empirical investigation to determine whether the wick characteristics limits the attainment of equilibrium between the opening of the outer tube and the water table in the inner tube; iv) field evaluations of five types of WFD under sprinkler

and natural rainfall to examine the accuracy and sensitivity of the different WFD designs; and v) analysis of the equilibrium between the WFD and the surrounding soil, and recommendations for the best design options based on the sensitivity requirement for different situations. The second phase of the study used observed data sets to validate the Hydrus-2D/3D model. After validation, the model was used to simulate different irrigation scenarios to develop guidelines for the deployment of WFD to schedule irrigation.

Field evaluations of various WFD designs showed that length has significant effect on the sensitivity of WFD ($P \leq 0.05$). The 90-cm-long Tube wetting front detector (90TD) was significantly more sensitive than the original FS design. The hydraulic conductivity function of two wick materials (Diatomaceous Earth and Fine sand) were not limiting for the attainment of the equilibrium between the Tube Detector and the surrounding soil, and the opening of the Tube Detector and the water level in the inner tube.

The Hydrus-2D/3D model performed well in simulating the measured responses of FS or 90TD and the experimental sensitivity thresholds of these detectors. This model was deployed to link WFD responses to different simulated irrigation scenarios to generate monitoring protocol such as detector placement depth, irrigation amount or interval. The model simulations showed that FS can be used to schedule irrigation objectively for sprinkler or drip irrigations, i.e. adjusting irrigation amount or interval based on the response of a detector. Though further study is warranted, model simulation has indicated that 90TD can be used to improving furrow irrigation management. It is envisaged that WFD technology can guide farmers to make informed irrigation decisions and alerting farmers to percolation losses below the root zone.

CHAPTER 1

INTRODUCTION

1.1 RATIONALE

Irrigated agriculture needs to play an important role in meeting the projected increase in food demand from a growing population (Howell, 2001). It is particularly important in the arid and semi-arid environments where water is the limiting factor for crop production, and where water use efficiency must be increased through better scheduling of irrigation. The most commonly used objective irrigation scheduling methods include soil water monitoring tools, atmospheric based quantification of evapotranspiration, plant based monitoring and integrated water balance models (Stevens *et al*., 2005). The use of these methods, however, is limited among farmers due to the cost and complexity in use and interpretation (Shearer and Vomocil, 1981; Stevens *et al*., 2005; Stirzaker, 2006).

In the face of this poor adoption, Stirzaker (2003) tried to find simpler ways to improve irrigation on-farm. This materialized in the development of a simple and affordable tool called the FullStop™ wetting front detector (FS WFD) for making irrigation decisions from the depth of a wetting front. This tool is a funnel-shaped device buried in the root zone with a mechanically operated indicator visible above the soil surface (see Section 1.3). It has shown promise in the field for water, nutrient and salt management in the root zone (Fessehazion *et al*., 2011; Tesfamariam *et al*., 2010; van der Laan *et al*., 2010).

The FS WFD responds well to relatively "strong" wetting fronts (30 cm tension or wetter), which are usually present in the upper soil layers during or in the few hours following irrigation. During the redistribution phase, however, wetting fronts become more diffuse (or "weak") with depth and time. In this case wetting fronts below the detection limit of the FS could pass without activating the indicator may cause substantial drainage water losses if this low flux persists (Stirzaker *et al*., 2004a). Therefore further research is needed to (i) specify the sensitivity of a WFD design in terms of the minimum water flux it can detect, and ii) evaluate new design options that respond to weak redistributing fronts.

The Water Research Commission (WRC) of South Africa initiated a project entitled 'Cheap and simple irrigation scheduling using wetting front detectors' (WRC Project No. 1135). Based on a survey of 54 irrigators and their advisors who used the WFDs on their own farms

for at least one season during the above project, 82% found that it conferred a relative advantage over their current practice. Some farmers who use centre pivot and furrow irrigation, however, reported that detectors did not respond to irrigation, hence their current practice was not challenged (Stirzaker *et al*., 2004a). This signalled that further work was required to develop a modified design of wetting front detector (WFD) that could be used, especially in furrow irrigation. A second WRC project was initiated in 2005 entitled 'Adapting the wetting front detector to the needs of small scale furrow irrigators and providing a basis for the interpretation of salt and nutrient measurements from the water sample'. Among others, two important objectives of this project were (i), to develop and test a modified WFD, dedicated to the needs of small-scale furrow irrigators, and (ii), to define the sensitivity of a WFD (the amount of water that could pass a detector without activating it). The research presented in this thesis on "Design features determining the sensitivity of wetting front detectors for managing irrigation water in the root zone" was conducted within the context of these two objectives of the latter WRC project.

1.2 A BRIEF REVIEW OF DRAINAGE LYSIMETRY

A WFD is essentially a type of passive lysimeter. In order to build a WFD, which can measure a weak, wetting front based on a sound theoretical principle governing water flux measurement, it is essential to understand the uses, designs and operating principles and factors affecting performance of a drainage lysimeters.

1.2.1 General

A lysimeter is typically a tank or container with defined boundary conditions designed to collect soil water and allow measurements of the soil water balance, vertical water flux and drainage water quality (Aboukhaled *et al*., 1982; Howell *et al*., 1991; Benson *et al*., 2001). Lysimetry has a long history of development, with different shapes and sizes designed for different purposes (Bergström, 1990; Payero and Irmak, 2008). Lysimetry has been used for nearly three centuries to study water percolation through soils (Hansen *et al*., 2000). A lysimeter can be used in a laboratory, greenhouse and controlled environment chambers to provide relative measurements of the measured variable; and under natural conditions to produce absolute measurements (Howell *et al*., 1991). Lysimeters link laboratory results to field scale studies and can reproduce natural conditions, but require knowledge of design details, good site selection and good management (Howell *et al*., 1991; Rupp *et al*., 2007).

The choice of a specific lysimeter type depends on the purpose and precision requirement of the measurement (Bergström, 1990). For instance, very accurate and detailed information is required for pesticide leaching studies in lysimeters, as leaching may occur in small quantities for a short duration. Lysimeters in general could be classified according to the method of (i) soil filling (packed or undisturbed core), (ii) water content measurement (weighing or non-weighing), and (iii) drainage water collection by gravity or vacuum or a water table formation (Dugas *et al*., 1990; Weihermüller *et al.*, 2007). In this review, however, only lysimeters based on drainage water collection are discussed due to their relevance to the research question.

1.2.2 Drainage lysimeter

The drainage system could be designed either to prevent saturation at the bottom of the lysimeter or to establish a water table within the lysimeter (Hansen *et al*., 2000). In the former type of lower boundary condition, the drainage system could be either (i) a free drainage that collects water from large pores or gravitational water by intercepting the downward flow of water in a collection unit (passive lysimeter), or (ii) a vacuum that sucks water out of the soil by applying suction at the bottom of the lysimeter (active lysimeter).

The lower boundary condition of the drainage lysimeter is usually the functional defect one has to live with due to the equilibrium between soil-water and atmospheric pressure creating a wetter soil at the bottom of the lysimeter than in a natural soil profile. These conditions, therefore, influence the interpretation and representation of soil water balance and nutrient studies (van Bavel, 1961). This functional defect can be caused due to (i) the no-flow boundary condition created by the pan at the bottom of the lysimeter, and (ii) the presence of a coarse drainage layer at the lower boundary of the lysimeter used to direct percolation to a collection unit, which induces a capillary break that may not exist under natural conditions. These artificial conditions may increase the storage capacity of the test material relative to natural conditions and hence reduce percolation rate by 8 to 14% (Abichou *et al*., 2006).

It has been claimed that lysimeters can measure percolation rates directly up to 0.5 mm/year (Ward and Gee, 1997; Benson *et al*., 2001). Despite this advantage, disturbances both inside and outside the lysimeter due to installation, geometry, and the boundary condition of the lysimeter have raised concerns about errors in estimating percolation rates (Jemison and Fox 1992; Brye *et al*., 1999; Zhu *et al*, 2002; Gee *et al*., 2003, 2004; Masarik *et al*., 2004; Weihermüller *et al*., 2007).

Two types of lysimeter used for measuring percolation rates including the pan lysimeter and passive wick lysimeter are discussed below.

1.2.2.1 *Pan (Zero tension) lysimeter*

A pan or zero tension lysimeter is a passive water sampling device designed in the shape of a pan (Fig. 1.1) and is buried below the ground surface to capture drainage water (Jemison and Fox 1992; Gee *et al*., 2004; Weihermüller *et al*., 2007).

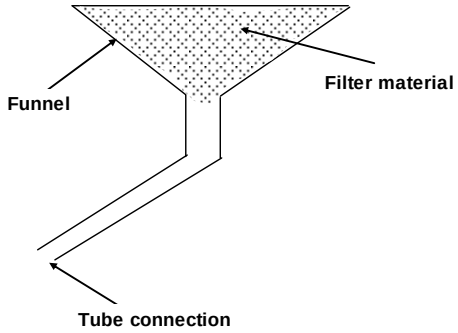

Figure 1.1 Sketch of a pan lysimeter (Weihermüller *et al*., 2007).

Zero-tension lysimeters were used primarily for solute monitoring and sometimes to quantify drainage rates. More recently, pan lysimeters have been used to estimate drainage rates over a wide range of soil conditions (Zhu *et al*., 2002; van der Velde *et al.*, 2005). The capture area of a pan lysimeter can be any size, the standard being 0.5 m^2. The materials used for constructing pan lysimeters can be stainless steel, glass, ceramic, or plastic, depending on the specific research requirements.

A pan lysimeter requires filling with coarse gravel or other highly conductive materials to ensure easy interception of drainage water and to divert it into a collection device (Gee *et al*., 2004; Weihermüller *et al*., 2007). This filling procedure creates non-capillary connection between the natural soil and filling material or a seepage flow boundary at the outflow, in which the soil water tension becomes equal to the atmospheric pressure (Richards, 1950). Therefore, the soil at the contact between the natural soil and coarse material reaches field saturation. This means that pan lysimeters operate well only in soils with pores near saturation, and are less successful when drainage fluxes are low (Zhu *et al*., 2002).

The textural difference between a filling material in the pan and natural soil creates a tendency for water to pass the lysimeter undetected. The amount of water flowing around the

lysimeter in general depends on the vertical water flux, textural contrast between fill material and surrounding soil, and gradients in water potential that persist at the contact between the fill material and surrounding soil.

Because of divergence of water around a lysimeter, it has been noted that water collection efficiencies for pan lysimeters were typically less than 40% (Jemison and Fox 1992; Zhu *et al*. 2002; Gee *et al*., 2004). In other words, only part of the naturally occurring drainage in a typical soil profile can be collected (Boll *et al*., 1992; Jemison and Fox, 1992). Thus, other approaches or improvements in design and fill materials should be considered to reduce divergence.

1.2.1.2 *Passive wick (fixed tension) lysimeters*

Passive wick lysimeters are sampling devices that exert tension on the soil using an inert wick material (Fig. 1.2). A wick lysimeter applies tension proportional to its length and drains the water passively to a collection device (Gee *et al*., 2003).

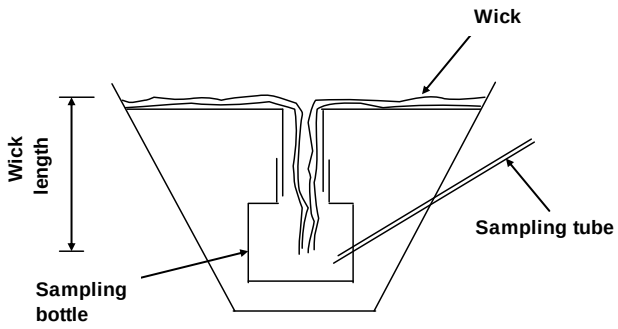

Figure 1.2 Sketch of a capillary wick sampler (after Brandi-Dohrn *et al*., 1996).

A wick lysimeter 'sucks' pore water from unsaturated soil by capillarity action and provides an additional fixed tension which acts as a hanging water column. Common inert wick materials are fibreglass (Holder *et al*., 1991) or rock wool (Ben-Gal and Shani, 2002). The maximum applied tension is in the range of 50 to 300 cm (Holder *et al*., 1991; Boll *et al*., 1992; Mertens *et al*. 2007; Weihermüller *et al*., 2007; Nichol *et al*., 2008).

The lower soil boundary inside the lysimeter is maintained at a pressure less than atmospheric pressure so that the soil stays unsaturated. The degree of unsaturation, however, depends on the length and diameter of wick material, flux rate, soil type and dimensions of the sampling

bottle (Boll *et al*., 1992; Knutson and Selker, 1994; Rimmer *et al*., 1995; Zhu *et al*., 2002; Weihermüller *et al*., 2007).

Extensive tests over several years have indicated that leachate collection efficiency, defined as measured drainage divided by the drainage estimated based on a mass balance approach from a water balance equation, have exceeded 100% for wick samplers (Louie *et al*., 2000; Zhu *et al*., 2002). This could be due to the artificial bottom soil boundary, which may increase the storage capacity of the soil and hence underestimates the drainage obtained from a mass balance method. Gee *et al*. (2003) modified the wick samplers by integrating a divergence barrier (extension tube) and a tipping bucket into their wick samplers to increase the temporal resolution of measuring water fluxes in field soils. The extension tube is filled with soil from the excavation of the hole into which the lysimeter is placed. Gee *et al*. (2003) have shown that the degree of flow divergence is controlled by the height of the divergence barrier and the knowledge of hydraulic properties of the soil. This modified water flux meter provides continuous monitoring of unsaturated water fluxes ranging from 1 to more than 1000 mm/yr.

1.2.3 Factors influencing lysimeter performance

1.2.3.1 *Lysimeter size and construction material*

The surface area of a lysimeter and the vertical length of the sidewalls determine the extent of flow diversion around the instrument and thus the magnitude of error in estimating percolation rates. Chiu and Shackelford (2000) indicated that lysimeters that are too small underestimate percolation rates. A large lysimeter with a thin wall (large soil area) is preferred over a small lysimeter to minimize errors in water flux measurement (Bergström, 1990). The wall area should not exceed 5% of the soil area for concrete containers, but is less significant for plastic and metal containers (Aboukhaled *et al*., 1982; Bergström, 1990).

Lysimeters are commonly constructed in circular, square or rectangular shapes designed to suit individual research requirements (Payero and Irmak, 2008). Dimensions of lysimeters could range between 0.05 to 2 m in diameter, and between 0.4 to 2.0 m in length. The size of a lysimeter in general is determined by the purpose and sensitivity requirement of the measurement.

A number of materials are used to manufacture lysimeter containers. The choice of material considers lightness, suitability to handle, inertness, cost, etc. The basic components of a

lysimeter include a sampling pipe, pan, screen, sampler, and collector chamber. Lysimeter containers are made up of materials such as reinforced concrete, butyl rubber sheets, steel and stainless steel, Teflon, fibreglass, filter material, and various types of plastic. It is important to ensure that the material used for construction of the lysimeter should not interfere with the leachate or soil solutions. For instance, an inert filter material should be placed in the lysimeter pan to reduce sediment collection in the pan and to create adequate capillary forces so that water in the vadose zone moves into the lysimeter, thus avoiding chemical alteration of the water sample.

1.2.3.2 *Hydraulic characteristics of wick and soil materials*

The matching of hydraulic characteristics between wicks and soil materials impacts on collected water samples significantly. Rimmer *et al*. (1995), who based their recommendations on a one-dimensional steady state model, advised that optimal wick lengths for sandy soils should range between 30 and 40 cm, and for silt loams, optimal lengths should exceed 100 cm. These wick lengths that matches the soil types (sand and silt loam) were determined using analytical solutions in order to minimize flow of water around the soil-wick contact area.

Mertens *et al*. (2007) tested the effect of wick materials of different lengths on leachate volume, and indicated that the longer the wick, the higher the sampling volume. The authors explained the reason for these differences by examining the conductivity functions of the soil and wick materials (e.g., AM3/8HI and PEP1/2 wicks). The leachate volumes in both wicks increase with increasing length for tensions where the conductivity of the wicks is higher than that of the surrounding soil. As the conductivity of the wicks drops below that of the soil, however, increasing wick length has a negligible effect on leachate volume.

Mertens *et al*. (2007) recommended that the length of a wick material such as AM3/8HI be seasonally variable, and be related to wet and dry periods, i.e. a longer wick is required during dry periods to collect water samples from low water fluxes. The approach used by Mertens *et al*. (2007) to match the wick and soil properties can be applicable to other soil and wick types and climatic conditions.

1.3 LINK BETWEEN LYSIMETER AND WETTING FRONT DETECTOR

Lysimeters have been used for decades in studies involving transpiration and evapotranspiration (Hillel *et al*., 1972; Allen and Pruitt, 1991), drainage measurement (Brye

et al., 1999; Gee *et al*., 2004; Masarik *et al*., 2004) and solution sampling (Brown *et al*., 1985; Lentz and Kincaid, 2003). However, no attempts have been made to apply lysimeter design principles for routine management of irrigation water in the root zone. The best ways to link lysimetry to irrigation water management is by deploying a lysimeter either to control the amount of irrigation water by stopping irrigation when it responds to a wetting front at the upper part of a root zone, or adjust irrigation amount based on the response of a lysimeter at the bottom of a root zone.

Section 1.2 presented a brief review of drainage lysimetry. The implications of drainage lysimetry review toward this study can be summarized as follows.

Dr. Richard Stirzaker from the CSIRO in Australia proposed that a simple technology that resemble to a passive water sampling device could be used for irrigation water management purposes. Stirzaker (2003) developed the commercially available version called the FullStop^{TM} wetting front detector (Fig. 1.3). It has a funnel 20 cm in diameter and 25 cm in depth (Stirzaker, 2008). "The FS WFD works by converging water films as they move into the wide end of the funnel. The soil in the funnel gets wetter and wetter as the cross-sectional area narrows. At the base of the funnel, the soil becomes completely saturated and free water starts to flow through the mesh screen and into the reservoir. The indicator floats on the water and then locks into the up position with a pair of magnets."

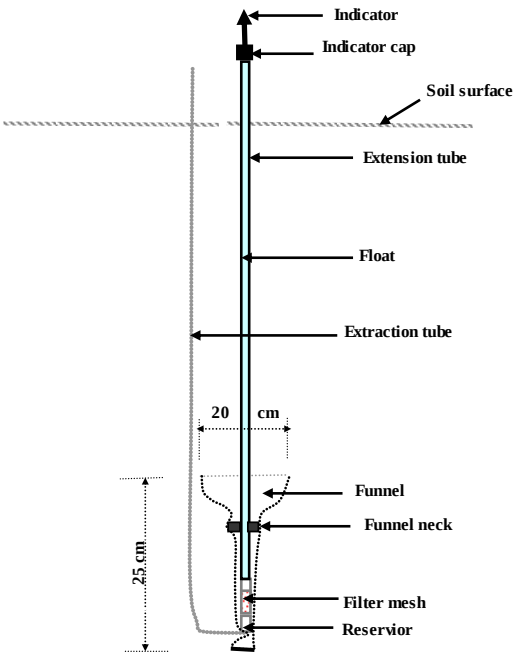

Figure 1.3 Components of the FullStop^{TM} wetting front detector (FS WFD).

This detector is designed so that an indicator above the surface will be in the "up" position when the soil outside the funnel, but at a similar depth to the neck of the funnel from the soil surface reaches a pressure head of 30 cm or wetter (Stirzaker *et al.*, 2009). For detailed descriptions of the components and how this device operates one is referred (Stirzaker, 2003; Stirzaker, 2008; Stirzaker *et al.*, 2009). More information can be also obtained from: www.fullstop.com.au.

In 2003, this technology won the WATSAVE award by the International Commission for Irrigation and Drainage (ICID) for contributions to water saving in agriculture.

The review has shown that the FS collects water under unsaturated conditions, while a pan lysimeter needs saturation conditions at the lower boundary of the soil in contact with the filter material inside the pan lysimeter. The FS on the other hand is analogous to a pan lysimeter where it uses a funnel to aid in collection of a water sample. It responds well to strong wetting fronts but is less sensitive to a weak wetting front, hence the need for further research. Specifically, it was decided to:

i. Determine the design features of a WFD that relate directly to sensitivity based on theory; and

ii. Build and evaluate different designs to test their sensitivity empirically under field conditions to test the theory in (i) above.

This materialized in the identification of design features that could help to build a more sensitive WFD technology, which fits the research question. These were:

i. Length of divergence barrier (extension tube);

ii. Length of a wick material;

iii. Hydraulic characteristics of wick and soil materials; and

iv. Appropriate drainage system.

A design must make use of the right combinations of the features (i) through (iv) mentioned above in order to create a more sensitive WFD prototype. The four design features of a WFD prototype are discussed below.

1.3.1 Length of divergence barrier (extension tube)

Gee *et al.* (2003) minimized flow divergence by increasing height of divergence barrier (extension tube) that matches with the soil hydraulic properties.

Hutchinson and Bond (2001) and Stirzaker (2008) suggested sensitivity of a WFD is determined by its length. In order to record every small wetting event, the wick and tube lengths combined (Chapter 2), which is similar to the Gee's divergence barrier plus a wick length should be a high walled WFD design (i.e. increasing length increases sensitivity) to counteract capillary emptying. Based on this recommendation, it was decided to build and test WFD prototypes of varying lengths.

1.3.2 Length of a wick material

Several authors (Rimmer *et al.*, 1995; Mertens *et al.*, 2007) showed the impact of different lengths of a wick material on collected water sample. The two main recommendations by these authors were:

i. Optimal lengths of wicks for sandy soils should range between 30 and 40 cm, and for silt loams, optimal length should exceed 100 cm; and
ii. Length of a wick material is determined by the season related to wet and dry periods, i.e. longer wick is required during drier periods to collect water samples from low water fluxes.

Stirzaker (2008) tested a 60 cm LongStop WFD filled with a fine sand material in furrow irrigated field site. The author found that the 60 cm LongStop was more sensitive than the FS WFD. Based on the results, it was recommended to further test different lengths of various types of wick materials.

1.3.3 Hydraulic characteristics of wick and soil materials

The matching of hydraulic characteristics between wicks and soil materials were examined (Rimmer *et al.*, 1995; Mertens *et al.*, 2007). The authors advised that the hydraulic conductivity functions of the wicks should be higher than that of the surrounding soil at each tension during the drainage event. This ensures that the wick can remove water from the soil and transport it to the reservoir. On the basis of this recommendation, it was needed to conduct measurements of hydraulic properties of various wick materials to facilitate the selection process of a suitable wick material.

1.3.4 Appropriate drainage system

Several authors (Dugas *et al.*, 1990; Hansen *et al.*, 2000; Weihermüller *et al.*, 2007) have reported two forms of drainage systems in a lysimeter. These include:

i. A drainage that prevents saturated condition at the bottom of a lysimeter; and
ii. A drainage that allow a water table formation inside a design.

Stirzaker (2003) designed the FS WFD so that free water produced at the soil-filter sand contact will be collected in the built in reservoir. Likewise, it was agreed to design a WFD prototype where the drainage system allows a water table formation within a prototype during a wetting event and self empties after irrigation or a rainfall event.

1.4 THESIS OBJECTIVES

The aim was to provide a WFD design option that detects a weak wetting front (low water flux), which can be used for irrigation management. The research presented in this thesis was conducted to meet the following objectives:

i. To analyze design features of a detector that relate to sensitivity,
ii. To empirically test how the length of a lysimeter is related to sensitivity under laboratory conditions,
iii. To determine the flux sensitivity of WFD designs based on theory,
iv. To select suitable wick materials for the operation of prototype WFDs in the field,
v. To test and evaluate performance of various prototype WFDs under field conditions,
vi. To determine, by experiment, how well WFD remain in equilibrium with the surrounding soil, and
vii. To recommend best design options based on the sensitivity requirements of the measurement.

1.5 APPROACH

This section sets out the methodologies used to meet the objectives of the thesis.

1.5.1 A brief review on lysimetry

A literature search was carried out on lysimetry in particular drainage lysimeters. In this thesis, a brief literature review followed by a section that links a lysimeter to a wetting front detector is presented (Chapter 1).

1.5.2 Analysis of design features and building of WFD prototypes

WFD prototypes of varying lengths and diameters were built (Chapter 2). In constructing these prototypes, sound theoretical and practical considerations were considered (Section 2.1). Prototypes were built for two reasons: (i) to vary one factor at a time i.e. diameter or length and (ii) to show that a working version could be manufactured simply and cheaply from locally available materials. In addition, the hydraulic properties of wick materials ideally suited to these prototypes were determined (Section 2.2).

1.5.3 Measurement of hydraulic characteristics of soil materials

In-situ measurement (neutron probe and tensiometer), including the methods listed in Table 1.1, were used for field soil hydraulic characteristic measurements. Analytical equations, numerical solutions and pedotransfer functions were also used in deriving some of the hydraulic characteristics of soil materials (Chapter 3).

Table 1.1 Laboratory methods used for measurements of hydraulic characteristics of wick and soil materials, data type and their applications.

Methods	Data types	Uses/applications
Multi-step controlled outflow	Water retention characteristic, $\theta(h)$	▪ Measure field capacity ▪ Estimate specific yield ▪ Estimate retention parameters
Constant head permeameter	Saturated hydraulic conductivity, K_s	▪ Input in analytical or numerical solutions to predict K(h)
Bruce and Klute	Soil water diffusivity function, $D(\theta)$	▪ Use $D(\theta)$ and slope of $\theta(h)$ to determine K(h) or $K(\theta)$

1.5.4 Measurement of hydraulic characteristics of wick materials

Several laboratory measurement methods (Table 1.1) and analytical equations were used to determine the hydraulic characteristics of wick materials (Chapter 4). This facilitated the selection process for an ideal wick material that would enable the detectors to remain in equilibrium with the surrounding soil.

1.5.5 Prototype testing and evaluation

Following the construction of WFD prototypes (Section 1.5.2) and measurement of hydraulic characteristic of soil and wick materials (Sections 1.5.3 and 1.5.4), the performance of each prototype were investigated under both laboratory and field conditions (Chapters 5, 6 and 7). This objective was achieved (i) by conducting empirical research on wick characteristics from directly observed variables such as water depth in the inner tube (see Chapter 2 for design components and descriptions) and wick tension measurement over time (Chapter 5), (ii) through field installation of prototypes together with supporting soil water measurement tools (Chapter 6), (iii) with the use of a sprinkler irrigation (Chapter 6) and rainfall (Chapter 7) to create different strengths of wetting fronts that enabled discrimination between designs, (iv) by evaluation of prototypes independently and in relation to the data from soil water measurement (Chapters 6 and 7), (v) by analysing and concluding if the prototypes do work well under both laboratory and field conditions for the purposes they were designed for (Chapter 8), and (vi) a synthesis showing how the varying sensitivities of the wetting front detector could be used to schedule irrigation (Chapter 9).

CHAPTER 2

ANALYSIS OF DESIGN FEATURES OF WETTING FRONT DETECTORS

Two types of WFD prototypes were built for measuring weak wetting front during the course of the study to compare with the original funnel design including:

i. A prototype of Tube WFD; and
ii. A prototype of Hybrid WFD.

"Design" throughout this thesis refers to the shape, physical dimensions and wick components for prototypes of Tube (Fig. 2.1a) and Hybrid (Fig. 2.1b) wetting front detectors. Note that in this thesis soil tension and pressure head are used interchangeably as needed.

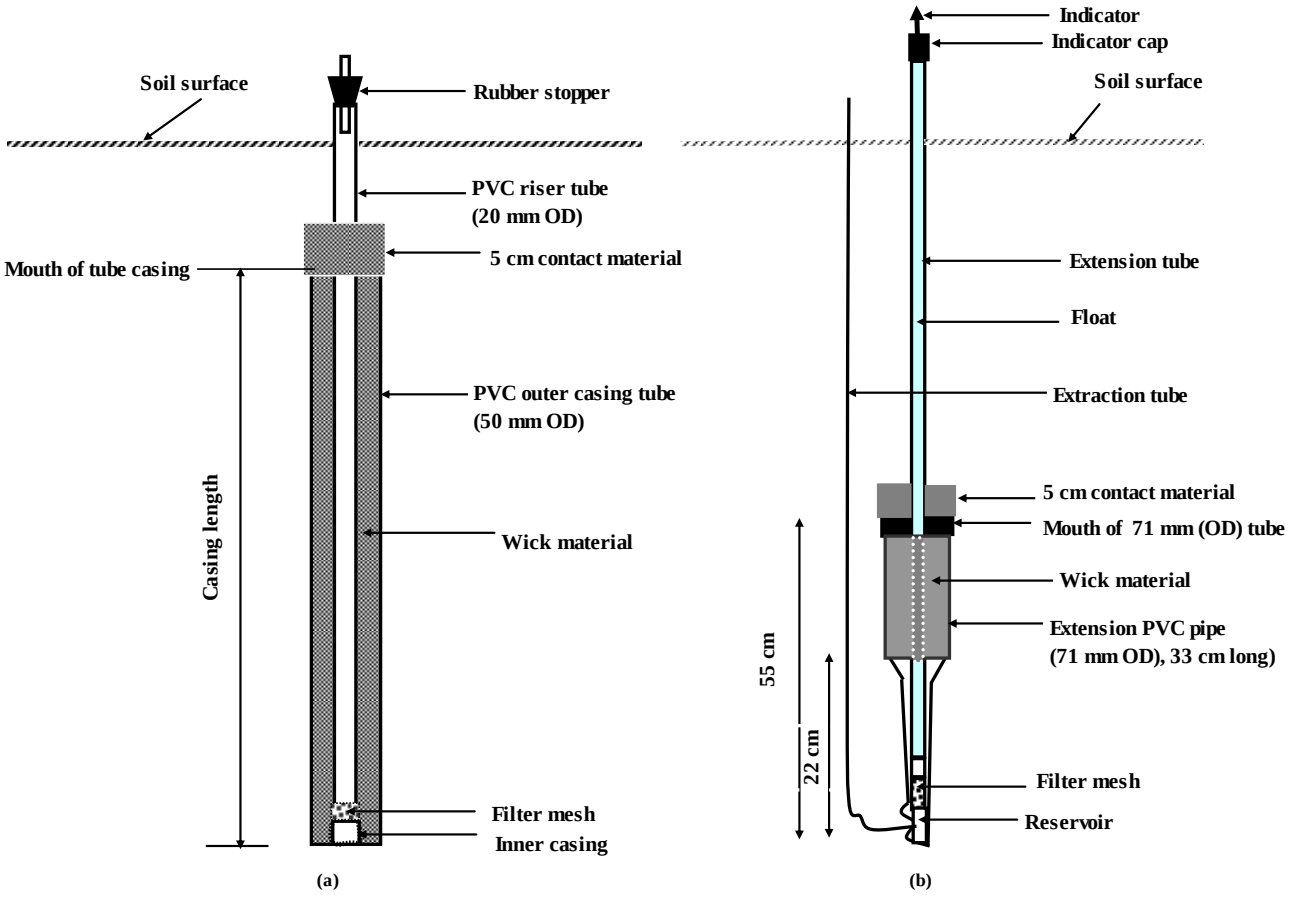

Figure 2.1 Components of a Tube (a) and Hybrid (b) wetting front detector - originally conceptualized (Stirzaker, 2008; Stirzaker *et al.*, 2010).

The first prototype is a Tube WFD (Fig. 2.1a) built to detect a weak redistributing front (low water flux) since it counteracts capillarity forces by the tube length, thereby increasing its sensitivity. The design does not attempt to increase water capture using the funnel shape i.e. it is straight-sided, but aims to prevent water that has entered the WFD from subsequently being removed by capillarity before saturation occurs at the base. Three different lengths of Tube WFD were selected and built according to the Figure 2.1a, as follows: i) 45 cm long Tube WFD (45TD), ii) 60 cm long Tube WFD (60TD), and iii) 90 cm long Tube WFD (90TD).

The second prototype is a Hybrid WFD (Fig. 2.1b), which is part tube detector above and part FullStop^{TM} WFD. The Hybrid WFD comprised some features of the funnel-shaped design such as wider opening than the tube version and a float mechanism for recording a response, together with a PVC tube extension of the wider opening to increase its sensitivity. This prototype has a length of 55 cm, which is the sum of a lower base (22 cm) and an extension tube (33 cm).

2.1 DESIGN CONSIDERATIONS

Factors governing the functionality and sensitivity of the WFD, including the theory of infiltration flux at the soil-wick interface and the flow of water to and from the WFD, length and diameter of the WFD, practical considerations that dictate the length of the WFD (e.g. soil depth), and the hydraulic conductivity and specific yield properties of soils and wick materials are discussed in Sections 2.1.1 to 2.1.4 below.

2.1.1 Theoretical and practical design considerations

The basic assumption in one-dimensional vertical flow of the wick-soil system is that soil tension becomes uniform at depths near the wick-soil contact and water flows only under gravity (Rimmer *et al*., 1995). One-dimensional analytical solutions of the Richards' equation can be used for wick analysis when the wick is conceptualised as a layer in a profile with the steady-state flow assumption being valid (water flows downward with a constant flux). In wicks installed at deeper depths with a high-frequency irrigation or rainfall, the water fluxes at these depths are usually damped by the overlying soil, and hence the steady-state flow assumption remains valid (Jury *et al*., 1991; Rimmer *et al*., 1995).

Whereas theory suggests a longer WFD would be more sensitive, there is a practical limit to the length of a WFD prototype and how deep it can be installed. This is particularly important

for deeper installations towards the bottom of the root zone, since the opening of the tube is at the depth of measurement. Considering the practicality of installation problems, it was decided that the length of a prototype to be less than a meter (i.e. a maximum tube length of 90 cm, that requires at least an installation soil depth of 1.8 m was considered in this study).

2.1.2 Boundary conditions and analytical solutions at the wick-soil layer

A good capillary continuity between the soil and wick material ensures that the tension from the wick is applied at the bottom of the soil in contact with the wick.

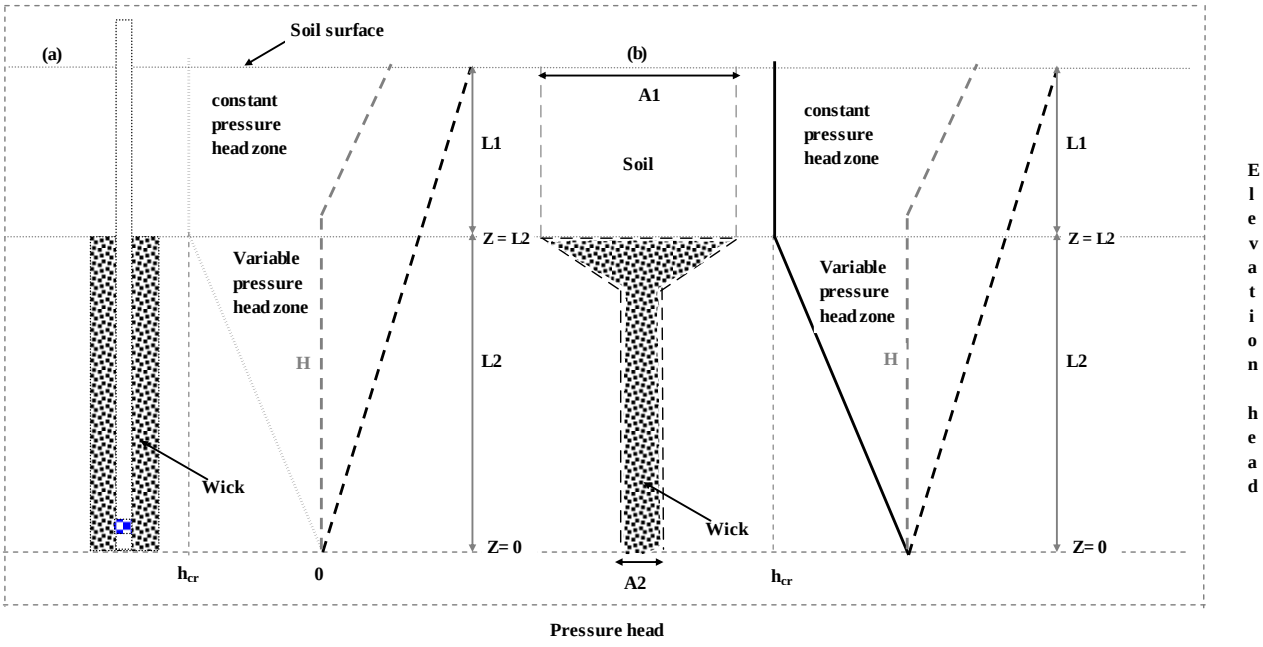

Figure 2.2 Schematic representations of the pressure head (solid line), gravitational head (bold dotted line) and hydraulic head (grey dotted line) profile distribution in a tube of uniform wick material with water table forming inside the tube (a) - (Kao *et al*., 2001) and a drainage lysimeter (b) - (Ben-Gal and Shani, 2002), for a steady infiltration rate. Note that H is the hydraulic head, which is the sum of pressure head and gravitational head, L1 is the depth of installation, L2 is tube length or drain length, h_{cr} is the critical pressure head with no water flow, A1 and A2 are cross-sectional areas of the soil and drain wick materials respectively.

The flow of water into the opening of the tube is determined by the pressure head conditions at the soil-wick contact and the soil above the contact area. If the pressure head at the opening of the tube is equal or less than the tube length (critical threshold, h_{cr}), saturation will occur at

its base. The basic requirement of the lower soil boundary in a tube and drainage lysimeter filled with wick materials is that the pressure head at the contact area (Fig. 2.2a and b) cannot exceed a critical threshold value (maximum measurable pressure head) when the layers above are drier.

These detectors are filled with homogenous and highly conductive materials to allow quick response to field water conditions. The pressure head conditions at the lower soil boundary shown (Fig. 2.2) can be described using the Ben-Gal and Shani relationship (2002) found in Appendix 1. The authors have described the boundary conditions and analytical solutions at the soil above a wick, at the bottom of a wick and at a wick-soil contact governing the functionality of the designs (Fig. 2.2). Among others, two important recommendations by Ben-Gal and Shani relationship (2002) related to the proper operation of these designs were, (i) the drainage water in the soil should be equal to that of the wick, and (ii), flux and pressure heads should be continuous at the wick-soil contact. The fulfilment of conditions (i) and (ii) in a WFD design therefore minimizes flow divergence around the detector thus improves its sensitivity. For detailed boundary conditions and analytical solutions on the wick-soil contact, see Appendix 1.

2.1.3 Pressure head and gravitational head distribution

A tube length (L2), sealed at the base and filled with a uniform wick material forming a water table within the inner tube (Fig. 2.2a) and a drainage lysimeter of length (L2) that drains water freely through the base (Fig. 2.2b) can be described using the one-dimensional steady infiltration rate theory.

The pressure head profiles for the vertical tube length (Fig. 2.2a) and drainage lysimeter (Fig. 2.2b) each buried at a soil depth of Z = L2 could be illustrated as a function of applied infiltration flux from the soil surface. When the infiltration flux applied to the soil surface is less than the saturated hydraulic conductivity (K_s) of the soil, the soil will be at some negative potential and water will enter the tube or lysimeter. This creates a water table (Fig. 2.2a) or saturation (Fig. 2.2b) at the base (L1+L2). Considering the reference level of each of these figures at Z = 0, the pressure head (h) at this reference point will be zero since water is in equilibrium with atmospheric pressure. Above the water table or saturated base, h will be less than zero. The gravitational head (Z) at each point within the wick or soil column is determined by the elevation above the reference level, with Z being positive above the

reference level. On the reference level since gravitational head (Z) and pressure head (h) are both zero, the hydraulic head (H) at this reference point is zero.

Above a free water surface, it is customary to assume a hydrostatic, equilibrium pressure head profile for the unsaturated zone inside the detector due to its strong hydraulic connection with the free water surface (Kao *et al*., 2001; Nachabe *et al*., 2004). In the variable pressure head zone (Fig. 2.2), the hydraulic head (H) remains zero (equilibrium condition) since both pressure head and gravitational head are equal in magnitude and opposite in sign. In the constant pressure head zone (Fig. 2.2), however, H > 0 showing a non-equilibrium condition exists.

Kao *et al*. (2001) described the shape of the pressure head profile (Fig. 2.2a) using the relationship between the slope of the pressure head, infiltration rate and hydraulic conductivity in a shallow water table under a vertical steady state flow condition by:

$$-\frac{\partial h}{\partial z} = \frac{q_{in}}{K(h)} + 1 \qquad (2.1)$$

where h is the pressure head; z the elevation; q_{in} the vertical infiltration flux and K(h) the unsaturated hydraulic conductivity. A similar pressure head profile is obtained (Fig. 2.2b) if analyzed instantaneously while its base is fully saturated (h = 0).

Equation 2.1 shows that if the infiltration flux applied on the top of the soil surface is less than K_s, a unit vertical hydraulic gradient will be attained at an elevation of Z = L2, which is above a water table. This point of elevation, which depends on the infiltration flux and hydraulic conductivity of the soil, will have zero pressure head gradient and a unit vertical hydraulic gradient. This defines the height of variable pressure head zone ranging from the free water surface (z = 0) to a length of the tube where Z = L2. Above the elevation Z = L2, the pressure head is constant and equal to h_{cr}. It follows that the hydraulic conductivity in the upper part of the soil is equal to the applied infiltration flux.

2.1.4 Specific yield of field soils

Specific yield is a parameter that needs to be determined for applications in transport or flow models. Specific yield can be defined as the drainable porosity or as the change in the volume of stored water within a unit area per unit change in water level (Bear, 1972; Sumner, 2007).Table 2.1 shows that clay has a higher porosity than sand, and sand has a higher

porosity than gravel. Although clay has the highest porosity, its specific yield is extremely low (2-10%), and that explains the difficulty of getting sufficient drainage water using wick samplers characterized by low-pressure head ranges.

Table 2.1 Typical porosity and specific yield of selected materials

Type	Porosity (%)	Specific yield (%)
Clay	50-55	2-10
Sand	40-47	25-33
Gravel	27-40	21-33

(*Stephens et al., 1998*)

It is important to consider drainage, which is closely related to the definition of specific yield for land reclamation integrated with cropping practices. Manjunatha *et al.* (2004) suggested that a relatively small drainage coefficient (1 to 2 mm per day) is required to leach salts that can lead to proper land reclamation.

2.2 DESIGN FEATURES OF WETTING FRONT DETECTORS

2.2.1 Design types

2.2.1.1 *Tube wetting front detector design and operation*

A Tube-shaped wetting front detector (Tube WFD) is a prototype design comprising of two concentric PVC tubes, a filter mesh, wick material and contact material (Fig. 2.1a). The inner tube (20 mm outside diameter) with a filter mesh just above its base is glued to the end cap of a second larger diameter PVC tube (44 mm inside diameter). The 20 mm tube extends to just above the soil surface, whereas the opening of the larger tube is at the depth of measurement. The gap between the inner and outer PVC tubes is filled with a wick material, unlike a wick used in a passive wick lysimeter; it is a porous media that keeps the tube in hydraulic equilibrium with the soil. A contact material similar to the wick material is placed above the mouth of the outer tube to ensure hydraulic contact between the wick and surrounding soil.

The mouth of the outer tube (50 mm outer diameter) is therefore buried in the root zone, with the inner tube (20 mm outer diameter) visible above the soil surface (Fig. 2.1a). Water infiltrates down through the soil and enters into the opening of the tube. This water flows

through the wick material, and if saturation occurs at the base, free water moves through the filter screen into the inner tube (Fig. 2.1a).

Water flows into the opening of the tube by the difference in hydraulic head. The two components of hydraulic head are the pressure head due to the attraction between water and soil particles and the gravitational head due to the forces pulling on the soil water. This water flows from high hydraulic head to low hydraulic head. From the field capacity concept, gravitational drainage becomes negligible when the pressure head reaches between 10 kPa and 33 kPa. This means that under ideal condition for example a 90TD should collect drainage water between 0 and 9 kPa soil tensions.

It follows that water enters the tube when the soil tension at the opening of the tube is equal to or less than the length of the Tube WFD (the maximum tube length used in this study is 90 cm). If the soil tension at opening of the tube is drier than a tube length, however, water will be wicked out to the soil. In a scenario where a soil tension is equal to or less than a tube length, a saturated condition will be formed at the base of the device. This creates an artificial water table inside the tube, which is a way of registering a wetting event. Under equilibrium condition, water content or pressure head at any point inside a tube can be defined by its height from a point of saturation or a water table (pressure varies linearly with depth from a free water surface). In other words, a wick material in the WFD 10 cm above a water table is at a tension of 10 cm, and 20 cm above a water table is at a tension of 20 cm and so on. Moreover, for any water depth inside a tube, the soil tension at the mouth of the tube is determined by multiplying the difference between the length of the outer tube and the water depth inside the tube by the hydrostatic pressure gradient of 9.8 kPa/m (Nichol *et al*., 2008).

The water depth in the tube is determined by extracting water from the inner tube using a flexible tube and syringe and measured with a graduated cylinder. This water volume was then converted to a depth of water (cm) using a conversion factor of 2.34 ml/cm (the volume of water in 100 cm long 20 mm outer diameter tube was measured and divided by 100 cm to get 2.34 ml/cm).

Two pressure profiles in a soil developed as a function of a zero and non-zero infiltration flux and three pressure profile scenarios for different tube lengths are illustrated (Fig 2.3). In the case of the soil, if the infiltration flux at the soil surface is zero, the pressure head will decrease hydrostatically for each increment of elevation above the water table. If the

infiltration flux applied at the soil surface is higher than zero but less than the K_s of the soil, a unit vertical gradient can be established at an elevation (Z = L1) above the water table.

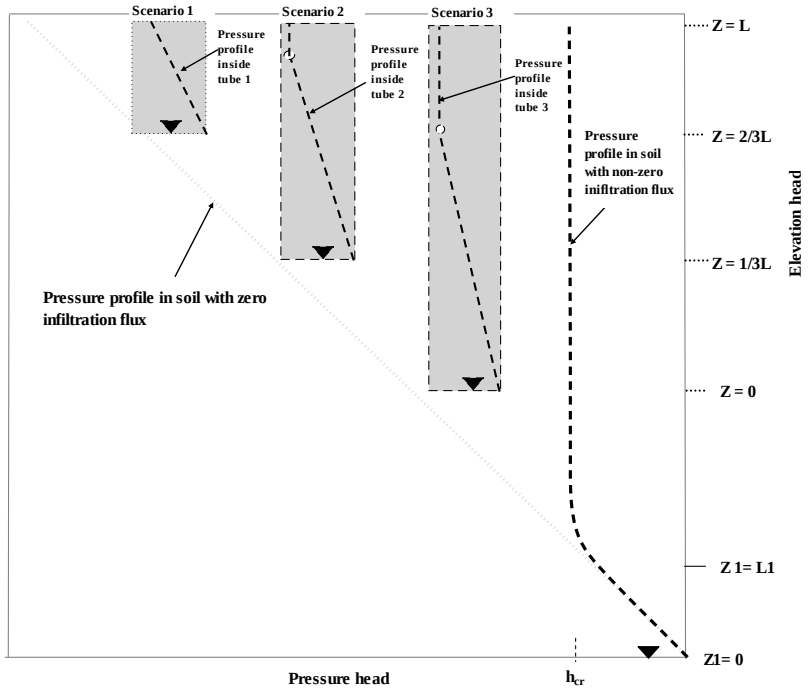

Figure 2.3 Pressure head profiles for three tube lengths compared to the *in-situ* soil. Note that all these pressure heads are under an equilibrium state for the surrounding soil (solid lines) and inside tubes (dashed lines).

The occurrence of an elevation at which a zero pressure head gradient (at a constant pressure head, h_{cr}) and a unit vertical gradient (Z = L1) depends on the applied infiltration flux and hydraulic conductivity of the soil.

During a non-zero infiltration flux to the soil surface, water will start entering the tube laterally and through a gravitational pull. It follows that an artificial water table will be created within each of the tubes buried below the soil surface (Fig. 2.3). This Figure illustrates three scenarios of pressure head profiles in different tube lengths. In scenario 1, the point of a zero pressure head gradient and unit vertical gradient does not occur within the tube1, which may result differences in pressure head conditions both inside and outside of the tube.

It follows that the tube will only collect part of the infiltration flux due to the flow of water around the tube. Besides, the water within the tube could be wicked out to the soil due to capillarity forces.

In scenarios 2 and 3 of Figure 2.3, the point of a zero pressure head and a unit vertical gradient (indicated by a circle) occurred within each tube length because the depth of the artificial water table is at a depth that allows for this condition to develop. In these two scenarios, the pressure head at the mouth of each tube is equal to the pressure head at the surrounding soil. Under an equilibrium condition, these pressures represent the maximum measurable pressure head at the elevation Z = L for each of the tube lengths (scenarios 2 and 3), i.e. the pressure head at the mouth of the tube corresponding to scenario 2 is equal to (2/3L)* 9.8 kPa/m and for scenario 3 is equal to (L)* 9.8 kPa/m. The pressure head developed at the mouth of these tubes therefore is dependent on the infiltration flux and hydraulic conductivity of a wick material. It follows that, any water level in each of the tubes (scenarios 2 and 3) under equilibrium conditions (no flow) can be related to the pressure head at the surrounding soil using the hydrostatic pressure gradient. The pressure head and gravitational head water distribution under equilibrium condition for this prototype is also similar to the one described (Fig. 2.2a).

2.2.1.2 *Hybrid wetting front detector design and operation*

The Hybrid wetting front detector is the second prototype design made up of an extension head tube (33 cm long and 71 mm in diameter) fitted above the top of the funnel neck (22 cm from the funnel base to its neck), a filter, floats and an indicator (Fig. 2.1b). This combines some features of the FullStop like the wider opening could have a slight convergence effect, the added tube length will reduce emptying due to capillarity forces, and a wick material with a higher hydraulic conductivity than the soil filling the extra tube length to ensure water flows to the tube. The Hybrid detector has a total length of 55 cm (base to the mouth of the device). With the hydrostatic pressure gradient in mind, it has potentially a tension sensitivity value of equal to its length (i.e. 55 cm or 5.5 kPa).

The open space between the 71 mm outer extension tube (providing length) and inner tube (housing the indicator float) is filled with a wick material. A contact material is placed above the mouth of the 71 mm diameter tube to provide hydraulic contact between the wick material in the Hybrid detector and the surrounding soil. The opening of the extension tube (71 mm in diameter) is buried in the root zone, with the indicator visible above the soil surface (Fig. 2.1b). The Hybrid detector intercepts water from the unsaturated flow via the contact material and flows down through a wick material and drains passively into the reservoir to activate the float mechanism. The pressure head and gravitational head water

distribution described for the tube length (Fig. 2.2a) works also in a similar way for the Hybrid design with some convergence effect at its mouth.

2.2.2 Wick material characteristics

The Tube-shaped WFD design needs to be filled with a wick material to keep the instrument and surrounding soil in hydraulic equilibrium. This, however, requires knowledge of the hydraulic properties of the wick material and soil. The basic hydraulic properties required for an ideal wick material include:

- A higher unsaturated hydraulic conductivity than the surrounding soil over the range of its tension sensitivity to intercept and divert water into the tube, and
- Water retention characteristics described by a high air entry potential that is inversely related to the specific yield, i.e. a wick with a large air entry potential will have a zero specific yield and remains saturated over its tension sensitivity range.

These ideas will be fully evaluated in Chapter 4.

CHAPTER 3

COMPARISON OF METHODS FOR DETERMINING UNSATURATED HYDRAULIC CONDUCTIVITY IN THE WET RANGE TO EVALUATE THE SENSITIVITY OF WETTING FRONT DETECTORS

3.1 INTRODUCTION

Irrigation is usually scheduled by measuring or predicting a soil water deficit. Another way to conceptualise the irrigation decision is to cease irrigation when the infiltrating water reaches a set depth in the soil (Zur *et al.*, 1994; Stirzaker, 2003). Stirzaker and Hutchinson (2005) demonstrated the success of using a funnel shaped wetting front detector (WFD) to irrigate grass by automatically switching off the sprinklers when the infiltrating water reached a depth of 15 cm.

The WFD used in the above study is essentially a passive lysimeter, i.e. it collects a water sample from an unsaturated medium by distorting the downward flow of water. Yet the limitations of passive lysimetry are well documented in the literature, in particular their failure to collect a sample when the flux is low (Gee *et al.*, 2002; Zhu *et al.*, 2002). In the same way, some water could drain past a WFD without a water sample being collected, and therefore give the irrigator incorrect feedback.

If a passive lysimeter or WFD were used to control irrigation, then it would be useful to be able to collect a water sample over the range from saturation to field capacity, since field capacity is usually accepted as the maximum soil storage with negligible drainage. However, field capacity has no universal definition. It is commonly defined in the field as the water remaining in a soil after 48 or 72 hours of free drainage following saturation (Soil Science Society of America, 1997). Others have defined field capacity as the time when the water flux falls below 0.1 mm/day (Stegman *et al.*, 1980) or when the absolute change in volumetric soil water content is 0.1 to 0.2% per day (Ratliff *et al.*, 1983) or as a particular soil tension (Romano and Santini, 2002).

The design of a passive lysimeter or WFD determines the soil tension at which it can collect a water sample, which for practical purposes ranges between 30 and 100 cm (Hutchinson and Bond 2001; Gee *et al.*, 2002; Weihermüller *et al.*, 2007; Stirzaker, 2008). Given the various definitions of field capacity, and the fact that it is highly dependent on soil type (Romano and

Santini, 2002), reliable methods of predicting the drainage flux within the 0-100 cm range of soil tensions would help to choose among various designs of wetting front detectors. However, the relationship between drainage rate and tension is notoriously difficult to determine since different field, laboratory and theoretical approaches can give very different results (Jones and Wagnet, 1984; Comegna, *et al*., 1996; Poulsen *et al*., 2002).

The instantaneous profile method (IPM) has been widely used to determine the hydraulic conductivity as a function of tension, K(h), in the field (Watson, 1966; Hillel *et al*., 1972; Reichardt *et al*., 1998) but can result in large errors, particularly at the wet end of the range (Fluhler *et al*., 1976; Reichardt *et al*., 1998). Results can be improved by using inverse modelling approaches. Inverse modelling uses the equations governing unsaturated flow to determine soil parameters by minimizing the differences between model predictions and observed data, and is believed to give the best estimate of unsaturated hydraulic conductivity (Fristerle and Faybishenko, 1999; Zhang, *et al*., 2003).

A disadvantage of the field IPM and inverse methods is the considerable time and cost they incur in comparison to laboratory tests. The laboratory procedure of Bruce and Klute (1956) is a rapid method for estimating the soil water diffusivity function, $D(\theta)$ or the hydraulic conductivity K(h) if water retention data is available. The original method has subsequently been improved by several groups (Clothier *et al*., 1983; Tyner and Brown, 2004; Prevedello *et al*., 2008). However, it is difficult to establish steady or transient-state flow conditions under laboratory conditions and the method does not fully represent actual field conditions (Nandagiri and Prasad, 1996).

Given the problems associated with field and laboratory techniques, the use of theoretical approaches has become common. Methods for estimating K(h) functions have been derived from water retention models (Brooks-Corey, 1964; Campbell, 1974; van Genuchten, 1980) combined with capillary models (Burdine, 1953; Mualem, 1976). These methods predict unsaturated hydraulic conductivity from easily measurable water retention data or basic soil properties such as texture and bulk density.

This chapter compares the field IPM method, the laboratory Bruce-Klute method and theoretical models to estimate unsaturated hydraulic conductivity between tensions of 0 and 100 cm on a Hutton soil type (Soil Classification Working Group, 1991). The application is two-fold. First, we need a way to choose between designs of wetting front detector that could

collect a water sample passively at 30, 60 and 90 cm tensions (Stirzaker *et al*., 2010). Second, we need to know the simplest method for getting a reasonable estimate of conductivity in the wet range to estimate the fluxes associated with each sensitivity level.

3.2 MATERIALS AND METHODS

This chapter is structured according to a detailed flow diagram shown (Fig. 3.1) and the list of symbols and equations used in manipulating the data are summarised in (Table 3.1, Table 3.2).

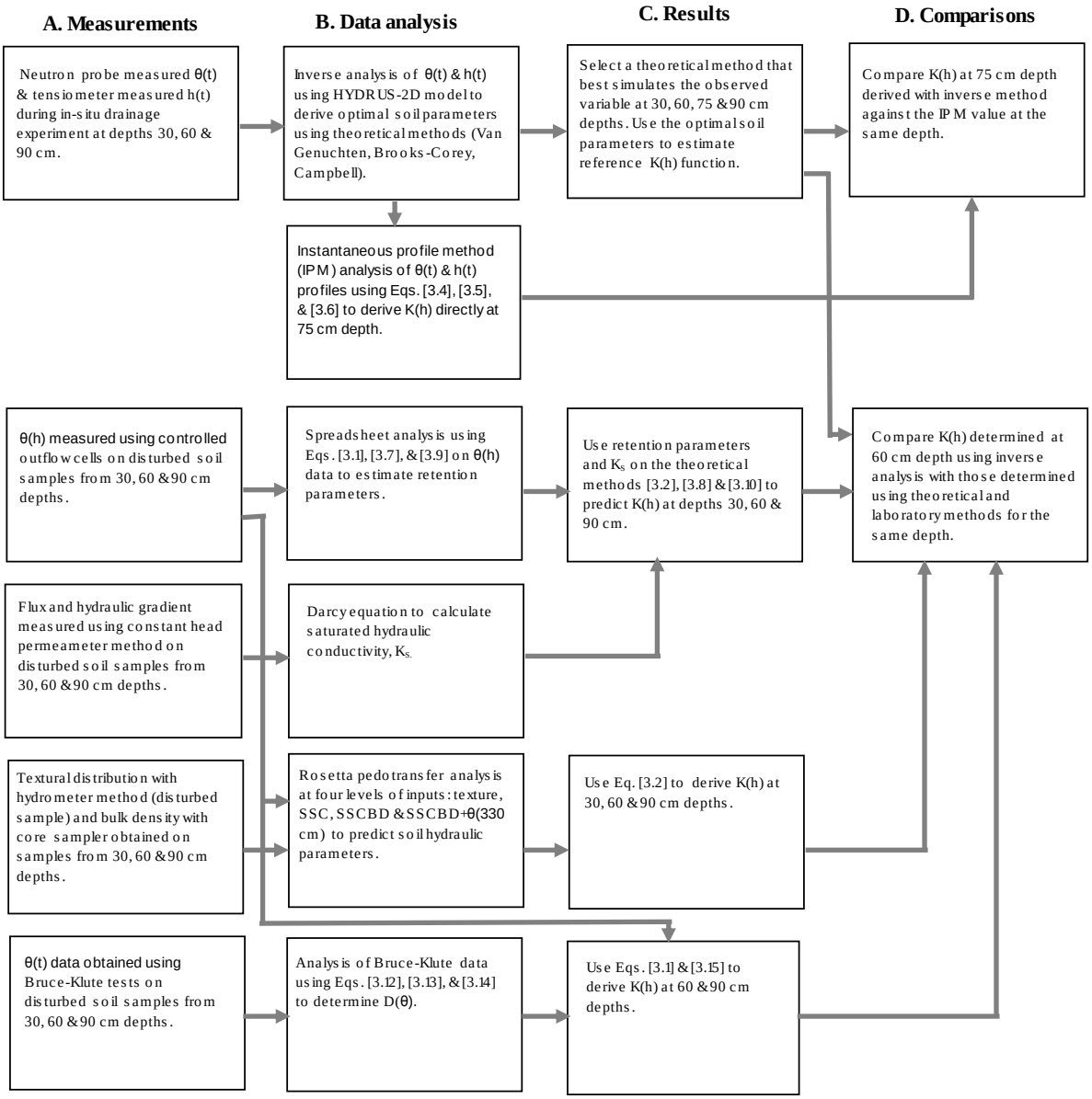

Figure 3.1 Flow charts describing all the processes involved to estimate unsaturated hydraulic conductivity of *in-situ* and disturbed soil samples using different methods.

Table 3.1 Equations used for analysing data.

Equation	Number	Reference	Equation	Number	Reference
$S_e(h)=\frac{\theta(h)-\theta_r}{\theta_s-\theta_r}=\left(1+(\alpha h)^n\right)^{-m}$	***3.1***	***Van Genuchten (1980)***	$\begin{cases} S_e=\left(\frac{h_d}{h}\right)^{\eta} & for \quad h>h_d \\ S_e=1 & for \quad 0<h<h_d \end{cases}$	***3.9***	***Brooks-Corey (1964)***
$\begin{cases} K(h)=K_s * S_e^{\,l} * \left(1-\left(1-S_e^{\,1/m}\right)^m\right)^2 \\ S_e=\frac{\theta-\theta_r}{\theta_s-\theta_r} \\ m=1-\frac{1}{n} \qquad n>1 \end{cases}$	***3.2***	***Van Genuchten (1980)-Mualem (1976)***	$\begin{aligned} K(h)&=K_s(S_e)^{\frac{(2+3\eta)}{\eta}} \quad for \quad h>hd \\ K(h)&=K_s \qquad\qquad\qquad for \quad 0<h<hd \end{aligned}$	***3.10***	***Brooks-Corey (1964)-Burdine (1953)***
$h_{75}(t)=a\ln t+b$	***3.3***		$\begin{cases} \theta=\theta_i \ for\ x>0\ and\ t=0 \\ \theta=\theta_o \ for\ x=0\ and\ t>0 \\ \theta=\theta_i \ for\ x=\infty\ and\ t>0 \end{cases}$	***3.11***	***Bruce-Klute (1956)***
$\theta_o-\theta=A_L\ln t+B_L$	***3.4***	***Reichardt et al (1998)***	$\lambda(\theta)=\left(\frac{P+1}{\theta_s-\theta_r}\right)S\left(1-\frac{\theta-\theta_r}{\theta_s-\theta_r}\right)^p$	***3.12***	***Clothier et al (1983)***
$Flux\ desnsity=-\sum_{i=1}^{n_f}\frac{A_L}{t}\Delta z$	***3.5***	***Reichardt et al (1998)***	$S=\int_{\theta_i}^{\theta_0}\lambda d\theta$	***3.13***	
$\left(dH/dz\right)=\frac{H_{90}(t)-H_{60}(t)}{\Delta z}$	***3.6***		$D(\theta)=p(p+1)S^2\left(\frac{(1-\theta)^{p-1}-(1-\theta)^{2p}}{2(\theta_s-\theta_r)^2}\right)$	***3.14***	***Clothier et al (1983)***
$\theta=\theta_s\left(\frac{h}{h_a}\right)^{-1/b}$	***3.7***	***Campbell (1974)***	$K(\theta)=\frac{D(\theta)}{dh/d\theta}$	***3.15***	***Klute (1952)***
$K=K_s\left(\frac{\theta}{\theta_s}\right)^{\omega}$, $where\ \omega=2b+3$	***3.8***	***Campbell (1974)***	$RMSE=\sqrt{\frac{1}{N}\sum_{i=1}^{n_f}\left(x_{measured}-x_{predicted}\right)^2}$	***3.16***	***Poulsen et al (2002)***

Table 3.2 Symbols and their definitions.

Symbol	Definition	Symbol	Definition
a, b, A_L, B_L	Empirical constants	θ_i	Initial water content
h_d, h_a	Air entry parameters	θ_o	Water content at the inlet
h(t)	Tension as a function of time	θx	Horizontal distance from the inlet
H	Total hydraulic head	$dh/d\theta$	Slope of water retention data
m, η, b	Fitting parameters	N	Number of observations
n_f	Last observation	Σ	Summation
t, λ	Time, Boltzmann variable	$xi, \bar{x}$	Observed and mean values respectively
Θ	Volumetric water content		
$\theta(h)$	Water content as a function of tension		
$\theta(t)$	Water content as a function of time		
S_e	Relative saturation		
z	Gravitational or vertical depth co-ordinate measured positively downward from the soil surface		

3.2.1 Soil data measurements

3.2.1.1 *In-situ drainage experiment*

An *in-situ* drainage experiment was conducted on a 250 x 200 cm levelled plot, located at the University of Pretoria Experimental Farm, Hatfield, South Africa (25° 45'S, 28° 16'E and altitude 1370 m). Particle size distribution, bulk density and volumetric water content at a tension value of 330 cm (θ_{330cm}) of the site are described in Table 3.3. These values were used as inputs by a pedotransfer function described in Section 3.2.1.5 to predict soil water flow parameters. The vertical sides of the drainage plot were hydrologically isolated from other plots by fibre cement sheets to a depth of 120 cm to prevent lateral water flow. The plot was ponded by applying water in excess of the infiltration rate for about 10 hours until the tensiometer installed at a depth of 90 cm below the soil surface read close to saturation. The surface of the drainage plot was then covered with a plastic sheet to prevent evaporation losses.

Table 3.3 Basic soil data and θ_{330cm} at the three soil depths of the Hutton soil on Hatfield Experimental Site.

Depth (cm)	Particle size distribution (%)			ρ_b (Mg/m^3)	θ_{330cm}	Texture
	Sand	Silt	Clay			
30	79.0	6.0	15.0	1.674	0.127	Sandy loam
60	60.5	5.0	34.5	1.475	0.209	Sandy clay loam
90	60.0	15.0	25.0	1.412	0.246	Sandy clay loam

Water content was monitored daily to a depth of 120 cm using a site-calibrated neutron probe with a standard error of less than 0.03 cm^3/cm^3, which is within the acceptable tolerance range (Hignett and Evett, 2002). Tension was recorded with SoilSpec tensiometers (SoilSpec Tensiometer System, Model SST101G, NH & TS Electronics, Australia) connected to a HOBO logger (Onset Computer Corporation, MA02532, USA) at 15 minute intervals to an accuracy of within ± 1 cm at 30, 60 and 90 cm depths. The tensiometer were placed about50 cm from the neutron probe access tubes, which is sufficient to avoid the interference of water in the tubes of the tensiometer from affecting the neutron probe readings. The drainage measurements were monitored for a total period of 16 days.

3.2.1.2 *Sample preparation and laboratory measurements*

On completion of the drainage measurements, disturbed soil samples were obtained for various laboratory tests at depths of 30, 60 and 90 cm. The samples were air-dried and ground to pass a 2 mm sieve. Particle size distribution (PSD) and textural class were determined using the hydrometer method and USDA textural classification respectively. Dry bulk density (BD) was determined from the core sampler volume (80.5 mm diameter and 105 mm long) and the dry mass of the sampled soil. The θ_{330cm} was determined from the water retention characteristics of each soil depth.

3.2.1.3 *Water retention characteristics*

The drying soil-water retention curve was determined using a multi-step controlled outflow method (Fig. 3.2). Soil samples were packed (metal ring 54 mm diameter and 30 mm height) at field bulk density to measure the water retention characteristics between 0 and 1000 cm tension (Lorentz, *et al*., 2001). This measurement on packed samples was made purposefully to estimate the deviation of hydraulic conductivity (HC) predicted using soil water parameters derived from measurements made on packed samples, from that of the *in-situ*

based HC values. When the equilibrium condition for the highest tension applied was obtained, the soil was removed and the final water content of the soil measured by oven drying. This final water content, together with the previous changes in water volume, was used to back calculate the water contents corresponding to the different tensions.

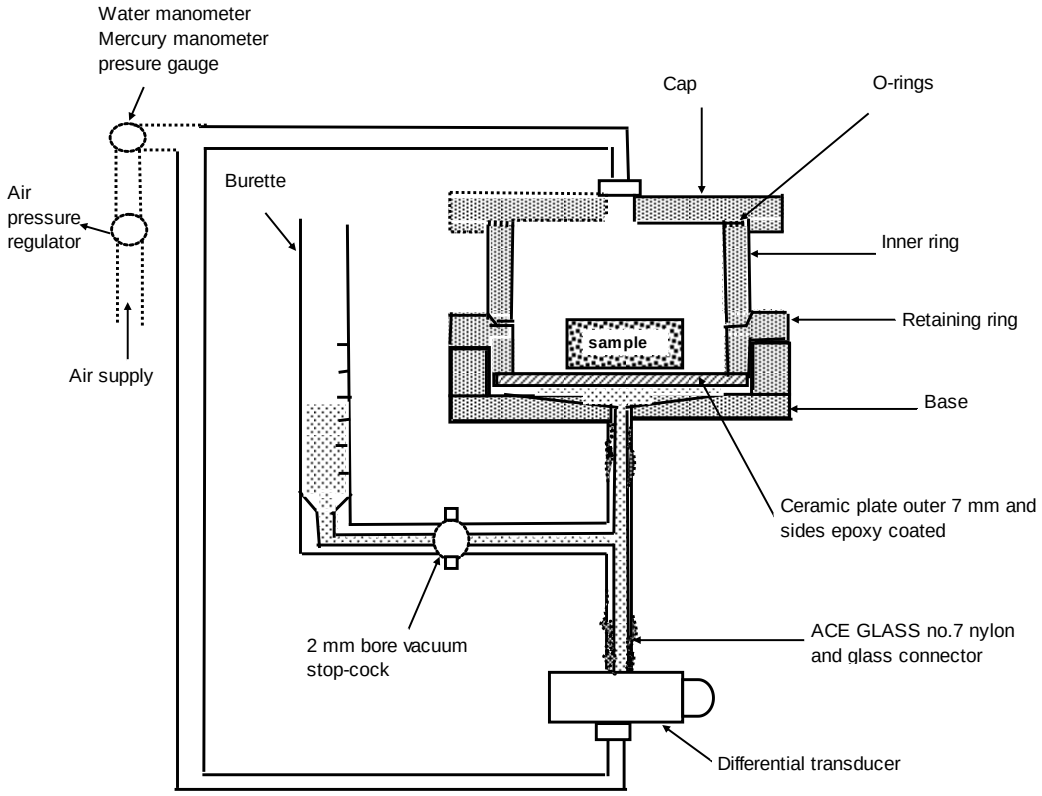

Figure 3.2 Schematic presentation of the Controlled Outflow Cell assembly (Lorentz *et al*., 2001).

3.2.1.4 *Saturated hydraulic conductivity*

Saturated hydraulic conductivity (K_s) was determined on packed soil columns using a constant-head permeameter. Soil samples were packed in permeameters to the field bulk densities indicated (Table 3.3) to imitate field conditions. Each soil sample was packed in layers where the top of each layer was disturbed to create a rough surface to improve contact between layers. A Marriott bottle was then used to supply water at a constant head, while wetting the sample with upward infiltration to minimize air entrapment. This method applies Darcy's principle to a saturated soil tube of uniform cross-sectional area (Klute, 1965). The tubes (60 mm diameter and 300 mm height) were packed at bulk densities, which varied on

average by < 10% of the field bulk density (Table 3.3). The hydraulic head difference between two permeameters ports and the flux measurements from the tube was used to calculate K_s.

3.2.1.5 *Rosetta Pedotransfer Function*

A pedotransfer function (PTF) provides an estimate of the relationship between the soil hydraulic properties and basic soil properties. The Rosetta Pedotransfer Function (Schaap *et al*., 1998; 2001) is a user-friendly computer program that facilitates the use of PTF models to predict soil hydraulic parameters, including residual volumetric water content (θ_r), saturated volumetric water content (θ_s), air entry parameter (α), pore size distribution parameter (n) and K_s from basic soil data and θ_{330cm}. The analyses using the Rosetta function were performed by entering a combination of predictors based on the level of available information through a text input file for each soil sample. These predictors included four levels: i) Textural class, ii) %Sand, %Silt, %Clay (SSC), iii) SSC+Bulk Density (BD), and iv) SSC+BD+θ_{330cm}. Outputs from the Rosetta program include θ_r, θ_s, α, n and K_s.

3.2.1.6 *Bruce-Klute test*

A Bruce-Klute imbibition test (Fig. 3.3) was performed on a uniformly packed horizontal tube of soil comprising 10 transparent cells (each cell 20 mm long and 25 mm diameter). Packing was done by compacting 4.0 cm layers with a 20 mm diameter-tamping rod and loosening the soil surface between packing. Dry bulk density was calculated from the tube volume and the dry mass of the packed soil. Porosity was calculated from the dry bulk density of the packed soil and the assumed soil particle density of 2.65 Mg/m^3.

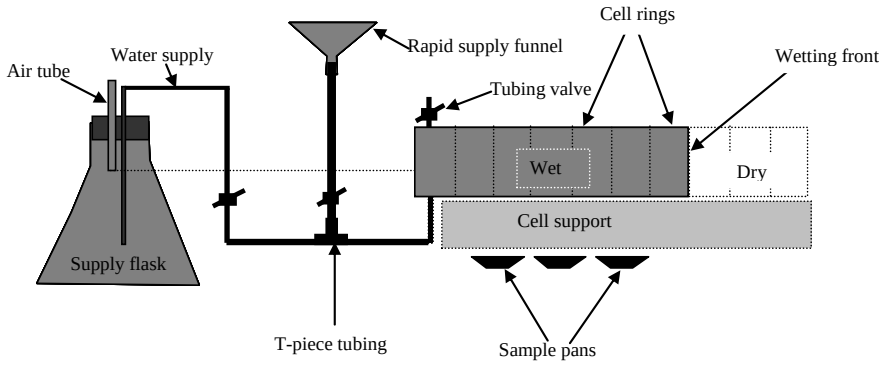

Figure 3.3 Schematic presentation of Bruce-Klute test for measuring soil water diffusivity by horizontal infiltration (Lorentz *et al*., 2001).

The inlet chamber on one end of the tube was connected to the supply flask to establish a zero tension at the centre of the sample (Fig. 3.3). An instantaneous supply of water was applied to the tube from a funnel with an immediate shift to the supply flask as soon as the inlet chamber was filled. The starting time was recorded and the advance of the wetting front observed. The source of water was removed as soon as the wetting front reached the second last ring and the time was recorded. All the cell rings were quickly sectioned and placed into separate aluminium weighing pans and wet and oven-dry mass were taken to determine the water content of each sample.

3.2.2 Data analysis

3.2.2.1 *The instantaneous profile method (IPM)*

The measured soil water contents and soil tensions from the field trial were used to obtain hydraulic conductivity as a function of water content or tension using the *IPM* procedures presented by Reichardt *et al.*, (1998) and the equations presented in Table 3.1. The water content profile, $\theta(z, t)$ was smoothed with respect to time for each depth using Eq. [3.4]. A finite difference over a given depth interval was applied to estimate the soil water flux density using Eq. [3.5]. The total hydraulic gradient at 75 cm depth was obtained by dividing the difference in hydraulic heads at depths of 60 and 90 cm by the vertical distance between these two depths using Eq. [3.6]. Finally, the hydraulic conductivity at 75 cm was determined as the ratio of water flux density Eq. [3.5] and total hydraulic gradient Eq. [3.6]. This IPM based hydraulic conductivity at a depth of 75 cm was then compared against the *in-situ* values determined using the inverse model at a similar depth.

3.2.2.2 *The in-situ inverse model*

Hydraulic properties were modelled using an inverse parameter estimation process using the HYDRUS-2D model (Šimůnek *et al.*, 1999) that solves the Richards' equation for two-dimensional vertical flow using the van Genuchten (1980)-Mualem (1976) hydraulic model. The profile was divided into four soil depth intervals (0-41 cm, 41-77 cm, 77-118 cm and 118-150 cm). The pore connectivity parameter (l) was set to 0.5, and initial estimates of residual and saturated water contents were entered in the data sheet for inverse solution of each depth interval to optimize the three soil parameters (n, α and K_s). These parameters were optimized simultaneously for each soil layer.

The drainage profile set in the HYDRUS-2D model was for this purpose divided into four soil materials each representing the depths of measurement of responses of wetting front detectors (0-41 cm, 41-77 cm, 77-118 cm and 118-150 cm), and not to any distinct soil layers. Each soil material was described in the form of van Genuchten parameters. The *in situ* water retention data were fitted to the analytic water retention models of van Genuchten Eq. [3.1] to estimate the water retention parameters. These fittings were performed manually in a spreadsheet analysis. The pore connectivity (l) parameter at 0.5, and the initial estimates of residual and saturated water contents obtained by fitting the analytic water retention models to a measured retention data were fixed in the data sheet for inverse solution for each material type. Three hydraulic parameters (n, α, and K_s) in the profile were optimized simultaneously for each soil material using the inverse method.

Four observation nodes at depths of 30, 60, 75 and 90 cm were configured within the flow domain of the profile (Fig. 3.4a) to simulate the *in situ* drainage data. The simulation had no flow boundary conditions at the topsoil surface and vertical sides of the profile, and free drainage conditions at the bottom of the profile, which simulated the boundary conditions of the drainage profile (Fig. 3.4b).

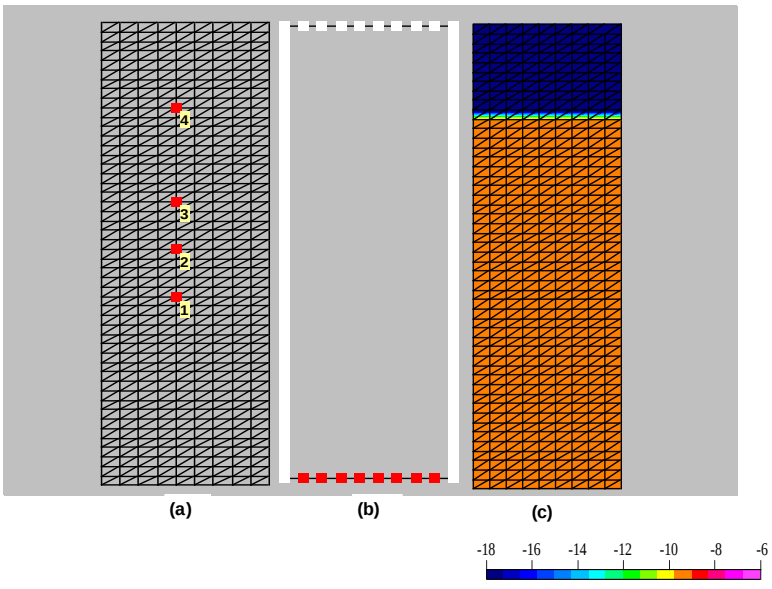

Figure 3.4 Observation nodes (a), boundary (b) and initial (c) conditions in HYDRUS-2D model to simulate observed data.

The initial conditions of each soil material were set to the *in situ* tension values observed at the start of the drainage experiment in the field: free drainage condition at the base selected

from the input file (SELECTOR.IN), h = 20 cm for depths between z = 0 and 41 cm, and 10 cm for depths between z = 41 and 150 cm (Fig. 3.4c). The *in situ* time series water content and tension data for each observation node at depths 30 (node 4), 60 (node 3) and 90 cm (node 1) and the *in-situ* time series water content at 75 cm depth (node 2) were entered into the data sheet for inverse solution in the HYDRUS-2D model to perform inverse parameter estimation (Fig. 3.4a).

The *in-situ* water contents were lower than those obtained with a multi-step controlled outflow method for similar tension values (data not shown), and may be due to air entrapment during field saturation of the profile (Reynolds and Elrick, 2002). Therefore, the *in-situ* water contents determined at 30, 60 and 90 cm depths were adjusted to coincide with the corresponding outflow cell retention data. Since there was no retention data at 75 cm, the *in-situ* water content for this depth was adjusted to the retention data measured at 90 cm below the soil surface.

A draining profile was simulated in HYDRUS-1D using the soil hydraulic properties obtained from the various methods described above. The profile was initially set to 10 cm tension with a zero flux upper boundary and a free drainage lower boundary condition. Water flow was simulated over a period of 16 days in (i) a uniform soil profile (150 cm depth) described by soil parameters determined at 60 cm depth using the inverse method to explore various definitions of field capacity and (ii) a two-layered soil profile (0-30 cm and 30-150 cm layers) using field and laboratory derived soil parameters to determine the flux at tensions of 30, 60 and 90 cm at a depth of 60 cm.

3.2.2.3 *Bruce-Klute test*

The soil water content profiles obtained for soil depths 30, 60 and 90 cm using a Bruce-Klute test were transformed into a Boltzmann variable $\lambda(\theta)$ by dividing the original data by the square root of the time required to complete the test. The $\lambda(\theta)$ data was then fitted with an appropriate function using Eq. [3.12] and the parameter 'p' in Eq. [3.14] was obtained during this fitting procedure. The sorptivity 'S' in Eq. [3.14] was calculated as the area under the fitted curve using Eq. [3.13]. The diffusivity function, $D(\theta)$ was then determined using the analytical form suggested by Clothier *et al*. (1983), Eq. [3.14]. This $D(\theta)$ function combined with the outflow data, was used to estimate the hydraulic conductivity as a function of water content, $K(\theta)$, Eq. [3.15]. Tension equivalent of the water contents in the $K(\theta)$ function were estimated using Eq. [3.1] to describe the hydraulic conductivity as a function of tension, K(h).

3.2.2.4 *Theoretical methods*

The independently measured retention data points fitted with the van Genuchten (1980), Campbell (1974), and Brooks-Corey (1964) analytical models and the K_s values measured in the laboratory with a constant head method were used to predict the unsaturated hydraulic conductivity function using theoretical models. These theoretical models are the van Genuchten-Mualem (VGM), Campbell, and Brooks-Corey-Burdine (BCB) represented by Eqs. [3.2], [3.8], and [3.10] respectively.

Four predictors obtained from the measurements of basic soil properties (Table 3.3) were entered into an input file in a Rosetta computer program to predict the soil parameters at depths 30, 60 and 90 cm. The four predictors used in the Rosetta computer program were: textural class, SSC, SSC+BD and SSC+BD+θ_{330cm}. Finally, the predicted soil parameters (θ_r, θ_s, n, α and K_s) were then used as input variables in Eq. [3.2] to predict K(h) function of each soil depth.

3.2.2.5 *Evaluation procedures*

Prediction accuracies of hydraulic conductivities (HC) determined using theoretical methods based on laboratory measured retention data and K_s, pedotransfer functions, laboratory method (Bruce-Klute), and the instantaneous profile method (IPM) were evaluated with respect to the *in situ* inverse analysis of drainage data. The root mean square error (RMSE) presented in Eq. [3.16] was used to calculate the prediction accuracy of the different models (Poulsen *et al*., 2002). The units used for HC include mm/day or mm/h ($mm.h^{-1}$) or cm/h ($cm.h^{-1}$) where necessary.

3.3 RESULTS AND DISCUSSION

3.3.1 Inverse method

Figure 3.5 shows the time series simulated and measured tension and water content data for the field drainage experiment. The simulated tensions and water contents were produced using the VGM hydraulic model.

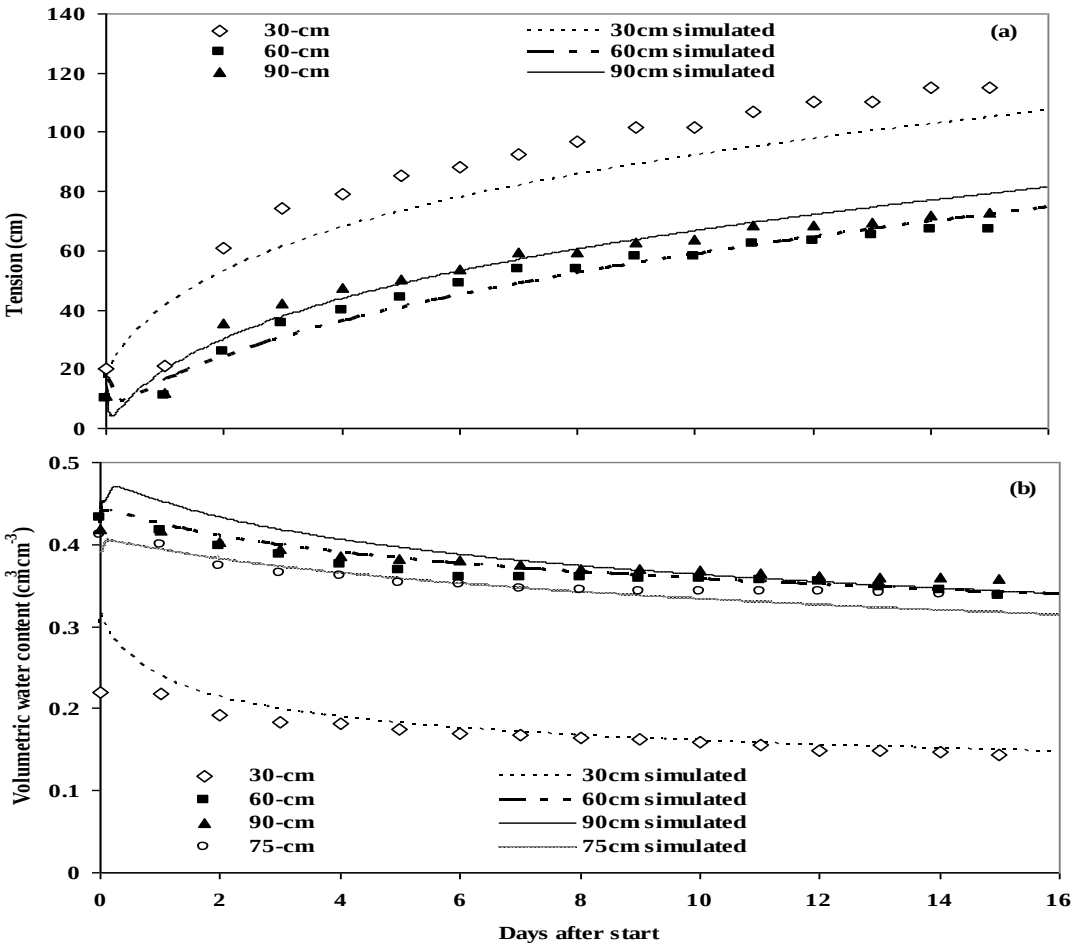

Figure 3.5 Comparisons between observed (data points) and inverse simulated (lines) for tensions (a) and water contents (b) determined at different observation depths.

The soil parameters obtained using the VGM model reproduced the measured data well at depths of 60 and 90 cm but not as well at 30 cm (Fig. 3.5a, b). The model also reproduced the measured water content well at 75 cm (Fig. 3.5b). The deviations at 30 cm are possibly due to the effect of diurnal surface temperature fluctuations on the performance of the tensiometer (Sisson *et al.*, 2002). The measured water contents also tended to be lower than the simulations, especially in the surface soil where the neutron probe is known to be less accurate. Similar analyses were performed using the BCB and Campbell hydraulic models, which performed adequately at most depths, but not as well as the VGM model overall (Table 3.4).

Table 3.4 R^2 values between measured and simulated tensions and water contents.

Depth (cm)	Campbell		van Genuchten		Brooks-Corey	
	Tension	Water content	Tension	Water content	Tension	Water content
30	0.37	0.89	0.91	0.88	0.93	0.78
60	0.94	0.94	0.96	0.97	0.59	0.95
75	-	0.87	-	0.97	-	0.87
90	0.95	0.83	0.97	0.97	0.95	0.82

The simultaneous use of water content and tension data in the optimization procedure produced unique parameter estimates (α, n, and K_s), as judged by the low correlation matrix, i.e. $R^2 < 0.95$, between optimized parameters, consistent with the findings of Zhang *et al.* (2003). The parameters obtained by inverse modelling of the drainage data at pre-selected depths (60, 75 and 90 cm), are therefore considered as reference values against which the other methods were compared (Table 3.5).

Table 3.5 Parameter estimates obtained with 95% confidence limits using an inverse method (VGM hydraulic model) at four observation depths.

Depth (cm)	Van Genuchten parameters					
	θ_r	θ_s	α (cm^{-1})	n	K_s(cm/h)	l
30	0.00	0.366	0.038	1.63	180.00	0.50
60	0.05	0.462	0.014	1.61	0.304	0.50
75	0.05	0.485	0.014	1.61	0.304	0.50
90	0.05	0.485	0.025	1.48	0.532	0.50

3.3.2 Instantaneous Profile Method, Bruce-Klute Test and Theoretical Methods

The soil parameters obtained by fitting the analytical retention models (van Genuchten, 1980; Campbell, 1974; Brooks-Corey, 1964) into the laboratory determined retention data; the regression values (R^2) between measured and fitted values are presented in Table 3.6.

The van Genuchten and Brooks-Corey models described the water retention data measured at depths 60 and 90 cm better than the Campbell model, judged by the higher regression values (R^2) > 0.98. Soil parameters generated from basic soil properties using the Rosetta pedotransfer function are also shown (Table 3.7).

Table 3.6 Estimated parameters using the three water retention models

Depth (cm)	K_s (cm/h)	van Genuchten					Campbell				Brooks and Corey				
		θ_r	θ_s	α	n	R^2	θ_s	h_a	b	R^2	θ_r	θ_s	η	h_d	R^2
30	1.197	0.07	0.366	0.019	1.38	0.91	0.366	5.5	4.0	0.92	0.07	0.366	0.400	5.00	0.91
60	1.197	0.10	0.462	0.027	1.55	0.99	0.443	22.0	3.4	0.86	0.16	0.443	1.000	38.46	0.98
90	1.100	0.17	0.485	0.031	1.60	0.99	0.467	10.0	5.6	0.94	0.16	0.467	0.464	22.22	0.99

The K (h) characteristic at 75 cm depth was estimated using the IPM (Fig. 3.6a). With the knowledge of soil parameters derived from laboratory measured retention data (Table 3.6), basic soil properties (Table 3.7) and Bruce-Klute test, for example at 60 cm depth, K(h) characteristics were determined (Figs. 3.6b and c).

Inferring flow parameters from conventional curve fitting method or pedotransfer functions, however, may lead to prediction errors due to the inadequacy of the derived parameters to describe the processes governing the flow. It is important, therefore, to know the deviation from the actual values by comparing K(h) functions predicted from these soil parameters with respect to those obtained by inverse modelling of drainage data.

Table 3.7 Estimated parameters for the three soil depths using Rosetta program

	Texture			SSC			SSCBD			SSCBD+ θ(330 cm)		
Parameter	**30**	**60**	**90**	**30**	**60**	**90**	**30**	**60**	**90**	**30**	**60**	**90**
θ_r	0.04	0.09	0.09	0.06	0.08	0.07	0.05	0.08	0.07	0.06	0.09	0.07
θ_s	0.39	0.48	0.48	0.37	0.39	0.39	0.35	0.43	0.43	0.35	0.43	0.43
α	0.027	0.008	0.008	0.029	0.027	0.026	0.031	0.025	0.021	0.050	0.036	0.028
n	1.45	1.52	1.52	1.51	1.24	1.32	1.49	1.28	1.39	1.87	1.63	1.39
K_s	1.59	0.46	0.46	1.85	0.62	0.58	1.45	1.06	1.25	6.40	8.13	2.43

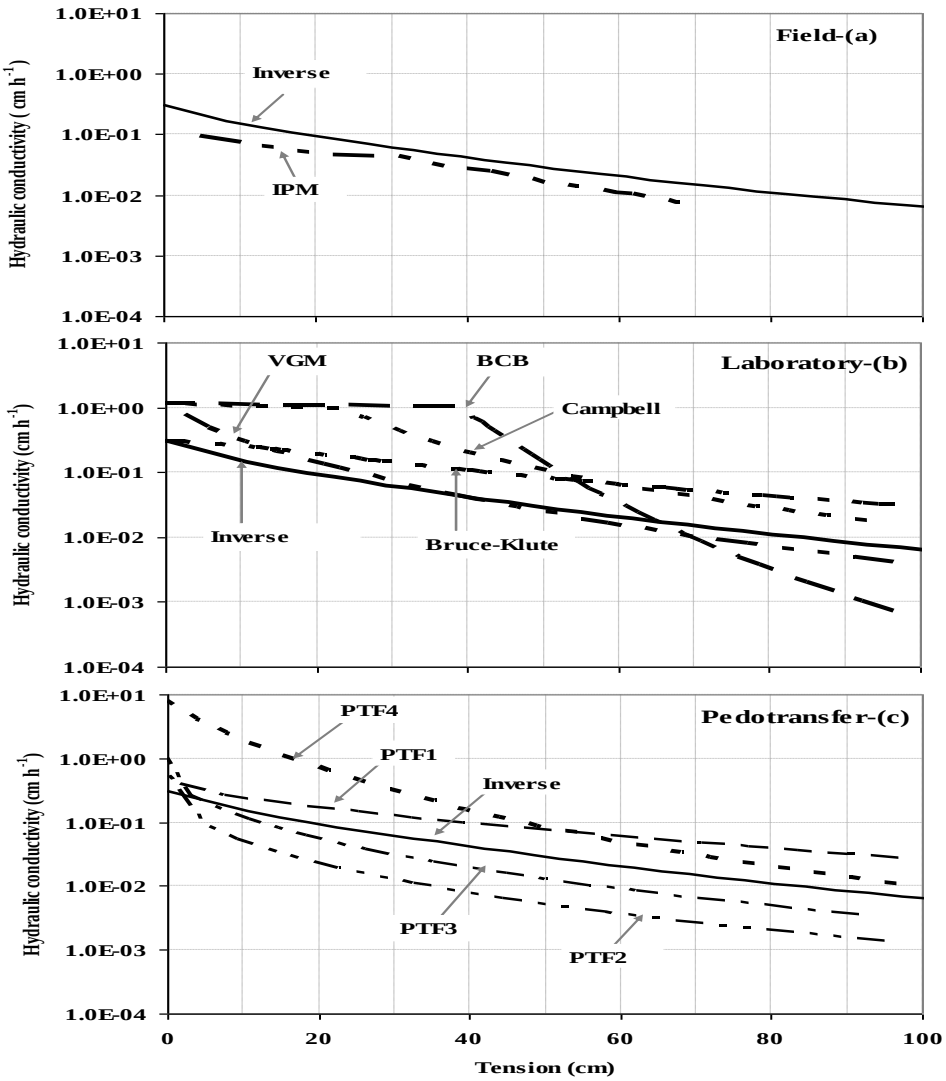

Figure 3.6 Comparisons between hydraulic conductivity estimated with the IPM against inverse results at 75 cm depth (a) and theoretical and laboratory (b) and pedotransfer (c) methods against inverse result at 60 cm depth.

3.3.3 Comparisons of hydraulic conductivity estimation methods

This part of the discussion will address the hypothesis: alternative methods can provide a reasonable substitute for the *in situ* inverse method of estimating K(h) characteristics. For illustration purposes, comparisons were made at two depths: (i) IPM against the inverse method at 75 cm depth (Fig. 3.6a) and (ii) three theoretical models and Bruce-Klute method with respect to the inverse method at 60 cm depth (Fig. 3.6b to c).

The field based IPM method produced K(h) curve slightly below the inverse reference (Fig. 3.6a). The VGM approach appeared to give the closest fit of the various laboratory based methods (Fig. 3.6b), especially for tensions drier than 20 cm. The Campbell and BCB methods overestimated K_s values in the wettest part of the range, consistent with the findings by Poulsen *et al*. (2002), namely that multi-modal pore size distribution models are required to predict the unsaturated hydraulic conductivity of undisturbed soils. The various pedotransfer models gave K(h) curves that were above or below the reference inverse method. PTF1 (textural class), PTF2 (SSC%) and PTF3 (SSC%+BD) were clearly superior to the PTF4 model, which included θ_{330cm} (Fig. 3.6c). The poor fit of the PTF4 model is most likely due to underestimation of the field capacity of the soil, i.e. water content at a tension value of 330 cm was too dry to represent the actual field capacity of this soil.

The performances of the field, laboratory and theoretical approaches were examined statistically by comparing their results with the inverse method (Table 3.8). This analysis shows that the VGM model and IPM field method predicted the reference K(h) with lowest error.

Three of the four pedotransfer models also displayed good prediction accuracy, followed by the Bruce-Klute test. The Campbell and BCB models showed considerable deviation from the inverse K(h) results over the 0 to 100 cm range. Given the small amount of input data required for the VGM model and the pedotransfer functions, these methods would seem an acceptable substitute for the more laborious field IPM and inverse approaches.

Table 3.8 RMSE values of the different models of estimating K(h) as calculated by Eq. [3.16]

Depth (cm)	**Methods**								
	VGM	**BCB**	**Campbell**	**PTF1**	**PTF2**	**PTF3**	**PTF4**	**Bruce-Klute**	**IPM**
60	0.01	0.46	0.28	0.04	0.03	0.02	0.45	0.07	-
75	-	-	-	-	-	-	-	-	0.02

Despite the apparent suitability of the simpler K(h) methods, there remain two dilemmas when it comes to choosing the sensitivity of a wetting front detector. The first dilemma is the difficulty in choosing a value for field capacity. Figure 3.7 uses the HYDRUS model and the hydraulic parameters from the inverse data at 60 cm depth to show a time series of tension, water content and flux. Two days after the start of drainage at a depth of 30 cm the tension

was 50 cm, the absolute water content change 1.8% per day and the flux 0.02 cm/h. The corresponding values at 90 cm depth were 30 cm, 1.3% per day and 0.05 cm/h. Even four days after the start of the simulation, the drainage flux was 0.03 cm/h. These values show that none of the field capacity definitions had been reached.

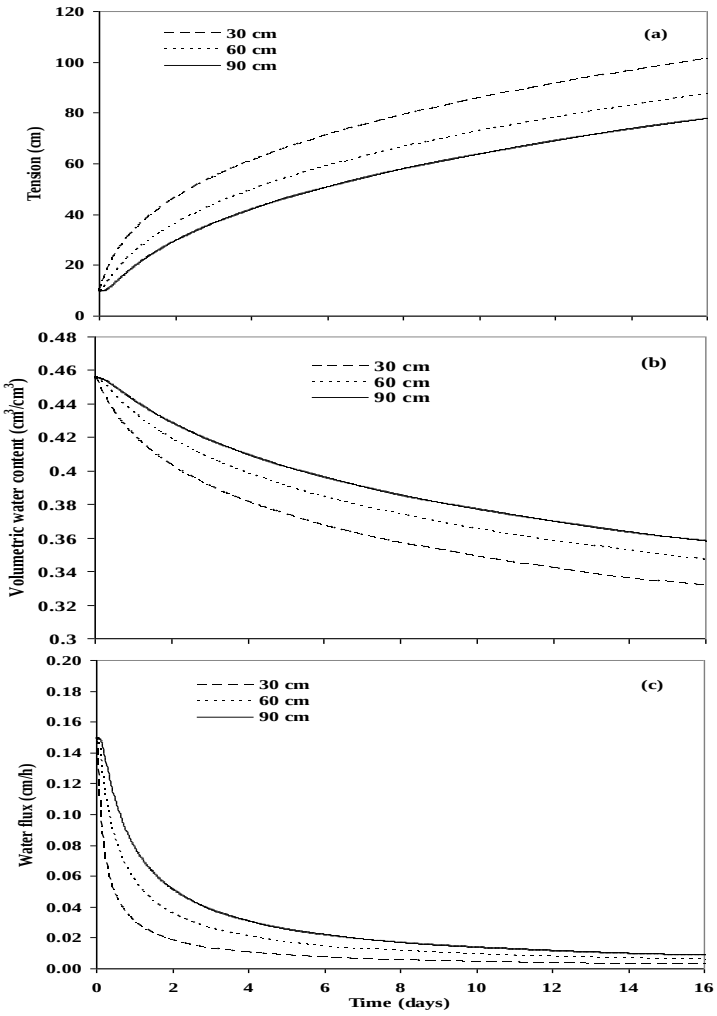

Figure 3.7 A time series of tension (a), water content (b) and water flux (c) at different observation nodes simulated using HYDRUS-1D model based on a uniform soil profile assumption described with soil parameters determined at 60 cm depth using inverse method.

The second dilemma relates to the large variability between the various K(h) estimation methods in the wet range (Table 3.9). Predicted hydraulic conductivity values are shown for the 30, 60 and 90 cm sensitivity level of wetting front detector used by Stirzaker *et al*. (2010). There is, for example, a coefficient of variability of 137% at a tension value of 30 cm. The point is further illustrated in Figure 3.8 where a two layer draining profile is simulated in the HYDRUS model using i) the field hydraulic properties derived from the inverse method ii)

the laboratory parameters derived using the van Genuchten approach and iii) default hydraulic properties from the HYDRUS model based on soil texture.

In this case the field and laboratory values show a four-fold higher simulated drainage than that obtained using the model default properties based on texture. This confirms other experimental observations reported by Reichardt *et al*. (1998), Jones and Wagnet (1984) and Fluhler *et al*. (1976). Even among methods that show low RMSE, there can be a large difference in conductivity at a given tension. This means that there will always be considerable uncertainty in specifying the minimum flux of water that could be detected by various designs of wetting front detector.

Table 3.9 Soil Hydraulic conductivities (K) at three pre-selected tensions estimated by the various methods for the 60 cm soil depth.

Method/Model	**Hydraulic conductivity (cm/h) at three tension values (cm)**		
	30	**60**	**90**
Field measurement			
Inverse	0.061	0.020	0.008
Lab measurements			
VGM	0.074	0.016	0.005
Campbell	0.485	0.065	0.020
BCB	1.197	0.034	0.001
Bruce-Klute	0.145	0.066	0.036
Pedotransfer			
PTF1	0.128	0.059	0.031
PTF2	0.012	0.004	0.002
PTF3	0.053	0.022	0.012
PTF4	0.322	0.050	0.014
SD (SE)	0.38(0.126)	0.02(0.008)	0.01(0.004)
CV (%)	137	62	87

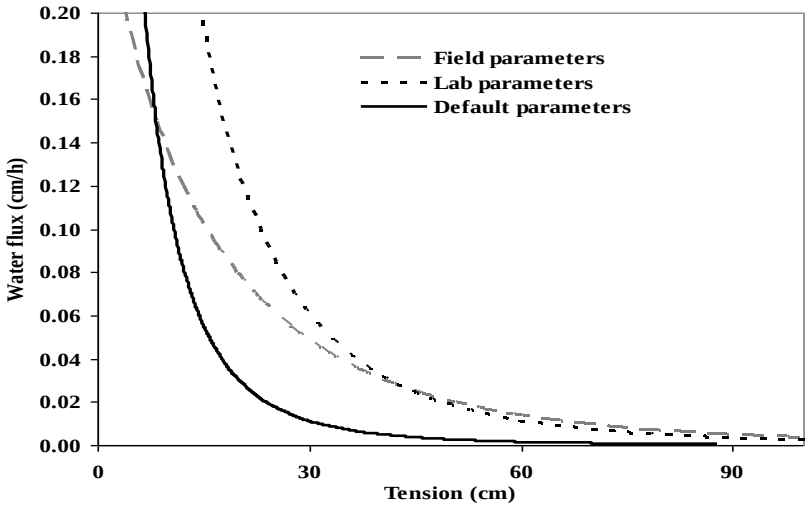

Figure 3.8 Water flux versus tension at 60 cm depth simulated using hydrus-1d model in a two-layered soil profile setting specified using soil parameters derived from field and laboratory measurements and default values.

3.4 CONCLUSIONS

Ideally a wetting front detector would be able to collect a water sample from a draining profile until field capacity was reached. In practice field capacity is hard to define. Ultimately the sensitivity of a wetting front detector depends on how it is going to be used. The less sensitive funnel shaped version used by Stirzaker and Hutchinson (2005) is suited to shallower placements and will record the early stages of redistribution. The Tube shaped designs used by Hutchinson and Bond (2001) and Stirzaker (2008), which record much lower fluxes, can be deployed deeper in the soil profile and would collect a water sample for many days after saturation.

The evaluation of different methods for determining unsaturated hydraulic conductivity was based on the assumption that the inverse analysis of the field drainage data provides a reference K(h) function. The VGM model and three of the pedotransfer models produced K(h) functions with an RMSE of less than 5% compared to the reference, and would appear to be simple methods of obtaining a reasonable estimate of unsaturated conductivity. However, the hydraulic conductivities estimated by the different methods were highly variable, particular at the wetter end of the tension range, so flux calculations are likely to contain large uncertainties.

CHAPTER 4

LABORATORY STUDIES ON HYDRAULIC PROPERTIES OF WICK MATERIALS

4.1 INTRODUCTION

A Tube wetting front detector (WFD) is a prototype designed to test the functionality of the instrument to aid in irrigation decisions using wetting front information at a set depth. This prototype is constructed using various components one of which is a wick material (Chapter 2). This material refers to a porous media filled in a Tube WFD prototype that draws water into the opening of the tube laterally by capillarity action and from above due to gravitational forces pulling on the soil water (Chapter 2).

This porous material must allow water to flow in and out of the tube to change the water level in the inner tube to attain an equilibrium condition quickly with the change in contact tension. Under equilibrium condition, the contact tension is determined by the height from a water level, which is the tension of the soil surrounding the tube. However, one of the problems with the use of wick for this purpose is a preferential flow mainly away from the Tube Detector due to differences in hydraulic properties between the wick material and the soil (Rimmer *et al*., 1995; Nichol *et al*., 2008). The illustration in Figure 4.1a shows the path flow water when the hydraulic conductivity of a wick material is higher than soil causing a slight decrease in contact tension that promotes water flow to the tube. If the hydraulic conductivity of a wick material is lower than the surrounding soil (Fig. 4.1b), however, water will move around the tube, which will potentially cause some irrigation water passing without activating a detector.

An equilibrium condition between water level in a tube and surrounding soil and a wick material that intercepts and diverts water to the tube quickly (Fig. 4.1a) are therefore the desirable criteria for the proper operation of the Tube Detector. These conditions can be achieved by designing the Tube Detector such that a wick material must have higher hydraulic conductivity than the soil (Fig. 4.1a) and must have high air entry potential or low specific yield (Fig. 4.2). Specific yield; S_y, can be defined as the change in the volume of stored water within a unit area per unit change in water level (Sumner, 2007).

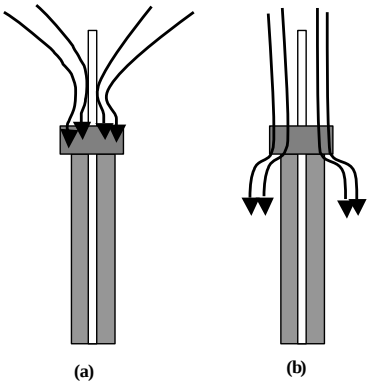

Figure 4.1 Schematic presentation of water flow paths in a Tube Detector when the K(h) of a wick material is higher than soil (a) and when the K(h) of the wick is lower than the soil (b).

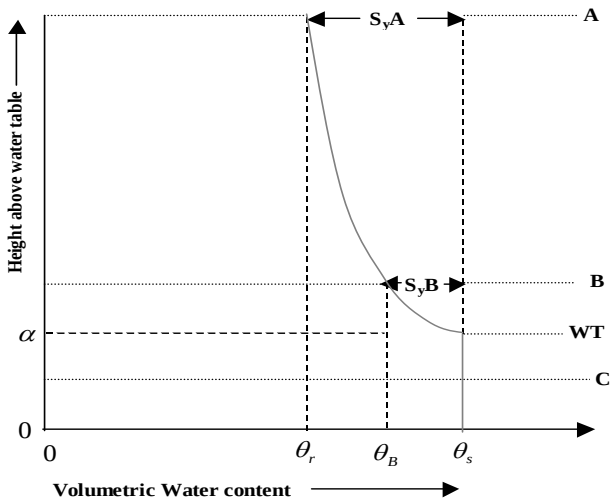

Figure 4.2 Equilibrium water content profiles above a water table with reference to soil surface positions A, B and C (taken from Sumner, 2007).

The water table depth determines the magnitude of the specific yield, which in turn depends on the water retention characteristics (Sumner, 2007). This condition can be illustrated using a generalized soil water profile at equilibrium above a water table in a homogenous soil (Fig. 4.2). Figure 4.2 shows soil tension increases and water content decreases with height above the water table under equilibrium condition. Water content remains constant at saturation from the water table to a height corresponding to the air entry potential (α), above which water content decreases asymptotetically with height above the water table to residual water content (Sumner, 2007). If the water table is deep (height from A to WT), causing large water content range corresponding to maximum storage capacity. Under this condition, the specific yield (**S$_y$A**) will be equal to the difference between water content at saturation and residual water content. On the other hand, if the water table is shallow (height from B to WT), the storage capacity and specific yield (**S$_y$B)** will be small. Finally, if the water table is at a depth

shallower than the air entry potential (soil surface at height C), there will be no change in water content with height due to a complete saturation condition producing zero specific yield (Fig. 4.2).

In this chapter, the specific yield described using equation 4.1 by Duke (1972) was combined with the van Genuchten (1980) soil water retention model shown in equation 4.2, and reproduced equation 4.3. This equation estimates the specific yield, S_y, from an experimentally measured water retention data with the assumption that it depends on the water table depth under an equilibrium condition (see Section 4.2.3, Fig. 4.4):

$$S_y(H) = \theta_s - \theta(H) \qquad (4.1)$$

$$\theta(H) = \theta_r + \frac{\theta_s - \theta_r}{\left(1 + (\alpha H)^n\right)^m} \qquad (4.2)$$

$$S_y(H) = (\theta_s - \theta_r) * \left(1 - \frac{1}{\left(1 + (\alpha H)^n\right)^m}\right) \qquad (4.3)$$

where θ is water content, θ_s is water content at saturation, θ_r is residual water content, α is air entry parameter, H is water table depth below soil surface, n is pore size distribution index, and m is fitting parameter.

Several silica sand and Diatomaceous earth materials were therefore tested to determine the hydraulic characteristics of each material. A suitable material for use in the proposed Tube prototypes with a maximum height of 90 cm can then be selected. In addition, these wick materials should allow rapid response of the water level to changes in tension. These materials must be also chemically inert, easy to install, and physically stable during and post installation. Some of the silica materials, such as silica flour, however, may be a risk to health and need appropriate handling or alternative material with similar hydraulic properties should be used (Nichol *et al*., 2008).

This chapter evaluates the measurements of hydraulic properties of five potential wick materials: Diatomaceous Earth (DE), D36-sand (Fine sand), Sand1, Sand2 and Sand3. Particle Size Distribution (PSD) and hydraulic characteristics of each material were determined to ensure rigorous selection of desirable wick characteristics.

The objectives of this chapter are therefore (1) to select a wick material with a high-unsaturated hydraulic conductivity; (2) to select a wick material that has a negligible specific yield over the tension range between 0 and 100 cm; (3) to identify cheap and accessible wick material; and (4) to interpret results obtained for the various wick materials with respect to the different lengths of Tube WFD.

The methods described previously in Chapter 3, including sample preparation (Section 3.2.1.2), the determination of water retention characteristics (Section 3.2.1.3), saturated hydraulic conductivity (Section 3.2.1.4) and Bruce-Klute measurement methods (Section 3.2.1.6), as well as the various methods of data analyses described in Sections 3.2.2.3 and 3.2.2.4, were used to determine and describe the hydraulic properties of wick materials.

4.2 ANALYSIS OF RESULT AND DISCUSSIONS

4.2.1 Particle size distribution (PSD)

The distribution of sand particle size affects total porosity as well as the shape of water retention curve of a porous material. Particle size distribution (PSD) analyses presented in Table 4.1 reveals all sand materials to have a predominantly sand fraction (> 76%). The textural classes for each of the materials shown in the type column of Table 4.1 are indicated in brackets.

Table 4.1 Particle size distributions of wick materials of all sizes (µm).

Type	Sand (%)				Silt (%)	Clay (%)
	Coarse 500-1000	**Medium 250-500**	**Fine 125-250**	**Very fine 50-125**	**2-50**	**< 2**
DE[2] (Sand)	99.70				0.10	-
DE[1] (Silty loam)	36.20				50.00	12.50
Fine sand* (Sand)	0.03	0.17	29.25	62.00	8.55	-
Sand1* (Loamy sand)	0.00	0.51	45.55	30.61	23.33	-
Sand2* (Sand)	1.33	7.23	66.51	19.82	5.11	-
Sand3* (Loamy sand)	0.00	0.84	61.43	17.60	20.13	-

[2] Particle size analysis taken (Bigelow *et al*., 2004), [1] UP Soil Science Lab results (hydrometer method), *Sieve method.

The PSD for DE determined at the UP Soil Science Lab was different from the one reported by Bigelow *et al.* (2004) in that 99.7% of the material was within the sand particle range (50-1000 µm). This suggests that the material from Bigelow *et al.* (2004) will have a lower air entry potential, steeper water retention and a steeper unsaturated hydraulic conductivity characteristic compared to the DE material used for this study. This also suggests that the DE material varies from place to place.

4.2.2 Water retention characteristics

A Tube detector requires a wick material that has negligible change in water content over the operating range of its length so that a quick response in water level to changes in contact tension could be maintained. This enables establishing a linear hydrostatic pressure profile within the Tube detector.

The measured water contents are plotted against the tension ranges between 0 and100 cm to establish the soil water retention characteristics curves that have special significance to the Tube Detector prototypes (Fig. 4.3).

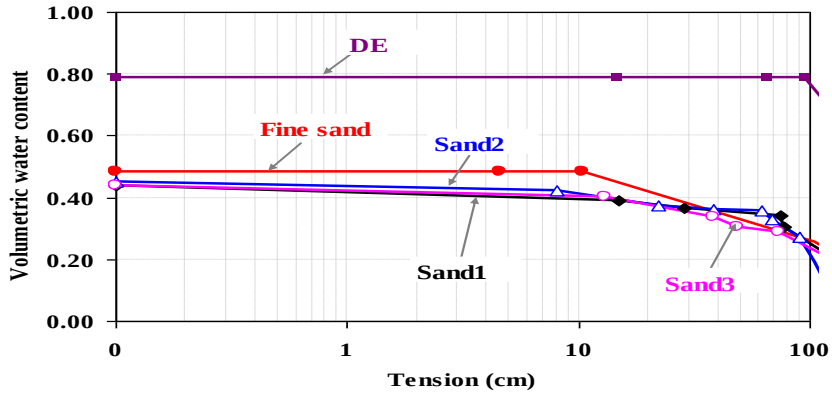

Figure 4.3 Measured water retention characteristics for all tested wick materials.

The air entry potential of DE exceeds 100 cm while the other materials, dominated by the sand fractions, have low air entry potentials (~10 cm). The DE material has the highest volumetric water content at saturation with little change in water content within the operating range of the prototypes (< 100 cm tension). On the other hand, all the sand type materials start to de-saturate under tensions far less than the lengths of each of the Tube Detectors (45-, 60- and 90-cm). This would mean a change in the unsaturated hydraulic conductivity of wick materials and require a larger volume of water to cause a unit change in the wick tension and associated water level in a tube. Therefore, these sands are likely to take a longer time to

respond than DE when experiencing de-saturation within the operating range of each tube length used for this study.

4.2.3 Specific yield

The calculated specific yields based on the water table depth for all the tested wick materials are shown (Fig. 4.4).

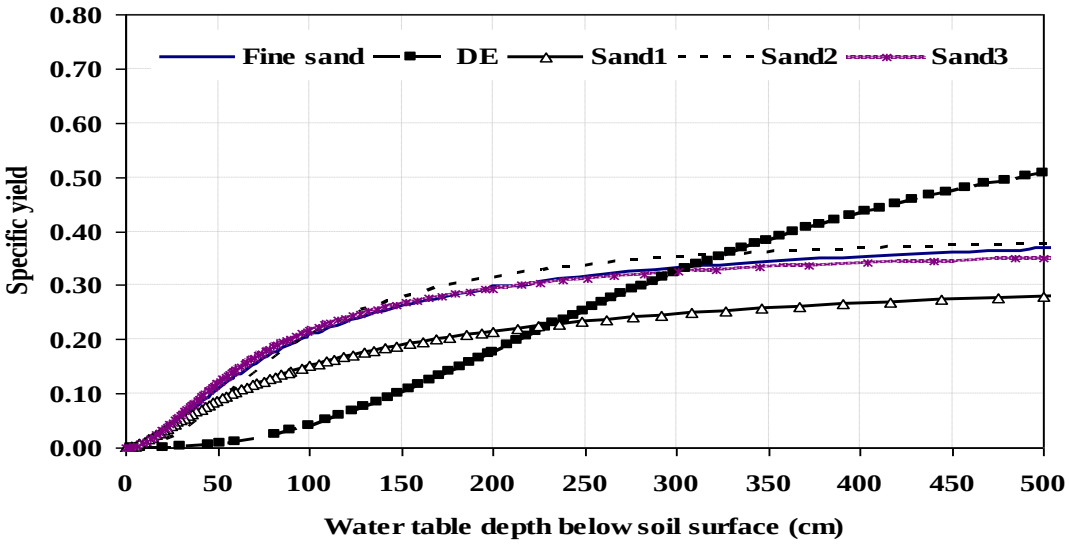

Figure 4.4 Specific yields for the tested wick materials dependent on water table depth.

The computed specific yield in most of the tested wick materials showed (Fig. 4.4) typically approach zero in the near saturation zone (soil surface at or below the water table) and increase rapidly to a maximum as water drains out such that the water content at the soil surface approaches residual water content (not shown on the scale). Table 4.2 shows the computed specific yields at pre-selected water table depths below the soil surface 45-, 60-, 90-, 100-, 200- and 500-cm for all the tested wick materials.

Table 4.2 Computed specific yields at pre-selected water table depths

Water table depth (cm)	Specific yields				
	DE	Fine sand	Sand1	Sand2	Sand3
45	0.006	0.098	0.079	0.071	0.105
60	0.012	0.136	0.103	0.114	0.144
90	0.032	0.195	0.141	0.190	0.202
100	0.042	0.210	0.151	0.210	0.216
200	0.177	0.298	0.214	0.316	0.294
500	0.507	0.370	0.280	0.378	0.351

For water table depth at 100 cm, the specific yield according to increasing in size are DE (0.042), Sand1 (0.151), (Sand2 = Fine sand = 0.210) and Sand3 = 0.216. Large specific yields within the operating range of Tube Detectors in Samd2, Sand3 and Fine sand shows that more liquid water is required to cause a unit change in the hydrostatic pressure (Table 4.2). In the DE material, the specific yield within the medium is almost negligible and the desirable linear hydrostatic pressure profile could be established for water table depths < 100 cm (Fig. 4.4). However, the specific yield of DE is the largest of all tested wick materials at 500 cm height from a water table as a result requiring the largest volume of water to cause a unit change in water table depth (Fig. 4.4).

4.2.4 Response time of wick materials

The equilibrium soil tension profiles were evaluated for the tested wick materials by plotting the tension at each equilibrium point as a function of drainage time obtained from the multi-step controlled outflow method. This relationship estimates the time required for a wick material to drain to an equilibration state following an incremental change in an applied pressure (Fig. 4.5). The results in Figure 4.5 indicate that all wick materials except Sand3 took less than 140 minutes to reach a new equilibrium state to a step change in applied pressure.

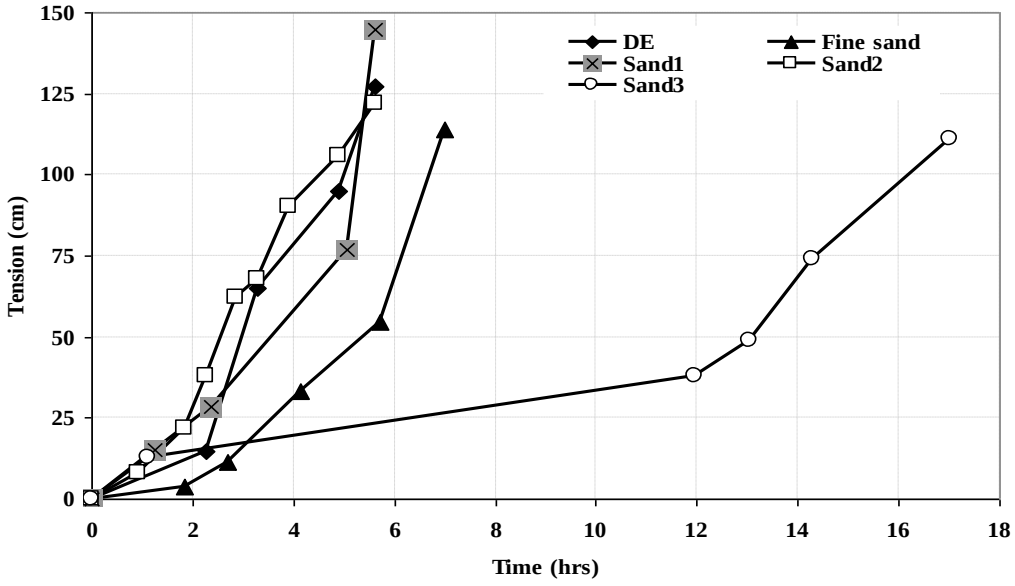

Figure 4.5 Equilibrium tension profile and drainage time data derived from the multi-step controlled outflow cells for the tested wick materials.

The time required for a wick material to reach a new equilibrium state within the 100 cm tension was generally quick (DE, Sand1, Sand2 and Fine sand) compared to Sand3. The quick re-equilibrium time in the first four wick materials for tensions lower than 100 cm supports an assumption of a rapid equilibrium tension profile in these wick materials (Fig. 4.5). The re-equilibrium state in Sand3, however, was relatively slower to a step change in pressure when compared to the other tested wick materials due to the hydraulic conductivity of the material limiting the rate of water transfer into the ceramic plate.

In general, the time required to reach a new equilibrium in these tested wick materials depends on the hydraulic properties of the wick and ceramic plate used during the test. In this specific test (Fig. 4.5), it was observed that the type of wick material determines the length of time response to a step change in an applied pressure. With the view of the general complexity in field conditions, it is suggested to estimate an *in-situ* response time of each wick material.

4.2.5 Unsaturated hydraulic conductivity

A wick material that has higher hydraulic conductivity than the soil over the operating range of the Tube detector (0 to100 cm tension) causes a decrease in the contact tension that promotes water to be drawn to the opening of the Tube WFD.

In this section, the van Genuchten-Mualem (VGM) pore size distribution model (Eq. 3.2) was used to predict the K(h) curve following the recommendation (Chapter 3) i.e., the VGM model can be used as a reasonable substitute to an inverse method of estimating K(h) function. This predictive model requires measured saturated hydraulic conductivity (K_s) and water retention parameters (Table 4.3) derived by fitting the van Genucthen analytical equation (1980) to the measured water retention data.

This equation was fitted to the measured data manually (Fig. 4.6). Table 4.3 shows fitting parameters, goodness of fit (R^2) between measured and fitted variables and physical properties of the wick materials. The predicted water retention curves presented (Fig. 4.6) fit closely to the measured data ($R^2 > 0.90$). This suggests that the water retention parameters determined by a manual fitting technique could adequately estimate the hydraulic conductivity functions of each wick material.

There is little change in hydraulic conductivity between tensions 0 and 10 cm for Fine sand, Sand1 and Sand3 and becomes steeper with increasing tensions (Fig. 4.7). This means with increasing tension, water content and hydraulic conductivity of the wick materials decrease requiring more water volume to fill the pores in the contact and wick material to cause a unit change in water table in the tube.

Table 4.3 Wick physical properties and model parameters

Type	Physical property		Retention parameters				Regression
	K_s (cm/h)	ρ gcm^{-3}	θ_s	θ_r	$\alpha(cm^{-1})$	n	R^2
DE	3.81	0.471	0.79	0.045	0.004	2.51	0.99
Fine sand	22.86	1.371	0.48	0.045	0.019	1.84	0.98
Sand1	0.67	1.466	0.44	0.045	0.021	1.52	0.97
Sand2	21.39	1.453	0.45	0.045	0.015	2.34	0.92
Sand3	1.10	1.484	0.44	0.045	0.021	1.93	0.98

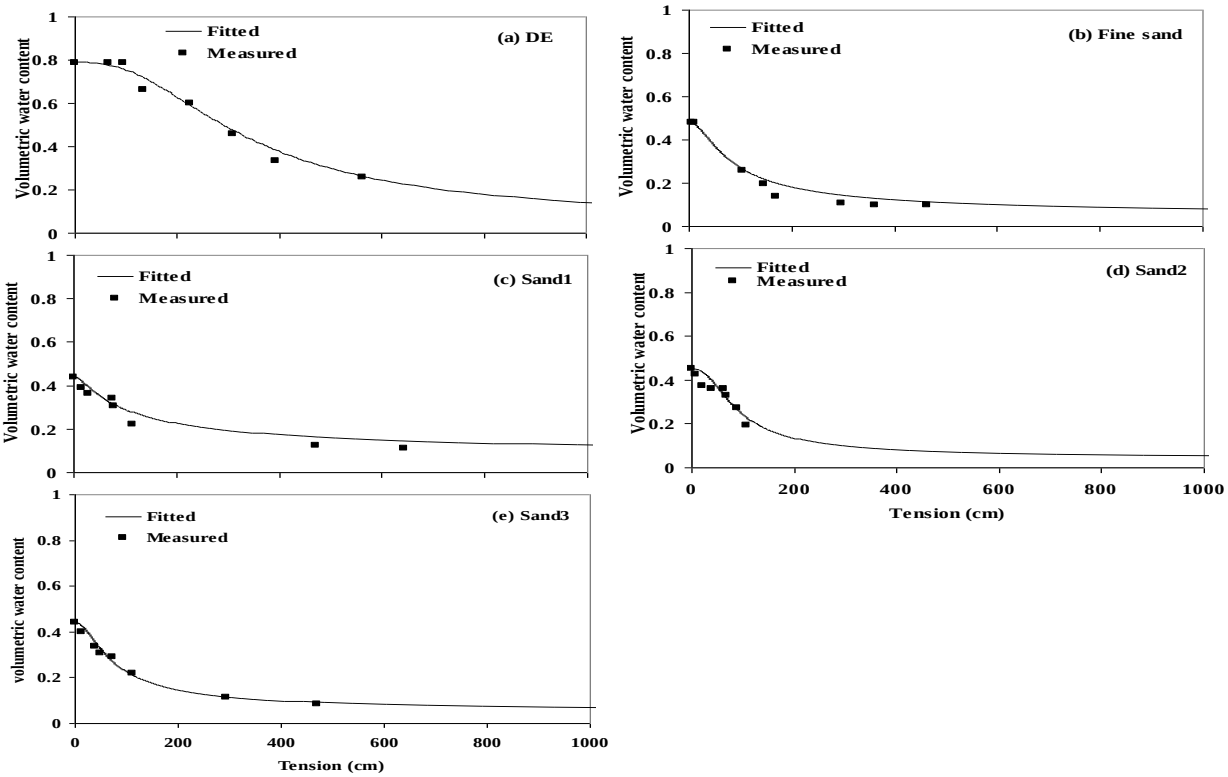

Figure 4.6 Measured retention data (symbols) and corresponding best-fit van Genuchten model (lines) for each of the five wick materials.

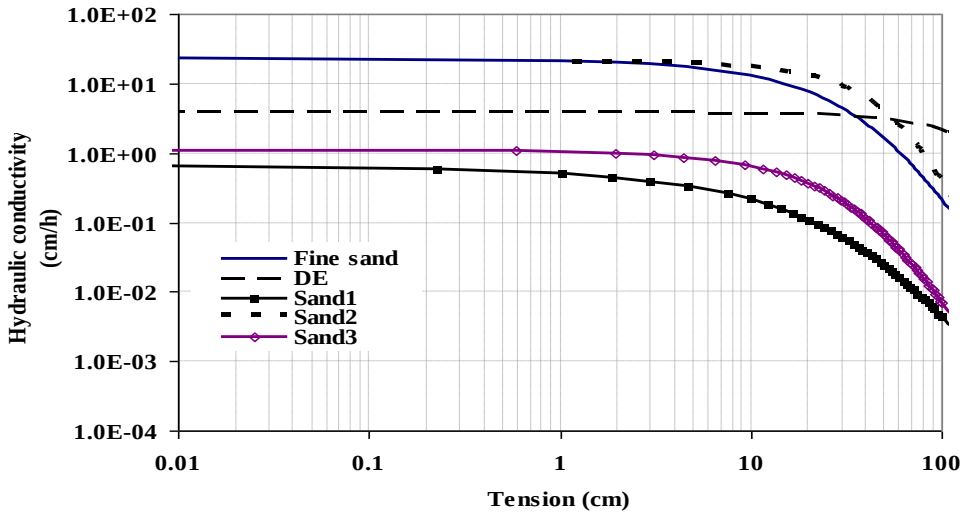

Figure 4.7 Predicted hydraulic conductivity curves for the tested wick materials.

Moreover, the hydraulic conductivity of a wick material could be lower than the soil violating the assumption of an equilibrium state within the tube under which the Tube Detector operates. There is a gentle decrease in hydraulic conductivity (K) in Sand2 for tensions lower than 50 cm but has the highest K of all tested wick materials within this narrow tension range.

The DE material conducts water at its saturation value between 0 and 100 cm tension range (Fig. 4.7). This implies that DE will maintain the equilibrium state within the Tube detector range provided that its conductivity remains higher than the surrounding soil (Section 4.2.6).

4.2.6 Use of Hydraulic Properties in the Application of the Tube Detector

The water retention and hydraulic conductivity functions of wick materials could be used in a Tube WFD:

4.2.6.1 *Determine the maximum height of the Tube Detector*

The tension at which the hydraulic conductivity of a wick material crosses the soil infiltration rate determines the height of the Tube detector. This means at the point of intersection, the slope of pressure head distribution will become zero and hence water flows only under gravity. When the hydraulic conductivity of a wick material is higher than infiltration rate, it causes water to flow to the tube thereby maintains the tube functional. If the hydraulic conductivity of a wick material becomes lower than the infiltration rate, it causes the water to

flow around the Tube detector lowering the performance of the design, i.e., the design will no longer function as expected.

The concept of maximum tube height determination is illustrated using Fig. 4.8. This maximum height of the design will enable the collection of most of the infiltrating water, provided that there is no flow divergence problem. Figure 4.8 was compiled using eight hydraulic conductivity functions representing six of the USDA textural classes and two hydraulic conductivities of the wick materials, i.e. DE and Fine sand. The soil parameters for the six textural classes were obtained from the soil catalogue section of the HYDRUS-1D model.

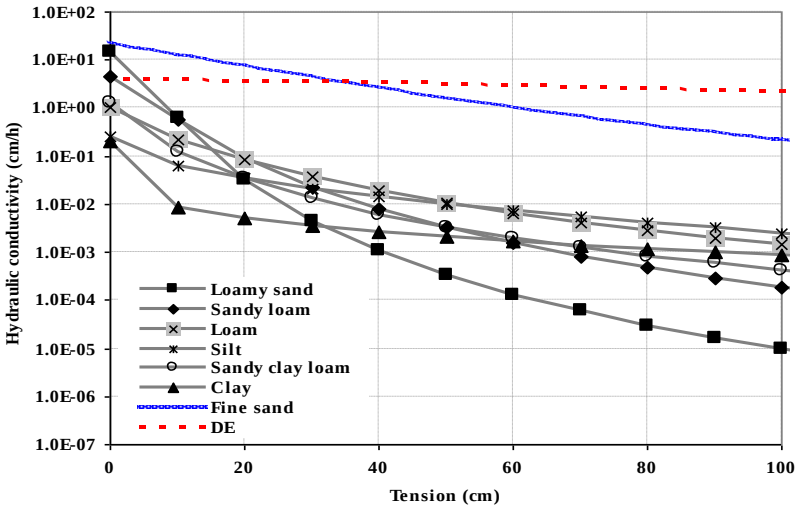

Figure 4.8 The hydraulic conductivity characteristics of Fine sand and DE with respect to the hydraulic conductivities of six textural classes determined from the soil catalogue in HYDRUS-1D model.

In Figure 4.8, a Tube Detector might fail to operate at tensions lower than 5 cm when the hydraulic conductivity of DE crosses that of loamy sand soil, otherwise both wick materials seem to operate well in most of these soils.

4.2.6.2 *Select a wick material with a rapid response time*

The time response characteristic of a wick material has a practical significance in selecting a material that responds rapidly to the soil water pressure change under field conditions (Fig. 4.9).

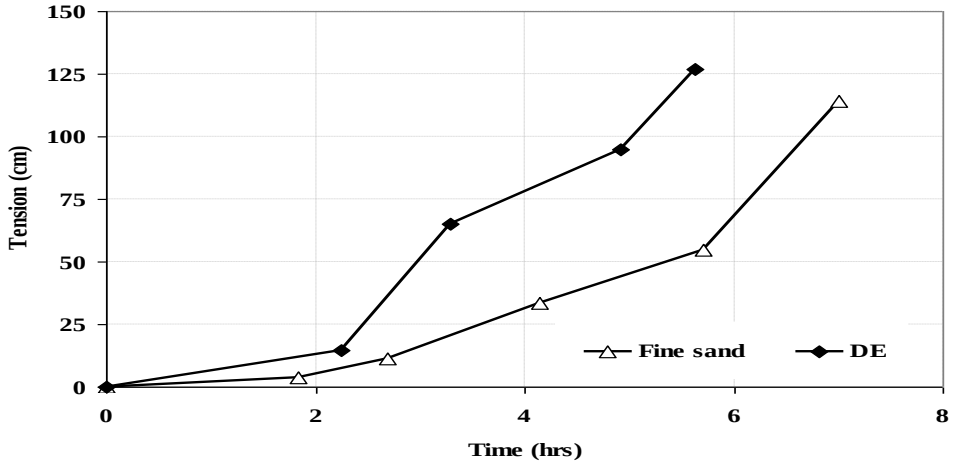

Figure 4.9 Time response characteristics of Fine sand and DE (taken from drainage-time curve of the outflow data).

This Figure was derived in the same way as in Figure 4.5 (Section 4.2.4). In Figure 4.9, it is noted that DE takes shorter duration than Fine sand in establishing an equilibrium condition for a given change in tension.

4.2.6.3 *Select a material that validates the assumption of equilibrium state*

A wick material with a zero specific yield within the operating range of the Tube Detector requires less water volume than with those with large specific yield to cause a unit change in the water table. The size of specific yield therefore determines how quickly the level of water in the tube changes to a unit change in tension surrounding the tube thereby maintains an equilibrium state (Section 4.2.3).

4.3 CONCLUSIONS

The unsaturated hydraulic conductivity K(h) of all tested wick materials were predicted using VGM predictive model that make use of water retention parameters and measured K_s. The K(h) of the two wick materials (Fine sand and DE) was overlaid with the K(h) functions of six USDA soil textural classes. The result indicated that Tube Detector < 100 cm in length filled with any of the two wick materials can operate well in most of these soils, i.e. the hydraulic conductivities in wicks are higher than infiltration rates, which is one of the desirable criteria to maintain an equilibrium state within the Tube Detector.

The data from the laboratory measurements of soil water retention characteristics indicate that the sand dominated wick materials have lower air entry potential than DE material. DE

shows little change in volumetric water content over the full tension range (0 to 100 cm). In the sand dominated wicks, however, de-saturation starts for tensions higher than 10 cm. The specific yield derived using a quantitative description that relates the measured water retention data to water table depth has also indicated that DE has the lowest specific yield within the operating range of the Tube Detector. Both the water retention curve and specific yield therefore showed that DE is the best candidate from the other tested wick materials in responding rapidly to changes in soil infiltration fluxes (requires least volume of water per unit change in water level or soil tension).

The response time for DE filled in a 100 cm tube length will not be affected because the material shows no volumetric water content change at least over this length. But in the other tested materials, the response time is likely to increase for higher tensions as the materials undergo de-saturation.

The DE and Fine sand materials are locally available. These materials need no special treatment or calibration and are to be easy to handle and cheap for the intended use.

CHAPTER 5

EMPIRICAL CHARACTERISTICS OF THE WICK MATERIALS

A wick material is a porous medium filled in a Tube Detector used to intercept and divert water into the opening of the tube, which creates a water table inside the inner tube. The wick material is placed in the open space between the outer and inner tube of the Tube Detector. A contact material is the same in texture and type as the wick material but is added above the open end of the outer tube to provide hydraulic contact between the wick in the tube and the surrounding soil (or air when exposed to the atmosphere, such as in the laboratory experiments described below). Tension in the contact material is hereafter called contact tension.

In this chapter, two types of wick material, (namely Diatomaceous Earth (DE) and D36-sand (Fine sand)) recommended from Chapter 4 were investigated empirically to evaluate the following hypotheses:

1) The contact tension is inversely related to the water level in the inner tube for tensions between zero and a tension equal to the length of the outer tube.

As a corollary to the above hypothesis, the following two inferences could be made:

2) When the contact tension (cm) is close to zero, the inner tube will be completely filled with water.

3) When the contact tension (cm) in the contact material is equal to the height of the outer tube, the inner tube will be empty.

5.1 INTRODUCTION

The loss of water from a wet contact wick material into the air is analogous to the process of evaporation of water from the soil. The process of drying in air occurs as liquid water is converted into water vapour and transported into the atmosphere (Saravanapavan and Salvucci, 2000). The rate of drying is influenced by atmospheric factors (wind speed, radiation, temperature gradient, air turbulence and vapour pressure) and soil physical characteristics such as texture (Qiu *et al*., 1998; Yanful and Mousavi, 2003).

The drying process following wetting occurs in three stages (Hillel, 1980). Initially water is lost from a wet soil at a rate determined by the atmospheric conditions until a threshold value of tension at the soil surface is reached (Ritchie, 1972). In the second stage, the evaporation rate falls progressively below the atmospheric potential because the hydraulic conductivity of the soil becomes the limiting factor to water movement (Aydin *et al*., 2005). In the third stage, a few centimeters of soil at the surface approach air dryness and water must diffuse as vapour through the dry layer, at which point the loss of water is exceedingly slow (Hillel, 1980).

Consider the example of the contact material exposed to the air on one side and the saturated wick material in the vertical tube on the other. Upward capillary movement of water from the saturated wick provides water to the evaporating surface of the contact material. As water leaves the wick material, its tension increases while its conductivity decreases. If the conductivity falls below the rate needed to satisfy the atmospheric conditions, the wick material enters the second stage evaporation.

It is important to choose a wick material that supplies water to the evaporating surface of the contact material at the rate of drying (the hydraulic conductivity of a wick material must not be a limiting factor), i.e. stays in the first stage of evaporation. This must occur over the range of tensions as defined by the length of the tube. This characteristic enables the detector to establish a hydraulic equilibrium between the evaporating surface of a wick material and the water level in the inner tube. A wick material that fulfils this desirable characteristic will ensure acceptance of the above-mentioned three hypotheses.

5.2 MATERIALS AND METHODS

This test was subdivided into two categories: one set of the Tube Detectors were filled with wick materials, wetted to saturation and subjected to the air for drying to take place. Another set of tube were filled with the same wick materials, buried 15 cm below the soil surface, irrigated and subjected to capillary emptying by the surrounding soil.

For the first test in air there were two different surface area sizes of contact material exposed to air-drying. This allowed investigating the effect of increasing or decreasing surface area on the inverse relationship between water level in a tube and a contact tension.

5.2.1 Tube Detector: Indoor wick drying test

The open space between two concentric tube of each of the two 90 cm long Tube Detectors were packed with Diatomaceous Earth (DE) to a density (ρ_b) of 0.433 g cm^{-3} (Fig. 5.1a and b).

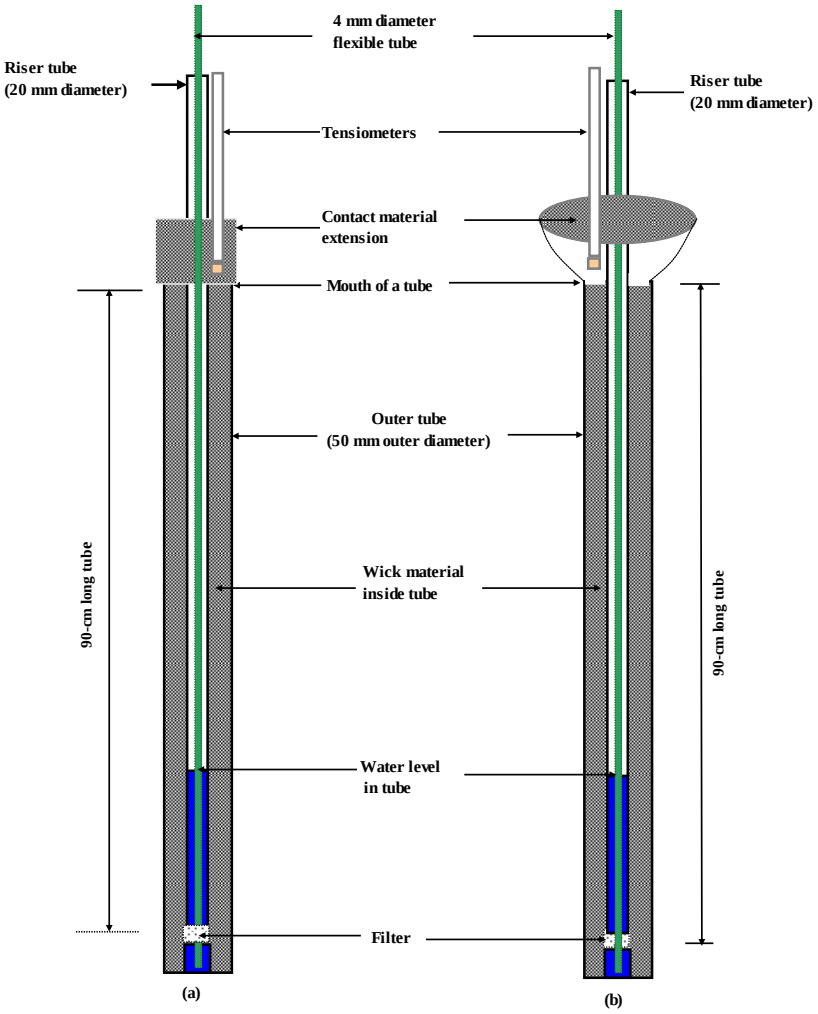

Figure 5.1 A schematic presentation of Tube Detectors with exposed contact material surface areas of 16.5 cm^2 (a) and 310.9 cm^2 (b) placed on the opening of the tube, with a saturated column of wick and contact material, and subjected to drying by the air.

In the first Tube Detector (Fig. 5.1a), an extra 5 cm height of DE was placed on top of the outer ring to simulate the contact material that would interface with the soil. The area of the contact material exposed to the drying air was 16.5 cm^2 (area of the outer tube with internal diameter of 44 mm minus the area of inner tube with an outer diameter of 20 mm). The

second tube had a funnel placed on top, 10 cm high and 20 cm in diameter, giving a surface area of 310.9 cm^2 that was exposed to the drying air (Fig. 5.1b).

A second pair of 90 cm long Tube Detectors with contact material of exposed surface areas (16.5 or 310.9 cm^2) were setup, but this time they were filled with a fine sand and packed to a density (ρ_b) of 1.32 g cm^{-3}. In both wick types, the aim of placing a contact material with a large exposed surface area was to increase the rate of drying, which would cause the wick material to enter second stage evaporation at a tension closer to zero.

A tensiometer (ceramic cup of 4.8 cm length and 1.8 cm outside diameter) was placed with the ceramic cup in the contact material. Water was applied to the inner tube, which then flowed into the outer tube through a 100 micron nylon mesh at about 3 cm from the base of the tube. A process of upward infiltration wetted the wick material in the outer tube, which avoided the problem of entrapped or dissolved air. Water was continually added until the level in the inner tube remained full, indicating that the wick material was saturated and the tensiometer in the contact material remained near zero for several days.

Following saturation for several days, the wick and contact material were allowed to dry out. The contact tension and water volume inside the inner tube were measured on a daily basis until the water volume in the inner tube read zero. The tensiometers were read using a hand-held electronic vacuum gauge (SoilSpec Tensiometer System, Model SST101G, NH & TS Electronics, Australia). This gauge pierces through a rubber septum sealing a tensiometer tube with a hypodermic needle itself connected to a pressure transducer and periodically reads the tensiometer with a precision of ± 1 cm. The water level in the inner tube was measured in the same way as described in Section 2.2.1.1. After each water volume measurements, the water was replaced back to the inner tube.

5.2.2 Tube Detector: Buried in the soil

Four Tube Detectors, each 90-cm-long, were installed 15 cm below the soil surface in a sandy loam soil. Two of the detectors were filled with DE (ρ_b = 0.433 g cm^{-3}) and the other two filled with fine sand (ρ_b = 1.32 g cm^{-3}). The soil-wick contact area for each of the tube was 16.5 cm^2. Only the 5 cm high wick material on top of the open end of the tube was in contact with the surrounding soil, while the bottom and vertical sides of each tube had impermeable boundaries (Fig. 5.2).

Tensiometers were placed in the contact material of each Tube Detector to measure contact tension. Manual tension measurements were made as described above in Section 5.2.1. Automated tensiometers with a cup size similar to those described in Section 5.2.1 were fitted with pressure transducers and were connected to a HOBO logger (Onset Computer Corporation, MA02532, USA) to record the change in tension in every 15 minutes with a precision of ± 1 cm.

The soil containing the tensiometers and Tube Detectors was irrigated to saturation. Following irrigation, contact tension at the soil-wick interface and water level inside the inner tube were monitored. The water level inside the inner tube was measured as discussed in Section 2.2.1.1.

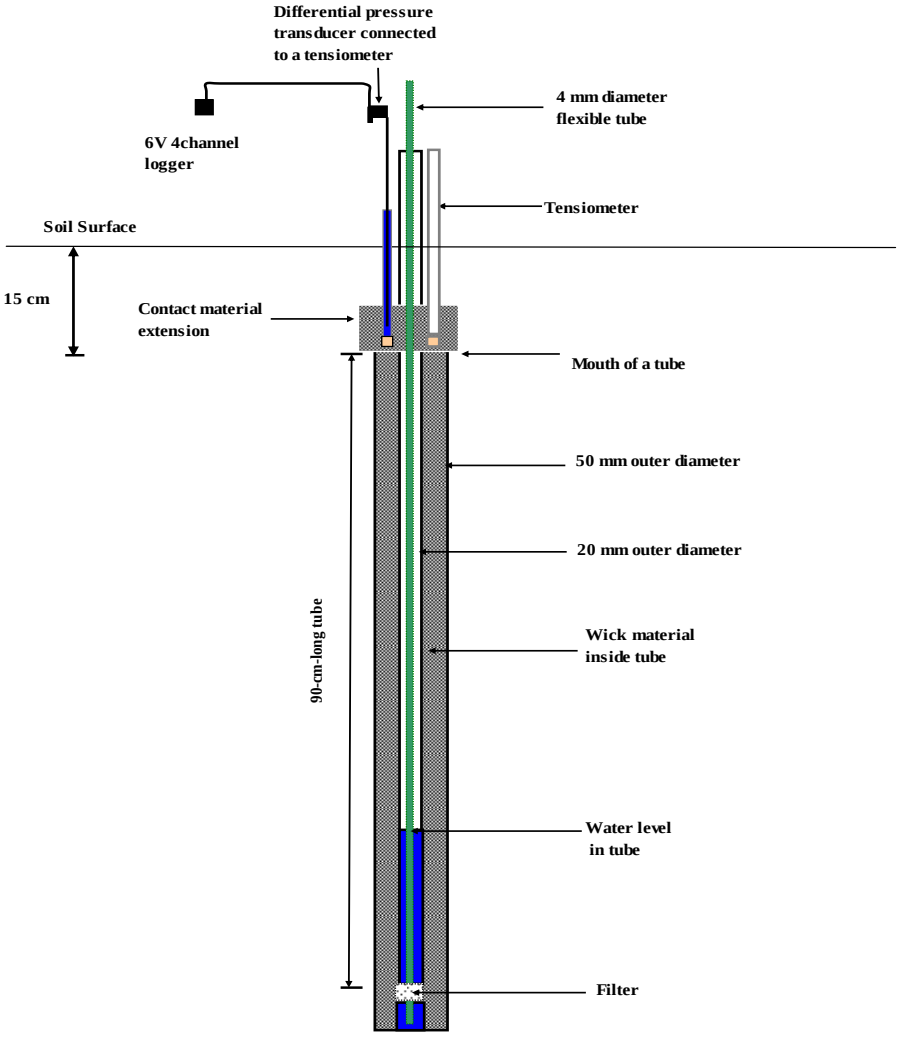

Figure 5.2 A 90 cm long Tube Detector filled with wick material, buried 15 cm below the soil surface, irrigated and subjected to drying.

5.3 RESULT AND DISCUSSIONS

5.3.1 Tube Detector: Indoor wick drying test

5.3.1.1 *Water level in a tube and contact tension*

The water level in a tube as a function of contact tension for the fine sand and DE filled Tube Detectors with two different exposed surface areas for each of these wick types are shown in Figure 5.3.

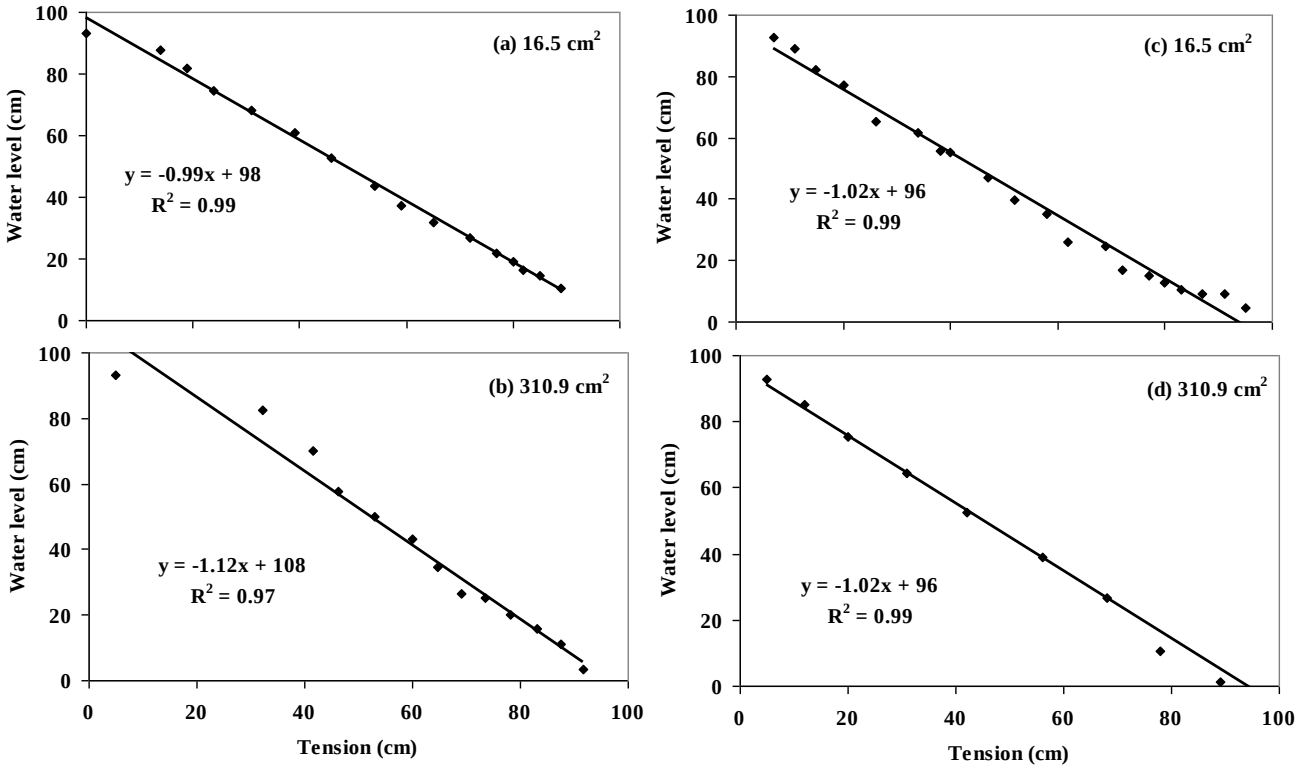

Figure 5.3 Water level in a Tube Detector as a function of contact tension for fine sand (a and b) and DE (c and d).

This result should answer the first hypothesis, i.e. between zero tension and a tension equal to the length of the outer tube, the contact tension is inversely related to the water level in the tube assuming the base of the outer tube to be the reference elevation. To accept this hypothesis, the slope of the regression line between contact tension and water level in the tube should be close to one with high coefficient of regression ($R^2 \approx 1$) under equilibrium conditions, while the y intercept reading should be equal to the length of the tube. The R^2 values indicated in Figure 5.3 are greater than 0.96 and the slopes ranged from -1.12 to -0.99.

These values generally indicate good correlation, i.e. the contact tension is inverse to the water level in the inner tube during both slow (16.5 cm^2) and fast (310.9 cm^2) surface areas drying. This confirms the hydrostatic equilibrium conditions, which reflects an inverse relationship between the water level in the inner tube and contact tension, and therefore hypothesis (1), can be accepted for both wick materials.

The intercepts of the regression functions (Fig. 5.3) indicate the maximum tension (cm) in the contact material when the water level in the tube is nearly emptied. The intercept value should therefore be equal to the length of the tube filled with wick material. Based on the regression lines (Fig. 5.3), the tension offsets between the intercept values and physical length of the wick (93 cm) were on average 3.0 cm for DE and 10.0 cm for fine sand filled tube. Considering the accuracy of tension measurement due to gauge and gauging errors, the tension offsets obtained in these Tube Detectors are small. These tension offsets observed in both wick types are generally low suggesting that a Tube Detector can be used as a tensiometer, which supports hypothesis (1), i.e. the intercept should equal the length of the outer tube.

5.3.1.2 *Contact tension and water level as a function of time*

This test investigated to what extent the wick type and size of the contact materials (i.e. speed of drying) affects the change in contact tension and water level drawdown over time using the same set-ups (Section 5.2.1). This investigation will determine if the two inferences made as the result of accepting hypothesis (1) are true, i.e. when the contact tension (cm) is close to zero, the inner tube will be completely filled with water hypothesis (2) and when the contact tension (cm) in the contact material is equal to the height of the outer tube filled with a wick material, the inner tube will be empty hypothesis (3).

The changes in contact tension and water level drawdown over time as a function of wick type and exposed contact surface area are presented (Fig. 5.4). In both wick types, the contact tensions increased while the water levels dropped continuously until it nearly emptied the tube and contact tensions were equal to the length of the outer tube.

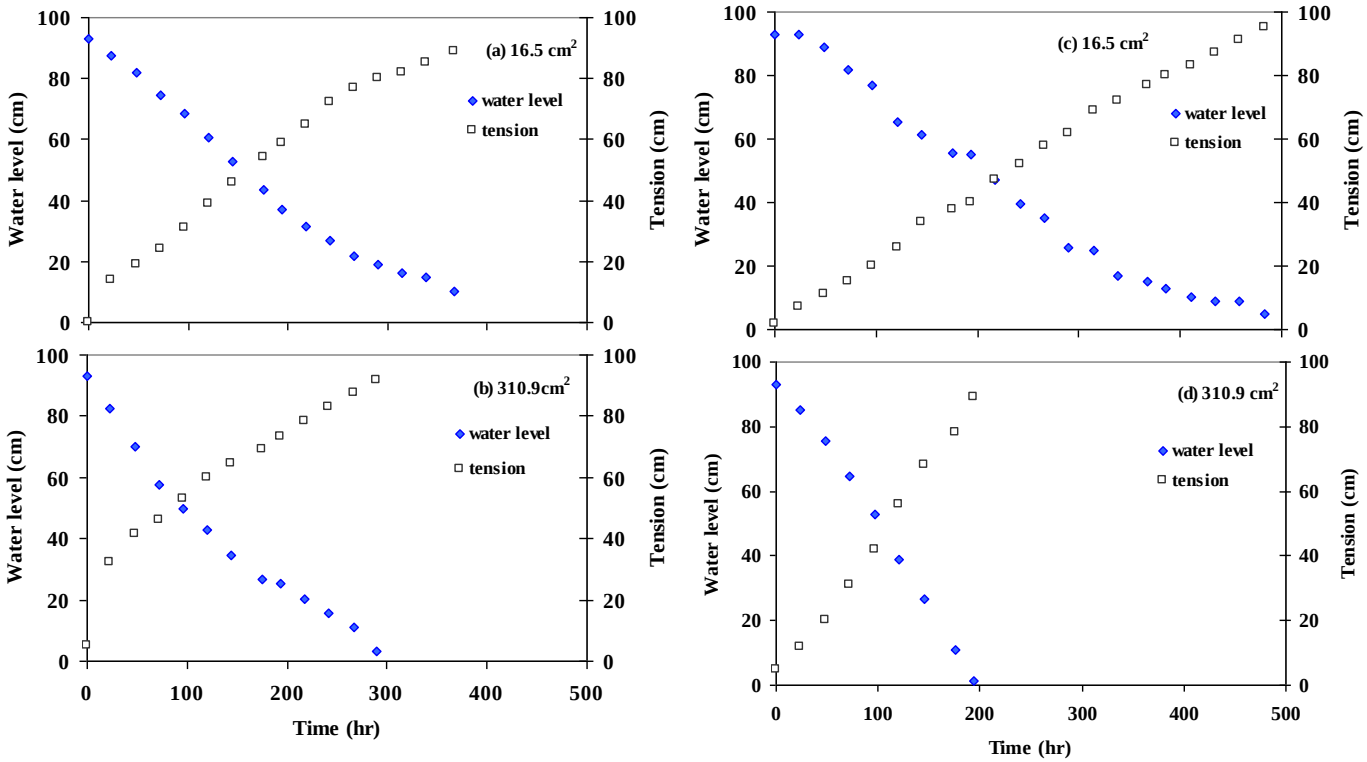

Figure 5.4 Contact tension and water level drawdown as a function of drying time for fine sand (a and b) and DE (c and d).

At the start of the drying process, the tension values corresponding to the full water level in the inner tube were 0 cm (Fig. 5.4a) and 5 cm (Fig. 5.4b) for fine sand filled Tube Detectors; and 2 cm (Fig. 5.4c) and 5 cm (Fig. 5.4d) for DE filled Tube Detectors. These initial tension values shown in each of the graphs (Fig. 5.4) have closely estimated the saturation values of the contact materials. This supports the first inference that the contact tension (cm) is close to zero when the inner tube is completely filled with water (Hypothesis 2).

The contact tension readings corresponding to the nearly empty water level in the inner tube were 89 cm (Fig. 5.4a) and 92 cm (Fig. 5.4b) in the fine sand filled Tube Detectors and 95 cm (Fig. 5.4c) and 89 cm (Fig. 5.4d) in the DE filled Tube Detectors. Therefore, these tensions have approximated the length of Tube Detector used for this study well (Fig. 5.4). This confirms the second inference, which states that the contact tension (cm) is equal to the height of the tube (cm) (Hypothesis 3).

The patterns of tensions over time have indicated that the contact materials with small exposed surface areas (Figs. 5.4a and c) took longer time to reach a tension value equivalent to the height of the tube than the contact materials with large exposed surface areas (Figs.

5.4b and d). In other words, Tube Detectors with large exposed surface areas of wick extensions (310.9 cm^2) were relatively quicker in establishing nearly constant tension values (equal to the height of Tube Detector) than those with small exposed surface areas (16.5 cm^2). This variability in speed of emptying due to differences in sizes of evaporating surface areas, however, had negligible effect on the equilibrium condition of the two materials, i.e. In both cases, water level and contact tensions were inversely related and the slopes of regressions between these two variables were close to -1.

The time needed to dry the contact and wick materials in this laboratory test (Fig. 5.4a to d) is controlled by the indoor atmospheric condition and wick hydraulic properties and is probably longer than what can be expected under field conditions, where the duration is determined by the physical properties of the soil and wick materials, and the atmospheric evaporative demand (see results in Section 5.3.3).

This data of measured tensions over time, however, are not adequate to distinguish between stage 1 (energy-limited) and stage 2 (hydraulic conductivity limited) evaporation from the wick materials. In future research, accurately measured mass loss and time step measurements of humidity at the wick surface during the drying cycle should be included in order to distinguish between these two stages. The results presented in this section demonstrate the significance of incorporating climatic effects and wick characteristics into the design of Tube Detectors.

5.3.2 Tube Detector: Buried in the soil

5.3.2.1 *Water level in a tube and contact tension*

Figure 5.5 shows measured water level in a tube against contact tension for fine sand and DE filled Tube Detectors, which were buried 15 cm below the soil surface. This investigation tested the hypothesis that between zero tension and a tension equal to the length of the tube, contact tension is inversely related to water level in a tube when buried in the soil (Hypothesis 1).

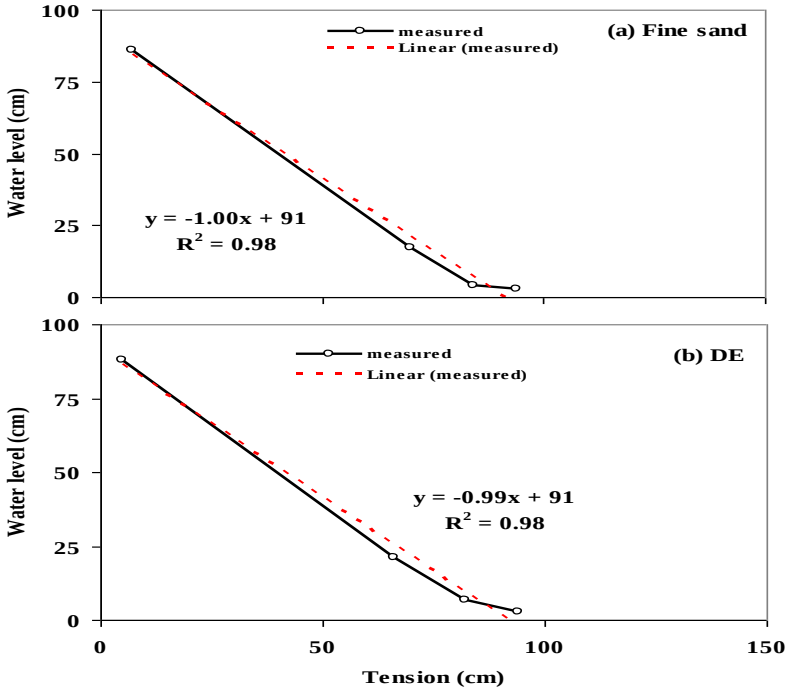

Figure 5.5 Water level drawdown in a tube as a function of contact tensions in Tube Detectors filled with fine sand (a) and DE (b) with measured variables (solid line and symbol) and inversely fitted (dotted line) to the measured values.

The regression line (dotted line) is fitted to the measured variables. In both Figures 5.5a and 5.5b the water level drawdown per unit change in contact tension is unity (inverse of the slope of regression line fitted to measured variables), i.e. for every 1 cm water level change, the contact tension changes by 1 cm. The slope, intercept and R^2 values shown in both figures showed a hydrostatic equilibrium condition between water level in the inner tube and contact tension. Therefore hypothesis 1 can be accepted for both wick materials.

5.3.2.2 *Contact tension and water level as a function of time*

Figure 5.6 shows tension in the soil-wick interface (contact tension) measured at 15 cm depth below the soil surface and water level in the inner tube. According to Figure 5.6, the general trend is that contact tension increases as the water level decreases over time.

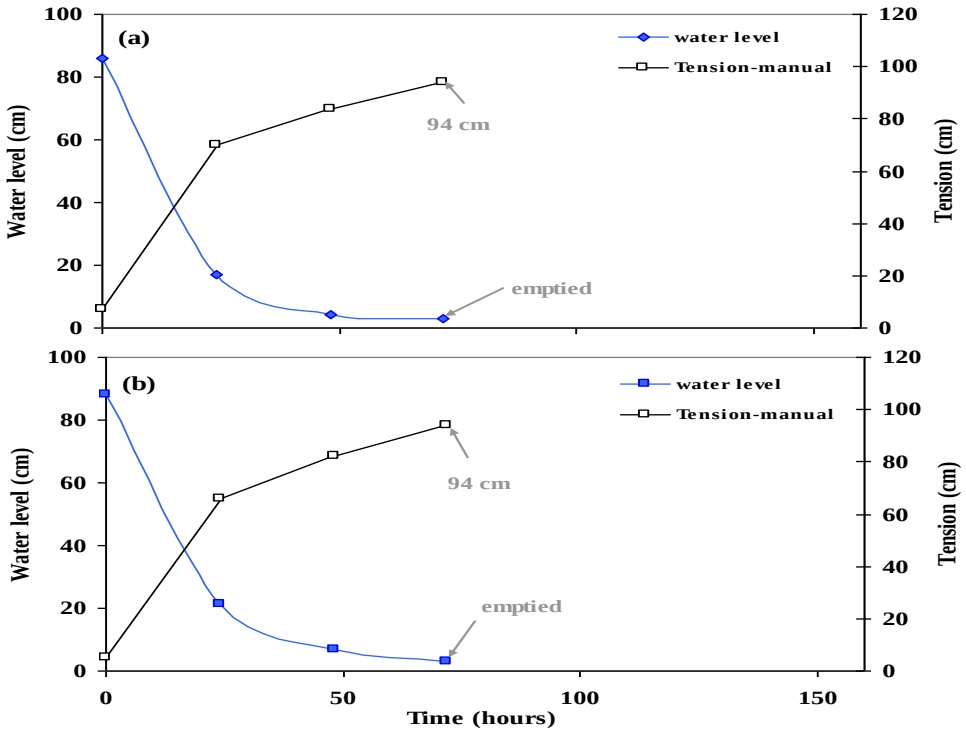

Figure 5.6 Water levels and contact tensions as a function of time with contact material exposed surface area of 16.5 cm^2 for fine sand (a) and DE (b).

The contact and wick material in Tube Detectors buried below the soil surface were saturated with watering cans at the start of the tests. Drying of wick materials started from below saturation, i.e. tensions between 5 and 7 cm, and water level at these tensions were 88 and 86 cm respectively. These initial tension values shown in each of the graphs (Fig. 5.6) estimated the saturation values of the contact materials well. This supports the first inference that the contact tension (cm) is close to zero when the inner tube is completely filled with water (Hypothesis 2). The contact tension readings corresponding to the nearly empty water level in the inner tube were 94 cm in both wick materials (Fig. 5.6a and b). Therefore, these tensions have approximated the length of Tube Detector used for this study well. This leads to confirm the second inference, namely that states the contact tension (cm) is equal to the height of the outer tube when the water level in the inner tube empty (Hypothesis 3).

According to Figure 5.6, the contact tensions in the fine sand Tube Detector varied from 7 to 94 cm and in the DE Tube Detector from 5 to 94 cm. The wettest contact tensions were therefore 5 and 7 cm for DE and fine sand filled Tube Detectors respectively. These initial

tensions showed that the materials were not completely saturated, possibly due to the inadequacy of the method of water application to completely saturate the wick and contact materials. The upward infiltration method, which prevents air trapping, is recommended to initially saturate both contact and wick materials in the Tube Detectors buried below the soil surface before allowing emptying.

5.4 CONCLUSIONS

In the indoor laboratory test, the regression values between the water level in the inner tube and contact tension for both wick materials (fine sand and DE) agreed well with the hydrostatic equilibrium condition, with only slight deviations from the theoretical hydrostatic equilibrium condition. Given the circumstances and possible minor measurement errors, the first hypothesis is accepted: the water level in the inner tube is inversely related to the contact tension.

In the buried tube test, water level in the inner tube was also inversely related to the contact tension for both the fine sand and DE wick materials, and therefore hypothesis 1 can also be accepted for field conditions.

In the indoor test, the initial contact tensions were nearly equal to tension-saturated conditions when the inner tubes were completely filled with water. A slight deviation from complete saturation was observed before the start of drying for contact materials with large surface area. However, this condition had less impact on the equilibrium between water level and contact tension. Results from indoor and buried tests support the first inference, namely that contact tension is close to zero when the inner tube is completely filled with water (Hypothesis 2). In the buried test, the same finding was observed supporting this inference.

Results from the indoor and buried tests also showed that the contact tensions at the end of evaporation (nearly empty water level) correlated well with the height of the Tube Detectors for both wick materials, and therefore the second inference can be accepted: contact tension is equal to the height of the tube when the water level emptied (Hypothesis 3).

CHAPTER 6

FIELD EVALUATION OF WETTING FRONT DETECTORS

6.1 INTRODUCTION

A field experiment was set up in order to evaluate the various designs of a wetting front detector. The experiment consists of two parts. In the first part, a crop of ryegrass was irrigated by sprinklers with a range from small to large irrigation events. The second part evaluated much lower fluxes of water by utilising natural rainfall in the absence of a crop.

The objectives of this field experiment are (1) to show all wetting front detector designs can be used for recording wetting fronts, (2) to show that wetting front detector designs can be discriminated from each other based on the strength of the fronts created using rainfall (potentially low fluxes) or sprinkler irrigation (high fluxes that vary with depth), and (3) to evaluate how well a Tube Detector remains in equilibrium with the bulk soil by comparing the tension in the wick material and the bulk soil.

This field evaluation investigates the following aspects:

- Overview of logged tensiometers record and wetting front movements;
- Evaluate performances across designs of wetting front detectors (WFD) based on the 'YES' type of response only as a function of rainfall and irrigation (i.e. a water sample was/was not collected);
- Evaluate performances of a WFD against the bulk soil tension readings based on the four different response types namely true positive, true negative, false positive and false negative (i.e. a water sample was/was not collected when the suction was within the theoretical sensitivity range of the WFD;
- Test any significant difference in the mean performance between different wetting front detector designs;

  - Due to differences in lengths of Tube Detectors
  - Due to difference in wick material (DE and Fine sand)
  - Due to difference in designs (Tube, Hybrid and FullStop^{TM})

- Investigate factors contributing to false negative and false positive responses;
- Estimate flux sensitivity of wetting front detectors; and

- Estimate drainages by cumulating the fluxes determined by Darcy's method and the water content-time curve relationships.

6.2 FIELD EXPERIMENTAL MATERIALS AND METHODS

This section of the chapter describes the materials and methods used for field evaluation of wetting front detectors.

These include field calibration of the neutron probe; field installation of the different versions of wetting front detector, water content and tension measuring equipment; field measurements and analyses of water applications, responses of wetting front detectors (water level in Tube Detectors and notes of visual observation of indicators), and water content and tension data; and water flux estimation methods.

6.2.1 Field Description, Calibration and Installation

6.2.1.1 *Experimental site*

The study was carried out in the rain shelter facility at the University of Pretoria, Experimental Farm at Hatfield, South Africa (25^{o} 45′S, 28^{o} 16′E and altitude of 1370 m). The study was conducted under rainfall only in 2006 and sprinkler irrigation system in 2007. This site was selected because all the plots (200 cm by 250 cm) are hydrologically isolated with vertical fibre cement sheets installed to a depth of 120 cm. The other advantage was that it had a rain-shelter facility that prevented incoming rainfall during the sprinkler evaluation period.

The soil profile ranges from sandy loam in the top layer (0 to 30 cm) to sandy clay loam in the 30 to120 cm depth. Of the 60 plots in the rain-shelter, 15 inner plots were selected for the trial, leaving two border rows on each side. The different designs of wetting front detectors included: three different lengths of Tube Detectors, the FullStop^{TM} detector, and a Hybrid Detector, which was a compromise between the funnel and Tube designs. Each design was replicated three times and allocated into the 15 plots in a completely randomized block design. Tension and water content measuring devices were installed in each of the 15 plots.

6.2.1.2 *Calibration*

Neutron probe

Two aluminium access tubes were installed in the experimental site to determine the calibration equations for water content measurements using a neutron probe (Model503DR, Campbell Pacific Nuclear International Martinez, CA). The soil profile around the first tube was saturated and covered with plastic sheet preventing evaporation losses and permitted to drain for 72 hours. Neutron probe raw counts at 15 s intervals (Hignett and Evett, 2002) were made at the drained site and standard counts in the air were taken to determine the count ratio (CR). Immediately after the measurements, core samples (80.5 mm diameter and 105 mm deep) were taken to determine the gravimetric soil water content at 20 cm depth interval to a depth of 120 cm next to each access tube. The mean bulk density and water content were determined by weighing the samples, placing in a drying oven at 105 ^{0}C for 72 hours and reweighing. In the second soil profile, similar procedures were used to determine the relationship between volumetric soil water content and the neutron probe raw counts except that the profile was dry. The calibration equations were then determined by plotting the volumetric soil water content against the neutron probe count ratio for both wet and dry conditions for depths 0 to 20 cm and 20 to 120 cm (Fig. 6.1). The calibration equations for both depths are:

$$\theta_v = 0.2436\ CR - 0.0528, \quad R^2 = 0.88, n = 10 \quad for \quad 0\ to\ 20\ cm\ depth \tag{6.1}$$

$$\theta_v = 0.2862\ CR - 0.2031, \quad R^2 = 0.81, n = 10 \quad for \quad 20\ to\ 120\ cm\ depth \tag{6.2}$$

The development of a separate calibration curve for the 0-20 cm soil depth was necessary because a substantial fraction of neutrons are lost from surface soil during near surface readings.

The volumetric water content was determined using the calibration equations (Eqs. 6.1 and 6.2) that correlate measured count ratio values with independently measured volumetric water contents.

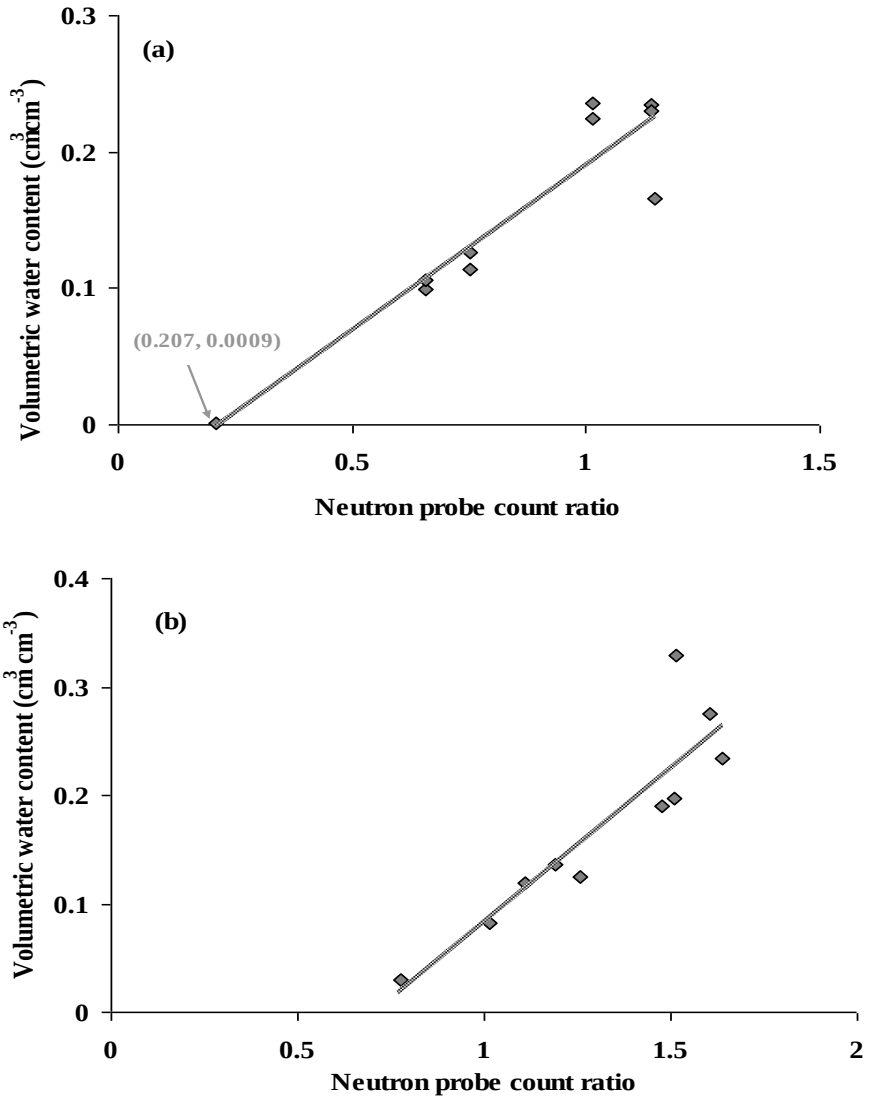

Figure 6.1 Relationship between gravimetrically determined volumetric soil water content and neutron probe count ratio for sandy loam soil 0 to 20 cm depth (a) and sandy clay loam of 20 to 120 cm depth (b).

Diviner 2000 probe

The Diviner 2000 probe was not calibrated on site and the default calibration equation for mean volumetric soil water content was used to determine water content in a profile at every 10 cm increments between depths 10 and 160 cm (Sentek Pty Ltd, 2003). The Diviner 2000 display unit also automatically displays the percentage of water contents on the chosen default screen.

$$\theta_v = 0.5017\left(SF^{3.0175}\right), \quad R^2 = 0.9985, \qquad (6.3)$$

where SF = the scaled frequency and R^2 is coefficient of determination.

6.2.1.3 *Installation procedures*

This section describes the procedures used during field installations of the different designs of a wetting front detector and soil water-monitoring equipments (neutron probe, diviner probe and tensiometers).

Tube wetting front detectors and soil water measuring equipment

Three different lengths of Tube Detectors referred as 45TD, 60TD and 90TD were installed to test their performances under field conditions. These abbreviations stand for prototypes made of two concentric tubes with inner tube of 20 mm (OD) and an outer tube of 44 mm (ID) in lengths of 45, 60 and 90 cm representing 45TD, 60TD and 90TD, respectively. Six Tube Detectors of the same lengths were installed in a plot, with each plot replicated three times. Three of the six detectors were filled with DE and the other three with Fine sand as described in Section 5.2.1. The open end of each Tube Detector was placed at depths 30, 60 and 90 cm below the soil surface and the holes were backfilled by compacting with the same soil material to avoid any preferential flow into a WFD (Fig. 6.2). Reliable responses of these wetting front detectors may be obtained by allowing a period of stabilization after soil disturbance caused during installation.

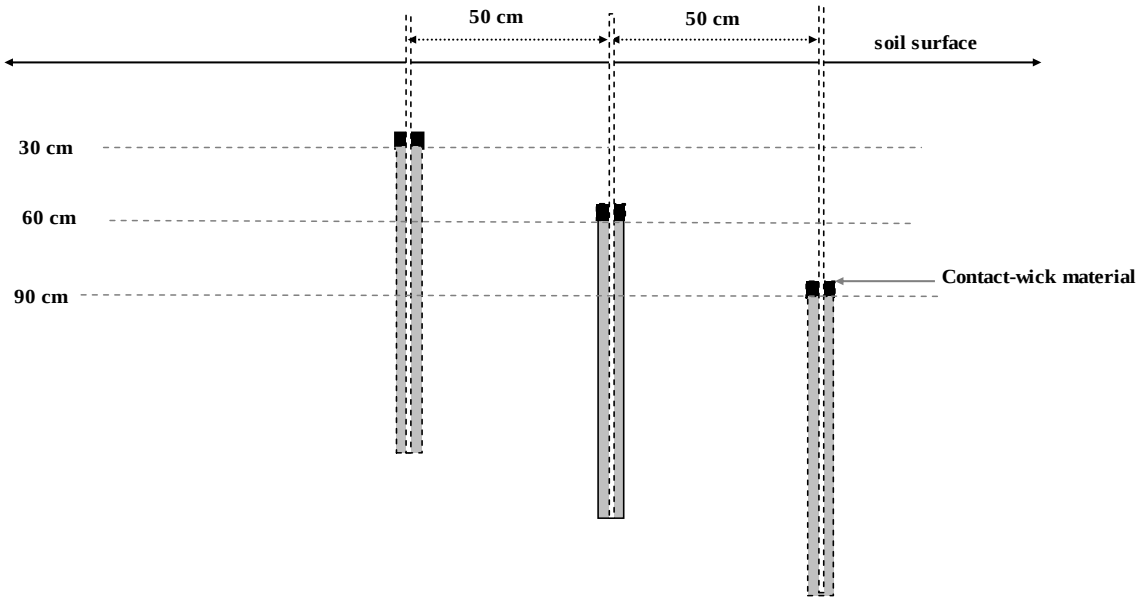

Figure 6.2 An example of 90TD prototype filled with DE and/or Fine sand installed in a plot at depths 30, 60 and 90 cm below the soil surface indicated by dashed lines, a 5 cm layer of contact wick material connecting the open end of a tube to the soil and a horizontal distance of 50 cm between the open ends of each prototypes.

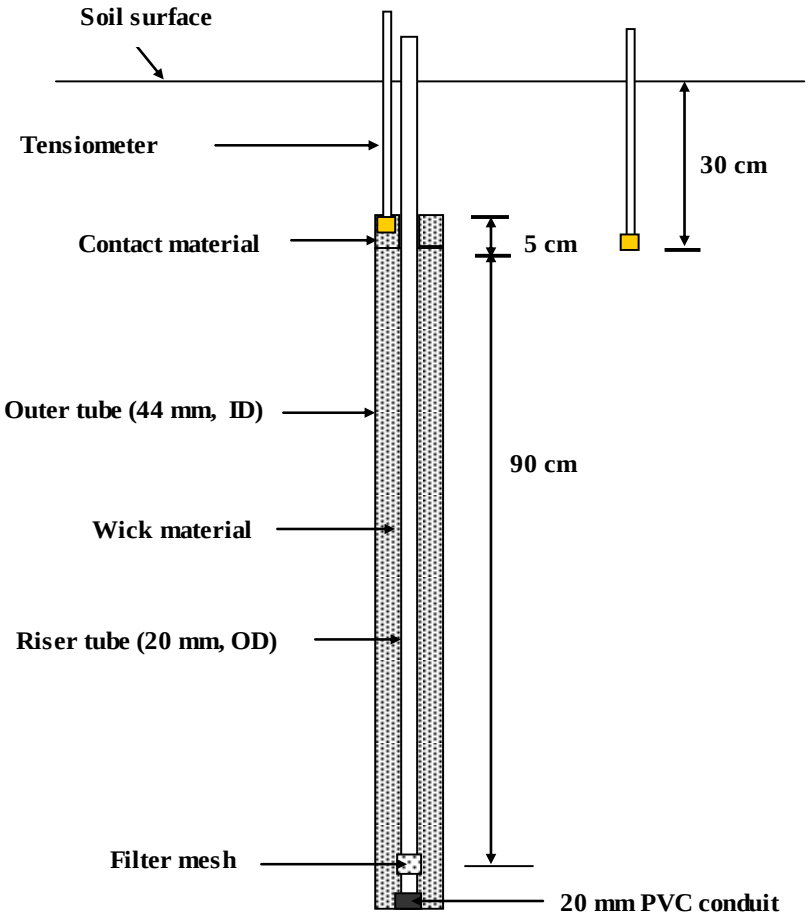

Figure 6.3 An example of longitudinal section of a Tube Detector showing two concentric pipes with the outer tube length of 90 cm and the cups of two manual tensiometers, one placed in the contact-wick material and the other in the bulk soil.

An amount of fill material 5 cm high is continued above the open end of a detector to provide hydraulic contact between fill material inside a tube and surrounding soil (Fig. 6.3). We refer to this as the contact-wick material (See Chapter 5).

In each test plot with Tube Detectors, each detector has one tensiometer in the contact-wick and another one in the bulk soil installed at similar depths approximately 50 cm away (Fig. 6.4). Each plot has therefore six tensiometers in the contact-wick area (2 contact materials x 3 depths) and another three in the bulk soil at three depths (Fig. 6.4). The manual tensiometer was used to measure tension as described in Section 5.2.1. All Tube Detectors were installed using an auger diameter of 55 mm in a grid of 50 cm by 100 cm within a plot (Fig. 6.4). The manual tensiometers were installed using 45 mm diameter auger after saturating the ceramic tips for 24 hours. All access holes were filled with slurry prepared from the same soil to ensure good contact between the tensiometer cup and soil.

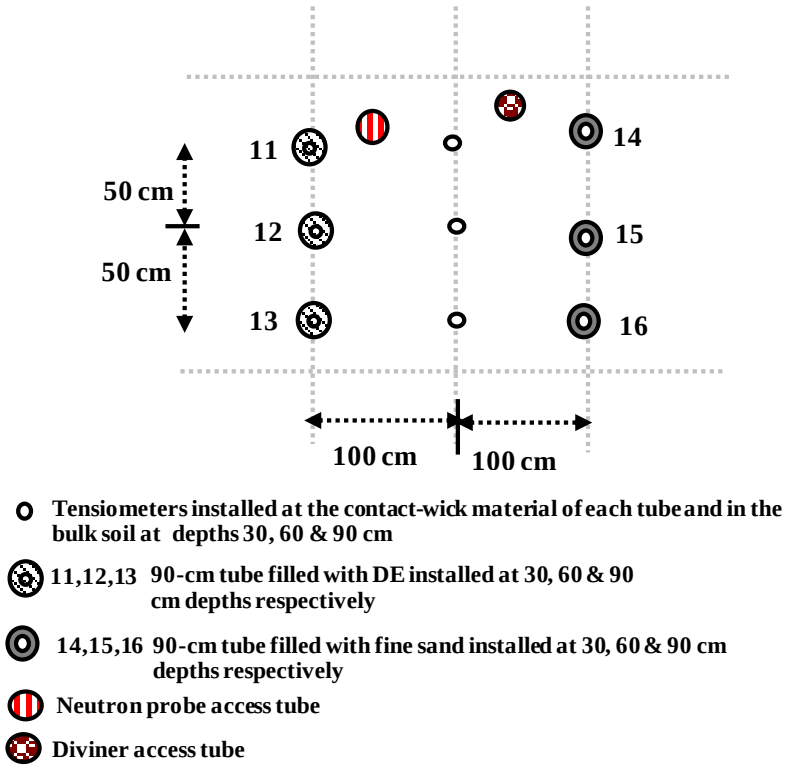

Figure 6.4 Plane view showing the positioning of tensiometer, neutron probe access tube, Diviner 2000 probe access tube and 90TD within a test plot.

A set of automatic tensiometers were installed with the HOBO logger system (Onset computer Corporation, MA02532, USA) that has four input channels each of which were used for a separate pressure transducer to capture time series tension data in the bulk soil at depths 30, 45, 60 and 90 cm in one plot of each treatments (90TD, 60TD and 45TD). Tensiometer data were logged at 12-minute interval using a pressure transducer with an accuracy of ± 1 cm. The installation procedures are similar to the manual tensiometer. Unlike the manual tensiometers, this was in just one rep per treatment.

In addition, each plot has one access tube for neutron probe and another one access tube for diviner probe measurements (Fig. 6.4). Access tubes for diviner probe were installed using the installation kit supplied by Sentek Pty Ltd for access tubes for Diviner 2000 measurements. Aluminium access tubes each 150 cm long were installed using an auger of 50 mm in diameter for neutron probe measurements._Tensiometers and wetting front detectors were about 50 cm from the access tubes used for neutron probe measurements (Fig. 6.4).

A total of 54 Tube Detectors and 84 tensiometers were installed in the nine plots identified by Tube Detector designs. A total of nine access tubes for neutron probe and another nine access tubes for diviner probe were installed to measure soil water content profile in these plots.

Hybrid and FullStop™ wetting front detectors and soil water-measuring equipments

A Hybrid Detector has a base to neck component of the FullStop™ (22 cm long) filled with a filter sand and continued with an extension pipe of 33 cm long with a diameter of 71 mm, i.e. the combined length of 55 cm making it a Hybrid between the funnel and the Tube Detector. The extension pipe is filled with either Fine sand or soil. The open end of each Hybrid Detector was buried at depths 30, 60 and 90 cm below the soil surface, and the holes were filled with the same soil material obtained during excavation (Fig. 6.5a). A soil or Fine sand wick material of 5 cm high was placed above the open end of each Hybrid Detector to ensure good hydraulic contact between the wick and bulk soil (Fig. 6.6a). Six Hybrid Detectors of which three of them filled with soil and the other three with Fine sand were installed in each replicate (Fig. 6.7a). The Hybrid Detectors were installed using auger sizes of 45 and 75 mm in diameter.

Eight FullStop™ (FS) detectors with four of them filled to just the stem of the funnel with filter sand and the other four with DE filter material were installed at depths 15, 30, 45 and 60 cm below the soil surface (Fig. 6.5b). The soil obtained while excavating access hole for installation of these detectors was backfilled into the funnel (from neck to the rim of the funnel) by compacting all the way to the soil surface to ensure good hydraulic continuity between the funnel and bulk soil and to avoid any preferential flow into a WFD. One tensiometer inside the funnel and another one tensiometer in a bulk soil were installed at similar depths (Fig. 6.6b). The FS detectors were installed using auger sizes of 45 and 200 mm diameter in a grid of 50 cm by 100 cm within a test plot (Fig. 6.7b). The above installations related to Hybrid and FS detectors were replicated three times.

A set of automatic tensiometers were installed at depths 15, 30, 45 and 60 cm in one replicate of the FS treatment and depths 30, 45, 60 and 90 cm in one replicate of the Hybrid treatment to record time series tension data. In addition, each test plot of the FS and Hybrid treatments has one access tube for neutron probe and another one access tube for diviner probe measurements (Fig. 6.7).

Hybrid and FullStop^{TM} wetting front detectors

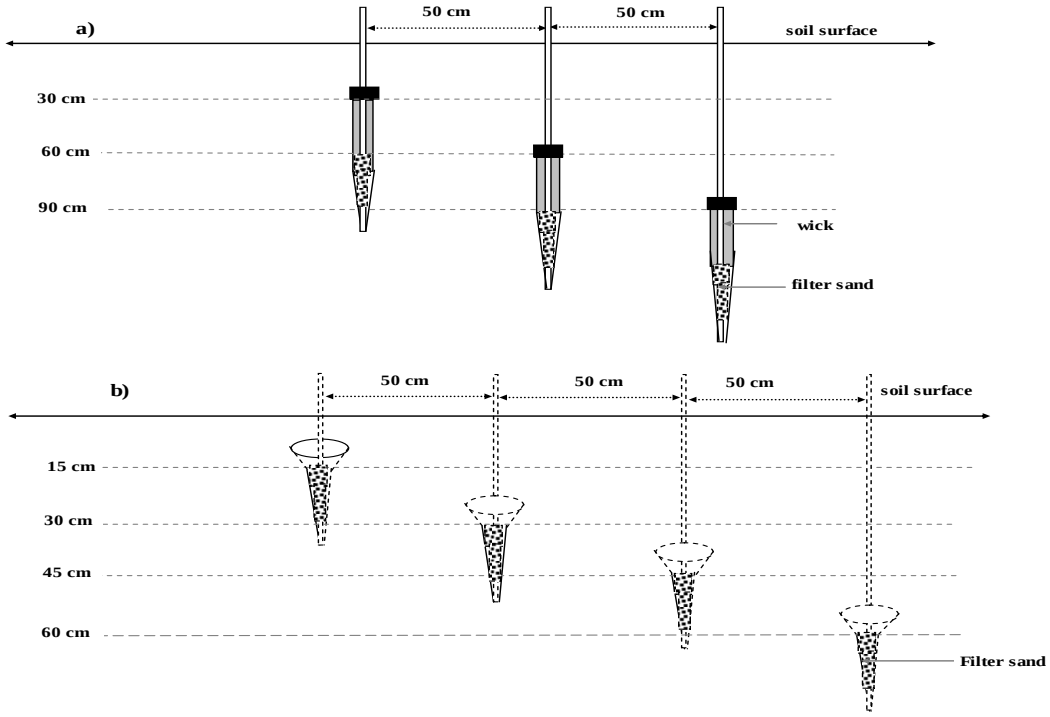

Figure 6.5 Diagram of the field layout of Hybrid wetting front detectors filled with local soil and/or Fine sand installed within a test plot at depths 30, 60 and 90 cm below the soil surface with the dashed horizontal lines indicating the depth of placements, and 50 cm horizontal distance between detectors (a); FS detectors with filter sand and/or DE used as filter materials installed at depths 15, 30, 45 and 60 cm below the soil surface with the dashed horizontal lines indicating the depths of installations and 50 cm horizontal distance between detectors (b).

In each of the three replicates of a Hybrid Detector treatment and following the installation detail (Fig. 6.7a), six Hybrid Detectors, nine tensiometers, one access tube for neutron probe and another one access tube for diviner probe measurements were installed. In each of the three replicates of the FS detector treatment (Fig. 6.7b), 8 funnel detectors, 12 tensiometers, one access tube for neutron probe and another one for diviner probe measurements were installed. Tensiometers and wetting front detectors were about 50 cm from the access tubes used for neutron probe measurements (Fig. 6.7).

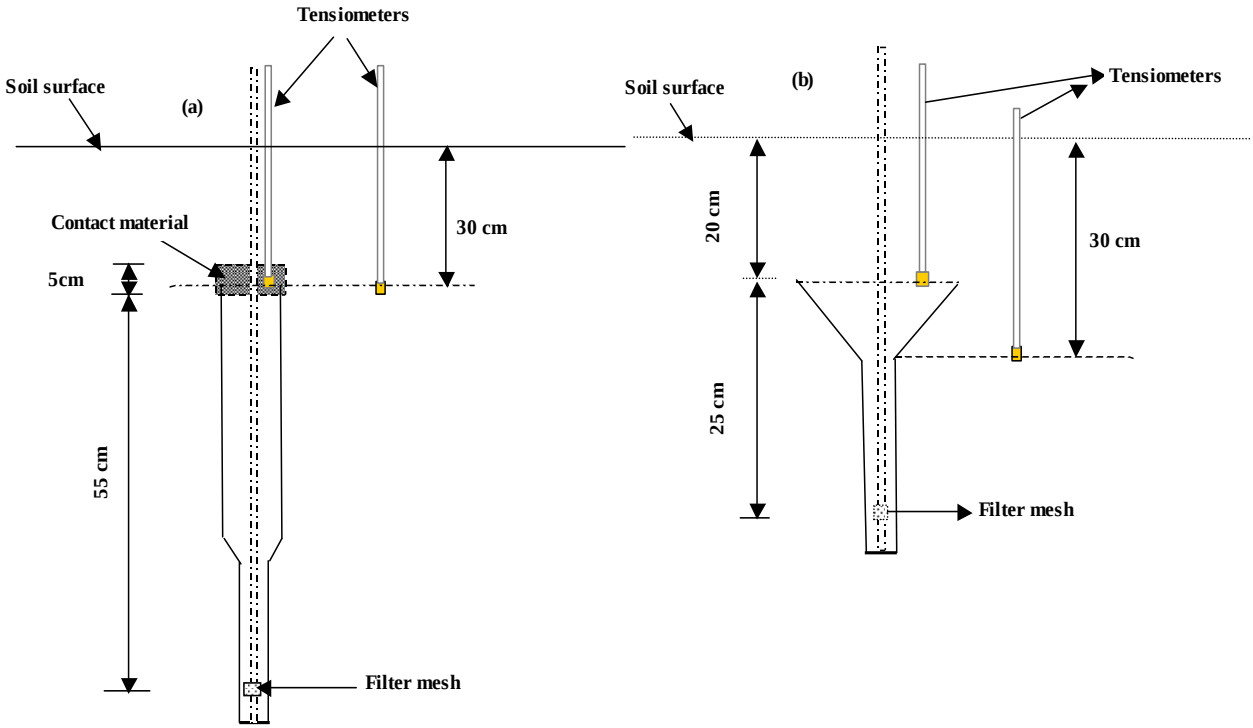

Figure 6.6 Examples of longitudinal sections showing a Hybrid Detector and two tensiometers (a) and the funnel detector and two tensiometers (b) buried below the soil surface.

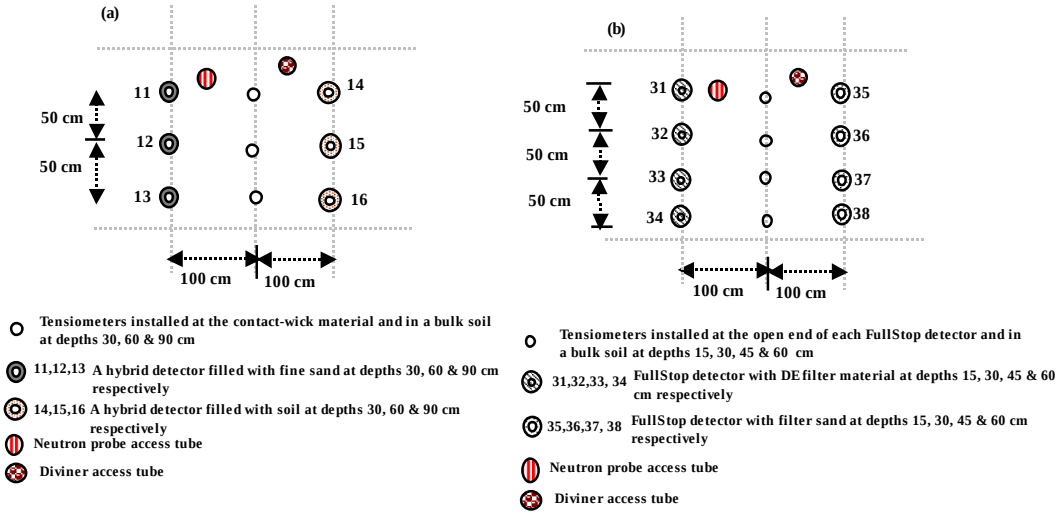

Figure 6.7 Plane view showing the positioning of tensiometer, neutron probe access tube, Diviner 2000 probe access tube in a Hybrid Detector test plot (a) in a FS detector test plot (b).

A total of 54 Tube Detectors, 18 Hybrid Detectors, 24 funnel detectors, 128 manual tensiometers, 20 automatic tensiometers, 15 access tubes for neutron probe and another 15 access tubes for diviner probe measurements were installed in all the 15 test plots of the experiment.

6.2.2 Field data measurements and analyses

6.2.2.1 *Water applications*

Following the field installations of wetting front detectors and soil water measuring equipment, the rain shelter facility was opened at 20-Nov-06 in order to allow the rainfall to produce a perfectly uniform wetted area. In the first season natural rainfall was used to test the sensitivity of each design because we wanted a very uniform application of low amounts of water that may not be possible to get from an irrigation system. The plots were mulched with dry grass to prevent evaporation and increase the penetration of water into the soil profile. The rainfall data was taken from the automatic weather station. Manual rain gauges were also placed within the rain shelter. The rainfall events ranged from 0.3 to 41.8 mm that produced a total of 220.1 mm from 20-Nov-06 until 02-Mar-07. Soil water content, manual tension and detector responses measurements were made on 15 separate occasions. Ten of these measurement dates occurred on the day following a rainfall event. (The remaining five was performed for periods with no rainfall on the preceding day to the measurements.

In the second season of evaluation of the sensitivities of wetting front detectors, the water application method used was sprinkler irrigation with two lateral lines each consisting of three sprinkler stands (full rotation) at 6 x 12 m. In this period, ryegrass was planted at a rate of 40 kg ha^{-1} in each of the plots in order to speed up the rate of drying from the soil. The mean application rate of the sprinkler irrigation during this evaluation period was 9.7 mm h^{-1} with standard deviation of 1.28 mm h^{-1}. A total of 696.1 mm of water was applied in 18 irrigation events. Water content, tension, WFD response measurements were taken at regular intervals during the 14 weeks period (22-Aug-07 to 28-Nov-07). The measurements were conducted prior to the start of irrigation, immediately after and then at 24 h intervals for several days after each irrigation event. The soil was allowed to dry for a period ranging from 1 to 13 days between irrigation events. The Distribution Uniformity (DU) and the coefficient of uniformity (CU) were calculated for all irrigation events using 60 catch cans placed on each plot in a grid of 3 m by 3 m within the rain shelter facility.

The uniformities of water application (DU and CU) were calculated using the lowest quarter method and Christiansen's method. The distribution uniformity (DU) is a measure of how uniformly an irrigation system applies water to a piece of land. It is calculated based on the lowest quarter method that compares average of lowest quarter of catch cans with the average of total catch cans.

$$DU = 100 * \left(\frac{lowest\ quarter}{average of\ total} \right) \quad (6.4)$$

The coefficient of uniformity (CU) calculates irrigation uniformity based on the Christiansen's method:

$$CU = 100 * \left(1 - \left(\frac{\sum x_i - \bar{x}}{\sum x_i} \right) \right) \quad (6.5)$$

where x_i *and* $\bar{x}$, are observed and mean values respectively.

The DU and CU for the 16 irrigation events were on average 70 and 80% respectively.

6.2.2.2 *Measurements of responses of wetting front detectors*

To investigate the performance of a wetting front detector in response to the rainfall or irrigation events, the amount of water collected in a Tube Detector was measured in the same way as described in Section 2.2.1.1. The Hybrid and FullStop were evaluated by means of system of mechanical floats and a magnetically latched indicator (www.fullstop.com.au). The indicator mechanism needs to collect approximately 20 ml of water in order to be activated. Thus the evaluation was judged as either on or off, i.e. more than or less than 20 ml of water (4 cm depth of water in the reservoir as measured) was collected during a wetting event.

6.2.3 Estimation of water fluxes

Water fluxes at the lower boundaries of 45 and 60 cm depths were estimated using the Darcy-Buckingham flux equation in order to compare water flux to the responses of wetting front detectors installed at similar depths. Soil depths at 45 and 60 cm are treated as a homogenous soil layer due to similar textural class i.e. the *in-situ* hydraulic conductivity function estimated for 60 cm soil depth was also used to estimate water flux past 45 cm soil depth.

The hydraulic conductivity function at 60 cm soil depth obtained with the inverse method and tensions measured at depths 30 and 60 cm were used to estimate water flux below 45 cm soil depth. Similarly, hydraulic conductivity function at 60 cm soil depth and tensions measured at depths 30 and 90 cm estimated water flux below 60 cm soil depth.

A pair of these tensiometers placed at two different depths, were used to determine the total tension gradient (∇H) at a given lower boundary by means of finite difference (ΔH/Δz). ΔH is the head difference between two observation depths and Δz is the vertical distance between two observation depths. The total head (H) is obtained by subtracting tension (h, cm) from the gravitational head (z, cm).

Given the relative homogeneity between these internodes, point estimates of flux in the internodes using *in-situ* estimated hydraulic conductivities and water potential gradients could be a representative of the point midway between the individual nodes. Tensiometer readings' were logged every 12 minute; hence the water flux was estimated for every 12-minute intervals over the measurement period. The hydraulic conductivity characteristics obtained with inverse method and the observed tensions at two nodes estimate water fluxes (q_L) at the internode by:

$$q_L = -K(h).\nabla H \qquad (6.6)$$

where q_L is the Darcy-Buckingham flux density (cm/h), $K(h)$ the conductivity as function of tension of the soil in question, and ∇H the hydraulic gradient determined by a finite difference.

6.3 RESULT AND DISCUSSIONS

Result and discussions of the field experiments described in Section 6.2 are presented in two parts. The first part provides field evaluation of the performances of wetting front detectors under 'strong', 'intermediate' and 'weak' soil water conditions created with sprinkler irrigation (Chapter 6). This is followed by the second part of evaluation of the performances of wetting front detectors of the same experimental set-up but under an 'intermediate' to dry soil water conditions produced by a natural rainfall (Chapter 7).

6.4 EVALUATION OF WETTING FRONT DETEECTORS UNDER SPRINKLER IRRIGATION

6.4.1 Irrigation, responses of tensiometers and wetting front detectors

6.4.1.1 *General overview of irrigation and wetting front movement*

The experiment received 696.1 mm of irrigation water over a period of 99 days (22-Aug-07 to 28-Nov-07). Wetting fronts produced in response to these irrigation events are indicated by

the lines of continuous tension measured by automatic tensiometers (Fig. 6.8) representing one replicate of each treatment. The continuous tension readings at depths 30, 45, 60 and 90 cm (Fig. 6.8b and d) and 30 cm (Fig. 6.8c) are shown for less than the days indicated (in some cases) on the scale because of technical problems associated with the proper operation of the pressure transducers. There were 13 large irrigation events (≥ 25 mm) and another five events with low irrigation amounts (≤ 12 mm) under which the various WFD designs were evaluated. Irrigation events are indicated by vertical dotted lines (Fig. 6.8b to d).

During a large irrigation event, all tensiometers at depths 15 to 90 cm responded on the same day of the irrigation (Fig.6.8b to d). The penetration of wetting front was, however, limited between 15 and 45 cm depths (Fig.6.8d) and 30 and 45 cm (Fig.6.8b and c) during low irrigation events as indicated by the responses of tensiometers at these depths.

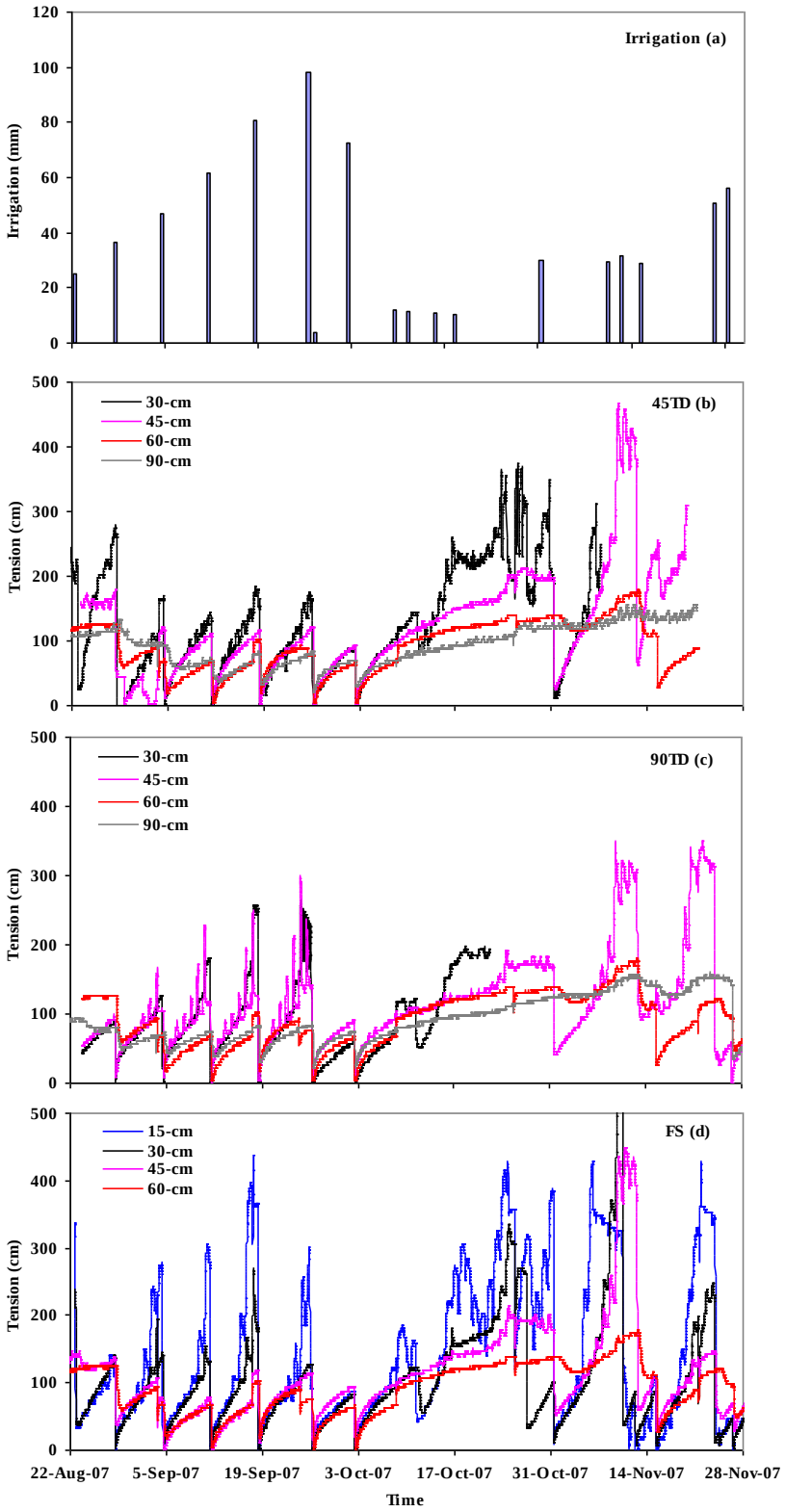

Figure 6.8 Responses of automatic tensiometers (b to d) measured at different depths in response to irrigation events (a).

From theory and laboratory experiments, the sensitivity of a Tube Detector is equal to its length (see Chapter 5), for example, a 90 cm long Tube Detector should be able to collect a water sample over the tension ranges from 0 to 90 cm occurring at the open end of the detector. Therefore, wetting events within these tension ranges are potentially recordable events. Following the above finding and illustration, the numbers of wetting events potentially recordable by a 45 cm long Tube Detector at depths 30, 60 and 90 cm are 9, 7 and 4 respectively (Fig. 6.8b). A 90 cm long Tube Detector potentially should detect 10 to 11 wetting events at depths 30, 60 and 90 cm that fell within the operating range of this length (Fig. 6.8c). Figure 6.8d indicated that the FS detector should record 14, 12, 9 and 8 wetting events at depths 15, 30, 45 and 60 cm, respectively. Note that a 60 cm long Tube Detector and HD treatments had no test plots with properly or 'fully' operating automatic tensiometer during this evaluation period.

6.5 EVALUATIONS OF THE PERFORMANCE OF WETTING FRONT DETECTORS

Two measures of evaluating the performance of wetting front detectors are discussed below. The first approach evaluates the performance of each design against the rest i.e. which design records the most fronts at each depth. It considers only the number of 'YES' type of responses recorded by the various WFD designs. The second approach evaluates the performance of a WFD design against its own sensitivity range based on the theoretical and experimental results discussed in Chapter 5 as a result identifies factors that contribute to the deviation of WFD from its 100% performance. The second approach produces four categories of responses for assessing the performance of each WFD design: true positive, true negative, false positive and false negative responses.

The first approach tested hypotheses (i), (ii) and (iii), while the second approach tested hypothesis (iv) as described below:

i) The 90 cm long Tube Detector is likely to record significantly higher wetting front events ('YES' responses) than the 60 and 45 cm long Tube Detectors

ii) DE filled Tube Detector is likely to record wetting event fronts ('YES' responses) significantly more often than those filled with Fine sand

iii) Tube Detectors longer than each of the FS and HD designs are likely to record wetting fronts event ('YES' responses) significantly more often than the latter two designs

iv) The length of a Tube Detector determines the driest tension value of wetting front that can be detected

6.5.1 First approach: 'YES' type of response as a measure of performance

This section ranks the performances of three lengths of Tube Detectors, HD and FS detectors to select the most sensitive design. It shows the performance of each design of a wetting front detector in response to the irrigation events described in Section 6.4.1.1. In this case, the performance indicator is the sum across replicates of each treatment based on the 'YES' type of responses recorded by each WFD design over the 18 irrigation events, i.e. measurements taken immediately after irrigation has stopped. These data sets therefore mainly tested hypotheses (i), (ii) and (iii) to select the WFD design/design feature, which records the most wetting event fronts.

The numbers of 'YES' type of responses recorded by a WFD design installed at different depths were evaluated based on the criteria listed below:

- A wetting front is registered as 'YES' type of response if the water volume in the inner tube of a Tube Detector ≥ 7 ml. This 7 ml volume of water is taken as a baseline located below a nylon filter mesh of 100-µm opening, i.e. this water cannot be wicked out even when the surrounding tension increases to large values.
- A 'YES' type of response is registered by the FullStop^{TM} and Hybrid Detectors, if more than 20 ml of water was collected in the reservoir, i.e. the indicator is magnetically latched in the up position.

Note that the above evaluation criteria between Tube Detectors and FS or HD are different, i.e. FS or HD detectors may have collected ≥ 7 ml of water that cannot activate the float and hence is not regarded as 'YES' response. The comparisons between these designs therefore reflect differences in their design requirements, i.e. the volume of water required to score a 'YES' response. Using the above sets of criteria, the numbers of 'YES' responses were evaluated based on the water volume in the Tube Detectors and the status of FS or HD indicator after each irrigation event as a function of depth, wick or filter material (Tables 6.1 and 6.2). The differences in the numbers of 'YES' responses observed at depths 30, 60 and 90 cm using the different WFD designs as shown in these tables were examined using the General Linear Model (GLM) procedure of SAS software (SAS Institute, 1999-2001). Means

were compared using the t Tests (LSD) at 5% probability level and shown in Tables 6.3, 6.4, 6.5 and 6.6.

Table 6.1 Summary of the number of 'YES' responses in a Tube and Hybrid Detectors (summed across the 3 replicates of each treatment): Tube Detectors have only one record per irrigation while the Hybrid can only respond once per event.

	DE			**Fine sand**		
	Depth (cm)			**Depth (cm)**		
Type	**30**	**60**	**90**	**30**	**60**	**90**
45TD	31	21	17	23	17	13
60TD	26	21	22	33	20	16
90TD	34	30	31	36	32	35
	Soil*			**Fine sand**		
HD	11	2	1	20	10	6

Soil* hereafter in this document refers to the soil removed from the installation hole and filled into the Hybrid WFD.

Table 6.2 Summary of the number of 'YES' responses in the FullStop^{TM} detectors (summed across the 3 replicates of the FS treatment): FS responds once per event.

	DE				**Filter sand**			
	Depth (cm)				**Depth (cm)**			
Type	**15**	**30**	**45**	**60**	**15**	**30**	**45**	**60**
FS	33	15	13	9	35	22	16	11

Based on the result summary (Tables 6.1 and 6.2) and the statistical analyses of length effect (Table 6.3), wick effect (Table 6.4) on the mean 'YES' responses and comparisons among the six Tube Detector treatments (Table 6.5) and ten WFD treatments (Table 6.6) are commented:

a) At the 60 and 90 cm depths, length has significant effect on the performance of Tube Detectors ($P \leq 0.05$) such that 90 cm long Tube Detector produced significantly higher mean "YES' responses than the 60 and 45 cm long Tube Detectors. Therefore hypothesis (i): the 90 cm long Tube Detector is likely to record significantly higher wetting front events ('YES' responses) than the 60 and 45 cm long Tube Detectors is accepted. At the 30 cm depth, however, length has no significant effect on the performance of Tube Detectors (Table 6.3).

b) Table 6.4 shows that wick type has no significant effect on the mean 'YES' responses of Tube Detectors in all the three depths ($P > 0.05$). Therefore hypothesis (ii): DE filled Tube Detector is likely to record wetting event fronts ('YES' responses) significantly more often than those filled with Fine sand is rejected (Table 6.4).

Table 6.3 Length effect in the mean 'YES' responses of Tube Detectors.

Length-cm (TD)	**Mean 'YES' responses at three depths**		
	30 cm	**60 cm**	**90 cm**
90	11.7a	10.3a	11.0a
60	9.8a	6.8b	6.3b
45	9.0a	6.3b	5.2b

Notes: column response means followed by the same lower case letter are not significantly different ($P > 0.05$); column response means followed by different lower case letter are significantly different ($P \leq 0.05$).

Table 6.4 Wick effect in the mean 'YES' responses of Tube Detectors.

Wick type	**Mean 'YES' responses at three depths**		
	30 cm	**60 cm**	**90 cm**
DE	10.1a	8.0a	7.8a
Fine sand	10.2a	7.7a	7.2a

Notes: column response means followed by the same lower case letter are not significantly different ($P > 0.05$); column response means followed by different lower case letter are significantly different ($P \leq 0.05$).

c) Table 6.5 shows that at 30 cm depth, there is no significant difference between the six Tube Detector treatments ($P > 0.05$) where as the mean 'YES' response in the 90 cm long Tube Detector is significantly higher than the 60 and 45 cm long Tube Detectors at depths 60 and 90 cm ($P \leq 0.05$). This supports hypothesis (i).

Table 6.5 Tube Detector treatments effect in the mean 'YES' responses of Tube Detectors.

Type	Mean 'YES' responses at three depths		
	30 cm	**60 cm**	**90 cm**
90TD-Fine sand	12.0a	10.7a	11.7a
90TD-DE	11.3a	10.0a	10.3a
60TD-Fine sand	11.0a	6.7bc	5.3b
60TD-DE	8.7a	7.0bc	7.3b
45TD-Fine sand	7.7a	5.7c	4.7b
45TD-DE	10.3a	7.0bc	5.7b

Notes: column response means followed by the same lower case letter are not significantly different ($P > 0.05$); column response means followed by different lower case letter are significantly different ($P \leq 0.05$).

Table 6.6 Mean of 'YES' responses as affected by WFD treatment type at the three depths

Type	Mean 'YES' responses		
	30 cm	**60 cm**	**90 cm**
90TD-Fine sand	12.0a	10.7a	11.7a
90TD-DE	11.3ab	10.0a	10.3a
60TD-Fine sand	11.0abc	6.7b	5.3bc
60TD-DE	8.7abcde	7.0b	7.3b
45TD-Fine sand	7.7bcde	5.7bc	4.7c
45TD-DE	10.3abcd	7.0b	5.7bc
HD-Fine sand	7.3cdef	3.7c	2.0d
HD-Soil*	5.0ef	3.0cd	0.3d
FS-DE	3.7f	0.7d	-
FS-Filter sand	6.7def	3.3cd	-

Notes: column response means followed by the same lower case letter are not significantly different ($P > 0.05$); column response means followed by different lower case letter are significantly different ($P \leq 0.05$); dash (-) in the 90 cm depth column indicates there was no FS detector installed at this depth.

d) Table 6.6 shows that at 30 cm depth, only the 90 cm long Tube Detector filled with either DE or Fine sand has significantly higher mean 'YES' responses than the FS or HD designs ($P \leq 0.05$). At the 60 and 90 cm depths, however, both the 60 and 90 cm long Tube Detectors filled with either DE and/or Fine sand have significantly higher mean responses than the FS or HD designs ($P \leq 0.05$). This finding provides users the flexibility to select a WFD of appropriate sensitivity for a particular application (e.g. to manage furrow irrigation in soil depths less than 1.8 m, install a 60-cm long tube detector at a depth of 0.90 m).These results therefore accepts hypothesis (iii): Tube Detectors longer than each of the FS and HD designs are likely to record wetting front events ('YES' responses) significantly more often than the latter two designs.

6.5.2 Second approach: Performance against the sensitivity ranges of WFD

This approach evaluates the WFD performances against (1) the theoretical sensitivity ranges of each design (45TD, 60TD, 90TD and HD) and (2) empirically determined sensitivity of the FS design in response to the irrigation applications described in Section 6.4.1.1. In this case, performance indicators are the sums of replicates of each treatment based on the four categories of responses: true positive (TP), true negative (TN), false positive (FP) and false negative (FN) responses recorded by each of the five WFD designs over the 18 irrigation events. This data set tests mainly the hypothesis (iv) associated with the applicability of the Tube WFD for a measurement of wetting front defined by tension within its detection ranges. The WFD design that measures tension of a wetting front with no or low drift in accuracy from its sensitivity range will be best suited for measuring a wetting front.

6.5.2.1 *Response types of wetting front detectors*

In this investigation, the following four types of responses were identified in each of the WFD designs. These responses help to understand factors that may contribute to the deviation of WFD performances from the theoretically or empirically determined tension sensitivity values.

Tube wetting front detector

Bulk soil determines the equilibrium condition of a Tube Detector with its surrounding soil; therefore, responses of a Tube Detector were evaluated with respect to the tensions measured in a bulk soil.

a) True positive (TP): the inner tube of a Tube Detector collects a volume of water ≥ 7 ml when a tension in the bulk soil at similar depth falls within the sensitivity range of a specific design (i.e. equal to the length, see Table 6.7).
b) False positive (FP): the inner tube of a Tube Detector collects a volume of water ≥ 7 ml when a tension in a bulk soil at similar depth falls outside the sensitivity range (e.g. drier than) of a specific design.
c) True negative (TN): the inner tube of a Tube Detector collects no water or a volume of water < 7 ml when a tension in a bulk soil at similar depth falls outside the sensitivity range of a specific design.
d) False negative (FN): the inner tube of a Tube Detector collects a volume of water < 7 ml when the tension in a bulk soil at similar depth falls within the sensitivity range of a specific design.

FullStop or Hybrid wetting front detector

e) True positive (TP): FS or HD detector collects > 20 ml of water and keeps the indicator latched in the up position when tension in a bulk soil came within the sensitivity range of each design. The maximum tension sensitivities for the FS and HD designs are 30 and 55 cm respectively.
f) True negative (TN): FS or HD detector collects < 20 ml of water and the indicator remains in the down position when tension in a bulk soil is drier than the sensitivity of each design
g) False positive (FP): FS or HD detector collects > 20 ml of water and showing the indicator in the up position when tension in a bulk soil is drier than the sensitivity of each design
h) False negative (FN): FS or HD detector collects < 20 ml of water and keeps the indicator in the down position when tension in a bulk soil is wetter than the sensitivity of each design

6.5.2.2 *Tension sensitivities of wetting front detectors*

The Tube Detector sensitivity is determined by length and the FS detector has a tension sensitivity of 30 cm or wetter as determined empirically (Stirzaker, 2003). The Hybrid design has a wide opening, which promotes water flow to converge to the tube with the extension tube for increasing its sensitivity and potentially will have a tension sensitivity of 55 cm. It is good therefore to determine the error in tension measurements that occur under field

conditions before evaluating each design against their defined tension sensitivity limits. The tension sensitivities of each of the WFD designs are shown (Table 6.7).

Table 6.7 Tension sensitivity limits of WFD designs

Design-WFD	90TD	60TD	45TD	HD	FS
Tension sensitivity (cm)	90[1]	60[1]	45[1]	55[1]	30[2]

[1] theoretical; [2] empirically determined values

These values are limited by the measurement accuracy due to instrument error (tension gauge) and spatial variation in the soil (e.g. spatial variability in tensiometer readings). The measurement accuracy of the pressure transducer gauge was generally within ± 1.0 cm. (See Section *Accuracy of manual pressure transducer gauge*). The errors due to uncertainty in tension measurements in the wet events were calculated between ± 5.5 and ± 8.4 cm (see Section *Uncertainty in tension measurements below*). In other words, the measurement error ranges of tensions within the operating range of wetting front detectors were generally within ± 6.5 to ± 9.4 cm.

Accuracy of manual pressure transducer gauge

The midpoint of a ceramic cup of each tensiometer in lengths 30, 45, 60 and 90 cm were submerged in water to calibrate the accuracy of the manual pressure transducer gauge used for the study. In general, the measured tensions were within ± 1.0 cm of the height of water column in each tensiometer tube.

Uncertainty in tension measurements

Figure 6.9 provides the uncertainty in tension measurements using error bars. Based on the 68 measurement dates conducted during the irrigation period, the mean tensions in the bulk soil, DE and Fine sand with the corresponding standard error values are presented for each depth (Fig. 6.9 and 6.10). In these figures, the error bars are quite small in the wet period (large irrigation amounts) that includes 22-Aug-07 to 01-Oct-07 and 07-Nov-07 to 30-Nov-07 (Fig. 6.9a and 6.10a). In most cases, the error bars become large in the dry periods (small irrigation amounts) that include periods between 02-Oct-07 and 16-Nov-07 (Fig. 6.9a and 6.10a).

The data used for illustrating uncertainty in tension measurements is based on the tensions measured at depths 30, 60 and 90 cm in each of the bulk soil, DE and Fine sand. The mean

tensions in the bulk soil, DE and Fine sand were determined by averaging tensions measured across 15, 9 and 12 plots, respectively, which were then used to calculate standard errors across depth and soil material. The averaged standard errors calculated from these data sets range from ± 8.4 to ± 18.1 cm in bulk soil and ± 5.5 to ± 14.9 cm in wick materials (Table 6.8). The standard error in tension measurements is determined by dividing the standard deviations by the square root of the number of measurements.

Table 6.8 Statistical summaries of uncertainty in tension measurements

Soil material	**Period**	**Depth and standard error (SE)**			**Average SE**
		30-cm	**60-cm**	**90-cm**	
Bulk soil	Wet	11.3	5.1	8.8	8.4
	Dry	36.4	8.7	9.2	18.1
DE	Wet	5.0	5.7	7.2	6.0
	Dry	27.4	11.0	6.2	14.9
Fine sand	Wet	3.7	6.5	6.3	5.5
	Dry	17.8	8.9	5.8	10.8

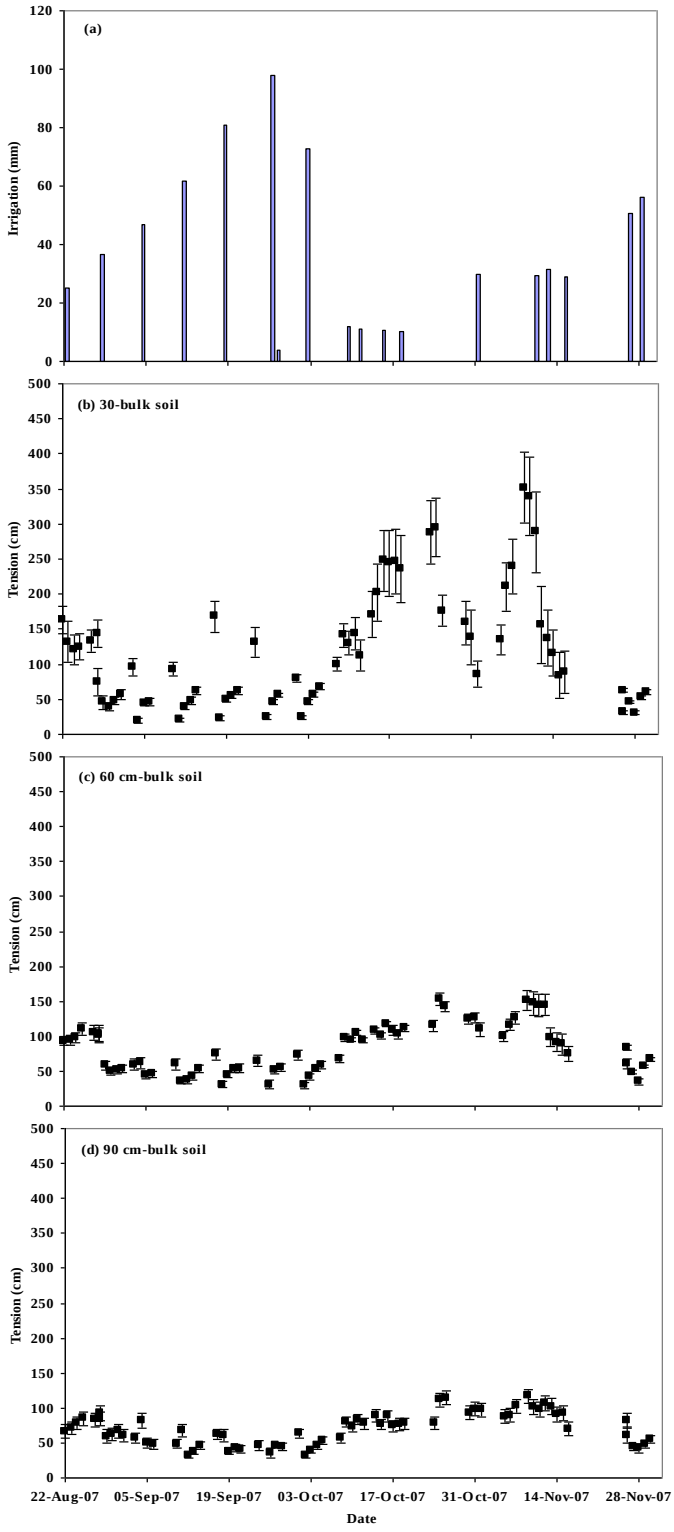

Figure 6.9 Averaged tensions across 15 plots in the bulk soil (b to d) with error bars at depths 30, 60 and 90 cm in response to irrigation applied (a).

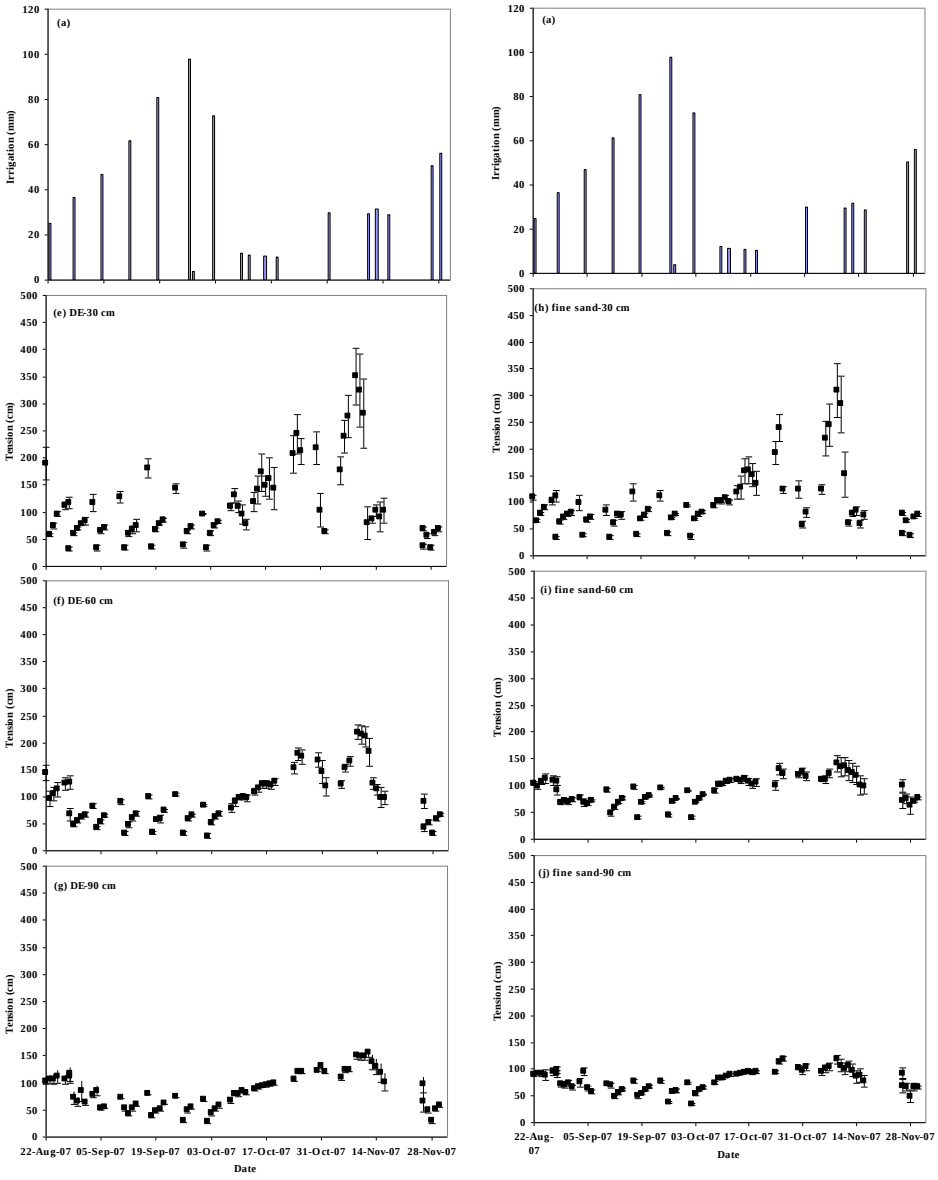

Figure 6.10 Averaged tensions across 9 plots with DE (e to g) and across 12 plots with Fine sand (h to i) with error bars at depths 30, 60 and 90 cm in response to irrigation applied (a).

Table 6.8 indicated a low spatial variability in tensions measured in the wet periods and a relatively high spatial variability of tensiometer readings during the dry periods. This suggests procedures used in evaluating the responses of the wetting front detector to irrigation events, with respect to tension sensitivities of the WFD, should take into account the average standard error of the tensions measured in the bulk soil for the corresponding wet or dry period as shown in Table 6.8.

6.5.2.3 *Performance evaluations with respect to tension sensitivities of WFD*

This section presents the numbers of responses recorded by the different designs of wetting front detectors in response to a change in tensions measured in the bulk soil.

Response evaluations based on irrigation event measurements

The TP, FP, TN and FN were evaluated against the sensitivity limits of each design, illustrated for one replication of each 90TD, the FS and HD (Figs. 6.11 to 6.13) and summarized in Table 6.9. The same evaluation procedure is then used to summarize the overall responses of wetting front detectors measured in each treatment of 90TD, 60TD, 45TD, FS and HD replicated three times over the 18 irrigation events (Appendix 2a to o), with the summary presented in Table 6.10.

Table 6.9 Response summaries of Figs. 6.11, 6.12 and 6.13 (One replication of 90TD, FS and HD treatments)

Detector-wick/filter-depth	Response numbers and types				Detection (%)
	TP	TN	FP	FN	
90 cm Tube Detector					
90TD1-DE-30cm	10	8	0	0	100
90TD1-DE-60cm	10	8	0	0	100
90TD1-DE-90cm	9	6	0	3	75
90TD1-Fine sand-30cm	10	7	1	0	100
90TD1-Fine sand-60cm	7	9	0	2	78
90TD1-Fine sand-90cm	12	5	0	1	92
FullStop detector					
FS1-DE-15cm	8	5	5	0	100
FS1-DE-30cm	5	12	1	0	100
FS1-DE-45cm	4	14	0	0	100
FS1-DE-60cm	3	15	0	0	100
FS1-Filter sand-15cm	8	5	5	0	100
FS1-Filter sand-30cm	7	10	1	0	100
FS1-Filter sand-45cm	4	13	1	0	100
FS1-Filter sand-60cm	3	15	0	0	100
Hybrid Detector					
HD1-Fine sand-30cm	6	11	0	1	86
HD1-Fine sand-60cm	2	13	0	3	40
HD1-Fine sand-90cm	0	15	0	3	0
HD1-Soil*-30cm	0	11	0	7	0
HD1-Soil*-60cm	0	13	0	5	0
HD1-Soil*-90cm	0	15	0	3	0

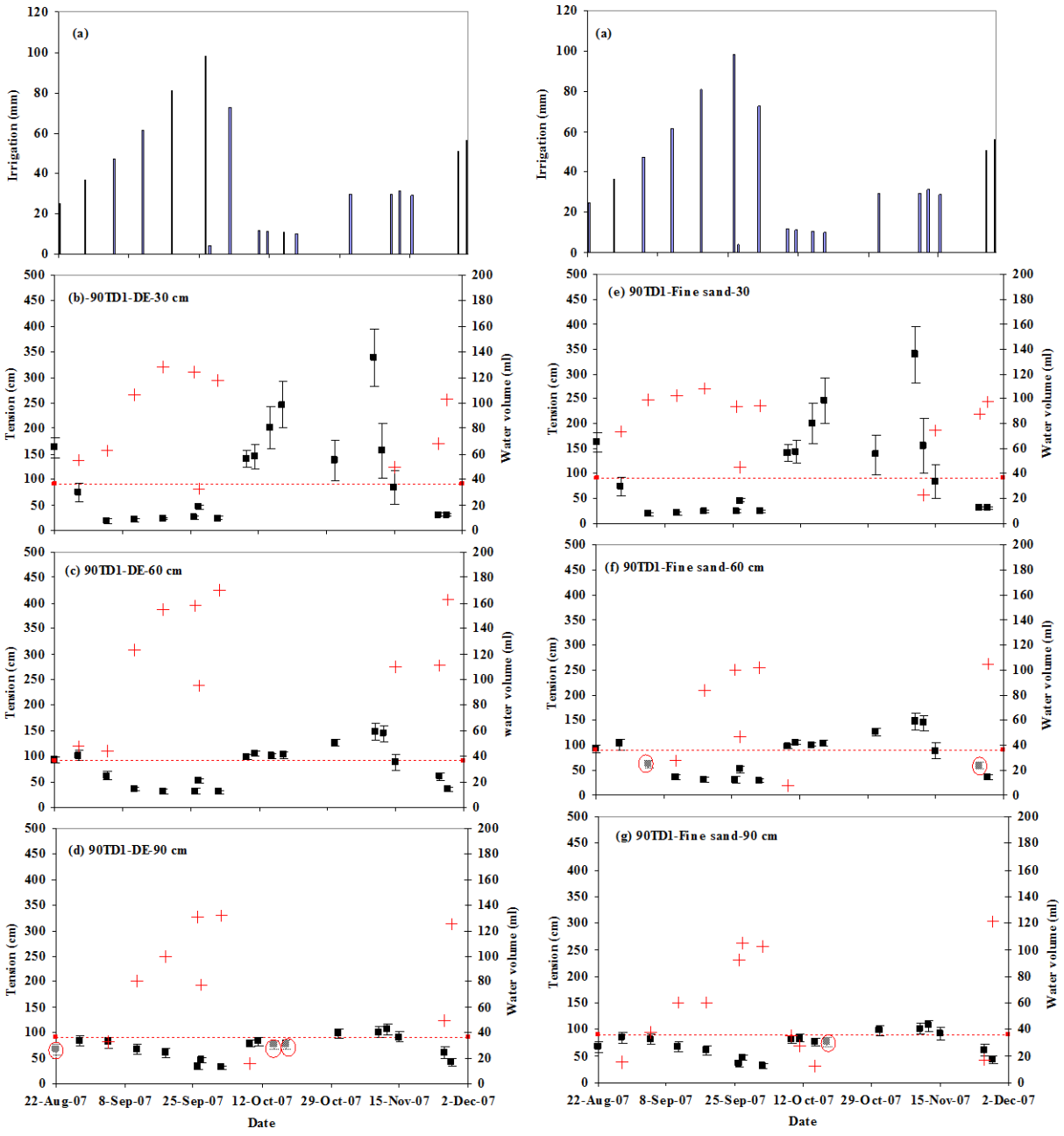

Figure 6.11 True positive response (+) represents water volume > 7 ml, false negative responses (circles), mean bulk soil tensions with error bars (squares), and tension sensitivity (dotted line) for a 90 cm long Tube Detector filled with DE (b to d) and Fine sand (e to g) at depths 30, 60 and 90 cm in response to irrigation applied (a).

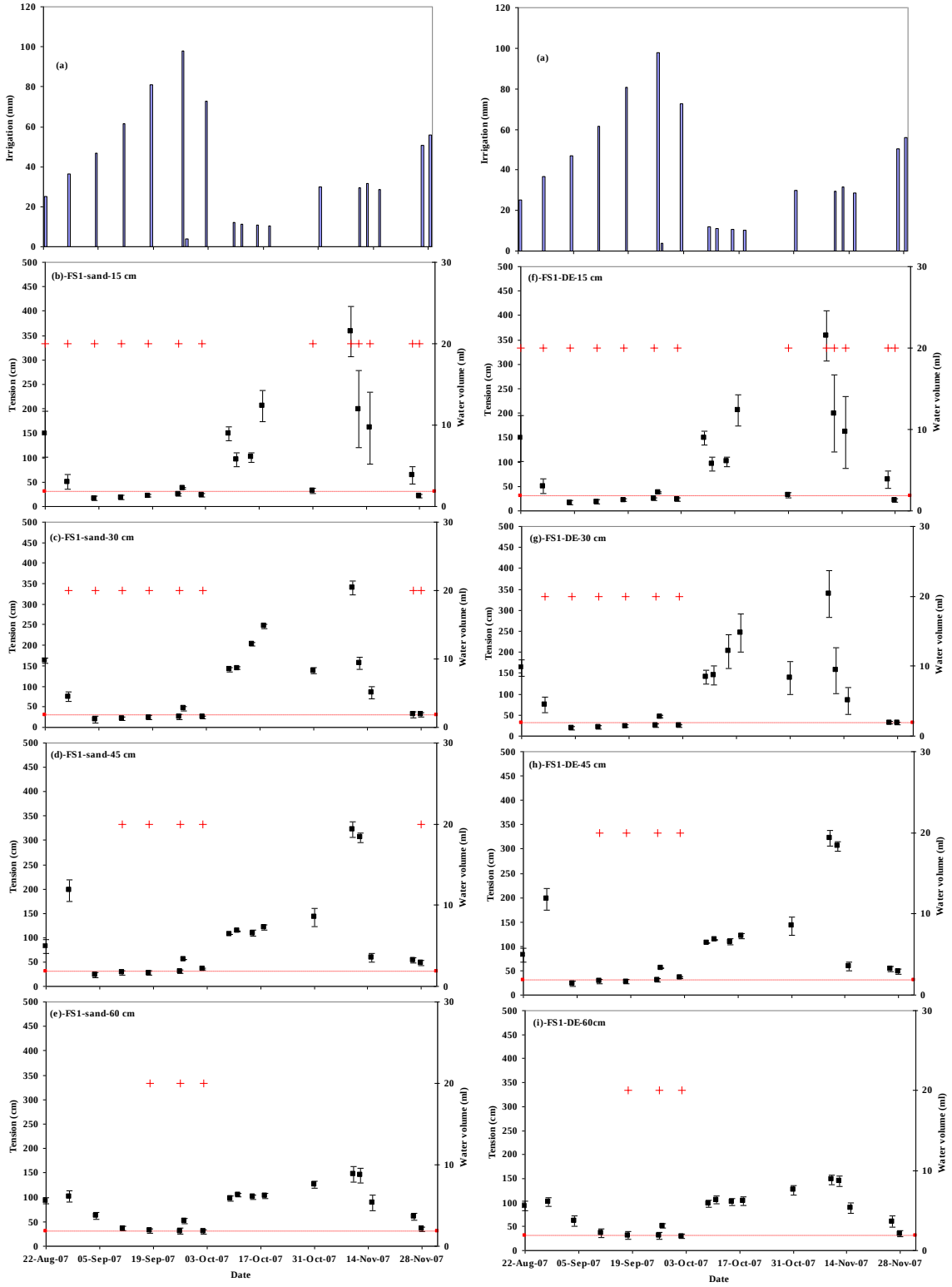

Figure 6.12 True positive response (+) represents water volume > 20 ml, mean bulk soil tensions with error bars (squares), and tension sensitivity (dotted line) for the FullStop detector with filter sand (b to e) and DE (f to i) at depths 15, 30, 45, and 60 cm in response to irrigation applied (a).

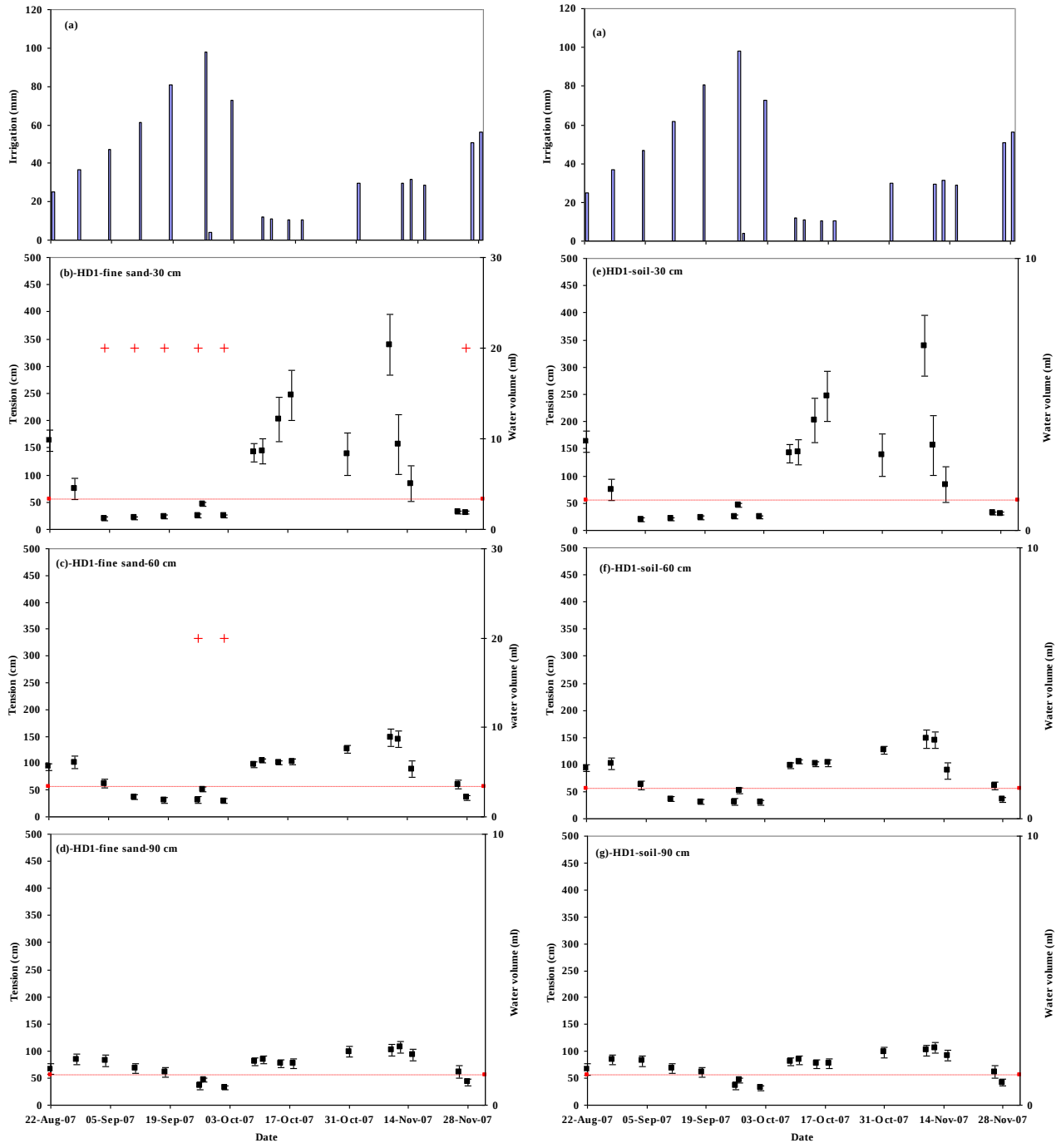

Figure 6.13 True positive response (+) represents water volume > 20 ml, mean bulk soil tensions with error bars (squares), and tension sensitivity (dotted line) for a Hybrid Detector filled with Fine sand (b to d) and soil (e to g) at depths 30, 60 and 90 cm in response to irrigation applied (a).

Testing a statistical significance for the observed differences in WFD responses

The numbers of response categories for each design is shown (Table 6.10).

Table 6.10 Response summaries of figures Appendix 2a to o.

Detector-wick/filter-depth	Response numbers and types				Detection (%)
	TP	TN	FP	FN	
90 cm Tube Detector					
90TD-DE-30cm	29	20	5	0	100
90TD-DE-60cm	29	24	1	0	100
90TD-DE-90cm	30	18	1	5	86
90TD-Fine sand-30cm	30	18	6	0	100
90TD-Fine sand-60cm	23	20	9	2	92
90TD-Fine sand-90cm	35	16	0	3	92
60 cm Tube Detector					
60TD-DE-30cm	23	24	3	4	85
60TD-DE-60cm	20	31	1	2	91
60TD-DE-90cm	19	32	3	0	100
60TD-Fine sand-30cm	26	18	7	3	90
60TD-Fine sand-60cm	17	30	3	4	81
60TD-Fine sand-90cm	16	37	0	1	94
45 cm Tube Detector					
45TD-DE-30cm	24	23	7	0	100
45TD-DE-60cm	16	32	5	1	94
45TD-DE-90cm	10	36	7	1	91
45TD-Fine sand-30cm	17	27	6	4	81
45TD-Fine sand-60cm	14	36	3	1	93
45TD-Fine sand-90cm	10	39	4	1	91
FullStop detector					
FS-DE-15cm	21	20	12	1	95
FS-DE-30cm	13	36	2	3	81
FS-DE-45cm	12	40	1	1	92
FS-DE-60cm	9	44	0	1	90
FS-Filter sand-15cm	21	18	14	1	95
FS-Filter sand-30cm	18	30	4	2	90
FS-Filter sand-45cm	11	37	5	1	92
FS-Filter sand-60cm	10	42	1	1	91
Hybrid Detector					
HD-Fine sand-30cm	20	31	0	3	87
HD-Fine sand-60cm	10	39	0	5	67
HD-Fine sand-90cm	6	43	0	5	55
HD-Soil*-30cm	11	36	0	7	61
HD-Soil*-60cm	2	48	0	4	33
HD-Soil*-90cm	1	49	0	4	20

Detection percentage (%) column in Tables 6.9 and 6.10 is calculated by multiplying by 100 for the ratio obtained by dividing the TP by the sums of TP and FN, i.e. 100*(TP/ (TP+FN)). The observed differences in the mean responses shown in Table 6.10 indicate that:

- The longer the tube length, the more the number of TP responses
- The numbers of responses of Tube Detectors in DE is slightly higher than in Fine sand.
- The three lengths of Tube Detector designs respond more frequently than HD and/or FS designs installed at similar depths.
- The average detection % within the sensitivity limit of each treatments of 90TD, 60TD, 45TD, FS and HD are 95, 90, 92, 91 and 54% respectively.

The subsequent statistical analyses of the data in Table 6.10 using the GLM procedure of SAS software (SAS Institute, 1999-2001) and the comparisons of the means using the t Tests (LSD) at 5% probability level_allows drawing the following conclusions concerning the tube length (Table 6.11) and wick type (Table 6.12) effects on the deviation of each Tube Detector in measuring a wetting front. It also compares the extent of these deviations among the WFD type (Table 6.13), six Tube Detector treatments (Table 6.14) and the ten WFD treatments (Table 6.15). The following are commented based on the measurements made at each of the three depths (Tables 6.11, 6.12, 6.14 and 6.15) and summed over these depths (Table 6.13):

1) The FN column in Table 6.11 shows a deviation in each of the 90TD, 60TD and 45TD treatments in measuring wetting event fronts at the three depths of observations within their sensitivity ranges. The three tube lengths generally underestimate in measuring a wetting front that falls within their ranges by 5% to 13% (drift in accuracy is calculated as 100*(FN/ (TP+FN)).
2) Table 6.11 also showed that the deviations among these three designs are not significantly different from each other. Given these low deviations, it can be concluded that the length of a Tube design can be matched to the ranges of wetting fronts to be measured. Therefore this finding supports the hypothesis (iv) that states the length of a Tube Detector determines the driest tension value of wetting front that can be detected.

3) The FN column in Table 6.12 shows that DE and Fine sand are similar at 30 and 90 cm depths. At 60 cm depth, however, Fine sand significantly underestimates in measuring a wetting front than DE.
4) Table 6.13 shows a deviation of 5% to 10% in each of the 90TD, 60TD, 45TD and FS treatments in measuring wetting event fronts within their sensitivity ranges. The FN column also showed that the deviations among these four designs are not significantly different from each other. Given these low deviations, it can be concluded that the length of a WFD design can be matched to the ranges of wetting fronts to be measured. Therefore this finding supports the hypothesis (iv) that states the length of a Tube Detector determines the driest tension value of wetting front that can be detected. However the HD design showed large deviation (46%) from its sensitivity range therefore not recommended for a wetting front measurement.
5) Table 6.14 shows that at 30 cm depth there is no significant difference in the FN column between the six Tube Detector treatments (drift in accuracy in measuring a wetting front ranges from 0% to 15%). The drift in accuracy as computed for the six Tube Detectors from the same table but at 60 and 90 cm depths indicated in the range of 0% to 18%.
6) The FN column in Table 6.15 shows that the 90TD, 60TD and 45TD in DE and/or Fine sand, and the FS detector in Filter sand and/or DE underestimates a wetting front that falls within the range of each design by 0 to18%. In the HD design filled with Soil* and/or Fine sand, however, the deviation in measuring a wetting front ranges from 13% to 81%. Given the relatively low deviations in the first four designs of WFD, each of these designs can be used to measure a wetting front within their ranges. This finding therefore, supports the hypothesis (iv). In other words, 90, 60 and 45 cm long Tube Detectors can be matched to wetting events range from 0 to 90, 0 to 60 and 0 to 45 cm tensions respectively.
7) There is no significant effect of a wick material difference in the performance of Tube Detectors of the same length, which can be seen in the TP, FP and FN columns for each of the tube lengths (Table 6.15). Wick materials therefore are reasonably staying in equilibrium with the bulk soil. In addition, no significant effect of filter material differences on the performances of FS detector.
8) Even though the length of a TD is beneficial, there seems to be no benefit in lengthening the FullStop. Even at 55 cm length (and with some convergence) a Hybrid did not improve performance over FullStop and was not as good as a 45TD.

This probably relates to the 7 ml vs. 20 ml, which is the design requirement to score a response (triggering point).

Table 6.11 Means of TP, TN, FP and FN responses as affected by tube length

Length	Mean responses at three depths											
	30-cm				60-cm				90-cm			
	TP	TN	FP	FN	TP	TN	FP	FN	TP	TN	FP	FN
90	9.8a	6.4b	1.8a	0.0a	8.7a	6.7b	1.6a	1.0a	10.8a	4.3b	0.2b	2.7a
60	8.2b	7.0ab	1.6a	1.2a	6.2b	10.3a	0.7a	0.8a	5.8b	11.5a	0.5b	0.2b
45	6.8b	8.3a	2.2a	0.7a	5.0c	11.5a	1.3a	0.2a	3.3c	12.9a	1.8a	0.0b

Notes: column response means followed by the same lower case letter are not significantly different ($P > 0.05$); column response means followed by different lower case letter are significantly different ($P \leq 0.05$). This applies also to Tables 6.12 and 6.13.

Table 6.12 Means of TP, TN, FP and FN responses as affected by wick type

Wick	Mean responses at three depths											
	30-cm				60-cm				90-cm			
	TP	TN	FP	FN	TP	TN	FP	FN	TP	TN	FP	FN
DE	8.4a	7.5a	1.7a	0.4a	7.2a	9.9a	0.8a	0.1b	6.6a	9.1a	1.2a	1.1a
Fine sand	8.1a	7.0a	2.1a	0.8a	6.0b	9.1a	1.7a	1.2a	6.8a	10.0a	0.4a	0.8a

Table 6.13 Means of TP, TN, FP and FN responses as affected by WFD type

WFD type	TP	TN	FP	FN
90TD	9.3a	6.5d	1.7a	0.5b
60TD	7.2b	8.9c	1.1ab	0.8b
45TD	5.9b	9.9bc	1.7a	0.5b
FS	4.2c	12.8a	0.6bc	0.4b
HD	3.6c	11.4ba	0.0c	3.0a

Table 6.14 Means of TP, TN, FP and FN responses of Tube Detector treatments

Wick	Mean responses at three depths											
	30-cm				60-cm				90-cm			
	TP	TN	FP	FN	TP	TN	FP	FN	TP	TN	FP	FN
90TD-DE	9.7ab	6.7ab	1.6a	0.0a	9.7a	8.0bc	0.3a	0.0b	10.0a	5.4b	0.3b	2.3a
90TD-Fine sand	10.0a	6.0b	2.0a	0.0a	7.7b	5.3c	3.0a	2.0a	11.7a	4.3b	0.0b	2.0b
60TD-DE	7.7bc	8.0ab	1.0a	1.3a	6.7bc	10.7ab	0.3a	0.3b	6.3b	10.7a	1.0ab	0.0c
60TD-Fine sand	8.7ab	6.0b	2.3a	1.0a	5.7cd	10.0ab	1.0a	1.3a	5.3bc	12.4a	0.0b	0.3c
45TD-DE	8.0ab	7.7ab	2.3a	0.0a	5.3cd	11.0ab	1.7a	0.0b	3.3c	12.5a	2.2a	0.0c
45TD-Fine sand	5.7c	9.0a	2.0a	1.3a	4.7d	12.0a	1.0a	0.3b	3.3c	13.4a	1.3ab	0.0c

Notes: column response means followed by the same lower case letter are not significantly different ($P > 0.05$); column response means followed by different lower case letter are significantly different ($P \leq 0.05$).

Table 6.15 Means of TP, TN, FP and FN responses of all WFD treatments

Wick	Mean responses at three depths											
	30-cm				60-cm				90-cm			
	TP	TN	FP	FN	TP	TN	FP	FN	TP	TN	FP	FN
90TD-DE	9.7a	6.7de	1.6ab	0.0b	9.7a	8.0fg	0.3b	0.0c	10.0a	5.4c	0.3bc	2.3a
90TD-Fine sand	10.0a	6.0e	2.0a	0.0b	7.7b	5.3g	3.0a	2.0a	11.7a	4.3c	0.0c	2.0ab
60TD-DE	7.7abc	8.0bcde	1.0ab	1.3ab	6.7bc	10.7def	0.3b	0.3bc	6.3b	10.7bc	1.0bc	0.0d
60TD-Fine sand	8.7ab	6.0e	2.3a	1.0ab	5.7cd	10.0ef	1.0b	1.3ab	5.3bc	12.4bc	0.0c	0.3cd
45TD-DE	8.0abc	7.7cde	2.3a	0.0b	5.3cd	11.0de	1.7ab	0.0c	3.3cd	12.5bc	2.2a	0.0d
45TD-Fine sand	5.7cde	9.0bd	2.0a	1.3ab	4.7de	12.0cde	1.0b	0.3bc	3.3cd	13.4b	1.3ab	0.0d
HD-Fine sand	6.7bcd	10.3ab	0.0b	1.0ab	3.3ef	13.0bcd	0.0b	1.7a	2.0de	14.3ab	0.0c	1.7bc
HD-Soil*	3.7e	12.0a	0.0b	2.3a	0.7g	16.0a	0.0b	1.3ab	0.3e	16.4a	0.0c	1.3bcd
FS-DE	4.3de	12.0a	0.7ab	1.0ab	3.0f	15.0ab	0.0b	0.0c	-	-	-	-
FS-Filter sand	6.0bcde	10.0abc	1.3ab	0.7ab	3.3ef	14.3abc	0.3b	0.0c	-	-	-	-

Notes: column response means followed by the same lower case letter are not significantly different ($P > 0.05$); column response means followed by different lower case letter are significantly different ($P \leq 0.05$).

6.6 CONCLUSIONS

Length has significant effect on the performance of Tube Detectors such that a 90TD has significantly higher mean 'YES' responses than 60TD and 45TD designs at depths 60 and 90 cm ($P \leq 0.05$). This finding therefore supports the hypothesis (i) that states the 90TD detector is likely to record significantly higher wetting front events ('YES' responses) than the 60TD and 45 TD detectors. However there is no significant difference between tube lengths at the 30 cm depth.

There is no significant difference in the mean 'YES' responses between DE and Fine sand ($P > 0.05$). Therefore, hypothesis (ii) that states DE filled Tube Detector is likely to record wetting event fronts ('YES' responses) significantly more often than those filled with Fine sand is rejected.

At the 60 and 90 cm depths, both the 60TD and 90TD filled with either DE or Fine sand have significantly higher mean responses than the FS or HD designs ($P \leq 0.05$). This result therefore supports hypothesis (iii) that states Tube Detectors longer than each of the FS and HD designs are likely to record wetting front events ('YES' responses) significantly more often than the latter two designs. At the 30 cm depth, however, only the 90TD filled with either DE or Fine sand has significantly higher mean 'YES' responses than the FS or HD designs.

The three Tube WFDs (90TD, 60TD and 45TD) generally underestimate in measuring a wetting front that falls within their ranges by 5 to 13%. Given these low deviations, each of these designs can be used to measure a wetting front within their ranges. In other words, 90, 60 and 45 cm long Tube Detectors can be matched to wetting events range from 0 to 90, 0 to 60 and 0 to 45 cm tensions respectively. The drift in accuracy in measuring a wetting front in these Tube WFDs in DE and/or Fine sand, and the FS detector in Filter sand and/or DE underestimates a wetting front that falls within the range of each design by $\leq 20\%$. Therefore these findings related to the Tube Detector lengths and all WFD treatments support the hypothesis (iv) that states the length of a Tube Detector determines the driest tension value of wetting front that can be detected. However the HD design and treatments showed large deviation (13 to 81%) from its sensitivity range. Therefore, HD design is not recommended for a wetting front measurement.

CHAPTER 7

EVALUATION OF WETTING FRONT DETEECTORS UNDER RAINFALL CONDITIONS

7.1 RAINFALL, RESPONSES OF TENSIOMETERS AND WETTING FRONT DETECTORS

7.1.1 General overview of rainfall and wetting front movement

The entire test plots received 220.1 mm of rain over a period of 103 days (20-Nov-2006 to 02-Mar-2007). Wetting fronts produced in response to these rainfall events are indicated by lines of continuous tensions as measured by automatic tensiometers, which were in one plot of each treatment (Fig. 7.1). The continuous tension readings are shown for less than the days indicated on the scale because of some technical problems associated with the operation of the pressure transducers (Fig. 7.1).

Figure 7.1a shows that the plots received rainfall amounts ranging from 0.3 to 41.8 mm. The rainfall period was dominated by small rainfall events with few large rain events that fell on 29-Dec-06, 17-Jan-07 and 10-Feb-07, indicated by the dotted vertical lines (Fig. 7.1b to f) in which the measurements were conducted in these dates. The shallow tensiometers installed at depths 30 cm (Fig. 7.1b, c, d and f) and 45 cm (Fig. 7.1f) responded on the same day of the large rainfall events. However, tensiometers installed at 60 and 90 cm depths responded more slowly, i.e., 1 to 2 days at 60 cm depth (Fig. 7.1c, e and f) and 2 to 3 days at 90 cm depth (Fig. 7.1c to e) after the large rainfall events.

From theory and laboratory experiments, the sensitivity of a Tube Detector is equal to its length (See Chapter 5); for example, a 90 cm long Tube Detector should be able to collect a water sample over the tension ranges from 0 to 90 cm. Therefore wetting events that are potentially recordable by WFD can be predicted from the tension time curves (Fig. 7.1). Potentially recordable wetting events by the different WFD designs during the rainfall period can be expected given that there are sources of errors (Fig. 7.1): ≤ 5 at 30 cm depth, ≤ 3 at 45 cm depth and ≤ 2 at depths 60 and 90 cm.

In other words, the numbers of wetting events potentially recordable by 90, 60 and 45 cm long Tube Detectors ranges from 1 to 5 depending on the length of a tube, i.e. the longer the tube the higher the number of wetting event records. The tension time curve also showed that

≤ 2 wetting events at depths 30 to 60 cm fell within the detectable ranges of the FS detector (Fig.7.1f).

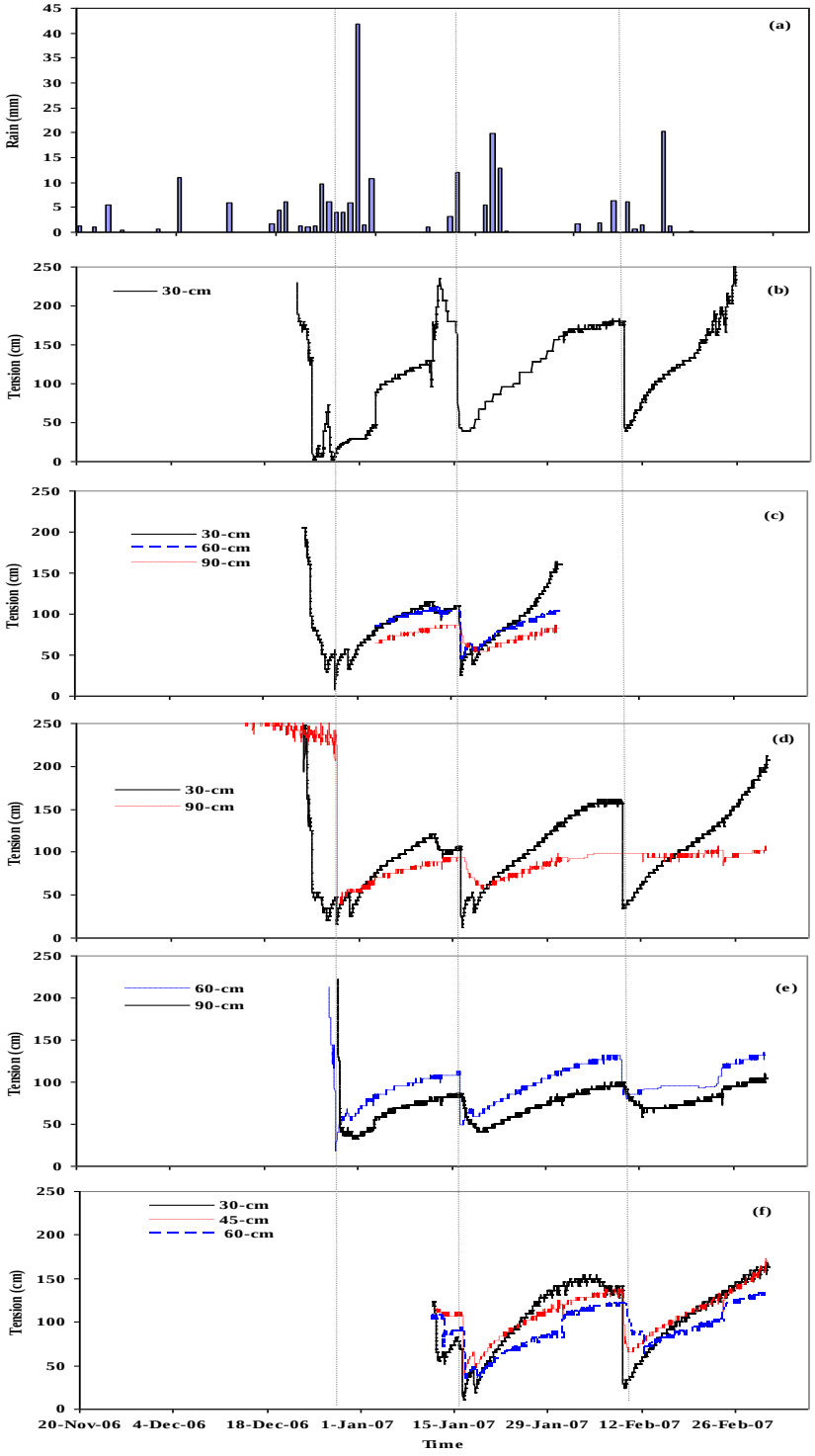

Figure 7.1 Rainfall (a) and continuous tensions data measured at different depths in a plot of each treatment: 45TD (b), 60TD (c), 90TD (d), HD (e), and FS (f).

7.2 EVALUATIONS OF THE PERFORMANCE OF WETTING FRONT DETECTORS

Exactly the same two measures of performance of wetting front detectors and hypotheses presented and discussed in Section 6.5 are used and tested in evaluating responses of WFD under a rainfall period.

7.2.1 First approach: 'YES' type of response as a measure of performance

This section ranks the performance of three lengths of Tube Detectors, HD and FS detectors to select the most sensitive design. It shows the performance of each design of a wetting front detector in response to the irrigation events described in Section 7.1.1. In this case, the performance indicator is the sums across replicates of each treatment based on the 'YES' type of responses recorded by each WFD designs over the 15 measurement dates during the rainfall period, i.e. measurements taken the next day after rain. These data sets therefore mainly tested hypotheses (i), (ii) and (iii) to select a WFD design (See Section 6.5), which records the most wetting event fronts.

The numbers of 'YES' type of responses recorded by a WFD design installed at different depths below the soil surface were evaluated based on the criteria discussed in Section 6.5.1. The differences in the numbers of 'YES' responses observed at depths 30, 60 and 90 cm with the various WFD designs as shown in Tables 7.1 and 7.2 were examined using the GLM procedure of SAS software (SAS Institute, 1999-2001) and mean was compared using the t Tests (LSD) at 5% probability level and shown in Tables 7.3, 7.4, 7.5 and 7.6.

Table 7.1 Summary of the number of 'YES' responses in a Tube and Hybrid Detectors (summed across the 3 replicates of each treatment).

	DE			**Fine sand**		
	Depth (cm)			**Depth (cm)**		
Type	**30**	**60**	**90**	**30**	**60**	**90**
45TD	11	3	5	6	2	1
60TD	16	7	6	8	2	1
90TD	15	9	5	13	11	8
	Soil*			**Fine sand**		
HD	4	3	3	7	6	3

Table 7.2 Summary of the number of 'YES' responses in the FullStop™ detectors (summed across the 3 replicates of the FS treatment).

	DE				Filter sand			
	Depth (cm)				Depth (cm)			
Type	**15**	**30**	**45**	**60**	**15**	**30**	**45**	**60**
FS	6	6	5	3	9	5	4	3

Table 7.3 Mean 'YES' responses as affected by Tube Detector length.

Length-cm	**Mean 'YES' responses at three depths**		
	30 cm	**60 cm**	**90 cm**
90	5.0a	3.5a	3.3a
60	4.0ab	1.4b	1.2b
45	2.7b	1.1b	1.0b

Notes: column response means followed by the same lower case letter are not significantly different ($P > 0.05$); column response means followed by different lower case letter are significantly different ($P \leq 0.05$).

Table 7.4 Mean 'YES' responses as affected by wick type.

Wick type	**Mean 'YES' responses at three depths**		
	30 cm	**60 cm**	**90 cm**
DE	4.8a	2.1a	2.2a
Fine sand	3.0a	1.8a	1.4a

Notes: column response means followed by the same lower case letter are not significantly different ($P > 0.05$); column response means followed by different lower case letter are significantly different ($P \leq 0.05$).

Table 7.5 Mean of 'YES' responses as affected by Tube Detector treatments.

Type	Mean 'YES' responses at three depths		
	30 cm	**60 cm**	**90 cm**
90TD-Fine sand	4.7ab	4.0a	3.7a
90TD-DE	5.3a	3.0ab	3.0a
60TD-Fine sand	2.7ab	0.8d	0.3b
60TD-DE	5.3a	2.3bc	2.0ab
45TD-Fine sand	2.0b	1.2cd	0.3b
45TD-DE	3.7ab	1.0d	1.7ab

Notes: column response means followed by the same lower case letter are not significantly different ($P > 0.05$); column response means followed by different lower case letter are significantly different ($P \leq 0.05$).

Table 7.6 Mean of 'YES' responses as affected by WFD treatment type at the three depths.

Type	Mean 'YES' responses at three depths		
	30 cm	**60 cm**	**90 cm**
90TD-Fine sand	4.7ab	4.0a	3.7a
90TD-DE	5.3a	3.0ab	3.0ab
60TD-Fine sand	2.7abc	0.7c	0.3c
60TD-DE	5.3a	2.3bc	2.0abc
45TD-Fine sand	2.0bc	0.7c	0.3c
45TD-DE	3.7abc	1.0c	1.7abc
HD-Fine sand	2.3bc	2.0bc	1.0bc
HD-Soil*	1.3c	1.0c	1.0bc
FS-DE	2.0bc	1.0c	-
FS-Filter sand	1.7c	1.0c	-

Notes: column response means followed by the same lower case letter are not significantly different ($P > 0.05$); column response means followed by different lower case letter are significantly different ($P \leq 0.05$); dash (-) in the 90 cm depth column indicates there was no FS detector installed at this depth.

Based on the result summary (Tables 7.1 and 7.2) and the statistical analyses of length effect (Table 7.3), wick effect (Table 7.4) on the mean 'YES' responses and comparison of the performances among the six Tube Detector treatments (Table 7.5) and the ten WFD treatments (Table 7.6) are commented:

a) At the 60 and 90 cm depths, length has significant effect on the performance of Tube Detectors such that 90 cm long Tube Detector produced significantly higher mean "YES' responses than the 60 and 45 cm long Tube Detectors ($P \leq 0.05$). Therefore hypothesis (i): the 90 cm long Tube Detector is likely to record significantly higher wetting front events than the 60 and 45 cm long Tube Detectors is accepted. At the 30 cm depth, however, there is significant difference between 90 and 45 cm long Tube Detectors but not between 60 and 90 cm long Tube Detectors (Table 7.3).
b) Table 7.4 shows that wick type has no significant effect on the mean 'YES' responses of Tube Detectors in all the three depths ($P > 0.05$). Therefore hypothesis (ii) that states DE filled Tube Detector is likely to record wetting event fronts ('YES' responses) significantly more often than those filled with Fine sand is rejected (Table 7.4).
c) Table 7.5 shows that at the 30 cm depth, there is no significant difference between the six Tube Detector treatments ($P > 0.05$) where as the mean 'YES' response in the 90 cm long Tube Detector filled with fine sand is significantly higher than the 60 and 45 cm long Tube Detectors at depths 60 and 90 cm but no significant differences between the three Tube Detectors filled with DE at the latter two depths.
d) Table 7.6 shows that at 30 cm depth, only the 90 cm long Tube Detector filled with DE has significantly higher mean 'YES' responses than the FS or HD designs. At the 60 for FS and at depths of 60 and 90 cm for HD, only the 90 cm long Tube Detectors filled with Fine sand has significantly higher mean responses than the FS or HD designs ($P \leq 0.05$). These results therefore show the range of wetting fronts created at the lower two depths were not quite adequate to discriminate between Tube Detectors filled with DE and the FS or HD designs.

7.2.2 Second approach: Performance against a theoretical sensitivity ranges of WFD

This approach evaluates the WFD performances against (1) the theoretical sensitivity ranges of each design (45TD, 60TD, 90TD and HD) and (2) empirically determined sensitivity of the FS design in response to the rainfall period described in Section 7.1.1. In this case,

performance indicators are the sums of replicates of each treatment based on the four categories of responses: TP, TN, FP and FN responses recorded by each of the five WFD designs over the 15 rainfall events. This data set mainly tests the fourth hypothesis (iv) associated with the applicability of a WFD for a measurement of tension based wetting front within its detection ranges (see Section 6.5). The WFD design that measures tension of a wetting front with no drift in accuracy from its sensitivity range will be best suited for the intended purpose.

7.2.2.1 *Response types of wetting front detectors*

Response types and definitions described in Section 6.5.2.1 are used for evaluating performances in the FS, TD and HD detectors measured or observed during the rainfall period.

7.2.2.2 *Tension sensitivities of wetting front detectors*

The effects of measurement accuracy due to instrument error and uncertainty in measurements (e.g. spatial variability in tensiometer readings) on the tension sensitivity values of WFD are discussed in Section 6.5.2.2. The measurement accuracy of the pressure transducer gauge generally fell within ± 1.0 cm. The error ranges due to uncertainty in tension measurements are calculated between ± 6 and ± 8 cm (See Section *Uncertainty in tension measurements below*). In other words, the measurement error ranges of tensions within the operating range of wetting front detectors are generally within ± 7 to ± 9 cm.

Accuracy of manual pressure transducer gauge

The measured tensions were within ± 1.0 cm of the height of water column in each tensiometer tube (See Section 6.5.2.2).

Uncertainty in tension measurements

Figures 7.2 and 7.3 provide the uncertainty in tension for the bulk soil measurements and measurements in each of the contact materials using error bars. Based on the 15 measurements days taken during the rainfall period, the mean tensions in the bulk soil, DE and Fine sand with their corresponding standard error values are presented for each depth. In these figures, the error bars are quite small in most of the cases especially after the largest rainfall event (29-Dec-06). The error bars are, however, relatively large for tensions measured before this large rain event.

The methods of averaging tensions in the bulk soil, DE and Fine sand and calculating standard errors for the data measured during the rainfall period is similar to the one described in Section 6.5.2.2. This data set is used for illustrating uncertainty in tension measurements during a rainfall period. In general, the averaged standard errors calculated from this data set range from ± 6 to ± 8 cm during the wet period and ± 11 to ± 37 cm in the dry period (Table 7.7). For convenience, dry and wet periods represent measurements taken before and after the largest rain event respectively.

Table 7.7 Statistical summaries of uncertainty in tension measurements

Soil material	**Period**	**Depth and standard error (SE)**			**Average SE**
		30-cm	**60-cm**	**90-cm**	
Bulk soil	Wet	11	7	7	8
	Dry	40	31	38	36
DE	Wet	8	5	4	6
	Dry	23	24	64	37
Fine sand	Wet	5	9	4	6
	Dry	5	9	20	11

Table 7.7 indicated a low spatial variability in tensions measured in the wet periods and a relatively high spatial variability of tensiometer readings during the dry periods. This suggests that the evaluation procedures for a response of a wetting front detector based on a tension measured in the bulk soil must allow for these tension error measurements (Table 7.7).

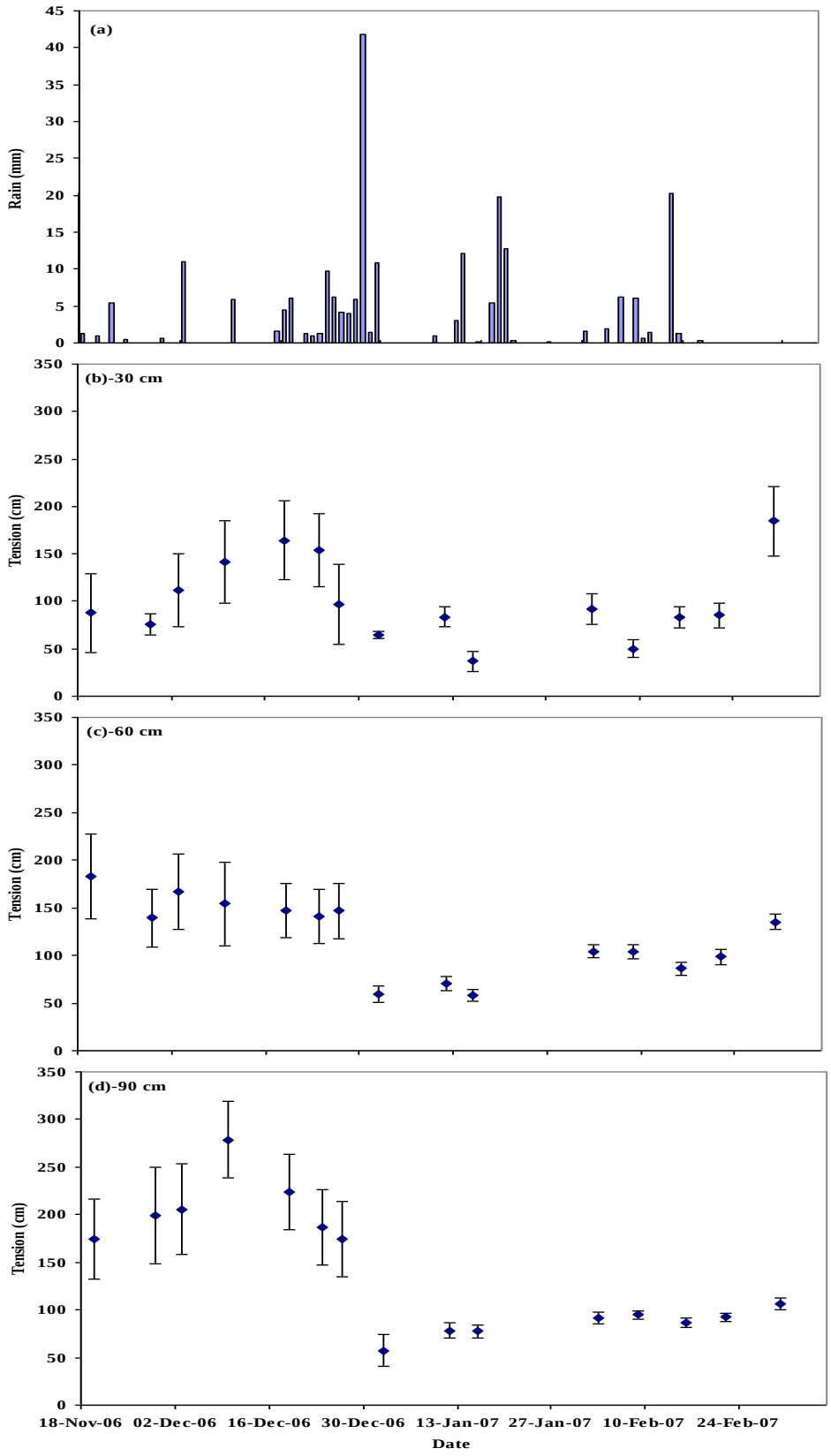

Figure 7.2 Averaged tensions measured in the bulk soil across 15 plots (b to d) with error bars at depths 30, 60 and 90 cm in response to rain (a).

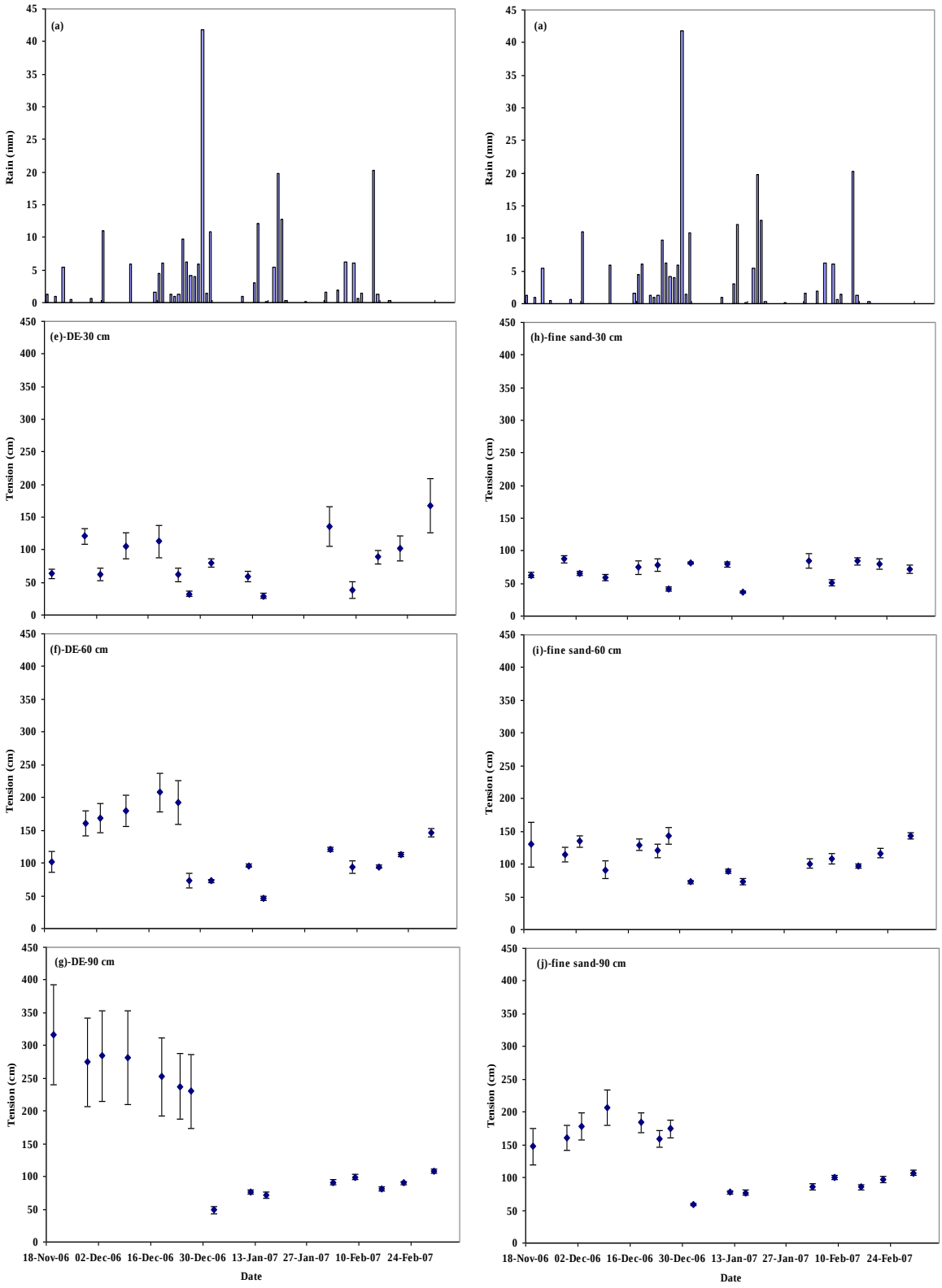

Figure 7.3 Averaged tensions measured in DE across 9 plots (e to g) and Fine sand across 12 plots (h to i) with error bars at depths 30, 60 and 90 cm in response to rain (a).

7.2.2.3 *Performance evaluations with respect to tension sensitivities of WFD*

This section presents the numbers of responses recorded by the various types of wetting front detectors in response to a change in tensions measured in the bulk soil. The responses were evaluated such that the numbers of responses of each type discussed in section 6.5.2.1 are determined. This section gives type and numbers of responses of each treatment: 90TD, 60TD, 45TD, FS and HD evaluated over the 15 measurement dates. In this part, TP, FP, TN and FN are evaluated against the tension sensitivity limits of each design, illustrated for one replication of each 90TD, FS and HD treatments (Figs. 7.4 to 7.6) and summarized in Table 7.8.

Table 7.8 Response summaries of Figs. 7.4, 7.5 and 7.6

Detector-wick/filter-depth	**Response numbers and types**				**Detection (%)**
	TP	**TN**	**FP**	**FN**	
90 cm Tube Detector					
90TD1-DE-30cm	6	7	1	1	86
90TD1-DE-60cm	3	10	1	0	100
90TD1-DE-90cm	2	12	0	1	67
90TD1-Fine sand-30cm	4	10	0	1	80
90TD1-Fine sand-60cm	2	11	1	1	67
90TD1-Fine sand-90cm	4	11	0	0	100
FullStop detector					
FS1-DE-15cm	3	12	0	0	100
FS1-DE-30cm	2	13	0	0	100
FS1-DE-45cm	1	14	0	0	100
FS1-DE-60cm	1	14	0	0	100
FS1-Filter sand-15cm	4	11	0	0	100
FS1-Filter sand-30cm	2	13	0	0	100
FS1-Filter sand-45cm	1	14	0	0	100
FS1-Filter sand-60cm	1	14	0	0	100
Hybrid Detector					
HD1-Fine sand-30cm	1	13	0	1	50
HD1-Fine sand-60cm	1	14	0	0	100
HD1-Fine sand-90cm	1	14	0	0	100
HD1-Soil*-30cm	2	13	0	0	100
HD1-Soil*-60cm	0	14	0	1	0
HD1-Soil*-90cm	0	15	0	0	-

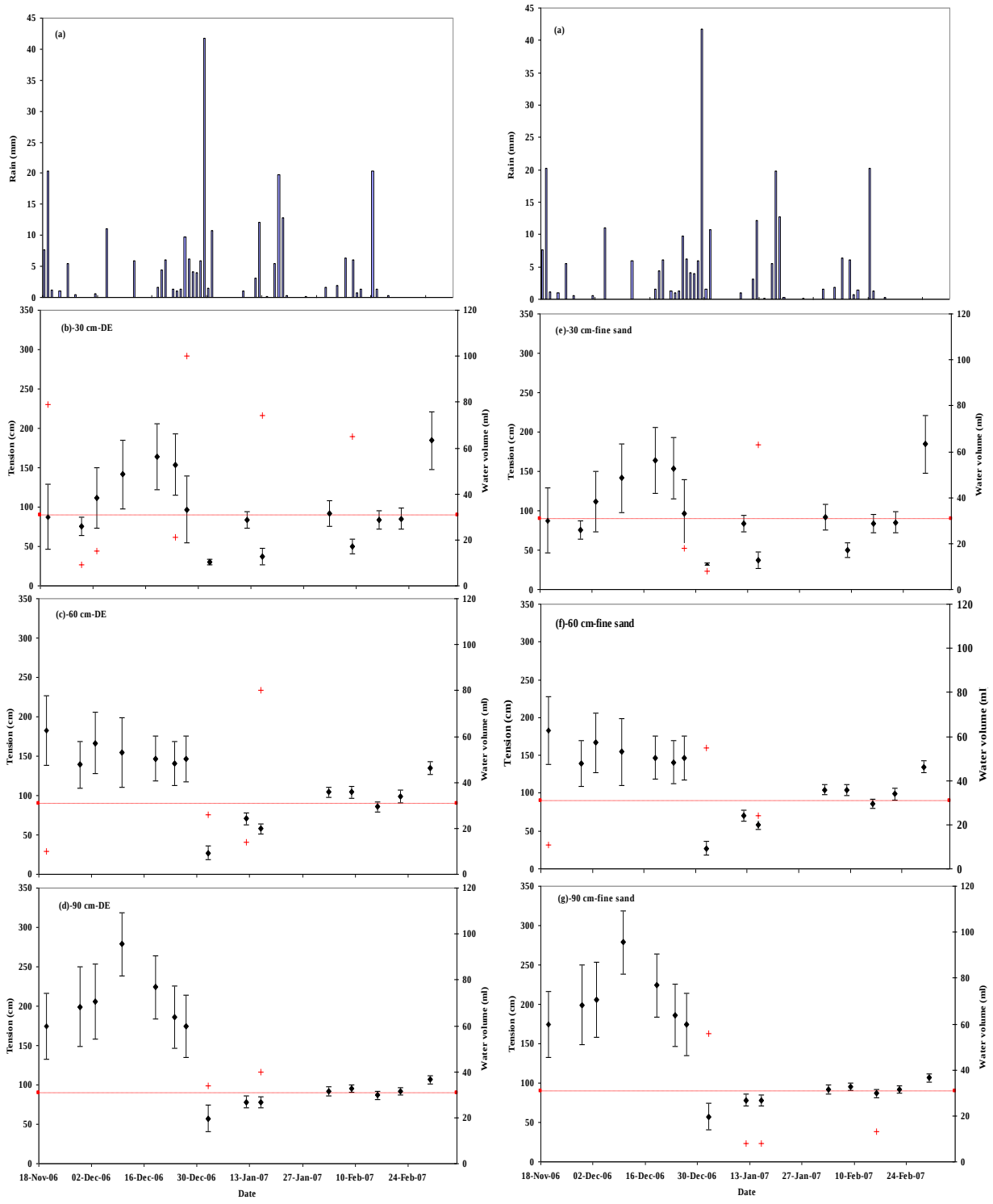

Figure 7.4 True positive response (+) represents water volume > 7 ml, false negative responses (circles), mean bulk soil tensions with error bars, and tension sensitivity (dotted line) for one selected replication of a 90 cm long Tube Detector filled with DE (b to d) and Fine sand (e to g) at depths 30, 60 and 90 cm in response to rain (a).

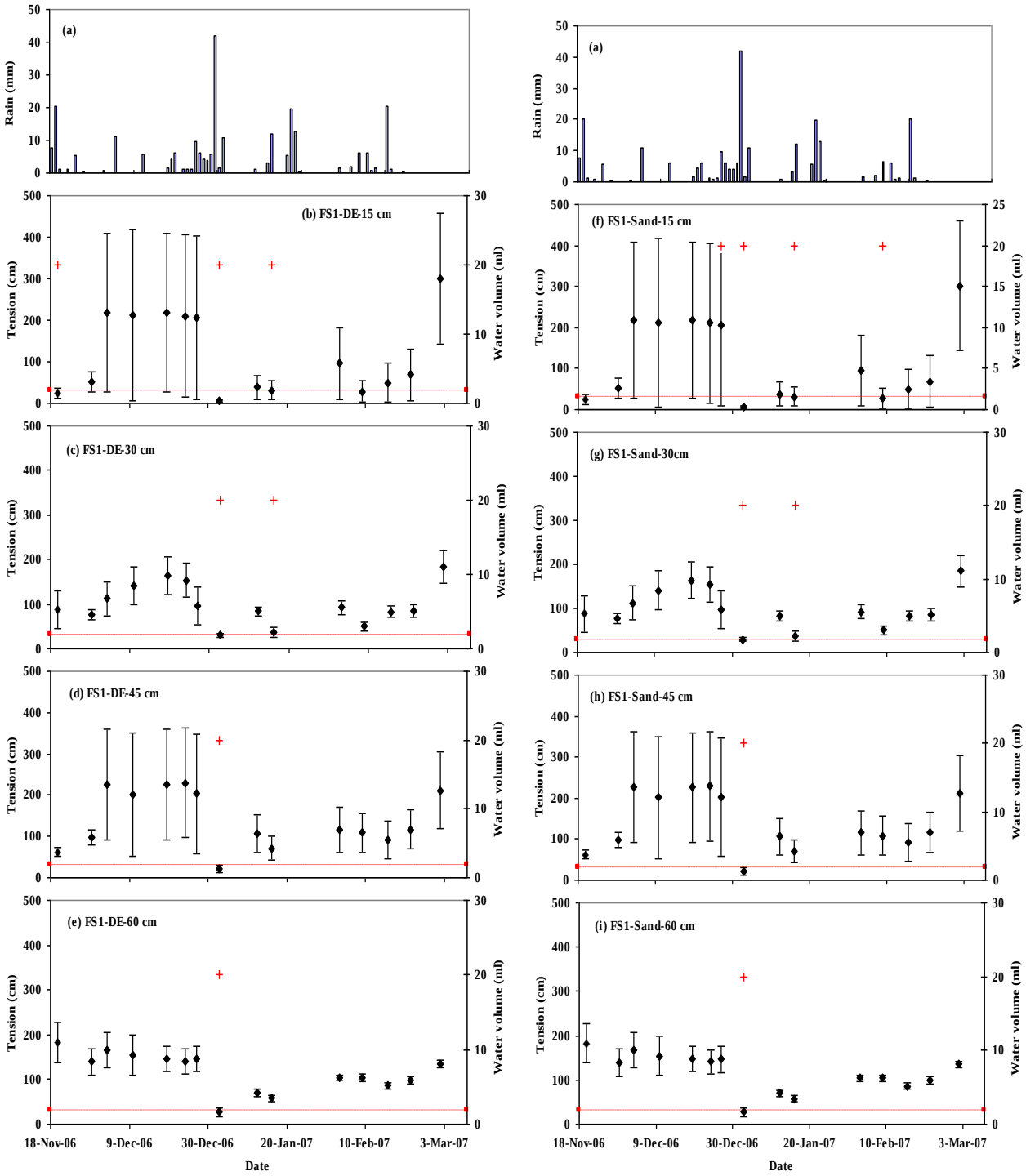

Figure 7.5 True positive response (+) represents water volume > 20 ml, mean bulk soil tensions with error bars, and tension sensitivity (dotted line) for one selected replication of the FS detector filled with DE (b to e) and filter sand (f to i) at depths 15, 30, 45 and 60 cm in response to rain (a).

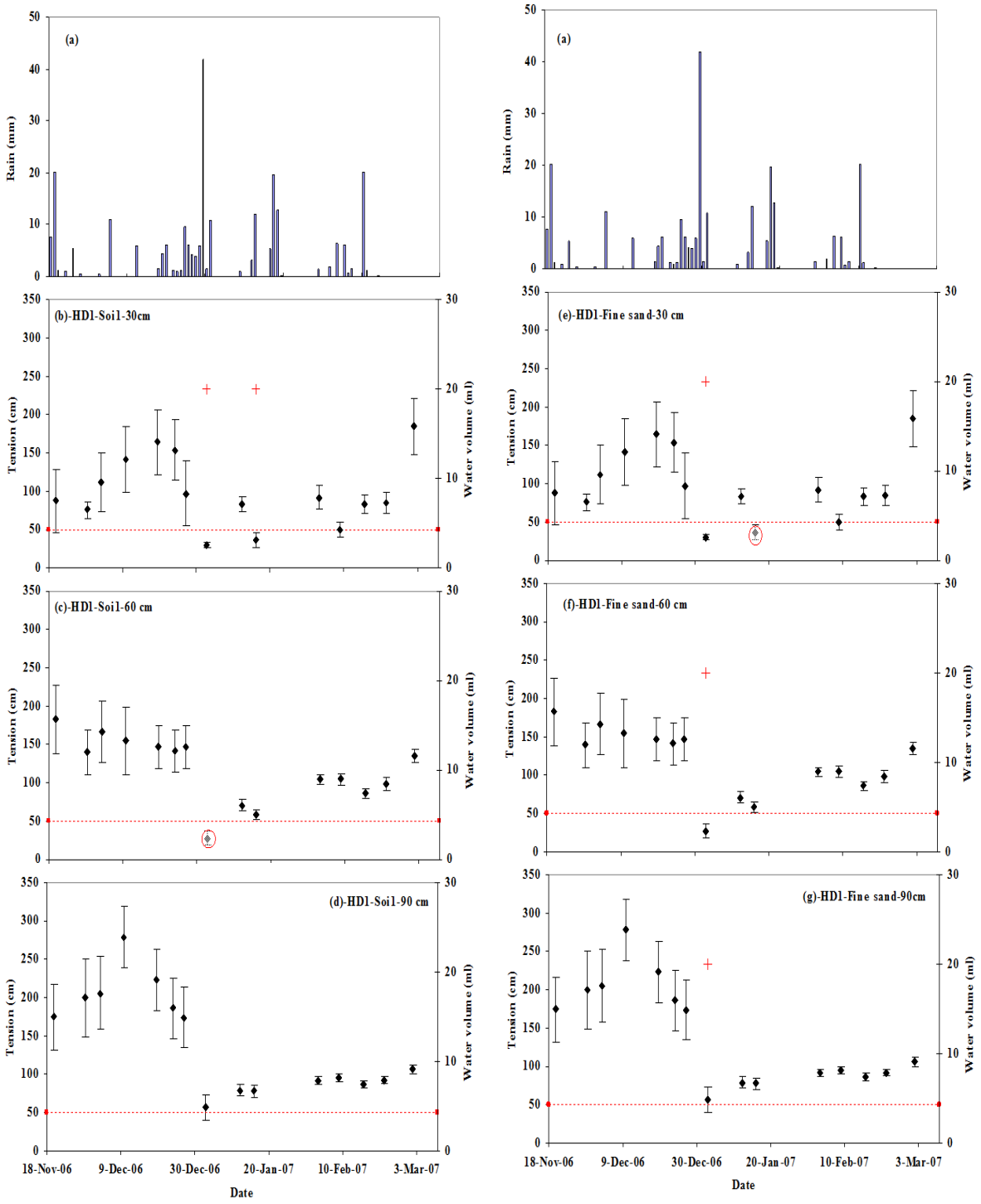

Figure 7.6 True positive response (+) represents water volume > 20 ml, mean bulk soil tensions with error bars, and tension sensitivity (dotted line) for one selected replication of a Hybrid Detector filled with soil (b to d) and Fine sand (e to g) at depths 30, 60 and 90 cm in response to rain (a).

Testing a statistical significance for the observed differences in WFD responses

Following the illustrations (Fig.7.4 to 7.6, Table 7.8), the numbers of responses of each treatment of a wetting front detector replicated three times are summarized.

Table 7.9 Response summaries of figures in Appendix 3a to o

Detector-wick/filter-depth	Response numbers and types				Detection (%)
	TP	TN	FP	FN	
90 cm Tube Detector					
90TD-DE-30cm	15	26	1	3	83
90TD-DE-60cm	9	34	0	2	82
90TD-DE-90cm	8	35	1	1	90
90TD-Fine sand-30cm	13	29	1	2	87
90TD-Fine sand-60cm	10	31	2	2	83
90TD-Fine sand-90cm	10	32	1	2	83
60 cm Tube Detector					
60TD-DE-30cm	10	29	6	0	100
60TD-DE-60cm	3	38	4	0	100
60TD-DE-90cm	2	39	4	0	100
60TD-Fine sand-30cm	8	37	0	0	100
60TD-Fine sand-60cm	0	43	2	0	-
60TD-Fine sand-90cm	0	44	1	0	-
45 cm Tube Detector					
45TD-DE-30cm	7	34	4	0	100
45TD-DE-60cm	0	42	3	0	-
45TD-DE-90cm	0	40	5	0	-
45TD-Fine sand-30cm	4	39	2	0	100
45TD-Fine sand-60cm	0	43	2	0	-
45TD-Fine sand-90cm	0	44	1	0	-
FullStop detector					
FS-DE-15cm	6	38	0	1	86
FS-DE-30cm	6	39	0	0	100
FS-DE-45cm	5	40	0	0	100
FS-DE-60cm	3	42	0	0	100
FS-Filter sand-15cm	9	36	0	0	100
FS-Filter sand-30cm	5	40	0	0	100
FS-Filter sand-45cm	4	41	0	0	100
FS-Filter sand-60cm	3	42	0	0	100
Hybrid Detector					
HD-Fine sand-30cm	2	37	5	1	67
HD-Fine sand-60cm	3	39	3	0	100
HD-Fine sand-90cm	3	42	0	0	100
HD-Soil*-30cm	2	39	2	2	50
HD-Soil*-60cm	3	41	0	1	75
HD-Soil*-90cm	3	42	0	0	100

These replications include for 15 measurement events (Appendix 7a to o) are summarized in Table 7.9. The average wetting front detection (%) at depths 30 and 60 cm within the sensitivity limit of each 90TD, 60TD, 45TD, FS and HD treatments are 84%, 100%, 100%, 100% and 72% respectively (Table 7.9).

The statistical analyses of the data in Table 7.9 using the GLM procedure of SAS software (SAS Institute, 1999-2001) and the comparisons of means using the t Tests (LSD) at 5% probability level allows drawing the following conclusions concerning the tube length (Table 7.10) and wick type (Table 7.11) effects on the deviation of each Tube Detector in measuring a wetting front. These statistical results are also used to quantify the drift in accuracy of wetting front measurements among the WFD types (Table 7.12), six Tube Detector treatments (Table 7.13) and the ten WFD treatments (Table 7.14). The following are commented based on the measurements made at the three depths (Tables 7.10, 7.11, 7.13 and 7.14) and summed over depths (Table 7.12):

1) The FN column in Table 7.10 shows a deviation in each of the 90TD, 60TD and 45TD treatments in measuring wetting event fronts within their sensitivity ranges. These tube lengths generally underestimate in measuring a wetting front that falls within their ranges by up to 16% (the drift in accuracy is calculated as 100*(FN/(TP+FN)).
2) The FN column (Table 7.10) shows that the 90 cm long Tube Detector produced significantly higher deviation than the 60 and 45 cm long Tube Detectors at the three depths ($P \leq 0.05$) but still better in measuring TP than the latter two tube lengths.
3) The FN column in Table 7.11 shows that there is no significant difference between DE and Fine sand at the three depths ($P > 0.05$).
4) From the FN and TP columns (Table 7.12), 90TD and HD designs showed deviations of 16% and 28% from their sensitivity ranges respectively, while there was no drift in accuracy in each of the 60TD, 45TD and FS detectors. Given zero to low deviations in the 90TD, 60TD, 45TD designs, it can be concluded that a length of Tube Detector can be matched to the ranges of wetting fronts to be measured. However the deviations observed in HD design needs further investigation.
5) Table 7.13 shows that the 90 cm long Tube Detector filled with either DE or Fine sand has significantly higher FN values than the 60 and 45 cm long Tube Detectors.

This means that the 90 cm long Tube Detector in this specific case underestimates the measurement of a wetting front by 14% to 20%.

6) The FN column in Table 7.14 shows that the 90TD, 60TD and 45TD in DE and/or Fine sand, and the FS detector in Filter sand and/or DE underestimates a wetting front that falls within the range of each design by 0% to 18% less from their sensitivity ranges. In the HD design filled with soil* and/or Fine sand, however, the deviation in measuring a wetting front ranges from 0% to 50%. Given the deviations in the first three designs of WFD, each of these designs can be used to measure a wetting front within their ranges. This finding therefore, supports the hypothesis (iv), which explains that the length of a Tube Detector can be matched to the tension values of wetting event fronts needed to be measured.
7) There is no significant effect of a wick material difference on the performance of the Tube Detectors of the same length, which can be seen in the TP, FP and FN columns for each of the tube lengths (Table 7.14). Wick materials therefore are reasonably staying in equilibrium with the bulk soil. In addition, no significant effect of filter material differences on the performances of FS detector.

Table 7.10 Means of TP, TN, FP and FN responses as affected by tube length

Length	Mean responses at three depths											
	30-cm				60-cm				90-cm			
	TP	TN	FP	FN	TP	TN	FP	FN	TP	TN	FP	FN
90	4.7a	9.2b	0.3a	0.8a	3.2a	10.8b	0.3a	0.7a	3.0a	11.0b	0.3a	0.7a
60	3.0b	11.0ab	1.0a	0.0b	0.5b	13.5a	1.0a	0.0b	0.3b	13.9a	0.8a	0.0b
45	1.8b	12.2a	1.0a	0.0b	0.0b	14.2a	0.8a	0.0b	0.0b	14.0a	1.0a	0.0b

Notes: column response means followed by the same lower case letter are not significantly different ($P > 0.05$); column response means followed by different lower case letter are significantly different ($P \leq 0.05$).

Table 7.11 Means of TP, TN, FP and FN responses as affected by wick type

Wick	Mean responses at three depths											
	30-cm				60-cm				90-cm			
	TP	TN	FP	FN	TP	TN	FP	FN	TP	TN	FP	FN
DE	3.6a	9.9a	1.2a	0.3a	1.3a	12.7a	0.8a	0.2a	1.1a	12.6a	1.1a	0.2a
Fine sand	2.8a	11.7a	0.3a	0.2a	1.1a	12.9a	0.7a	0.3a	1.1a	13.4a	0.3a	0.2a

Notes: column response means followed by the same lower case letter are not significantly different ($P > 0.05$); column response means followed by different lower case letter are significantly different ($P \leq 0.05$).

Table 7.12 Means of TP, TN, FP and FN responses as affected by WFD type

WFD type	TP	TN	FP	FN
90TD	3.6a	10.3ac	0.4ab	0.7a
60TD	1.8b	12.2b	1.0a	0.0c
HD	0.8b	13.0ab	0.9b	0.3b
FS	1.1b	13.6a	0.3b	0.0c
45TD	0.9b	13.2ab	0.9a	0.0c

Notes: Column response means followed by the same lower case letter are not significantly different ($P > 0.05$); column response means followed by different lower case letter are significantly different ($P \leq 0.05$).

Table 7.13 Means of TP, TN, FP and FN responses of Tube Detector treatments

Wick	Mean responses at three depths											
	30-cm				60-cm				90-cm			
	TP	TN	FP	FN	TP	TN	FP	FN	TP	TN	FP	FN
90TD-DE	5.0a	8.7b	0.3ab	1.0a	3.0a	11.3cd	0.0b	0.7a	2.7a	11.3bc	0.3a	0.7a
90TD-Fine sand	4.3ab	9.7ab	0.3ab	0.7a	3.3a	10.3d	0.7ab	0.7a	3.3a	10.7c	0.3a	0.7a
60TD-DE	3.3abc	9.7ab	2.0a	0.0b	1.0b	12.7bc	1.3a	0.0b	0.7b	13.0ab	1.3a	0.0b
60TD-Fine sand	2.7bc	12.3a	0.0b	0.0b	0.0b	14.3a	0.7ab	0.0b	0.0b	14.7a	0.3a	0.0b
45TD-DE	2.3bc	11.4ab	1.3ab	0.0b	0.0b	14.0ab	1.0ab	0.0b	0.0b	13.3ab	1.7a	0.0b
45TD-Fine sand	1.3c	13.0a	0.7ab	0.0b	0.0b	14.3a	0.7ab	0.0b	0.0b	14.7a	0.3a	0.0b

Notes: column response means followed by the same lower case letter are not significantly different ($P > 0.05$); column response means followed by different lower case letter are significantly different ($P \leq 0.05$).

Table 7.14 Means of TP, TN, FP and FN responses of all WFD treatments

Wick	Mean responses at three depths											
	30-cm				60-cm				90-cm			
	TP	TN	FP	FN	TP	TN	FP	FN	TP	TN	FP	FN
90TD-DE	5.0a	8.7b	0.3ab	1.0a	3.0a	11.3cd	0.0b	0.7a	2.7a	11.3bc	0.3a	0.7a
90TD-Fine sand	4.3ab	9.7ab	0.3ab	0.7a	3.3a	10.3d	0.7ab	0.7a	3.3a	10.7c	0.3a	0.7a
60TD-DE	3.3abc	9.7ab	2.0a	0.0b	1.0b	12.7bc	1.3a	0.0b	0.7b	13.0ab	1.3a	0.0b
60TD-Fine sand	2.7bc	12.3a	0.0b	0.0b	0.0b	14.3a	0.7ab	0.0b	0.0b	14.7a	0.3a	0.0b
45TD-DE	2.3bc	11.4ab	1.3ab	0.0b	0.0b	14.0ab	1.0ab	0.0b	0.0b	13.3ab	1.7a	0.0b
45TD-Fine sand	1.3c	13.0a	0.7ab	0.0b	0.0b	14.3a	0.7ab	0.0b	0.0b	14.7a	0.3a	0.0b
HD-Fine sand	0.7e	13.3a	0.7abc	0.3bc	1.0b	13.0ab	1.0a	0.0b	1.0b	14.0a	0.0a	0.0b
HD-Soil*	0.7e	13.6a	0.0c	0.7ab	1.0b	13.7ab	0.0a	0.3ab	1.0b	14.0a	0.0a	0.0b
FS-DE	2.0cde	13.0a	0.0c	0.0c	1.0b	14.0ab	0.0a	0.0b	-	-	-	-
FS-Filter sand	1.7cde	13.3a	0.0c	0.0c	1.0b	14.0ab	0.0a	0.0b	-	-	-	-

Notes: column response means followed by the same lower case letter are not significantly different ($P > 0.05$); column response means followed by different lower case letter are significantly different ($P \leq 0.05$).

7.3 CONCLUSIONS

Length has significant effect on the performance of Tube Detectors such that a 90TD has significantly higher mean 'YES' responses than the 60TD and 45TD designs at depths 60 and 90 cm ($P \leq 0.05$). This finding supports hypothesis (i) that states the 90TD is likely to record significantly higher wetting front events ('YES' responses) than the 60TD and 45TD designs. But, only a 90TD filled with Fine sand has significant mean 'YES' responses than the 60TD and 45TD filled with the same wick material at 60 and 90 cm depths ($P \leq 0.05$). At the 30 cm depth, however, there is no significant difference among the Tube Detector treatments.

There is no significant difference in the mean 'YES' responses between DE and Fine sand ($P > 0.05$). Therefore, hypothesis (ii) that states DE filled Tube Detector is likely to record wetting event fronts ('YES' responses) significantly more often than those filled with Fine sand is rejected.

At the 60 cm for FS and at depths of 60 and 90 cm for HD, only the 90 TD filled with either DE and/or Fine sand has significantly higher mean 'YES' responses than the FS or HD designs ($P \leq 0.05$). At the 30 cm depth, however, only the 90TD filled with DE has significantly higher mean 'YES' responses than the FS or HD designs. The comparison between various WFD designs was only successful among some of the designs due to a very low water flux occurred during the rainfall period.

The drift in accuracy in measuring a wetting front in the 90TD, 60TD and 45TD in DE and/or Fine sand is ≤ 16%. Given the natural variation in experiments and field variability, each of these designs can be used to measure a wetting front within their ranges. Therefore hypothesis (iv), which states that the length of a Tube Detector determines the driest tension value of wetting front that can be detected. In addition, the FS detector in Filter sand and/or DE underestimates a wetting front that falls within its range by ≤ 18%. However large deviation was observed in the HD treatments that range from 28% to 50%, hence not recommended for a wetting front measurement.

CHAPTER 8

ANALYSES OF HYDRAULIC CHARACTERISTICS OF WICK AND SOIL, WICK-SOIL EQUILIBRIUM CONDITIONS AND WATER FLUX SENSITIVITIES OF WETTING FRONT DETECTORS

8.1 GENERAL

Parameterization and measurements of hydraulic properties of soil (Chapter 3) and wick materials (Chapter 4) incorporated, as part of this thesis would increase our understanding how well a Tube Detector remains in equilibrium with the bulk soil. The hydraulic conductivities of both wicks and soils from the experimental site were compared to predict the equilibrium condition between wick and soil (Section 8.2.1). In addition, a difference in specific yield between DE and Fine sand was tested if it contributes significantly to the drift in accuracy (Section 8.2.2).

Length of a Tube Detector determines its sensitivity and has been confirmed using an empirical method (Chapter 5) and field performance evaluations of Tube Detectors (Chapters 6 and 7). During the building phase of WFD prototypes, a consideration was given to limit the physical dimensions that may cause installation problems and soil disturbances (small diameter and less than a meter in length was considered). The significance of the effect of wick types on the measured contact tension was evaluated (Section 8.3).

The *in-situ* inverse results coupled with a time series tension data increases the confidence to use water fluxes estimated by the Darcy's flux method for further applications. These fluxes could then be related to the positive responses (TP) of wetting front detectors so that a minimum flux detection capacity (Section 8.4) and minimum drainage limits (Section 8.5) could be assigned for each of the WFD designs.

8.2 HYDRAULIC CHARACTERISTICS OF WICK AND SOIL MATERIAL

8.2.1 Hydraulic conductivity characteristics of a wick and soil material

Hypothesis: the equilibrium condition between a wick and soil materials can be informed from the shape of their unsaturated hydraulic conductivity curves K(h). Theoretically, a Tube Detector requires a wick material that has higher unsaturated hydraulic conductivity than a soil over the

range of its sensitivity, to ensure that water will not flow around the tube. Figure 8.1 shows that DE and Fine sand have higher K(h) than the soil over the tensions indicated on the scale. This shape of K(h) functions predicts that the wick materials should stay in equilibrium with the soil, which is also supported by the results shown in Sections 6.5.2.3 and 7.2.2.3. Therefore, the above hypothesis is accepted, which implies that the Tube Detectors used for this study were not limited by the hydraulic conductivity of a wick material over the tension sensitivity ranges of each design.

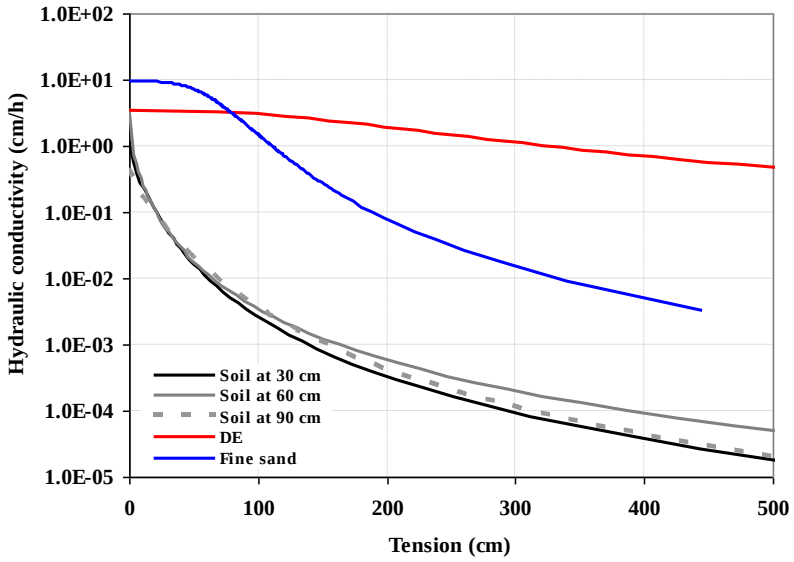

Figure 8.1 Hydraulic conductivity functions at the three soil depths (30, 60 and 90 cm) and two wick types (DE and Fine sand).

8.2.2 Specific yield of a wick material

Hypothesis: Fine sand has significantly higher mean false negative (FN) responses than DE over the operating range of a Tube Detector (Table 6.10). This may be due to Fine sand has larger specific yield than DE, i.e. the amount of water needed in Fine sand is higher than in DE to bring the wick material to saturation before a water sample can be collected in the inner tube. This causes relatively larger number of false negative responses in Fine sand than in DE. A specific yield can be predicted from a water retention characteristic as a difference between water content at saturation and water content at a given height above a water table assuming a hydrostatic equilibrium condition. The estimations from Figure 8.2 show that DE and Fine sand have

specific yields of 0.042 and 0.210 respectively at a depth to water table of 100 cm. This explains that Fine sand loses more water than DE under tensions within the operating range of Tube Detectors. This would change the K(h) of the wick material and require a volume of water to fill the contact-wick material, in addition to a water volume required to change the water level in the inner tube (0.43 cm cm^{-3}, which is calculated from a measurement of the cross-sectional area of the inner tube). This condition may be the cause of more false negative responses in Fine sand than in DE, which is evidenced in the columns of FN (Table 6.10) but statistically was found not significant. It is therefore rejected the hypothesis: Fine sand has significantly higher mean FN responses than DE within the operating range of a Tube Detector.

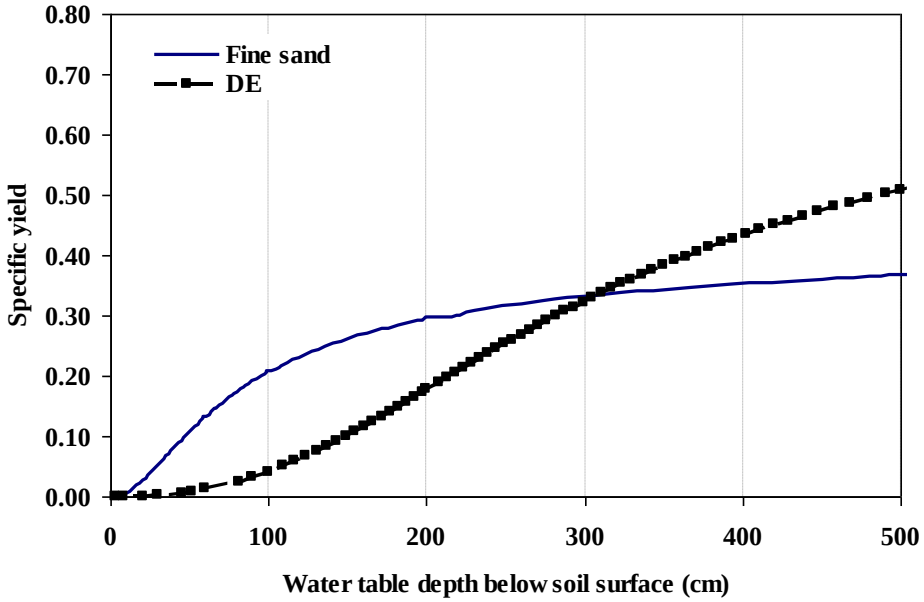

Figure 8.2 Computed specific yield in both wick materials based on the relationship between water retention data and height above a water table.

8.3 WICK-SOIL EQUILIBRIUM UNDER FIELD CONDITIONS

8.3.1 Effect of wick type and installation disturbance on a contact tension

Hypothesis: the tension in the contact wick material is the same as the bulk soil, and is not affected by the type of wick and installation disturbance.

Three different tube lengths were tested: 45, 60 and 90 cm. For each of the 45, 60 and 90 cm lengths, DE and Fine sand wick types were tested. The bulk soil tensions measured at depths 30, 60 and 90 cm in 15 plots were averaged to obtain mean tensions of each depth over the irrigation period, which are considered as reference tensions with standard error (SE) bars plotted corresponding to the wettest event of each measurement dates (Fig. 8.3).

Similarly, the contact tensions measured in the DE averaged over nine plots (three plots from each of the 90TD, 60TD and 45TD treatments) and Fine sand over 12 plots (three plots from each of the 90TD, 60TD, 45TD and HD treatments) to obtain the mean tensions at each depth over the same periods (Fig. 8.3).

The error bars indicated in Figure 8.3 show differences between a mean reference tension and mean contact tension (either DE or Fine sand) measured at the same time and depth below the soil surface. This Figure also indicates that these SE error bars shown at the three depths are small therefore low uncertainty in the data. There were few events with large SE error bars and large gaps between the means of data points measured at the same time (Fig. 8.3e and f), which might be due random measurement fluctuations. Despite these few cases, however, the SE bars between the bulk soil and wick material overlap or just touches each other, $P > 0.05$ (Cumming *et al*., 2007) therefore shows the effect of wick type on the measured contact tension is negligible. This leads to the conclusion that there was an equilibrium condition between the contact tension and the reference soil tension measured over the irrigation periods. This supports the hypothesis that states the tension in the contact wick material is the same as the bulk soil therefore not affected by the wick type and installation disturbance. The same hypothesis mentioned above was tested under a rainfall condition. All except few measurement events such as in Figure 8.4a, the SE bars do overlap hence the tensions measured in the bulk soil and wick materials were similar, $P > 0.05$.

It can also be concluded from this result that there were no effect of wick type and installation disturbance on the contact tension for the same period. This supports the effectiveness of both using auger sizes that match WFD openings and the backfilling of soil materials by compacting tightly to avoid any preferential flow to the detectors. It is expected that the reliability of the use

of detectors responses for irrigation management decision making will improve with time, and the effect of installation disturbance will likely be overcome after one season.

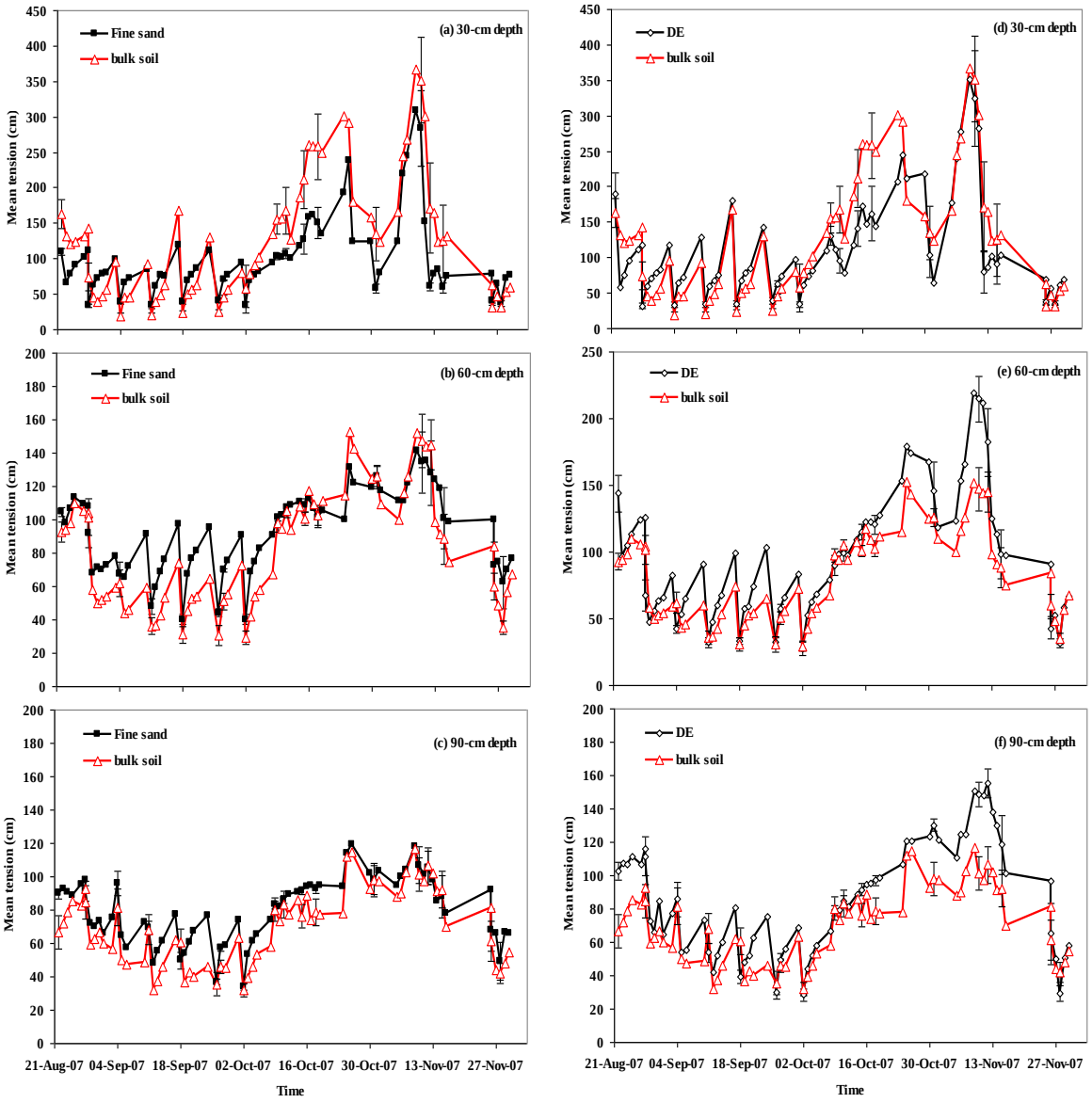

Figure 8.3 Inferences between soil tensions measured in the bulk soil and in the wick materials. Means and standard error (SE) bars for the soil tensions measured in a bulk soil across 15 plots and Fine sand across 12 plots (a to c) and bulk soil across 15 plots and DE across nine plots (d to f) measured at three depths over time during the irrigation season.

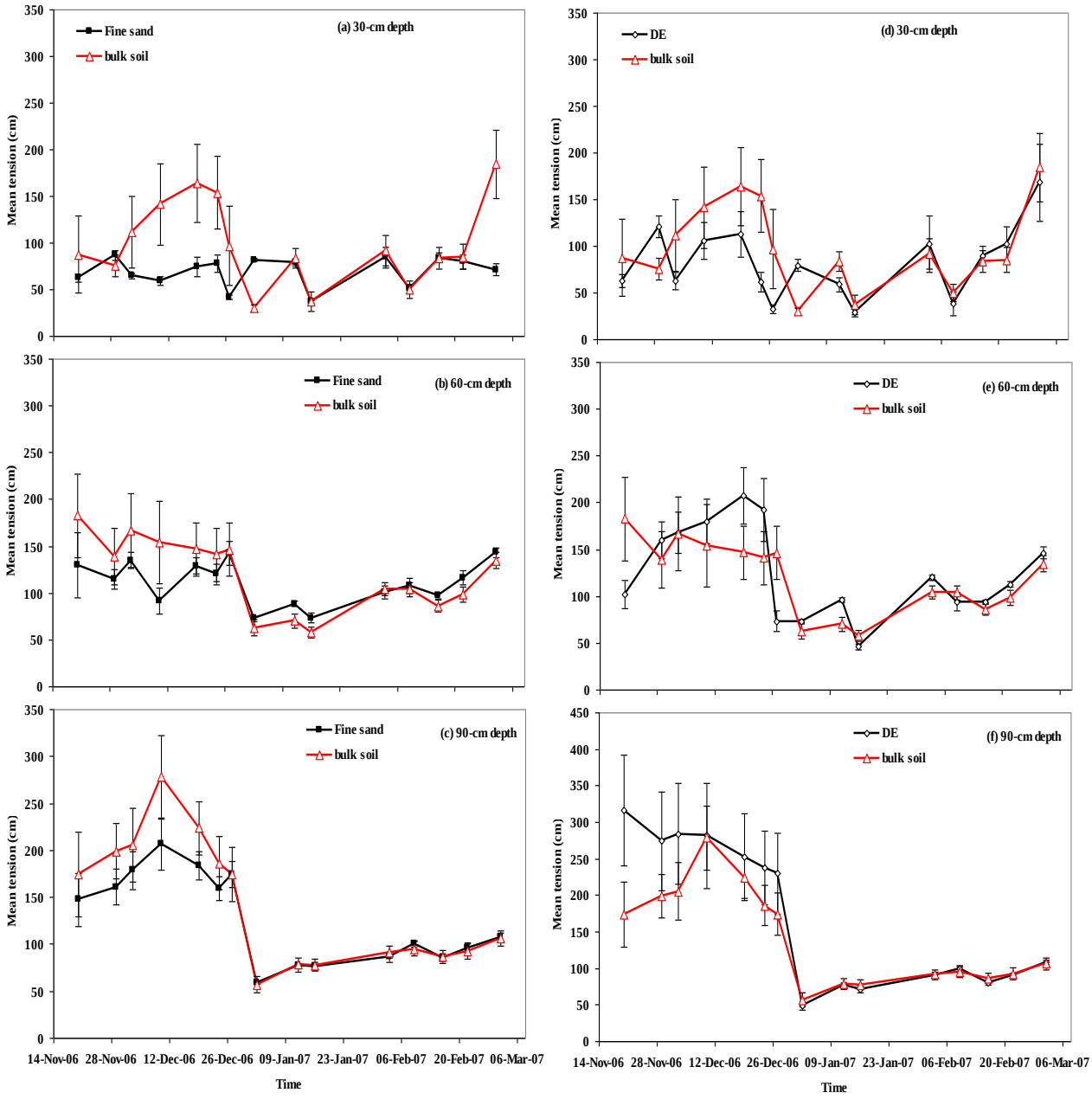

Figure 8.4 Inferences between soil tensions measured in the bulk soil and in the wick material. Means and standard error (SE) bars for the soil tensions measured in a bulk soil across 15 plots and Fine sand across 12 plots (a to c) and bulk soil across 15 plots and DE across nine plots (d to f) measured at three depths over time during the rainy season.

In summary, the analyses of factors that are potentially suggested to cause wick-soil non-equilibrium conditions hence increasing the numbers of FN responses showed that (1) there was equilibrium condition between a bulk soil tension and contact tension showing that wick type and installation disturbance have negligible effect on the contact tension therefore causing no effect on the numbers of FN responses; (2) the K(h) functions of wick materials stay higher than the bulk soil over the lengths of Tube Detectors used for this study. This shows that the hydraulic conductivity of wick materials was not limiting factor for the equilibrium between a wick and soil material; and (3) the higher specific yield of Fine sand over DE, i.e. Fine sand produced higher numbers of FN responses than in DE but statistically was found not significant to cause a non-equilibrium condition in the Tube Detector filled with the Fine sand.

8.4 SENSITIVITIES OF WETTING FRONT DETECTORS AND WATER FLUX PROFILES

8.4.1 Sprinkler irrigation

Automatic tensiometers operated from the beginning of August 2007 to the 15th of November 2007. During this period, the plots received 589.4 mm in about 85 days. *In-situ* soil hydraulic conductivities as shown (Fig. 8.1) coupled with the time series tensions measured at depths 30, 60 and 90 cm estimated the water fluxes profiles at depths 45 and 60 cm.

Considering the assumptions underlying the flux estimation, which are accurate measurements of soil tensions and *in-situ* hydraulic conductivity relationships, the estimated water fluxes are reliable. The water fluxes determined at these two depths were matched to the TP responses of WFD at similar depths obtained in one test plot of each FS, 45TD and 90TD treatment (see Section 6.5.2.3) to estimate the flux sensitivity of each design. The TP responses and water flux estimates are shown: FS (Fig. 8.5a), 45TD (Fig. 8.5b) and 90TD (Fig. 8.5c).

The lines in Fig. 8.5 represent the arrival of a range of water fluxes overtime at a specific depth. The symbols represented by ‘10’ and ‘20’ on the secondary y-axis stand for the TP type of responses in DE and Fine sand filled Tube Detectors; and for the FS detector with DE and Filter sand, respectively.

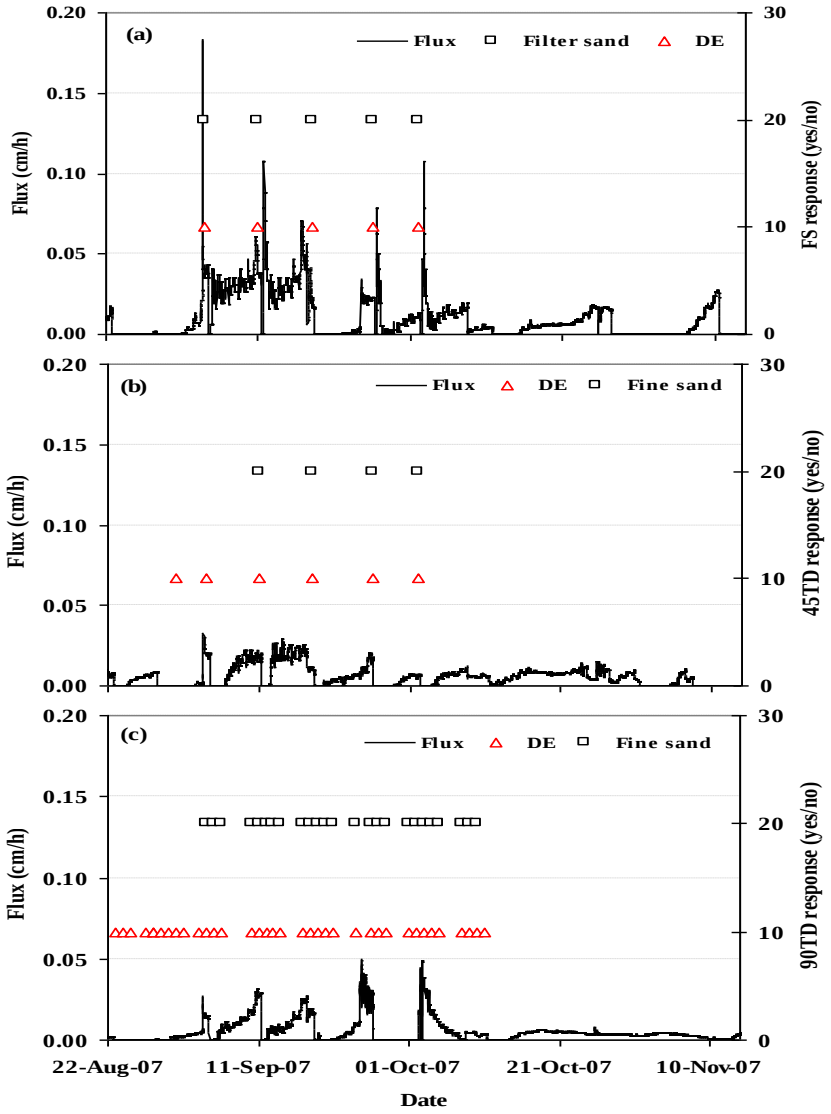

Figure 8.5 Estimated water fluxes (lines) and observed responses of WFD (symbols): (a) FS at 45 cm depth, (b) 45TD and (c) 90TD buried at 60 cm depth below the soil surface.

A blank response on the secondary y-axis for fluxes greater than zero indicates a WFD did not record the arrival of these water fluxes. The fluxes that triggered each of the TP responses in FS (Fig. 8.5a) were averaged to produce a mean flux of 0.047 cm/h and standard error (SE) of 0.007. The mean flux sensitivity values defining the TP responses observed in 45TD and 90TD are:

0.041 with SE 0.011 cm/h (Fig. 8.5b) and 0.018 with SE 0.008 cm/h (Fig. 8.5c), respectively. These mean fluxes minus the SE values calculated for each of the FS and Tube Detectors therefore are the minimum fluxes that can be recorded by each of these designs. Since the FS treatment had no tensiometer placed at 90 cm depth to estimate flux at 60 cm depth, flux shown (Fig. 8.5c) was used to estimate a minimum flux that could trigger FS detector at 60 cm depth under the assumption that fluxes calculated at 60 cm depth is similar in all plots of the WFD treatments (Fig. 8.6). This figure therefore shows fluxes in the range of 0.03 to 0.05 cm/h triggers the FS detector.

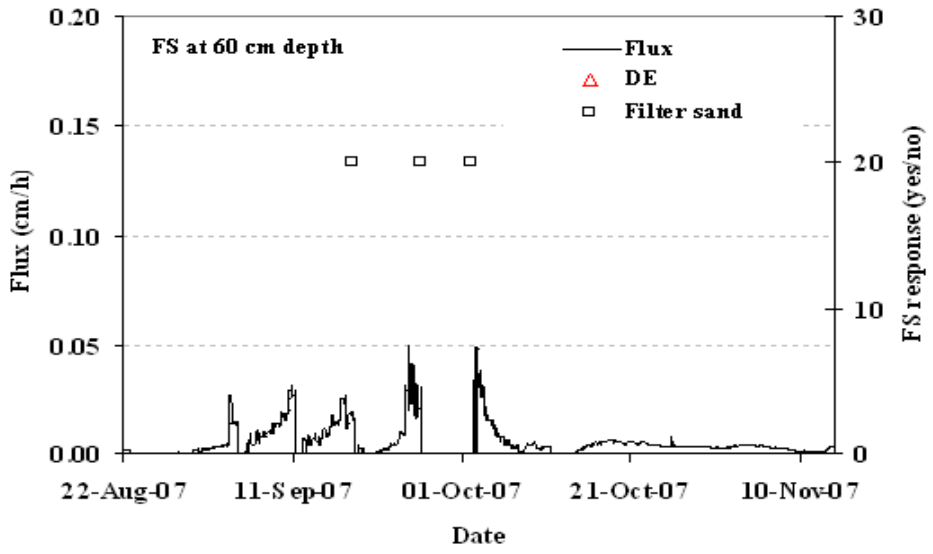

Figure 8.6 Estimated water fluxes (Fig. 7.5c) and observed responses of FS detector (symbols) at 60 cm depth in one plot of the FS treatment.

8.4.2 Rainfall

Automatic tensiometers operated from the 20-Nov-06 to 02-Mar-07. During this period, the plots received 220.1 mm in about 103 days. The water fluxes profiles are determined at depths 45 and 60 cm using the Darcy-flux estimation method (See Section 8.4.1). These water fluxes were matched to the TP responses of WFD at similar depths obtained in a plot of the FS, 60TD and 90TD treatments to estimate the flux sensitivity of each design. The TP responses and water flux estimates are shown: FS (Fig. 8.7a), 60TD (Fig. 8.7b) and 90TD (Fig. 8.7c).

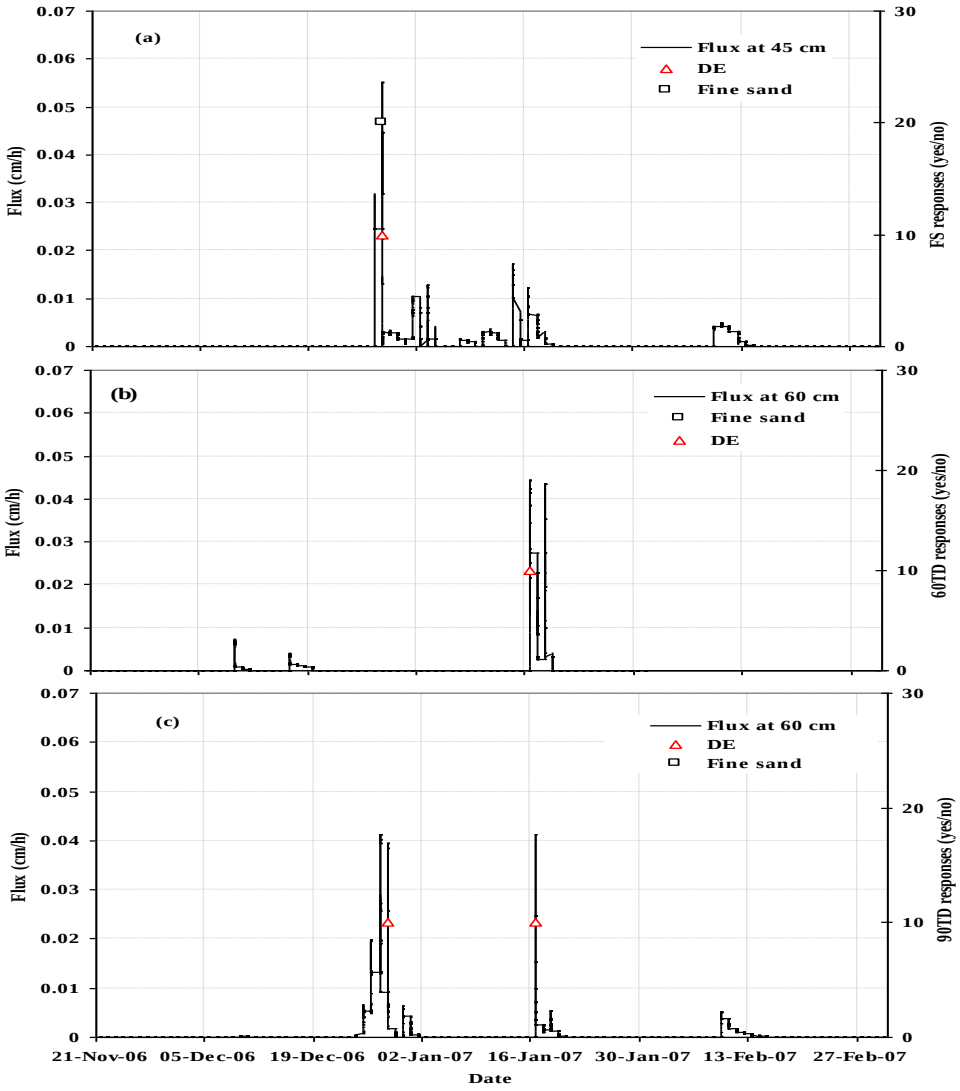

Figure 8.7 Estimated water fluxes (lines) and observed responses of WFD (symbols): (a) FS buried at 45 cm depth, (b) 60TD and (c) 90TD buried at 60 cm depth.

The lines and symbols in Fig. 8.7 are similar to the description provided in Figure 8.5. The maximum water flux corresponding to the TP response in the FS detector is 0.055 cm/h (Fig. 8.7a). The maximum water flux values at a depth of 60 cm corresponding to the TP responses observed in 60TD and 90TD include 0.044 cm/h (Fig. 8.7b) and 0.039 to 0.041 cm/h (Fig. 8.7c), respectively. The maximum water fluxes were used in the above because a note of time was not taken during the WFD response measurement periods.

8.5 DRAINAGE AND RESPONSE OF WETTING FRONT DETECTORS

8.5.1 Sprinkler irrigation

The discussion and conclusion of this section is based on the TP responses of FS at 45 cm, and 45TD and 90TD at 60 cm depths with respect to the drainage fluxes cumulated overtime at these two depths. The drainage water (Q) was calculated as the product of water flux estimated (Section 6.2.3) and a time interval of 12 minute. Summation of these individual drainages over a period of about 85 days provided an estimate of cumulative drainage water passed below depths 45 cm (8.8a) and 60 cm (Fig. 8.8b and c). These drainage results were used to determine the minimum drainage limits that can be detected by a wetting front detector.

The total irrigation amount (22-Aug-7 to 15-Nov-07) was 589.4 mm. Drainages past depths 45 and 60 cm were 35.4% and 15.3% of the total irrigation respectively (Fig. 8.8).

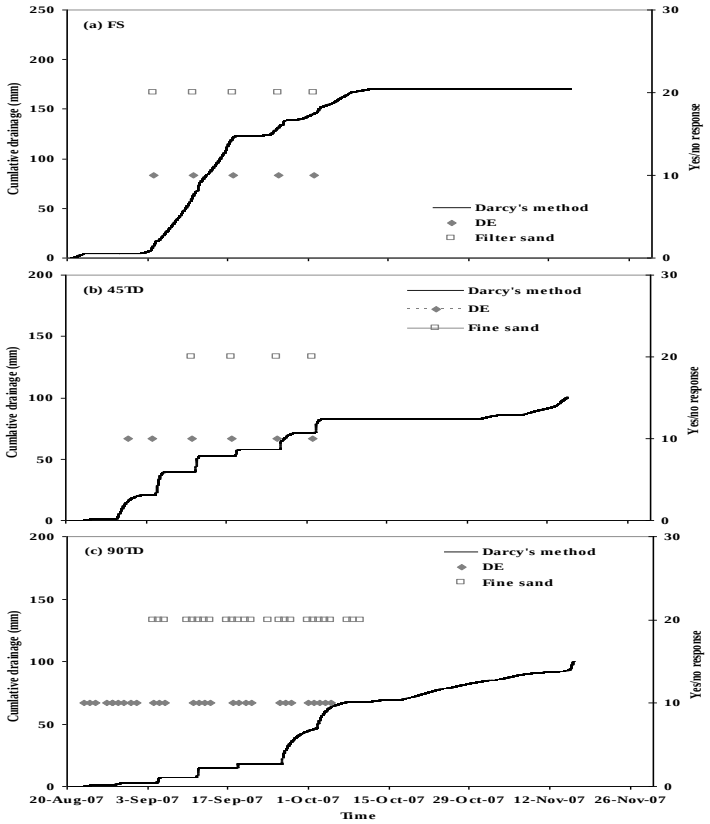

Figure 8.8 Cumulative drainage and TP responses of different WFD designs: 45 cm depth (a) and 60 cm depth (b and c).

This drainage data indicated that the FS detector could detect drainage as low as 11.8 mm/d (Fig. 8.8a), while 45 and 90 cm long Tube Detectors both at 60 cm depth can detect drainages as low as 4.8 and 2.8 mm/d respectively (Fig. 8.8b and c). These drainage rates were calculated by dividing the total amount of water drained between two successive measurement dates by the number of draining days.

8.5.2 Rainfall

The discussion and conclusion of this section is based on the TP responses of FS at 45 cm, 60TD and 90TD at 60 cm depths with respect to the drainage fluxes cumulated overtime at these two depths. The drainage water (Q) was calculated as the product of water flux estimated and a time interval of 12 minute. Summation of these individual drainages over a period of about 103 days provided an estimate of cumulative drainage water passed below depths 45 cm (8.9a) and 60 cm (Fig. 8.9b and c).

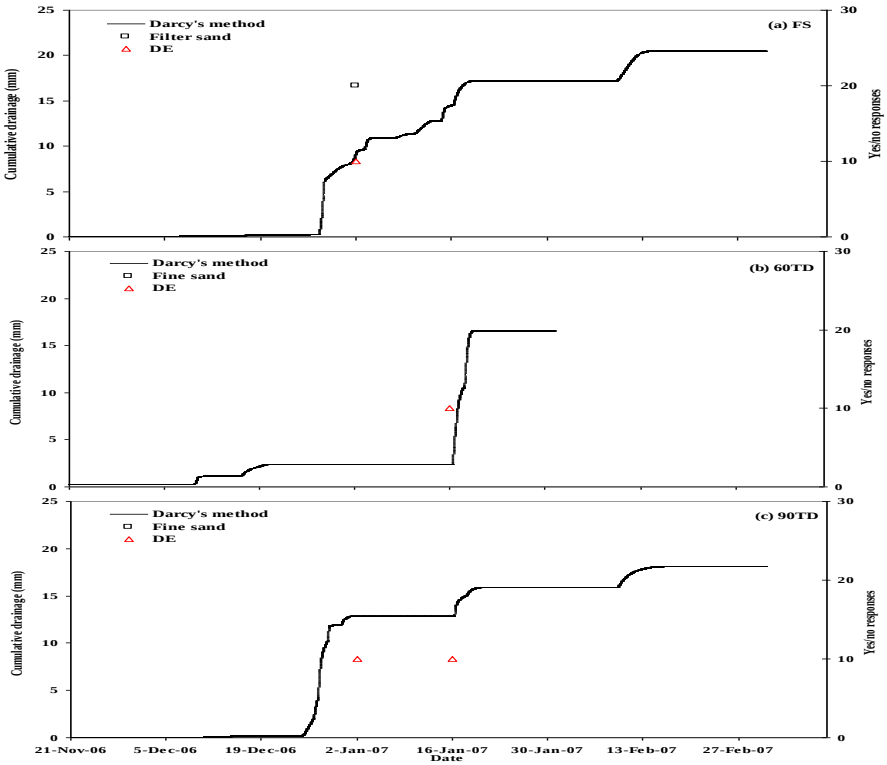

Figure 8.9 Cumulative drainage and TP responses of different WFD designs: 45 cm depth (a) and 60 cm depth (b and c).

Drainages past depths 45 and 60 cm were 9.2% and 8.3% of the total rain respectively (Fig. 8.9). This drainage data indicated that the FS detector started to respond to drainage of 2.3 mm/d (Fig. 8.9a), while 60 and 90 cm long Tube Detectors both at 60 cm depth can see drainages of 1.0 and 0.7 mm/d respectively (Fig. 8.9b and c). A set of tensiometers in 60TD plot (Fig. 8.9b) stopped working earlier than expected hence affected the shape of the curve. The low drainage rates assumed as triggering points for each of these designs could be possibly due to a relatively large time interval between two measurement events (Note that drainage rates were calculated by dividing the total amount of water drained between two successive measurement dates by the number of draining days).

In summary, the drainage estimated based on Darcy's flux method was used as reference against which the performances of wetting front detectors were judged. This is because of a reliable K(h) function and measured time series tension data. Drainage rates estimated at depths 45 and 60 cm using Darcy's method corresponding to the positive responses of FS and 90TD in sprinkler irrigation were higher than rainfall period. Based on these reference drainage rates expressed in mm/d, in this soil, a FS detector responds to drainage ranges from 2.3 to 11.8 mm/d, and a 90 cm Tube Detector responds to drainage ranges from 0.7 to 2.8 mm/d.

CHAPTER 9

SYNTHESIS OF THE THESIS

9.1 INTRODUCTION

The increasing competition for fresh water resources among various sectors of the economy calls for the development of efficient water use strategies. One way of increasing water use efficiency at field scale is to improve irrigation scheduling. Several methods are used to initiate and terminate irrigation. The most commonly used approach is to initiate irrigation when a predetermined soil water threshold is reached and then to apply a certain water volume or to irrigate for a certain time (Dabach *et al*., 2013). Since most irrigation farmers do not follow this straightforward measurement procedure, determining upper, refill and lower limits, and measuring or predicting soil water deficits may be more difficult than it appears (Stirzaker *et al., 2004*a ; Stevens *et al.*, 2005).

An alternative approach is proposed in which the objective is to refill the root zone sufficiently, while minimizing deep percolation losses, by linking the amount of water applied to the depth of penetration of a wetting front. This new approach encourages irrigators to adjust irrigation amount or interval based on response of a mechanical device, called the FullStop^{TM} Wetting Front Detector (FS WFD), to the previous irrigation event. This device can also be used to cease irrigation (automatic control mode) when a wetting front of defined soil tension or water flux reaches a set depth, i.e. when water moves from an upper to a lower soil layer (Zur *et al.*, 1994; Stirzaker, 2003). The FS WFD, hereafter called the FS, was specifically developed to be a simple affordable technology to help farmers manage water, nutrients and salt in the root zone.

The FS is a simple tool that shows the irrigator whether a wetting front of certain strength has passed a set soil depth or not. This design comprises a funnel, a filter, and a mechanical float mechanism (Stirzaker, 2008). The FS is buried in the soil within the root zone to capture a water sample from the unsaturated soil by intercepting the downward flow of the infiltrating (sharp front) or redistributing (diffuse front) water. As the water converges inside the funnel, the soil at its base increases to saturation and results in free water seeping through the screen filter into a small reservoir. The water volume collected in this reservoir triggers an indicator flag above the soil surface through a float mechanism (a sketch of the FS and its components is available in the

full thesis, Fig. 1.3).

Stirzaker and Hutchinson (2005) demonstrated the success of using an electronic version of a funnel shaped wetting front detector to irrigate turf by automatically switching off the sprinklers when the infiltrating water reached a depth of 15 cm. Stirzaker *et al* (2004a) also showed the success of the funnel shaped detector in automatic control mode for a deep rooted crop such as *Medicago sativa*, on the proviso that an appropriate irrigation interval is used. When used correctly, the FS has shown great promise in the field for water, nutrient and salt management in the root zone (Tesfamariam *et al*., 2010; van der Laan *et al*., 2010; Fessehazion *et al*., 2011).

The FS design is well suited for drip irrigation, has been used with some success under sprinkler irrigation, but is not well suited to furrow irrigation (Stirzaker *et al., 2010*). Furrow irrigation normally requires a large volume of water to be applied at one time (large wetted depth) and the fact that water cannot simply be turned off as it can be in the case of drip or sprinkler, a more sensitive design was needed to detect weak (diffuse) wetting fronts at deep placements. This dictated the direction of the new research initiated in 2005 entitled 'Adapting the wetting front detector to the needs of small scale furrow irrigators and providing a basis for the interpretation of salt and nutrient measurements from the water sample'. The present thesis entitled "Design features determining the sensitivity of wetting front detectors for managing irrigation water in the root zone," has addressed two important objectives of this project: (i), to develop and test a modified WFD for specific applications such as flood irrigation, and (ii), to define the sensitivity of different designs of WFDs.

The aims of the thesis are reiterated in this synthesis document and a summary of thesis findings is presented, guided by a flow chart (Fig. 9.1). While the focus of the thesis was on specifying WFD sensitivities, this synthesis aims to show how different WFD designs can be used in practice to schedule irrigation and hence improve water management. This is achieved with the aid of various model scenario simulations.

9.2 STRUCTURE OF SYNTHESIS

This synthesis is mainly made up of the five blocks (A, B, C, D and E) shown by the flow diagram (Fig. 9.1):

A - Thesis chapters 1 and 2 summarized the operation and functioning of passive lysimeters, based on a review of the literature (literature review), and used this knowledge to develop new WFD designs.

B - Thesis chapters 3 to 8 systematically presented experimental methodologies and results to evaluate the sensitivity of WFDs.

C - This synthesis used various WFD performance measures and/or depth of wetted soil to evaluate the efficacy of different WFD designs for irrigation scheduling.

D - The modeling part of the synthesis used the Hydrus-2D/3D model to simulate different irrigation scenarios, and

E - Makes recommendations on how to use detectors for improving irrigation management.

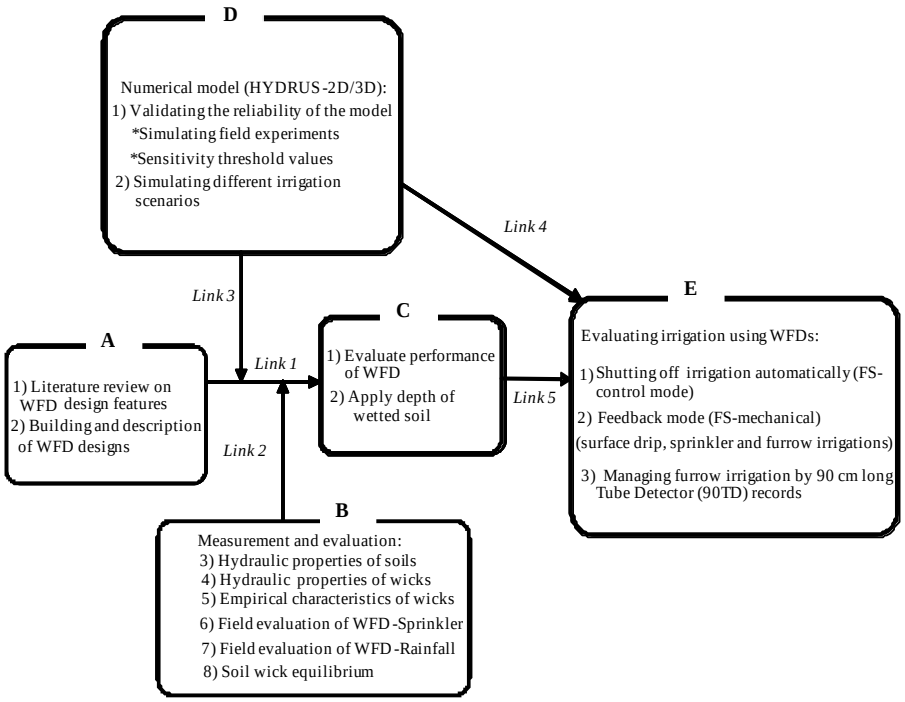

Figure 9.1 Diagram of the different components of the thesis chapters (1 and 2 of block A and 3 to 8 of block B) and model simulations including points (1 and 2 of block D and 1 to 3 of block E) as used in this synthesis for an assessment of irrigation with the WFD. Points 1 and 2 of block C serve as indicators of the performance of the WFD for scheduling irrigation.

The relationships among the various components of the flow diagram (Fig. 9.1) are described briefly as follows. If an individual component, for example 'building and description of WFD designs' is listed under point (2) within block 'A', then it is referred to as Fig. 9.1A-2 throughout this document. A similar procedure of referencing has been adopted throughout this synthesis so that the individual contents listed in each of the blocks (Fig. 9.1) can be described explicitly.

The literature review of passive lysimetery (Fig. 9.1A-1) was used to study the operation and functioning of the different components of the lysimeter so that the various WFD designs could be built and tested (Fig. 9.1A-2). Link 1 shows how WFD design features (Fig. 9.1A-1) relate to the sensitivity of detectors (Fig. 9.1C-1). Link 2 shows how various laboratory and field measurements (Fig. 9.1B) were used in order to choose the most significant design features (Fig. 9.1A-1) that determine the sensitivity of a WFD (Fig. 9.1C-1). Field evaluation of the different WFD designs for irrigation scheduling under a range of conditions is expensive and cumbersome, therefore model simulation was used. Assessment of the effect of design features on the performance of WFDs was performed through model simulation (Link 3) after validating the model by simulating field data sets (Fig. 9.1D-1). Different irrigation scenarios (Fig. 9.1D-2) were simulated to develop explicit recommendations on the deployment of WFDs for irrigation scheduling (Link 4), while depth of soil wetting (Fig. 9.1C-2) was utilized to assess whether detectors could be effectively used for irrigation scheduling (Link 5).

9.3 SUMMARY OF THESIS RESULTS

9.3.1 Purpose of the thesis

The objective of both laboratory measurements and field experimentation (described in the thesis) was to examine how design features of a WFD affect the performance of the instrument. The purposes of thesis chapters 1 and 2 were: (i) to review how design features of WFDs can be expected to determine sensitivity according to theory (literature review), and (ii) to describe the various components of WFD prototypes built and tested in the thesis and to ascertain how sensitive each design is.

A comprehensive literature study on passive lysimetry, focusing mainly on two specific design features (length and wick material), was conducted to explain how prototype WFDs should operate. The purpose of thesis chapter 3 was to show the significance of an accurately measured

unsaturated hydraulic conductivity function in defining the sensitivity of WFDs (published in Water SA Vol. 38 No. 1). Chapter 4 considered the relationship between hydraulic conductivity functions of soil and wick materials and the functioning of different WFD designs. It also examined the effect of water release curves of wick materials on the response of WFDs.

The purpose of the laboratory study and the field experiments over two seasons under sprinkler irrigation and natural rainfall, was to examine the accuracy and sensitivity of various WFD designs by exploring the association between the individual design features (length and wick) and the two modes of responses of the WFD, i.e. ON/OFF (Funnel and Hybrid versions - float indicator) and water volume collected in the inner tube (Tube Detector). Since the underlying theory of the design of a long walled Tube Detector makes it more sensitive than the short funnel shaped version, the expectation was that the tube version could measure lower water fluxes than the short funnel shaped detector. The relationship between soil-wick equilibrium and the performance of WFDs was also investigated in Chapter 8.

9.3.2 A summary of thesis findings

In the thesis summary, the results of the studies based on laboratory and field experimentation (Link 2) are discussed in relation to the design features and performance of WFDs (Link 1), following the relationships in the diagram.

9.3.2.1 *Design features and performance of wetting front detectors*

In the literature review (Fig. 9.1A-1), a tube shaped WFD that counteracts capillary emptying and a high wick hydraulic conductivity that conducts water easily from the soil to the base of the tube were identified as the most significant design features that determine the sensitivity of a WFD.

The two design features identified (Fig. 9.1A-1) were combined with the practicality of the device in the field, for example, less than a metre long in order to minimize installation problems (Fig. 9.1A-2). These prototypes include a Tube version comprising two concentric tubes with different outer tube lengths and a Hybrid version that comprises partly the Tube version and some features from the funnel shaped WFD. The Hybrid had a larger diameter funnel than a Tube Detector to increase convergence and hence response time, but also a straight-sided tube

section (tube length) to increase sensitivity. The effects of wick type and length of the WFD designs on the performance of the WFDs (Fig. 9.1C-1) are discussed in section 9.3.2.2 using the experimental data (Fig. 9.1B-3, B-4 and B-5).

9.3.2.2 *Hydraulic properties of wick and soil materials and performance evaluation of WFDs*

The WFD prototypes require a wick material characterized by 1) higher wick hydraulic conductivity than surrounding soil over the operating tension ranges, and 2) a wick that remains saturated over the operating tension range. In order to facilitate the selection of such desirable wick characteristics, measurements of hydraulic properties of five potential wick materials were conducted (Fig.9.1B-4). Two wick materials were selected from this screening study (Diatomaceous Earth (DE) and Fine Sand for further testing (Fig. 9.1B-5). It was shown that hydraulic conductivity of these materials were not limiting for the attainment of equilibrium between (i) the opening of the outer tube (contact tension) and the position of the water table in the inner tube (Fig. 9.1B-5); and (ii) the contact wick material above the open end of the outer tube and the surrounding soil (Fig. 9.1B-8). The empirical study (Fig. 9.1B-5) also indicated that both DE and Fine Sand stayed in the first stage of evaporation over the tension range of the outer tube length and in effect maintained an equilibrium condition. Given the fact that the equilibrium condition was met, this study also confirmed that the water table height in the inner tube was inversely related to the contact tension over the tension range defined by the length of the Tube Detector.

Although the air entry value of DE was considerably higher than that of the Fine Sand, the field based performance of both wick materials was similar, which was contrary to expectation. For example, the findings (Fig. 9.1B-6 and B-7) show that the difference in selected wick materials had no significant impact on the sensitivity of the Tube Detector (Fig. 9.1C-1). In the analysis of the accuracy of the tube version, however, it should be noted that the mean number of false negative responses (when a Tube Detector fails to collect water when it should), in Fine Sand was higher than those filled with DE, but they were not significantly different from each other ($P > 0.05$).

Length has a significant impact on the sensitivity of WFDs ($P \leq 0.05$). The sensitivity of WFDs differs significantly between different lengths of Tube Detector, and across most of the other

WFD designs tested. As predicted, the 90 cm long Tube Detector collected water more frequently than the 60 and 45 cm long Tube Detectors, and the 60 and 90 cm long Tube Detectors collected water from wetting fronts that passed without activating the FS or Hybrid WFDs. The performance of the Hybrid WFD was not significantly different from that of the FS ($P > 0.05$), which was contrary to expectation, as the Hybrids had a longer tube section that should have increased sensitivity. A possible explanation may be that there could have been design artifacts in the Hybrid prototype, such as a requirement for a large volume of water to fill all pores in the wick material in this design before it collects water in the reservoir.

In the analysis of the accuracy of tube-shaped WFDs, length determines the tension range of a wetting front that can be measured. For example, for a tension between zero and a tension equal to tube length, water was collected in the inner tube, i.e. ≥ 7 mL (see thesis document referred to in Fig. 9.1B-6 and B-7). In the controlled test (Fig. 9.1B-5), the water volume in the inner tube was inversely related to the contact tension measured by a tensiometer i.e. the tension in the soil immediately above the detector. In addition, since the contact tension corresponding to the time when water in the inner tube just empties was equal to the length of the outer tube, it was inferred that the tension sensitivity of the Tube Detector is determined by its length. Other results (Fig. 9.1B-6 and B-7) also confirmed that length determines the tension range of a wetting front that can be measured by Tube Detectors, as the deviation in measurement accuracy of infiltrating water was within a reasonable error limit (16%). This small deviation is associated with the number of false negative responses and could be explained by the air trapped in the tube of a tensiometer, decreasing the soil tension reading while the soil is dry.

Like all soil water monitoring equipment, there is a concern over soil disturbance during installation of the WFD. The analysis of soil-wick equilibrium (Fig. 9.1B-8) shows that installation disturbance does not significantly affect the equilibrium between contact tension (selected wick material) and bulk soil tension. This means that the tension in the contact wick material is the same as in the bulk soil and is therefore not affected by installation disturbance. The small impact of installation disturbance on the soil-wick equilibrium condition could be explained probably by the fact that the source of irrigation water (e.g. sprinkler system) is above the detector. This applies water to the soil at a rate less than the saturated hydraulic conductivity

of the soil; therefore the advance of a wetting front is affected mostly by the initial water content rather than soil texture.

The purpose of this synthesis is to show the practical application of the thesis findings for irrigation scheduling (how to deploy WFDs under field conditions to improve water management). It is believed that the success of irrigation scheduling using WFDs lies in the ability to optimize irrigation amounts and intervals for different soils and irrigation methods. This relationship could be determined by a series of field experiments that would require considerable expense, time and effort. As an alternative to such laborious field work, this synthesis chapter describes how a numerical model could be utilized to study the above relationships using the following links (Fig. 9.1): i) validation of the model (Fig. 9.1D-1, Link 3), ii) simulating various irrigation scenarios (Fig. 9.1D-2) for evaluating irrigation using WFDs (Link 4), iii) evaluating irrigation performance against WFD responses (Fig. 9.1E) using a wetted depth parameter (Fig.9.1C-2, Link 5).

In the analysis of the above three Links (3-5), the HYDRUS 2D/3D simulation model is validated against experimental data to confirm its usefulness as a prediction tool, and then used (i), to show the usefulness of the FS as a tool for irrigation management, (ii), to illustrate the potential use of the 90TD for managing furrow irrigation, and, (iii), to present explicit recommendations on how to use detector response to make irrigation scheduling decisions.

9.4 MODEL SIMULATIONS

Model simulations form the major part of this synthesis in order to (i), simulate experimental field data to develop the confidence to use the model (ii), compare the predicted sensitivity thresholds of WFDs obtained based on default soil parameters against the experimental values to increase the confidence in the model estimates, (iii), show the potential of WFDs for evaluating irrigation efficiency through optimization of irrigation intervals and irrigation amounts for different soil and irrigation types. A list of simulations performed in this synthesis is presented in Table 9.1.

Table 9.1 A summary of the model simulations performed in this synthesis.

No.	Type	Purpose (s)
1.	Simulating field experimental data.	To validate the HYDRUS 2D/3D model.
2.	Predicting the theoretical sensitivity threshold values of WFDs.	To compare predicted sensitivity thresholds values against experimental values.
3.	Controlling irrigation from a set depth (FS-automatic mode).	To test the ability of the suggested analytical equation to predict an appropriate placement depth of a FS.
4.	Simulating different hypothetical irrigation scenarios and registering FS responses.	To optimize irrigation amount and irrigation interval that provide a desired wetted depth.
5.	Simulating furrow irrigation and registering responses of the FS and the 90TD placed at a pre-defined soil depth.	To compare the sensitivities of the FS and the 90TD and show the implications to furrow irrigation management.

This model simulation section therefore addresses the following four sub-sections: 9.4.1 Validation of the Hydrus model, 9.4.2 Determining FS placement depth by analytical method, 9.4.3 Evaluating irrigation amounts and intervals by FS, and 9.4.4 Sensitivity of WFD under flood irrigation.

9.4.1Numerical model validation (HYDRUS 2D/3D model)

9.4.1.1 *Comparison between model simulations and field experimental data*

The aim of this simulation is to validate the HYDRUS 2D/3D model in order to gain confidence in the usefulness of model results.

Materials and methods

The thesis describes a field experiment carried out to evaluate the performance of different types of WFDs under a range of water fluxes created using sprinkler irrigation (Fig. 9.1B-6) and natural rainfall (Fig. 9.1B-7). The HYDRUS 2D/3D model (Šimůnek *et al*., 2008) was used to simulate the field experiment (Fig. 9.1D-1) to validate the model. Here emphasis is given to the FS and 90TD WFDs evaluated under sprinkler irrigation.

Experimental data collected during the evaluation of the performance of the various WFD types using sprinkler irrigation (application rate of 9 mm/h) were compared to the simulated variables obtained using the HYDRUS 2D/3D model. Details on soil type and amount of water applied

during each of the irrigation events are given in the thesis (Chapter 6 and Section 6.4.1.1). The purpose of these irrigation treatments was to create a range of water fluxes in the soil profile.

FullStop model setup

The HYDRUS 2D/3D model was used to simulate two dimensional water flow into the FS installed below the soil surface, assuming a homogenous soil profile. The flow domain and boundary conditions of this detector is described in the model as follows.

A finite element mesh was created with the axis of symmetry along the centre of a FS (Fig. 9.2). Because the flow through a FS is axisymmetric, the simulation was equivalent to a three dimensional simulation. The boundary of the flow domain was rectangular (290 cm deep and 200 cm wide), except near the upper left corner where a FS was located (Fig. 9.2a).

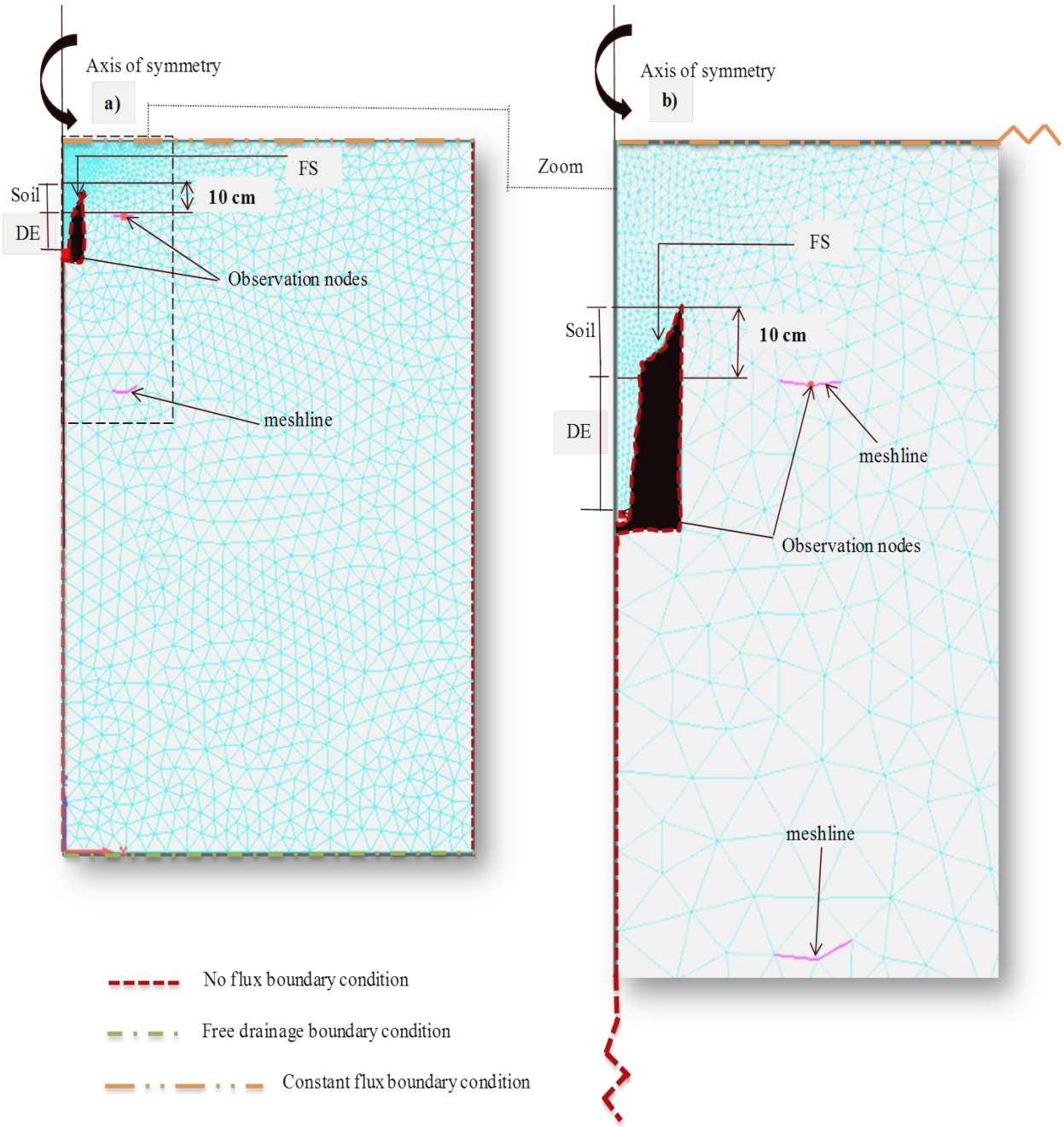

Figure 9.2 Typical geometry and finite element mesh used for the FS wetting front detector in HYDRUS 2D/3D simulations. (a) Detail of the FS and its immediate surroundings and (b) an enlargement of the area enclosed within the dashed rectangle. The arrow in the top left corner of (a) and (b) indicates the axis of symmetry.

The flow domain was subdivided into a grid with variable spacing, i.e. a high density mesh at the bottom and inside wall of the FS, and a lower density mesh in the flow domain outside the FS.

The boundary of the mesh (Fig. 9.2a) was curved inward following half of the perimeter of a detector. The FS (20 cm funnel diameter, 30 cm long) was incorporated into the flow domain. The flow domain in this design comprises two materials, a 15 cm thick layer filled with DE (base to neck of the FS); and the remainder is represented by the homogenous soil material (Fig. 9.2b).

Two observation nodes were inserted (Fig. 9.2b): one at the base of the FS to register soil tension variations inside the detector and to see when it will trigger the indicator, and another at the depth of placement (equivalent to the neck of the FS which is assumed as the depth of measurement) within the flow domain but outside the FS to record soil tension in the bulk soil. Two mesh lines were inserted: one at the placement depth of the detector to record water flux in the soil, and another at a depth below the root zone to record drainage water.

The lower boundary inside the bottom of the detector was set as a no flux boundary to allow the build up of positive pressure inside a detector, hence simulating pressure head variations inside the bottom of the detector. The sides of the flow domain were set up as no-flow boundaries. The upper boundary of the soil profile depends on the form of water application used, for example in Figure 9.2 it was set to a constant flux to simulate irrigation scenarios using a sprinkler system, while its bottom boundary was set to a free drainage condition.

Tube Detector model setup

The 90 cm long tube was incorporated into the soil profile and represented as a no-flow boundary in the model (Fig. 9.3). The wick inside the tube and the contact material (the same material as the wick) placed above the open end of a tube was incorporated as a second ‘soil type’ within the model (Fig. 9.3).

Water leaves the lower boundary of the soil-wick contact area and flows through the wick to enter the tube. The wick diameter was set equal to the internal diameter of the outer tube (4.7 cm). The lower boundary inside the bottom of the detector was set as a no flux boundary that allows the formation of a positive pressure inside the detector, therefore simulating pressure head variations inside the bottom of a Tube Detector. The sides of the flow domain were set up as no-flow boundaries. The upper boundary of the soil profile was set to a constant flux (for this specific example) and its bottom boundary was set to a free drainage condition.

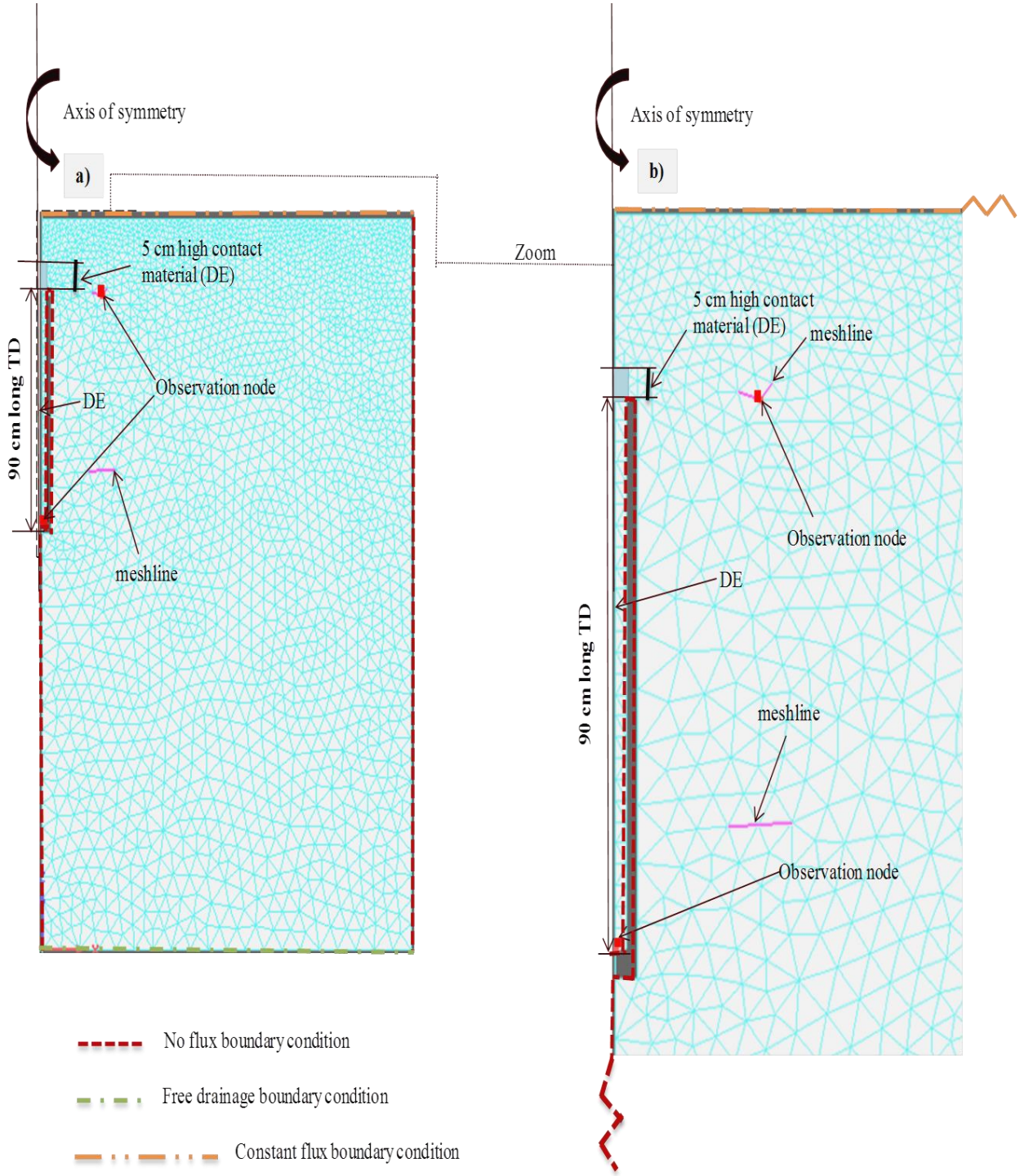

Figure 9.3 Typical geometry and finite element mesh used for the 90TD wetting front detector in HYDRUS 2D/3D simulations. (a) Detail of the 90TD and its immediate surroundings and (b) an enlargement of the area enclosed within the dashed rectangle. The arrow in the top left corner of (a) and (b) indicates the axis of symmetry.

The two measured soils of the study site were used to validate the model, the three default soils to generate various irrigation scenarios, and DE filter/wick material needed for proper functioning of a WFD are presented in Table 9.2.The hydraulic parameters selected for numerical simulations were the same as those in the field experiment (Fig. 9.1B-6 and B-7).The wick material parameters were derived from direct measurements (Fig. 9.1B-4). The hydraulic parameters for wicks and field experiment soils are all indicated by an asterisk ("*").

Note that since DE has a very high air entry value, it was used as a filter material in the FS and as a wick material in a 90TD in all the simulations. A filter material prevents fine materials from entering the reservoir of the FS, while a wick material was used to fill the inside of the Tube detector to carry water from the soil to the base of the detector.

Table 9.2 Hydraulic parameters used for soils and wicks in the simulations.

Soil/wick type	θ_r	θ_s	α (cm^{-1})	n (-)	K_s ($cm.\ h^{-1}$)
Loamy sand	0.057	0.410	0.124	2.28	14.59
Loam	0.078	0.430	0.036	1.56	1.04
Clay loam	0.095	0.410	0.019	1.31	0.26
Sandy loam*	0.070	0.366	0.019	1.38	1.197
Sandy clay loam*	0.050	0.462	0.014	1.61	0.304
DE*	0.045	0.790	0.004	2.54	3.81

Definition of water flow parameters: θ_r = residual water content, θ_s = water content at saturation, α = air entry parameter, n = pore size distribution index, K_s = saturated hydraulic conductivity, * = actual/measured values.

Results and discussion

Using the HYDRUS 2D/3D model (Šimůnek *et al*., 2008) and the measured soil characteristics in Table 9.2 (sandy loam and sandy clay loam), the responses of the FS and 90TD during the described monitoring period (Fig. 9.1B-6) were simulated and compared to actual observed WFD responses (Fig. 9.4). The WFD responses are described here either in volume or depth of water interchangeably (see also Chapters 6 and 7 of the thesis). Note that all the simulation results presented in this section are reported with a model mass balance error of < 3%.

Comparisons of the measured and simulated responses (water depth) of the WFDs are shown in Figure 4 as a function of time for the experiment, with the FS and 90TD installed at depths of 30 cm (sandy loam top soil in the field experiment) and 60 cm (sandy clay loam subsoil in the field experiment). This experiment was irrigated using sprinkler irrigation at a rate of 9 mm/h (for irrigation durations ranging from 0.44 to 11 hours). For the FS (Fig. 9.4c and d), the simulated numbers of responses (time series water depths registered by an observation node placed at the base of the FS), were 9 and 5 for depths 30 and 60 cm respectively.

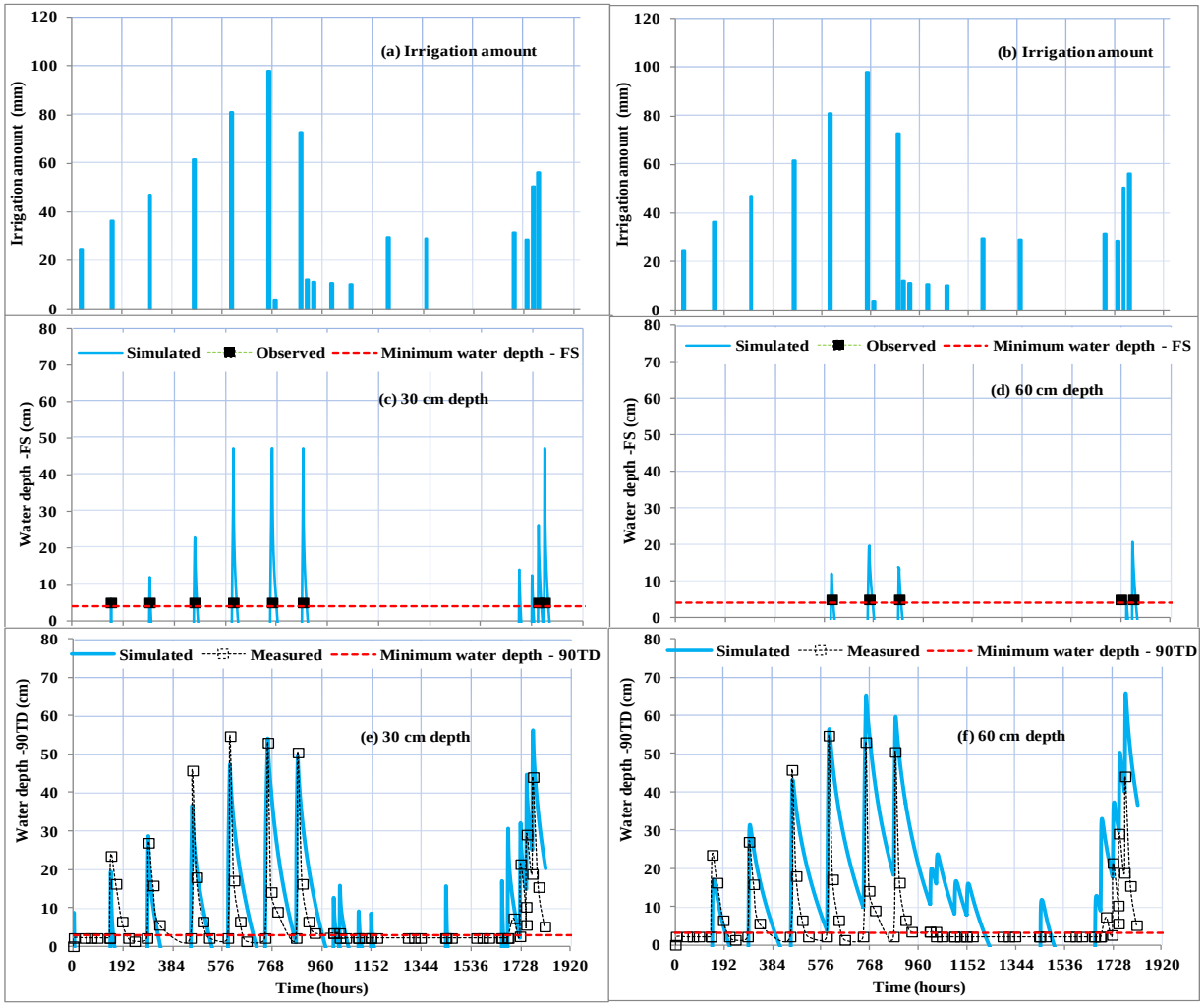

Figure 9.4 Measured and simulated WFD responses at depths of 30 (sandy loam) and 60 cm (sandy clay loam) for the FS (c and d) and 90TD (e and f) to irrigation applications (a and b are identical). A dashed horizontal line shows the minimum depth of water required to record a wetting event: 90TD = 3 cm (7 mL water) and FS = 4 cm (20 mL water).

Although the simulated positive pressures at the base of the FS were higher (due to the build-up of water in a detector) than a predefined depth of water required to trigger a FS (4 cm depth of water), the simulation model predicted the correct number of irrigation events that were measured by the FS. For the 90TD (Fig. 9.4e and f), the simulated responses (time series water depth record obtained from the observation node placed at the base of a Tube Detector) were also in good agreement with the experimental data, predicting all the major wetting and redistribution events. However, there were differences between simulated and measured 90TD responses for smaller irrigation events, for example at 960 to 1536 hours, where the simulated results showed small events but not the measured data. The potential explanation for these differences could be that in the field experiment a long dry period between irrigation events may have dried out the DE, requiring large volumes of water to first fill the pores of the DE before it could produce water in the tube.

The results in Figure 9.4 are therefore encouraging and support the use of this simulation model to i) compare the experimental sensitivity thresholds of a WFD with the predicted sensitivity values obtained using default soils (Fig.9.1D-1), and ii) evaluate irrigation performance by a WFD (Fig.9.1D-2) in order to develop guidelines on how to use detectors for irrigation scheduling.

9.4.1.2 *Predicting theoretical sensitivity thresholds of WFD*

The aim of these simulations was to build confidence in the model results by comparing the predicted theoretical sensitivity thresholds of the FS and 90TD to experimental values.

Materials and methods

The HYDRUS model was also used to predict the theoretical sensitivity thresholds of both WFD types (FS and 90TD) to compare to the experimental values. The HYDRUS 2D/3D model was used to analyse sensitivity thresholds of WFDs, assuming a homogenous soil profile. For this purpose, scenarios comprising one year of rainfall data, a sugarcane crop which could dry the sub-soil and hydraulic parameters selected for three hypothetical soils (Table 9.2) obtained from Carsel and Parrish (1988) were used. Roots were assumed to be linearly distributed to a depth of 100 cm. Initial conditions in the soil profile was set to an arbitrary selected tension value for these simulations.

Results and discussion

The sensitivity thresholds (soil tension and flux based values) for the FS and 90TD WFDs were determined using model simulations. Note that the sensitivity thresholds throughout this modelling section refer to the values obtained outside a detector in the bulk soil at the depths of 10 cm below the rim of the funnel (Fig. 9.2) and/or at the open end of the tube (Fig. 9.3). Soil tension and pressure head are used interchangeably.

Responses of the FS and 90TD placed at a depth of 30 cm in a loamy soil for one year of rainfall data are presented (Fig. 9.5b). The predicted soil tension (Fig. 9.5c) and water flux values (Fig. 9.5d), both marked with symbols, are read-off from the observation nodes placed within the flow domain but outside a detector at the depth of WFD placement. These marked responses correspond to those times when a minimum depth of water collected in the reservoir of a detector reaches just 4 cm (triggers the FS) and 3 cm (starts to register a response in the 90TD).

a) Rainfall

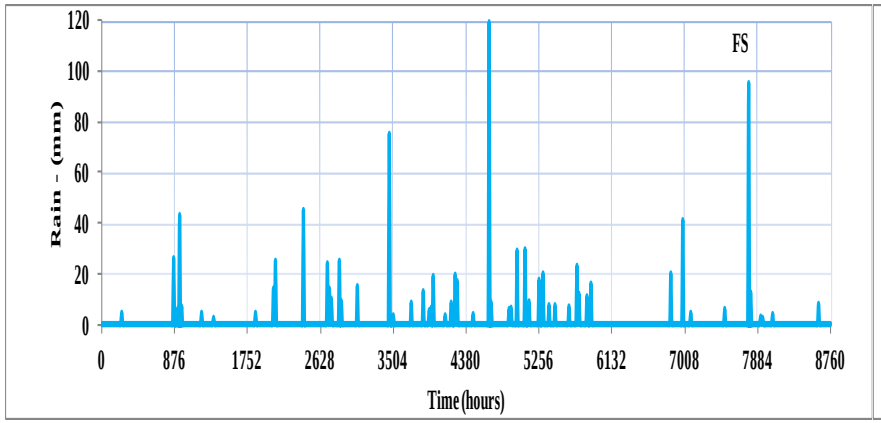

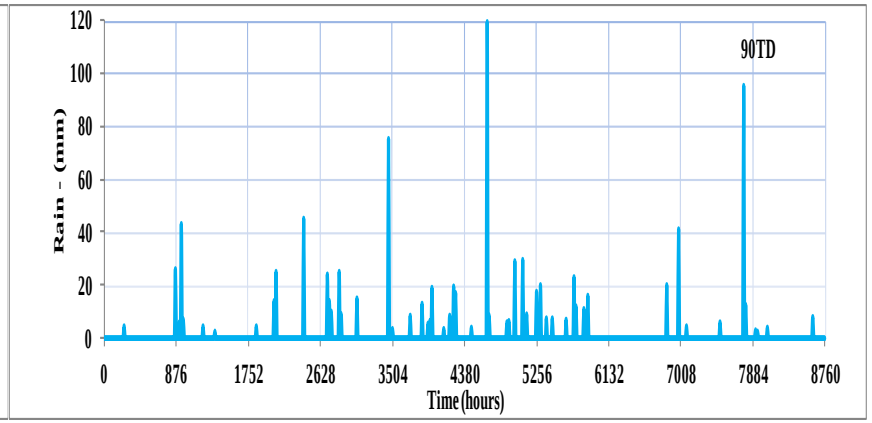

b) Water depth

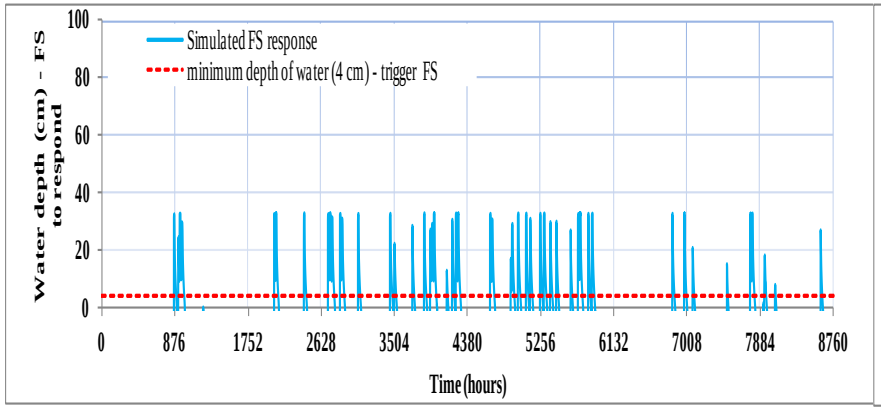

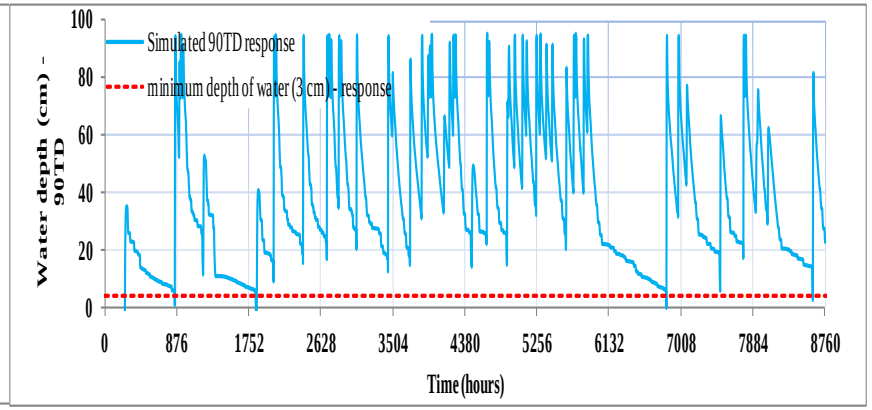

c) Pressure head

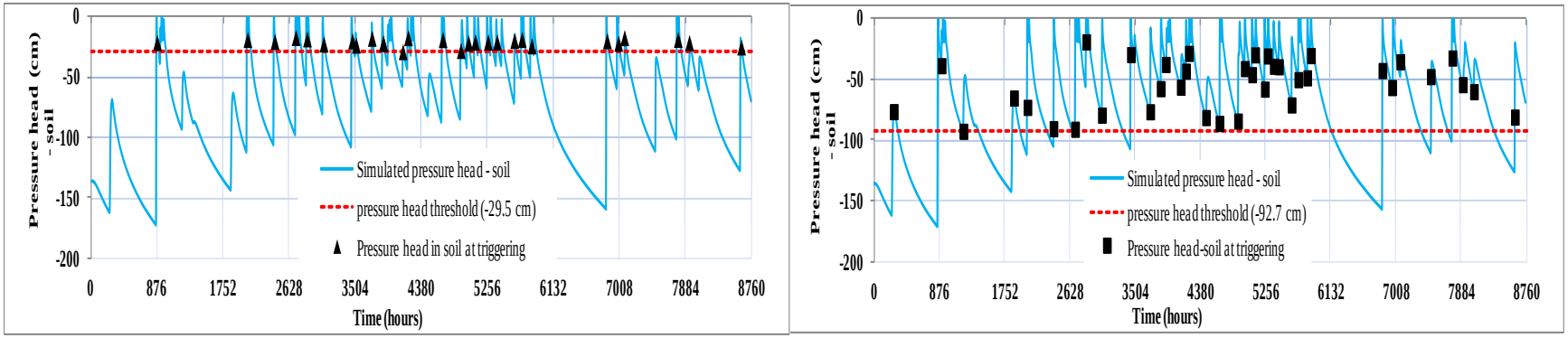

d) Water flux

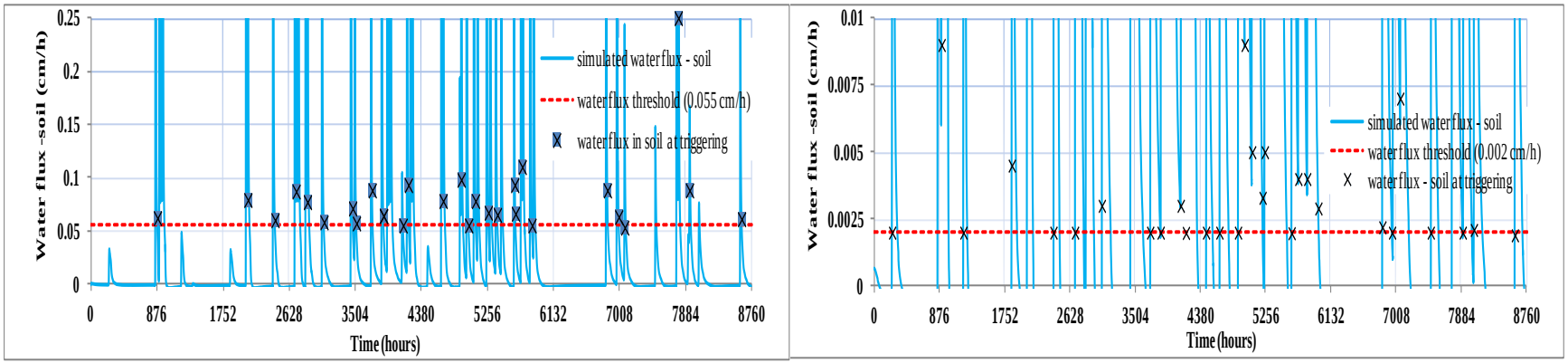

Figure 9.5 Relationship between (a) rainfall records and: (b) water depth records at the observation nodes placed inside the base of the FS or 90TD; (c) records of pressure head at the observation node, and (d) water flux at the meshline. Both (node and meshline) placed in the soil but outside a detector corresponding to the placement depth of a FS or 90TD - loam soil.

In evaluating Figure 9.5c and d, a dashed horizontal line that passes through the driest point for each of the marked variables was drawn to determine the soil tension and water flux threshold values. Based on this evaluation procedure, the soil tension thresholds of -29.5 cm for the FS and -92.7 cm for the 90TD (Fig. 9.5c); minimum water flux thresholds of 0.055 cm/h for the FS and 0.002 cm/h for the 90TD (Fig. 9.5d) were obtained. The same evaluation procedure was then used to summarize the overall soil tension and water flux thresholds for each of the WFD types in the three soils (Figures not shown), with the summary presented in Table 9.3.

Table 9.3 shows water flux and soil tension threshold values of the FS and/or 90TD operating under different soils. The water fluxes for the FS range from 0.01 to 0.055 cm/h. These water flux thresholds suggest that the FS captures 'sharp fronts', which are common with a relatively large irrigation application or found at shallow depths. The soil tension sensitivity limits for the FS range from -24.6 to -29.5 cm, which agree well with the experimental findings (Stirzaker, 2003; Stirzaker, 2008; Adhanom *et al*., 2012).

The water fluxes for the 90TD range from 0.0001 to 0.002 cm/h (Table 9.3), which also agrees with the findings of Adhanom *et al*. (2012). These values suggest that it responds to relatively 'low fluxes', which usually occur with smaller irrigation applications or found at deep placements where redistributing wetting fronts become diffuse. The predicted tension thresholds of -92.7 cm (loam) and -88.9 cm (clay loam) fit well with the experimental/thesis findings obtained in sandy loam to sandy clay loam soils. The soil tension threshold value for a 90TD buried in a loamy sand soil is, however, indicated by a dashed symbol (-) as the water flux in this soil becomes negligible for tensions drier than -59.4 cm, and it was therefore not possible to evaluate the 90TD over the full tension sensitivity limit thereof (90 cm soil tension).

Table 9.3 Predicted soil tension and water flux threshold values for the FS and 90TD in three default soils.

WFD type	Loamy sand		Loam		Clay loam	
	Soil tension (cm)	Water flux (cm/h)	Soil tension (cm)	Water flux (cm/h)	Soil tension (cm)	Water flux (cm/h)
FS	-24.6	0.010	-29.5	0.055	-26.0	0.021
90TD	-	0.0001	-92.7	0.002	-88.9	0.002

9.4.2 Determining FS placement depth by analytical approach (control mode)

In the early research (Stirzaker *et al*., 2004a) and field trials under sprinkler irrigation (Stirzaker and Hutchinson, 2005), an electronic FS detector was used to shut off the solenoid valve when the wetting front reached a detector buried at a certain soil depth (control mode). The authors have demonstrated the success of the method in the field, but cautioned that its usefulness depends on how well the placement depth and irrigation interval match with the potential transpiration rates. This section investigates the analytical relationship between the detector placement depth (control detector) and the irrigation amount required to wet a root zone.

Materials and methods

Figure 9.6 illustrates a simple analytical procedure that relates placement depth of an automatic control FS (Z_p) that allows sufficient water to be redistributed to the bottom of the root zone(Z_r). This analytical procedure uses the equation from Zur *et al.* (1994), which was developed based on a mass balance approach computed during irrigation and after redistribution.

The amount of water added to the area (BFHD) during irrigation must be equal to the amount of water after redistribution has taken place (BJKC). The amount of water added (Q_c)at the time when the WFD records the front can be estimated by:

$$Q_c = (\theta_{wf} - \theta_{MAD}) * Z_p \qquad (9.1)$$

The term θ_{wf} (in this synthesis) represents the water content in excess of field capacity immediately after triggering of a detector, which is a function of application rate and averaged over the wetted soil depth. This water content was estimated by shutting down irrigation automatically by a detector placed at arbitrary shallow and deep depths. The maximum allowable depletion (MAD) is expressed as a percentage of plant available water (PAW) in a rooting zone, which is the point below which excessive water stress could occur. The θ_{MAD} is determined by the water content at field capacity (θ_{fc}), permanent wilting point (θ_{pwp}) and MAD, i.e. θ_{MAD} = $(\theta_{fc}) - ((\theta_{fc} - \theta_{pwp}) * MAD)$.The irrigation amount applied to the soil is controlled by the response (triggering) of a FS placed at a predetermined depth (Z_p).

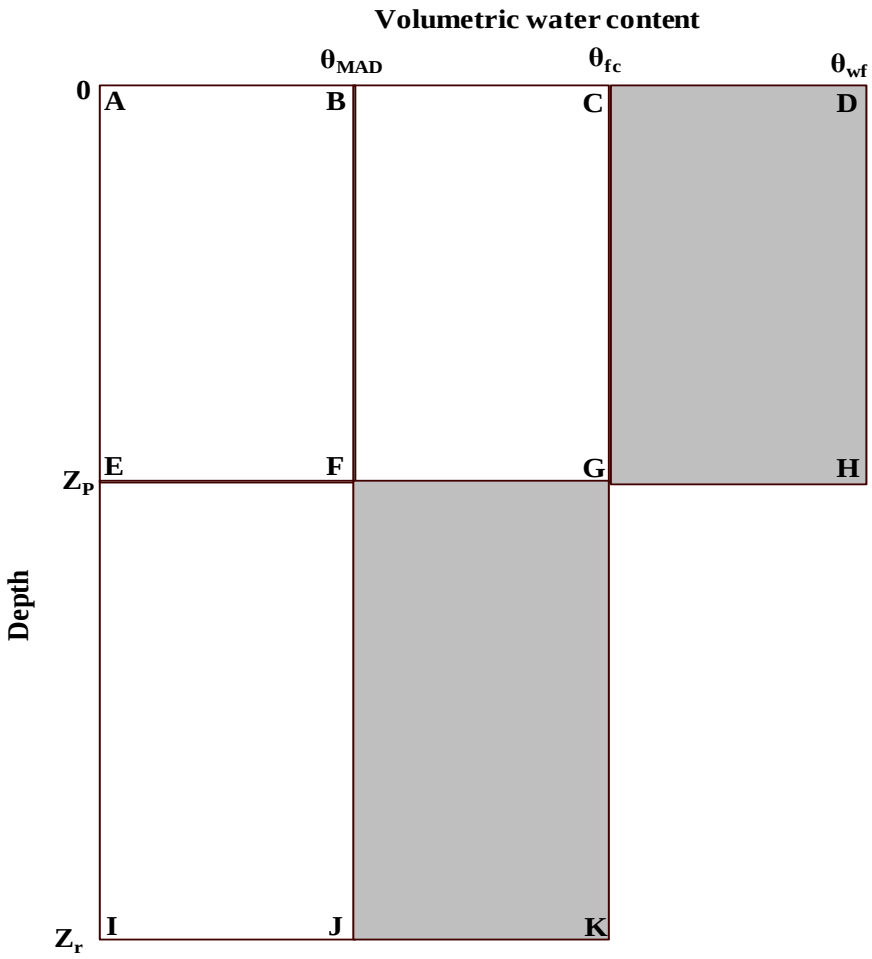

Figure 9.6 Sketch of a conceptual water balance during irrigation and redistribution.

The amount of water in the soil at the end of redistribution is given as:

$$Q_c = (\theta_{fc} - \theta_{MAD}) * Z_r \quad (9.2)$$

Where θ_{fc} is the water content at field capacity, obtained based on the two days of drainage after saturation (water content two days after saturation was averaged over each selected root depth to represent the field capacity of a root zone).

Equating Eq. (9.1) and (9.2):

$$(\theta_{wf} - \theta_{MAD}) * Z_p = (\theta_{fc} - \theta_{MAD}) * Z_r \quad (9.3)$$

Similarly, the amount of water in both shaded regions (Fig. 9.6) is equal and can be expressed as:

$$(\theta_{wf} - \theta_{fc}) * Z_p = (\theta_{fc} - \theta_{MAD}) * (Z_r - Z_p) \quad (9.4)$$

The left side of Eq. (9.4) represents the amount of water in excess of field capacity applied

during an irrigation that will sufficiently replenish the root zone through redistribution, and the right side of the equation shows the additional depth wetted to field capacity.

Re-arranging Eqs. (9.3) and (9.4)

$$\frac{(\theta_{wf}-\theta_{fc})*Z_p}{(\theta_{wf}-\theta_{MAD})*Z_p} = \frac{(\theta_{fc}-\theta_{MAD})*(Z_r-Z_p)}{(\theta_{fc}-\theta_{MAD})*Z_r} \quad (9.5)$$

Eq. (9.5) then simplifies to:

$$\frac{(\theta_{wf}-\theta_{fc})}{(\theta_{wf}-\theta_{MAD})} = \frac{(Z_r-Z_p)}{Z_r} \quad (9.6)$$

Finally Eq. (9.6) becomes:

$$Z_p = Z_r * (1 - \frac{(\theta_{wf}-\theta_{fc})}{(\theta_{wf}-\theta_{MAD})}) \quad (9.7)$$

The ideal depth of placement of a FS (Z_p) is inversely related to the expression($\theta_{wf} - \theta_{MAD}$). The above equations (9.1-9.7) are valid under the following assumptions: (i) the soil water content in a profile prior to irrigation (θ_{MAD}) is uniform with depth, and (ii) the water content in excess of field capacity (θ_{wf}) is obtained by controlling irrigation from a set of arbitrary shallow or deep detectors.

The application of an analytical equation (Eq. 9.7) to predict the placement depth of a control detector was tested for two arbitrary root depths 50 cm (shallow) and 100 cm (deep) and three soils (loamy sand, loam and clay loam). This equation, however, requires variables such as θ_{wf} and θ_{fc}, therefore the Hydrus model was used to determine these variables. The field capacity values for the three soils were determined using the two days of drainage time rule. The maximum soil water depletion of 50% PAW was considered as a trigger to irrigate.

The ability of equation 9.7 (Eq.9.7) to predict the placement depth of a FS from which sufficient water would be redistributed to wet a root zone was then tested using the Hydrus 2D/3D simulation model. For this purpose, the sides and lower boundary conditions of the flow domain were set similar to those described in Section 9.4.1. The upper boundary condition of the soil profile was set to a constant flux - sprinkler irrigation (5 mm/h). Irrigation was stopped when a FS installed at the placement depth predicted by Eq. 9.7 was triggered. This was followed by the simulation of the redistribution phase (two days) for each of the irrigation scenarios: (i) without root water uptake (by ignoring ET_o) in the soil profile, and (ii) by considering simultaneous

redistribution and root water uptake (ET_o = 6mm/day) to determine the depth of a wetted root zone ($Z_{r\prime}$). The redistribution depth was simulated by importing the final soil tension profile obtained during the infiltration phase as the initial condition for the redistribution phase, while the upper boundary was changed from a constant boundary flux to a no flux (assuming no plants) and atmospheric (when root water uptake was considered) boundary condition.

Results and discussion

Variables θ_{wf} and θ_{fc}, which were determined using Hydrus simulations, and θ_{MAD} were used in the analytical equation to predict the correct detector placement depth (Z_p) for two root depths and three soils, which is summarized in Table 9.4.The ratios obtained by dividing the placement depth of a FS (Z_p) predicted using Eq. 9.7 by the depth of a root zone planned to wet (Z_r) are shown in columns 10 and 11 (Table 9.4). The values ranged from 0.28 to 0.34 for loamy sand, 0.60 to 0.65 for a loam and 0.80 to 0.83 for a clay loam. These ratios (less than 1) imply that there is excess water above the FS available for redistribution, which supports the findings of Zur *et al*. (1994), and Stirzaker and Hutchinson (2005).

Table 9.4 Predicted FS placement depths (Z_p) for shallow and deep root depths and three soil types.

Soil type	θ_{wf}		θ_{fc}		θ_{MAD}		$Z_p$cm (Eq.9.7)		Z_p/Z_r- Eq.9.7 without plants		$Z_p/Z_{r\prime}$- Hydrus without plants		$Z_p/Z_{r\prime}$- Hydrus with plants (ET_o = 6mm/day)	
	S	D	S	D	S	D	S	D	S	D	S	D	S	D
Loamy sand	0.24	0.25	0.14	0.15	0.10	0.11	14	34	0.28	0.34	0.28	0.34	0.30	0.37
Loam	0.41	0.42	0.33	0.35	0.21	0.22	30	65	0.60	0.65	0.45	0.54	0.49	0.61
Clay loam	0.41	0.41	0.38	0.39	0.27	0.27	40	83	0.80	0.83	0.58	0.72	0.62	0.75

S = shallow root depth and D = deep root depth

The FS was then set in the Hydrus model at depths predicted by the analytical equation to control the irrigation amount and the subsequent simulations of the redistributed wetted depth for two days after irrigation was stopped by a control detector are shown (Fig. 9.7). Irrigation or drainage amounts are expressed in "mm", while wetted depths are shown in "cm" (Fig. 9.7).

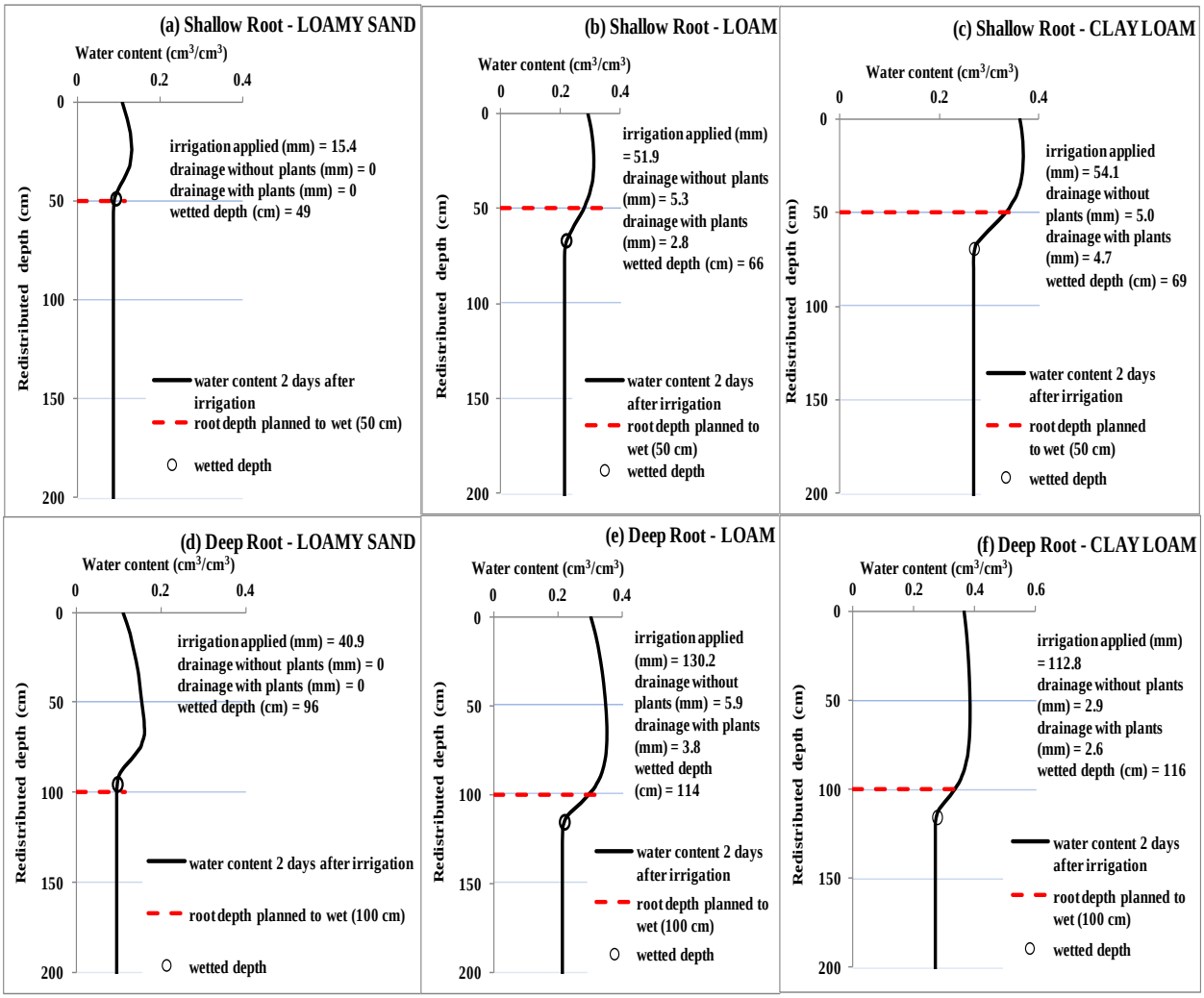

Figure 9.7 Wetting front redistribution two days after irrigation was stopped by a control detector for three soils (irrigated at soil water depletions of PAW 50%). The dashed lines represent the shallow and deep rooting depths(Z_r) respectively. The redistributed wetted depth- $Z_{r'}$ (circle) was determined when the increase in water content of a wetting front at any depth in a soil profile (after two days of irrigation with ET_o = 6 mm/day) with reference to its initial water content reaches 0.1 to 0.2%. The irrigation amount applied to trigger the FS are indicated for each of the above irrigation cases (a - f).

The ratios in the last four columns of Table 9.4 were produced by dividing the placement depth of a detector predicted using Eq. 9.7 by the simulated redistributed wetted depth (Fig. 9.7). The ratios derived based on the analytical approach were larger than those simulated for loam and clay loam soils (Table 9.4). This difference could be due to the fact that the numerical approach

gives deeper redistribution depth than the analytical method. The differences in wetted depths between simulations ($Z_{r\prime}$)with and without plants were small, explaining that the infiltration and redistribution processes are much faster than the root water uptake.

The ability of Eq. (9.7) to accurately predict the placement depth of a detector for loamy sand showed that the simulated redistributed wetted depth ($Z_{r\prime}$) was very close to the depth of the planned depth of root zone wetting (Z_r) hence the equation appears to work well for coarse textured soils. However, the $Z_{r\prime}$ for the loam and clay loam soils was deeper than Z_r and these differences in wetted depths ($Z_{r\prime} - Z_r$)were equivalent to drainage values ranging from 2.9 to 5.9 mm (without plants) and 2.6 to 4.7 mm (with plants). These values were obtained by integrating the water content over the wetted depth defined between Z_r and $Z_{r\prime}$ as indicated by the circles (Fig. 9.7). These drainages were, however, not accounted by the analytical approach. This explains that the analytical method uses the bucket analogy, which assumes negligible drainage two days after saturation, while the simulation model showed that soil drains well beyond the two days period. Hence the deployment of the analytical approach to predict the placement depth of a FS for medium and fine textured soils (loam and clay loam) to control irrigation amount and produce sufficient wetted depth without significant loss of drainage water below a root zone is not supported by the numerical simulation. This difference between the analytical and the numerical methods could be because of the way how the field capacity concept is defined and used.

9.4.3 Evaluating irrigation amounts and intervals by FS (mechanical mode)

The FS in control mode (automatically shutting down irrigation when a FS is triggered) resulted in successful irrigation scheduling (Stirzaker, 2003; Stirzaker and Hutchinson, 2005). However, this method requires irrigation controllers and electronic valves which most farmers do not have access to. For this reason, the commercial version of the FS was designed to be completely mechanical.

The irrigator uses the mechanical version to adjust irrigation amount or interval based on the response of a shallow or deep detector to the previous irrigation event. In this section, FS placement depths as recommended by Stirzaker *et al*. (2004a) for drip and sprinkler irrigation systems, based on practical experience (Table 9.5) were used to evaluate irrigation intervals for

each placement depths, irrigation methods and soil types. This section also uses a similar modelling approach to the above section to evaluate how much water would be required to get deep and shallow detectors to respond. Following the termination of irrigation by a shallow or deep detector, the redistribution phase was simulated for two days: i) to determine the wetted depth, and ii) to estimate the position of water content at the FS sensitivity during redistribution. The point in (ii) above helps to check whether redistributing water reached a deep detector after the irrigation was terminated by a shallow detector. These results were then used to evaluate whether the response of a FS could be used to adjust/guide irrigation management or decision.

Materials and methods

The different irrigation scenarios described below are simulated with the intention of developing rules of thumb around the responses of a pair of detectors (when none of the detectors respond, shallow detector responds, and both shallow and deep detectors respond).

Simulations - surface drip irrigation

The sides and lower boundaries of the soil profile were the same as described in the first sets of simulations (Section 9.4.1). The upper boundary condition was divided into two parts: one of variable flux (width being soil dependent) corresponding to the wetted radius created by a dripper, and the rest of the surface was assumed impermeable. Several simulations were made using a 2 L/h drip emitter and the FS placement depths from Table 9.5: the FS located directly under the dripper at depths of 30 and 50 cm controls the irrigation amount for each of the three default soils (loamy sand, loam and clay loam) and two actual field soils (sandy loam and sandy clay loam).

The hydraulic properties of these soils were taken from Table 9.2. In all the surface drip irrigation scenarios simulated, the initial conditions of the flow domain were set to soil water deficits of 10, 25 and 50% of the plant available water (PAW). These water deficits are based on the PAW used as a trigger to irrigate (PAW is defined as the water retained in the soil between field capacity and permanent wilting point).

Table 9.5 Recommended placement depths for the FS under different irrigation systems (*Stirzaker et al., 2004a*).

Type of irrigation	Notes	Shallow detector (cm)	Deep detector (cm)
Drip	Amount applied per dripper usually less than 6 litres at one time (e.g. row crops, pulsing)	30	45
Drip	Amount applied per dripper usually more than 6 litres at one time (perennial crops)	30	50
Sprinkler	Irrigation is usually less than 20 mm at one time (e.g. centre pivot, micro-jets)	15	30
Sprinkler	Irrigation is usually more than 20 mm at one time (e.g. sprinklers and draglines)	20	30
Flood (furrow)	Deeper placements than listed here needed for infrequent irrigations or very long furrows	20	40

Simulations - sprinkler irrigation

The flow domain, the sides and lower boundaries of the soil profile were the same as described for surface drip irrigation. The whole of the upper boundary, however, was set to a constant flux (5 mm/h) boundary condition. The initial soil water condition of the profile was the same as described above for drip irrigation. Irrigation amount was controlled by a FS located at depths 15 and 30 cm (Table 9.5) for the same soils described for drip irrigation.

Results and discussion

Table 9.6 reports the irrigation amounts required to trigger a FS at each soil depth and the redistributed wetted depth two days after irrigation for a range of soils and initial conditions. The pre-selected soil water depletion levels were used as criterion for the onset of irrigation (Table 9.6). This overcomes problems with the initial soil tensions that may over (coarse textured soils) or under estimate depletions (fine textured soils) than the selected allowable soil-water depletion levels. To know the initial soil tensions equivalent to the corresponding allowable soil-water depletions used to produce the results in Table 9.6, see Appendix 4-Tables 4 and 5. Some of these initial soil tensions (e.g. loamy sand and loam) appear to be wetter than recommended allowable soil tensions (Hanson *et al*., 2000). The reasons for this are likely to be the way the field capacity was defined and how the allowable soil-water content depletion was calculated.

Table 9.6 Irrigation amounts required to trigger a FS at different placement depths and the corresponding redistributed wetted depths for a range of soils and initial conditions (evapotranspiration was considered during the redistribution).

Soil type	Drip irrigation										Sprinkler irrigation									
	Placement depth-cm (Z_p)	Irrigation amount-(L) to trigger FS when irrigation starts at PAW of:			Wetted depth (cm) at ET_o: 6 mm/day ($Z_{r'}$)			Hydrus model: $Z_p/Z_{r'}$			Placement depth-cm (Z_p)	Irrigation amount-(mm) to trigger FS when irrigation starts at PAW of:			Wetted depth (cm) at ET_o = 6 mm/day ($Z_{r'}$)			Hydrus model: $Z_p/Z_{r'}$		
		10%	25%	50%	10 %	25%	50 %	10%	25%	50%		10%	25%	50%	10 %	25 %	50 %	10%	25%	50%
Loam sand	30	3.3	3.5	4.0	71	67	56	0.42	0.45	0.54	15	13.8	16.0	17.9	63	59	42	0.24	0.25	0.36
	50	9.2	10.2	11.5	111	106	87	0.45	0.47	0.57	30	28.0	31.1	36.3	105	99	87	0.29	0.30	0.34
Loam	30	7.2	9.8	13.9	87	70	52	0.34	0.43	0.58	15	15.0	18.9	25.8	60	52	43	0.25	0.29	0.35
	50	17.7	24.6	36.8	111	94	79	0.45	0.53	0.63	30	25.0	35.3	51.9	104	87	65	0.29	0.34	0.46
Clay loam	30	11.0	17.9	30.3	79	66	48	0.38	0.45	0.63	15	7.9	10.9	18.0	59	48	37	0.25	0.31	0.41
	50	21.8	34.8	58.1	100	85	72	0.50	0.59	0.69	30	14.5	22.3	38.6	81	66	50	0.37	0.45	0.60
Sandy loam	30	5.5	8.7	14.9	90	70	49	0.33	0.43	0.61	15	13.7	19.5	30.9	67	54	42	0.22	0.28	0.36
	50	18.6	31.8	58.8	115	95	78	0.43	0.53	0.64	30	19.5	32.6	57.3	112	95	68	0.27	0.32	0.44
Sandy clay loam	30	13.2	22.9	39.8	96	84	65	0.31	0.36	0.46	15	14.2	19.1	30.0	60	53	40	0.25	0.28	0.38
	50	36.3	61.8	110.3	121	106	89	0.41	0.47	0.56	30	21.3	35.2	59.4	96	85	69	0.31	0.35	0.43

The results (Table 9.6) combined with reference evapotranspiration data for the location of the farm, provides information on how much water to apply and the irrigation interval. This is illustrated assuming shallow (30-50 cm) and deep (50-120 cm) rooted crops and three different daily reference evapotranspiration values, under sprinkler (Table 9.7) and drip (Table 9.8) irrigation systems. Since drip irrigation distributes water over a small area of the field and the roots follow the same wetting pattern, water volume (Litre) was used to determine water use and storage in the plant root zone (a tree was used for this example) to estimate the irrigation interval.

Irrigation intervals in Tables 9.7 and 9.8 below were determined as follows:

The irrigation amount (mm) required to trigger a detector was determined by automatically shutting the irrigation off when a detector at a specific soil depth from Table 9.5 responds (Table 9.6). This irrigation amount will then refill the root zone to the wetted depth shown in Table 9.6. The starting condition is a MAD of 50%. For example, an irrigation amount of 25.8 mm triggers FS at 15 cm depth in a loamy soil when irrigated at 50% depletion (sprinkler irrigation) that resulted in a wetted depth of 43 cm. Similarly for drip irrigation, a 13.9 L irrigation amount triggers FS at 30 cm depth in a loamy soil when irrigated at 50% depletion that produced a wetted depth of 52 cm.

Irrigation interval (days) = Irrigation amount triggering FS (mm)/ET_o.

Table 9.7 Sprinkler irrigation: recommended detector triggering depths from Stirzaker *et al.* (2004a) and irrigation interval for shallow and deep root depths growing in different soil types.

	Shallow root depth (30-50 cm)				Deep root depth (50-120 cm)			
	Interval (days)			Detector depth (cm)-required to trigger	Interval (days)			Detector depth(cm)-required to trigger
Daily reference Evapotranspiration	High	Medium	Low		High	Medium	Low	
Loamy sand	3	4	5	15	5	7	12	30
Loam	4	5	9	15	7	10	17	30
Clay loam	3	4	6	15	6	8	13	30
Sandy loam	4	6	10	15	8	11	19	30
Sandy clay loam	4	6	10	15	8	12	20	30

Irrigation intervals (Table 9.7) were calculated by dividing the irrigation amount needed to trigger the FS (Table 9.6 – sprinkler irrigation) by the reference evapotranspiration (ET_o) value of a farm location (assumed values include: 7 mm/day - High, 5 mm/day – Medium, and 3 mm/day - Low):

The intervals in Table 9.8 (drip irrigation partially wets the soil surface area e.g. tree) were determined by dividing the volume of water applied to the root zone (L) by the water use in L/day (7.0 L/day - High, 5.0 L/day - Medium and 3.0 L/day - Low). These values were obtained by assuming 1 mm/day = 1 L/m^2/day.

Irrigation interval (days) = volume of water required to activate a FS at a specific placement depth (L)/water use (L/day).

Table 9.8. Drip irrigation: recommended detector triggering depths from Stirzaker *et al*. (2004a) and irrigation interval for shallow and deep root depths growing in different soil types.

	Shallow root depth (30-50 cm)				Deep root depth (50-120 cm)			
	Interval (days)			Detector depth (cm)-required to trigger	Interval (days)			Detector depth(cm)-required to trigger
Daily reference Evapotranspiration	High	Medium	Low		High	Medium	Low	
Loamy sand	1	1	1	30	2	2	4	50
Loam	2	3	5	30	5	7	12	50
Clay loam	4	6	10	30	8	12	19	50
Sandy loam	2	3	5	30	8	12	20	50
Sandy clay loam	6	8	13	30	16	22	37	50

Tables 9.7 and 9.8 above provide the soil depth at which the FS should be triggered for each soil type and also the intervals of days to apply irrigation to trigger a detector. The selection of root depths of crops to be irrigated with a particular irrigation system were decided based on the wetted depths obtained in Table 9.6. The irrigator should follow three steps:

1) Determine soil type and rooting depth (see Table 9.7 or 9.8).
2) Determine the daily reference evapotranspiration (ET_o) of the farm location.
3) Divide the irrigation amount triggered a FS at a specific soil depth (Table 9.6) by the ET_o of a location to determine an irrigation interval (Table 9.7 or 9.8). Match this interval (days) to the corresponding redistributed wetted depth (Table 9.6).

For example, look at Table 9.7 for the soil type and root depth (step 1) and ET_o (step 2) and determine the interval and the depth at which a detector should respond to adequately replenish the deficit at about 50% depletion and at the same time ensure the wetted depth doesn't exceed the root zone. For example, a shallow root crop grown in clay loam soil in an area with high ET_o (7 mm/day) requires a detector at 15 cm depth to get triggered every 3 days. In a similar fashion, a shallow rooted crop grown on a clay loam soil with high ET_o (7.0 L/day) needs a detector at 50 cm depth to be triggered every 4 days (Table 9.8).

This study also investigated whether the redistribution wetting depth (Table 9.6) was sufficient to trigger a deep detector. This investigation includes: i) determining the water contents at the tension sensitivity thresholds of the FS (see Table 9.3) from the generic water release curves (not shown), and ii) these values were then used to determine the redistribution depth that falls within the sensitivity range of a FS. Table 9 shows the results produced for this feedback analysis in, which were derived from the same redistribution curves used to develop Table 9.6. The summary of the feedback (Table 9.9) could be used: i) to determine whether redistribution water becomes out of the detection limit of the FS at the point of the lower detector, and ii) to assist irrigators to adjust the next irrigation with the help of the wetted depths (Table 9.6) and recommendations (Tables 9.7 and 9.8):

- For sprinkler irrigation, only the redistribution water (irrigated at 10 and 25% depletion of PAW) in loamy sand could trigger the FS at depths well below the placement depth of a control detector. For loam and clay loam, however, the redistributing wetting front was below the detection limit of the FS. This agrees with the findings of Stirzaker *et al.* (unpublished paper) which demonstrated that the FS was not capable of providing adequate feedback for deep depths, i.e. the inability of the FS to detect weak redistributing fronts.

Table 9.9 Redistribution depths (cm) within the detectable sensitivity range of a FS.

Soil type	Sprinkler irrigation				Drip irrigation			
	Depth (cm) triggered during irrigation	Redistribution depth (cm) within the detection limit of a FS when irrigated at MAD values of:			Depth (cm) triggered during irrigation	Redistribution depth (cm) within the detection limit of a FS when irrigated at MAD values of:		
		10%	25%	50%		10%	25%	50%
Loamy sand	15	49	34	-	30	-	-	-
	30	101	92	66	50	106	80	64
Loam	15	-	-	-	30	84	63	42
	30	-	-	-	50	99	86	74
Clay loam	15	-	-	-	30	59	54	40
	30	-	-	-	50	78	75	53

(-) means the water content during redistribution was below the detection sensitivity limit of FS.

- For drip irrigation, in all cases except when a shallow detector was placed at a depth of 30 cm (loamy sand), the water content sensitivity (detectable by FS) reached depths where the redistributing water could trigger a detector 3 to 24 cm below the point of a shallow detector (depends on the soil type and depth of a shallow detector). However, none of the irrigations (at 50% soil-water depletion) controlled by a shallow detector (30 cm) triggered a deep detector (50 cm). This also shows the sensitivity limitation of the FS.
- For additional indications of the detector response from set combinations of different irrigation amounts and MAD values for three soils and three irrigation systems, see Appendix 4 -Tables 1, 2, and 3.

The above model simulations (Section 9.4.3) showed the suitability of the FS at shallow placement depths (≤ 50 cm) where the wetting front is strong. The FS sensitivity reported in this Section 9.4.3 supports the findings by Stirzaker *et al.* (2008) and Stirzaker *et al.* (unpublished paper). The authors reported that the FS has sensitivity limitations for specific applications where deep detector placement is required (e.g. flood irrigation).

Since flood irrigators often need to apply large irrigation amounts at one time and the fact that water flux decreases with depth, deep detector placement is necessary. Several studies (the synthesis section 9.4.1.2, chapters 6 and 7 of the thesis document, and chapter 3 of the thesis

published in Water SA Vol. 38 No. 1) have shown that 90TD responds better than FS to low water fluxes. The following section 9.4.4 therefore illustrates the significance of a more sensitive detector in providing opportunity/flexibility to manage furrow irrigation.

9.4.4 Sensitivity of WFDs under flood irrigation

Sections 9.4.2 and 9.4.3 above focused on finding the match between the placement depth of a detector and the wetted depth to store the overhead/excess water below the FS (FS controls irrigation amount). Under flood irrigation (e.g. furrow irrigation), however, water cannot be turned off as can be done in the case of drip or sprinkler irrigation. In addition there is usually the need to apply a large water amount at one time, resulting in weaker fronts at depth and hence the need for a more sensitive detector.

The FS responds at soil tensions lower (less negative pressure) than field capacity for three different soils (Fig. 9.8).

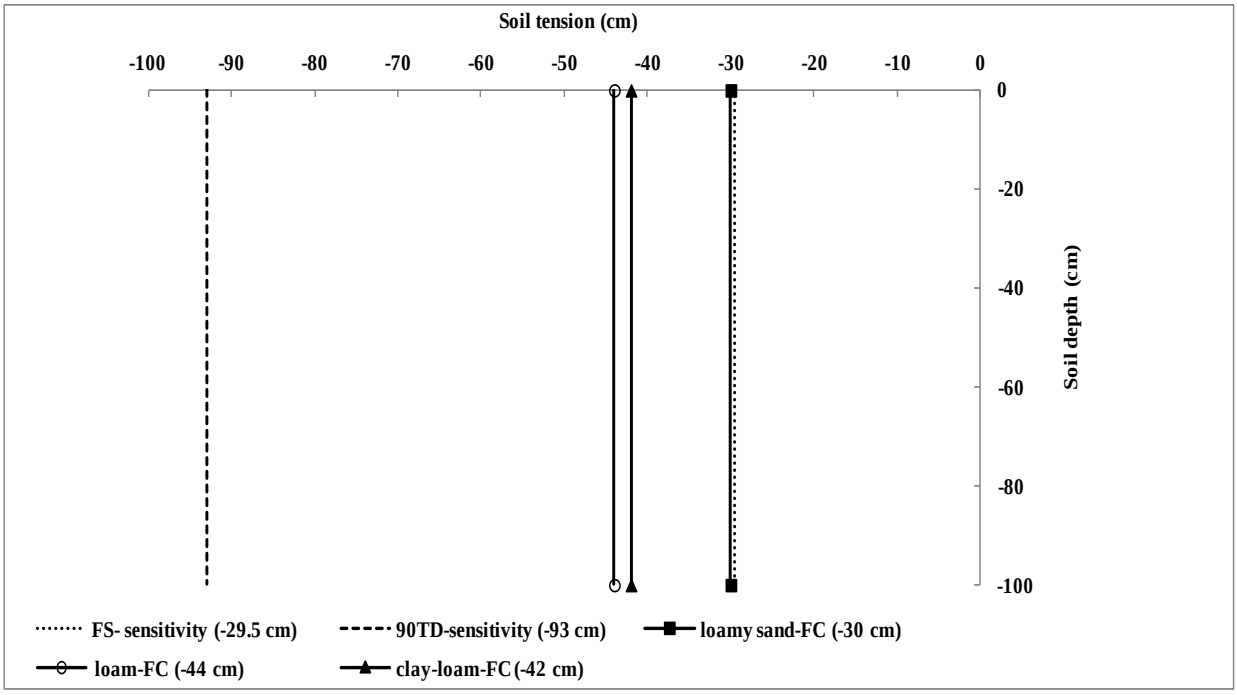

Figure 9.8 Soil tension values for each of the three soil types at field capacity (the driest tension observed among the different detector placement depths - 15 cm) based on the two days of drainage after saturation (symbol) and the tension sensitivity limits of the FS (dotted line) and 90TD (dashed line).

The response of the FS at these low soil tensions justifies the need for matching detector placement depth with the wetted depth after redistribution (see Sections 9.4.2 and 9.4.3). On the other hand the 90TD responds at soil tensions higher (more negative pressure) than the field capacities of the three soils, and should thus respond when the drainage rate is very low (Fig. 9.8). The information from the 90TD therefore can help a grower using flood irrigation: (i), to know whether previous irrigation has wetted the root zone sufficiently, and (ii), to take corrective action to refill the profile if the detector indicates no response. The problem of water draining undetected past of 90TD, as can be the case with a FS, should be overcome.

Materials and methods

Furrow irrigation was simulated based on the following field characteristics. The default soils (Table 9.2) were used with allowable soil water depletion of 50% PAW prior to irrigation. The soil profile was 290 cm deep with furrows 150 cm apart. The furrow was 13.2 cm deep and 50 cm wide at the top. This furrow provided water application volumes of 0.0375, 0.075 and 0.1125 m^2 (0.0375, 0.075 and 0.1125 m^3 per 1 m length of furrow).

The water flow boundary condition of the furrow and the shoulder of the bed were specified at a constant head of 11 cm with equilibrium from the lowest located nodal point (bottom of the furrow). The sides and the lower boundary of the flow domains were the same as described for the surface drip and sprinkler irrigation simulations. Different irrigation amounts (25, 50 and 75 mm) per irrigation event that are typically practised by small scale irrigators (FAO, 1989) were applied to a furrow instrumented with the 90TD and FS, each located at depths of 60 and 90 cm. Each soil was irrigated from an initial water condition of 50% PAW. In each case, the upper boundary condition remained constant throughout the application and was changed to atmospheric boundary condition with root water uptake of 6 mm/day when simulating the re-distribution phase.

Results and discussion

The performance of the two WFD versions of different sensitivity was compared over the three soils and three irrigation amounts. This investigated the relative advantage of the deployment of the 90TD over the FS to improve furrow irrigation management.

The responses of both FS and 90TD at a depth of 60 cm to the three irrigation amounts and the wetted depths after redistribution for each of the irrigation scenarios are depicted in Figure 9.9. The small irrigation application (25 mm) triggered the 90TD but not the FS for loam and clay loam soils (Fig. 9.9b-c), while both detectors were activated in a loamy sand (Fig. 9.9a). For this irrigation amount, the discrimination between the FS and 90TD (Fig. 9.9b-c) shows that the wetting front at the placement depth of the detector was at soil tensions higher (more negative pressure) than the tension sensitivity limit of the FS, but within the detection range of the 90TD.

The 50 and 75 mm irrigation amounts activated both the FS and 90TD in all three soils, indicating that the wetting fronts were within the detection range of the FS (Fig. 9.9d-i). These irrigations may be adequate (loam and clay loam) to satisfy the needs of a deep root zone. On the other hand, these irrigation amounts could cause over-irrigation on loamy sand. Similar evaluations were performed for both detectors placed at a depth of 90 cm and results are summarized in Table 9.10.

The 25 and 50 mm irrigation amounts activated the 90TD buried at a soil depth of 90 cm but not the FS at similar placement depth (loam soil) while activating both WFD types buried in loamy sand and clay loam soils (Table 9.10). The irrigation amount of 75 mm activated both detectors placed at the three different soils showing strong wetting fronts. The real question is whether irrigators could improve furrow irrigation management using the 90TD responses?

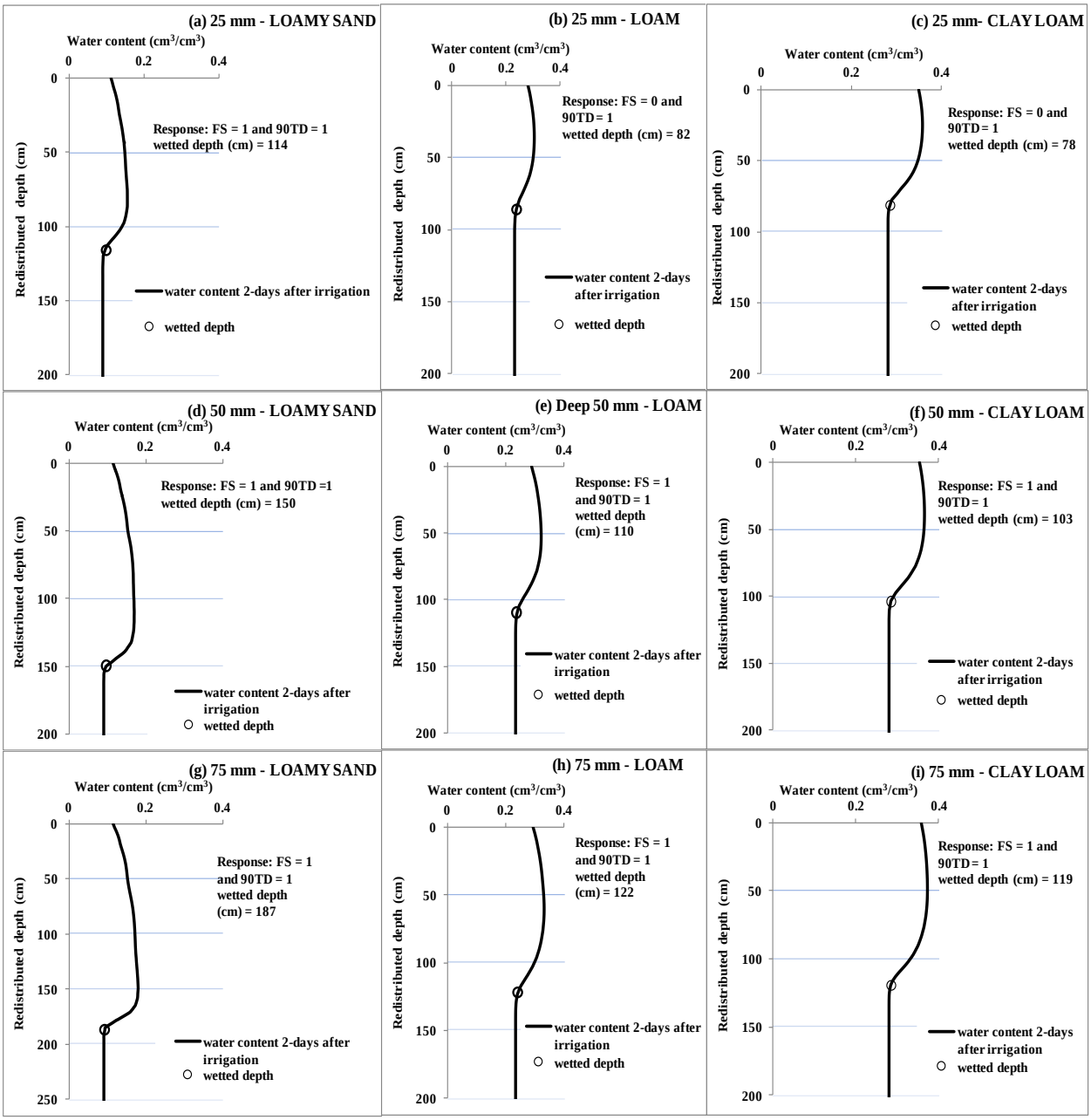

Figure 9.9 Simulated water content distribution (two days after irrigation) for three soils following irrigation applications of 25 mm (a-c), 50 mm (d-f) and 75 mm (g-i). The wetted depths two days after irrigation and the FS/90TD responses at a depth of 60 cm (1 = activated and 0 = not activated) to irrigations are also indicated (Fig. 9.9a-i). The position of a wetting front representing a wetted depth is shown by a circle.

Table 9.10 Simulated detector responses and wetted depths to furrow irrigation applied to different soil types (0 = not activated and 1 = activated).

Irrigation applied (mm)	WFD type	Detector response at a depth of 60 cm			Detector response at a depth of 90 cm			Wetted depth (cm)		
		Loamy sand	Loam	Clay loam	Loamy sand	Loam	Clay loam	Loamy sand	Loam	Clay loam
25	FS	1	0	0	1	0	0	114	82	78
	90TD	1	1	1	1	1	0			
50	FS	1	1	1	1	0	0	150	110	103
	90TD	1	1	1	1	1	0			
75	FS	1	1	1	1	1	1	187	122	119
	90TD	1	1	1	1	1	1			

Responses of the 90TD but not the FS to the 25 mm irrigation amount in loam and clay loam soils (at 60 cm soil depth) and 25 and 50 mm irrigation amounts in loam soil (at 90 cm soil depth) clearly show the significance of using a more sensitive WFD to detect weak redistributing fronts. The interpretations of these responses with respect to deep rooted crops showed an adequate irrigation (clay loam and loam) and over-irrigation conditions (loamy sand). The most obvious lesson from the above simulations is that the 90TD clearly identifies the different status of a furrow irrigation (adequate or over irrigated wetted depths), which the FS has failed to predict.

Over- and well- irrigated conditions were fairly evident from this simulation. Using responses from a Tube Detector hence can be used to improve furrow irrigation management by placing them roughly at 95 and 80% of the root zone for medium and fine textured soils, respectively. These values were obtained as the ratios of the distance of a wetting front from the soil surface (defined by a point in the redistributing water content profile equivalent to the tension sensitivity limit of the 90TD) to the redistributed wetted depth indicated (Table 9.10), expressed as a percentage. However furrow irrigation (large applications such as 50 and 75 mm) on coarse textured soils (e.g. loamy sand) produced excessive wetted depths (Table 9.10), and is therefore not recommended.

9.5 GUIDELINES FOR USING WETTING FRONT DETECTORS TO SCHEDULE IRRIGATION

FullStop wetting front detectors (FS) are recommended for use with sprinkler and drip irrigation systems only. For flood irrigation, please read the paragraph below. These guidelines on the use of FSs for irrigation scheduling are based on experience from field studies (Stirzaker *et al*., 2004a; thesis document) and Hydrus model simulations (this synthesis). The basic concept of using a FS for irrigation management is very simple. FSs are buried in the active root zone of the crop to indicate whether a specific irrigation amount has wetted the root zone to the desired depth. The FS will be activated (indicator flag triggered) once the infiltrating or redistributing water has reached the depth of placement of this detector. If the irrigation amount was not sufficient, the FS will not respond and the next irrigation amount or interval must be adjusted according to the guidelines below.

FullStops are not ideal for irrigation management of flood (e.g. furrow) irrigation. During flood irrigation a large amount of water is usually applied at a time. This requires detectors to be placed deeper in the soil profile. However, wetting fronts are usually weak at depth in the profile and hence a FS may not respond. Therefore a more sensitive detector, such as the *90-cm-long Tube Detector* (90TD), is recommended for flood irrigation. The placement depth of the 90TD is determined by the *in-situ* hydraulic conductivity of the different soils at the tension sensitivity threshold of this detector.

9.5.1 USE OF THE FULLSTOP WETTING FRONT DETECTOR

- Procedures for assembly and installation of the FS are available at the following web site: *www.fullstop.com.au*
- Placement depth, irrigation amount and interval for sprinkler and drip irrigation systems:
- ***Sprinkler irrigation***

➢ Use FS placement depths of 15 cm or 30 cm, depending on the rooting depth of the specific crop.

➢ Irrigation events should wet the soil profile to depths of 30-50 cm for shallow rooted crops and 50-120 cm for deep rooted crops to ensure sufficient wetting of the root zone.

✓ **For shallow rooted crops (30-50 cm):**

o Install a FS at 15 cm soil depth.

- Irrigate until the FS at 15 cm soil depth (*e.g. loam soil*) is activated and record the **irrigation amount (mm).**
- Divide this irrigation amount by the current daily reference evapotranspiration (ET_o, mm/day) of your farm location to estimate the **irrigation interval (days**), *e.g. 15.0 mm ÷ 5mm/day = 3 days*.
- Apply the **irrigation amount (mm)** at the **calculated interval** (*e.g. irrigate 15.0 mm every 3 days*). The FS at 15 cm soil depth should be activated after every irrigation interval to ensure that the entire root zone is sufficiently wetted.
- If the FS does not respond, increase the next irrigation amount or decrease the irrigation interval. Depending on knowledge of crop and site characteristics, therefore, the irrigator may develop certain algorithms or rules based on trial and error for fine tuning irrigation decisions, for example, if a FS does not respond, increase irrigation amount equivalent to one day's reference ET, or decrease irrigation interval by one day. This is applicable for sprinkler and drip irrigations described in Section 9.5.1 of this thesis.

✓ **For deep rooted depths (50-120 cm):**

- Install a FS at 30 cm soil depth.
- Irrigate until the FS at 30 cm soil depth (*e.g. loam soil*) is activated and record the **irrigation amount (mm).**
- Divide this **irrigation amount** by the current daily reference evapotranspiration (ET_o, mm/day) of your specific farm location to estimate the **irrigation interval (days)**, *e.g. 25.0 mm ÷ 5mm/day = 5 days*.
- Then irrigate the **irrigation amount** (**mm**) at the **calculated interval** (*e.g. irrigate 25.0 mm every 5 days*).The FS at 30 cm soil depth should be activated after every irrigation to ensure that the entire root zone is sufficiently wetted.
- If the FS does not respond, increase the next irrigation amount or decrease the irrigation interval.

- ***Drip irrigation***

➢ Use **FS placement depths of 30 cm or 50 cm**, depending on the rooting depth of the specific crop.

➢ Irrigation events should wet the soil profile to depths of 30-50 cm for shallow rooted crops and 50-120 cm for deep rooted crops, to ensure sufficient wetting of the root zone.

- For irrigation interval calculations consider the current reference evapotranspiration ($ET_{o,}$ mm/day) equivalent in L/m^2/day, i.e. 1mm/day = 1L/m^2/day.
    - ✓ **For shallow rooted crops (30-50 cm):**
- Install a FS at 30 cm soil depth **directly under a dripper**.
- Irrigate until the FS at 30 cm soil depth (*e.g. loam soil*) is activated and record the **irrigation amount (L/dripper)** *(e.g. 7.2 L),* and **time required (***e.g. 3.6 hours at an emitter discharge rate of 2.0 L/h***)**.
- Divide the **irrigation amount (L)** by the daily water use (L/day *e.g. 5L/day*) of your farm location to estimate the **irrigation interval (days)**, *e.g. 7.2 L ÷ 5L/day ≈ 1 day interval.*
- Apply the **irrigation amount (or time duration)** at the **calculated interval** (*e.g. irrigate 7.2 L/dripper every day, or irrigate e.g. 3.6 hours every day*). The **FS at 30 cm** soil depth should be **activated** after every irrigation event to wet the entire root zone sufficiently.
- If the FS does not respond, increase the next irrigation amount or decrease the irrigation interval.
    - ✓ **For deep rooted crops (50-120 cm):**
- Install a FS at 50 cm soil depth **directly under a dripper**.
- Irrigate until the FS at 50 cm soil depth (*e.g. loam soil*) is activated and record the **irrigation amount (L/dripper)** *e.g. 17.7 L* and **time required (***e.g. 8.85 hours at an emitter discharge rate of 2.0 L/h***)**.
- Divide this **irrigation amount** (**L**) by the daily water use (*L/day e.g. 5 L/day*) of your farm location to estimate the **irrigation interval (days)**, *e.g. 17.7 L ÷ 5L/day ≈ 4 days interval.*
- Apply this **irrigation amount** (or **time duration**) at the **calculated interval** (*e.g. irrigate 17.7 L/dripper every 4 days, or irrigate e.g. 8.85 hours every 4 days*). The **FS at 50 cm** soil depth should be **activated** after every irrigation event to wet the entire root zone sufficiently.
- If the FS does not respond, increase the next **irrigation amount** or decrease the **irrigation interval**.

9.5.2 USE OF THE 90-CM-LONG TUBE DETECTOR (90TD)

- The 90TD is specifically designed for application in flood irrigation (e.g. furrow irrigation). Unlike the responses of FS in sprinkler or drip irrigation, the 90TD response

provides flood irrigators less flexibility to shut off irrigation automatically. Given this condition, the farmer may use the 90TD response to know whether the previous irrigation has reached the required depth, or indeed if the soil is still wet at this depth. The interim guideline on the deployment of 90TD presented in this synthesis (Section 9.5.2) guides an irrigator by providing the depths of installations of the 90TD in medium and fine textured soils and the implications of the responses of this detector. Management responses related to the non response of this detector will depend on the irrigator's personal judgment/experience (knowledge of site and crop conditions).

- **The various components of a 90TD and its installation procedure** are available in the thesis document entitled "Design features determining the sensitivity of wetting front detectors for managing irrigation water in the root zone". This design has, however, not yet been commercialized but 90TD units can be provided for evaluation.

- **Deployment of the 90TD in furrow irrigation**

✓ ***Installation of the 90TD***

- 90TDs should be installed in the furrows.
- The placement depth is with reference to the furrow base.
- Install a 90TD at 95% of the root zone depth for **medium textured (loam) soils** and 80% of the root zone depth for **fine textured (clayey) soils**.

✓ ***Interpretation of 90TD responses***

- The **presence of water** in a 90TD placed at the prescribed depths following an irrigation event indicates that the root zone was wetted adequately.
- **No water** in the 90TD on the other hand indicates that too little water was applied during the last irrigation event and hence more water should be applied with the next irrigation.

9.6 SUMMARY AND CONCLUSIONS

Water use efficiency in irrigated agriculture can be increased through irrigation scheduling. Current scheduling technology is limited primarily to refilling the root zone based on the measured or predicted amount of water stored within the root zone. This method requires accurate measurement of water content or soil tension and specifying a soil's field capacity,

which can make it expensive and challenging. This synthesis report takes the thesis a step forward by providing more explicit instructions for how to use WFDs of varying sensitivity. This information can be used to decide on placement depths and irrigation intervals, without having to measure the initial soil water content.

This synthesis compared WFD response in a field experiment under sprinkler irrigation, with results of HYDRUS 2D/3D simulations. Model simulations were conducted for three "Hydrus soils" and two field soils, i.e. the top and subsoil from the field experiment. The results show that HYDRUS 2D/3D predictions of the measured responses of both FS and 90TD, and the simulated sensitivity thresholds of these detectors were in good agreement with the experimental results.

Field capacity is a frequently used concept in irrigation scheduling. Although there is some debate on how field capacity is defined, it represents a concept that is practical for field use. One should, however, be aware of the dilemma in choosing a value for field capacity and its subsequent effect to the interpretation of both the field measurement and model simulation results. In this synthesis, the water remaining in a soil after two days of free drainage following saturation was deployed to specify a soil's field capacity.

In light of the significance of field capacity analogy vis-à-vis the awareness of its limitations, numerical modelling was deployed to evaluate the effectiveness of WFDs for scheduling irrigation. The modelling work includes: a) controlling irrigation from a set depth (FS - automatic mode), b) adjusting irrigation amount and interval to the wetted root zone and ET_o of a farm location (FS - mechanical mode), and c) for deep placements or low water fluxes to be detected (90TD – mechanical mode). Knowledge gained from these simulations allows the existing recommendations to be revised in terms of: i) an irrigation interval that ensures that the last irrigation water is consumed by plants before applying the next irrigation to avoid percolation of water below a root zone (FS guidelines recommended for drip and sprinkler irrigation), and ii) the likely use of a 90TD in furrow irrigation.

The simulation results have illustrated the likely use of detectors to improve irrigation management practices in two ways. The first method showed that irrigation can be scheduled objectively by the FS - automatic mode. One of the most important parameters irrigators will know from the FS is whether a wetting front has passed a specific depth or not. The patterns of

detector response along with the simulated wetted depths and estimated irrigation intervals should guide irrigators in the right direction. The FS - feedback mode however was inadequate to provide information to make effective irrigation decisions due to its inability to detect weak fronts.

The second approach used the 90TD response (the presence or absence of water in the inner tube) in irrigation systems where deep placements or low water flux detection is required to make irrigation decisions (e.g. furrow irrigation). Since very limited research had been conducted on furrow irrigation management by a 90TD, no information on the deployment of this detector was given from previous studies. Though further study is warranted, model simulations (this Synthesis) and studies conducted by Stirzaker *et al.* (2010) have indicated that the 90TD can be used to improving furrow irrigation management.

This synthesis provided a simulated framework for managing irrigation water in the root zone effectively. Simulated results form the basis of many of the interpretations and management responses, in addition to the recommended placement depths from previous studies. As more experience is gained with the deployment of the simulated results in practice, it is expected that these recommendations will continue to be revised until the WFD method becomes a recognized technique for irrigation scheduling.

9.7 FUTURE RESEARCH NEEDS

This synthesis used the modelling approach to develop/revise practical guidelines, aiming for the deployment of detectors to manage irrigation water effectively. The model was useful in predicting detector responses with the aim of improving the guidelines for managing irrigation practices in a range of soil types, initial conditions and irrigation methods. It is believed that further numerical analysis should be conducted to equip the inexperienced irrigator with quick irrigation decisions from the WFD response.

Further simulations with real on-farm case studies involving WFD data sets would be an advantage to optimize detector response and water amounts applied per irrigation event. This builds confidence in the deployment of WFDs in the field with the aim of increasing the efficiency of water use.

REFERENCES

ABICHOU T, LIU X and TAWFIQ K (2006) Design considerations for lysimeters used to evaluate alternative earthen final covers. *J. Geotech. Geoenviron. Eng.* **132** 1519-1525.

ABOUKHALED A, ALFARO A and SMITH M (1982) Lysimeters. Food and Agriculture Organization of the United Nations, Rome, Italy. 68pp.

ADHANOM GT, STIRZAKER RJ, LORENTZ SA, ANNANDALE JG, and STEYN JM (2012) Comparison of methods for determining unsaturated hydraulic conductivity in the wet range to evaluate the sensitivity of wetting front detectors. *Water SA* **38**:67-76.

ALLEN GR and PRUITT WO (1991) FAO-24 reference evapotranspiration factors, *J. Irrig. Drain. Eng.* **5** 758-773.

AYDIN M, YANG SL, KURT N and YANO T (2005) Test of a simple model for estimating evaporation from bare soils in different environments. *Ecological Modelling.* **182** 91-105.

BEAR J (1972) Dynamics of fluids in porous media. Elsevier, New York.

BEN-GAL A and SHANI U (2002) A highly conductive drainage extension to control the lower boundary conditions of lysimeters. *Plant and Soil* **239**: 9-17.

BENSON C, ABICHOU T, ALBRIGHT W, GEE G and ROESLER A (2001) Field evaluation of alternative earthen final covers. *Int. J. Phytoremediation*, **3**:105-127.

BERGSTRÖM LE (1990) Use of lysimeters to estimate leaching of pesticides in agricultural soils. *Environ. Pollut.* **67** 325-347.

BIGELOW CA, BOWMAN DC and CASSEL K (2004) Physical properties of three sand size classes amended with inorganic materials or sphagnum peat moss for putting green root zones. *Crop Sci.* **44** 900–907.

BOLL J, STEENHUIS TS and SELKER JS (1992) Fibreglass wicks for sampling of water and solutes in the vadose zone. *Soil Sci. Soc. Am. J.* **56** 701-707.

BRANDI-DOHRN EM, DICK RP, HEW M and SELKER JS (1996) Field Evaluation of passive capillary samplers. *Soil Sci. Soc. Am. J* **60** 1705-1713.

BROOKS RH and COREY TA (1964) Hydraulic properties of porous media affecting fluid flow. *Proc. ASCE J. Irrig. Drain. Div.* **92** 61-88.

BROWN KW, THOMAS JC and AURELIUS MW (1985) Collection and testing barrel sized undisturbed soil monoliths. *Soil Sic. Soc. Am. J.* **49** 1067-1069.

BRUCE RR and KLUTE A (1956) The measurement of soil diffusivity. *Soil Sci. Soc. Am. Proc.* **20** 458-462.

BRYE KR, NORMAN JM, BUNDY LG and GOWER ST (1999) An equilibrium tension lysimeter for measuring drainage through soil. *Soil Sci. Soc. Am. J.* **63** 536-543.

BURDINE NT (1953) Relative permeability calculations from pore-size distribution data. *J. AIME* **198** 71-77.

CAMPBELL GS (1974) A simple method for determining unsaturated conductivity from moisture retention data. *Soil Sci.* **117** 311-314.

CARSEL RF and PARRISH RS (1988) Developing joint probability distributions of soil water retention characteristics. *Water Resour Res* **24**:755-769.

CHIU T and SHACKELFORD C (2000) Laboratory evaluation of sand underdrains. *J. Geotech. Geoenviron. Eng.* **126** 990-1001.

CLOTHIER BE, SCOTTER DR and GREEN AE (1983) Diffusivity and one-dimensional absorption experiment. *Soil Sci. Soc. Am. J.* **47** 641-644.

COMEGNA V, DAMIANI P, D'ANNA F and RUGGIERO C (1996) Comparisons of field methods for determining the hydraulic conductivity curve of a volcanic vesuvian soil. *Geoderma.* **73** 231-244.

CUMMING G, FIDLER F and VAUX DL (2007) Error bars in experimental biology. *The journal of Cell Biology*, **177**: 7-11.

DABACH S, LAZAROVITCH N, ŠIMŮNEK J, and SHANI U (2013) Numerical investigation of irrigation scheduling based on soil water status. *Irrig. Sci.* **31:**27-36.

DUGAS WA, MEYER WS, BARRS HD and FLEETWOOD RJ (1990) Effects of soil types on soybean crop water use in weighing lysimeters. II. Root growth, soil water extraction and water table conditions. *Irrig. Sci.* **11** 77-81.

DUKE HR (1972) Capillary properties of soils-influence upon specific yield. *Trans. of the American Society of Agricultural Engineers* **15** 688-691.

FAO (1989). Guidelines for designing and evaluating surface irrigation systems. http://www.fao.org/documents/en/detail/20964. Accessed 01 June 2013.

FESSEHAZION MK, STIRZAKER RJ, ANNANDALE JG, EVERSON CS and (2011) Improving nitrogen and irrigation water use efficiency through adaptative management: A case study using annual ryegrass. *Agriculture, Ecosystems and Environment.* **141** 350-358.

FLUHLER H, ARDAKANI MS and STOLZY LH (1976) Error propagation in determining hydraulic conductivities from successive water content and capillary pressure head profiles. *Soil Sci.Soc.Am.J.* **40** 830-836.

FRISTERLE S and FAYBISHENKO B (1999) Inverse modelling of a radial multi-step outflow experiment for determining unsaturated hydraulic properties. *Water Resour. Res.* **22** 431-444.

GEE GW, WARD AL, CALDWELL TJ and RITTER JC (2002) A vadose-zone water fluxmeter with divergence control. *Water Resour. Res.* **38** 35-41.

GEE GW, ZHANG ZF, WARD AL and KELLER JM (2004) Passive-wick water fluxmeters: theory and practice. *SuperSoil 2004: 3rd Australian New Zealand Soils Conference*, 5-9 December, University of Sydney, Australia.

GEE GW, ZHANG ZF and WARD AL (2003) A modified vadose-zone fluxmeter with solution collection capability. *Vadose Zone J.* **2** 627-632.

HANSEN JB, HOLM PE, HANSEN EA and HJELMAR O (2000) Use of lysimeter for characterization of leaching from soil and mainly inorganic waste materials. Nordtest technical report 473, DK-2970 Hørsholm, Denmark, 1-49 pp.

HIGNETT C and EVETT SR (2002) Neutron Thermalization. *In Dane JH and Top GC (ed.) Methods of soil analysis.* Part 4: Physical methods. 2nd ed. SSSA, Madison, WI, pp 501-521.

HILLEL D (1980) Applications of soil physics. Academic press, New York, London, p.385.

HILLEL D, KRENTOS VD and STYLIANOU Y (1972) Procedure and test of an internal drainage method for measuring soil hydraulic characteristics in-situ. *Soil Sci*. **114** 395-400.

HOLDER M, BROWN KW, THOMAS JC, ZABCIK D and MURRAY HE (1991) Capillary–wick unsaturated zone soil pore water sampler. *Soil Sci. Soc. Am. J.* **55** 1195-1202.

HOWELL TA, SCHNEIDER AD and JENSEN ME (1991) History of lysimeter design and use for evapotranspiration measurements. In: Allen et al (eds.) *Lysimeters for evapotranspiration and environmental measurements.* American Society of Civil Engineers, Reston, VA, 1-9 pp.

HOWELL TA (2001) Enhancing water use efficiency in irrigated agriculture. *Agron. J.* **93** 281-289.

HUTCHINSON PA and BOND WJ (2001) Routine measurement of the soil water potential gradient near saturation using a pair of tube tensiometers. *Aust. J. Soil Res.* **39** 1147–1156.

JEMISON JM and FOX RH (1992) Estimation of zero-tension pan lysimeter collection efficiency. *Soil Sci.* **154** 85-94.

JONES AJ and WAGENET RJ (1984) *In situ* estimation of hydraulic characteristics in situ. *Soil Sci.* **114** 395-400.

JURY WA, GARDNER WA and GARDNER WH (1991) Soil Physics. John Wiley and Sons, New York.

KAO C, BOUARFA S and ZIMMER D (2001) Steady state analysis of unsaturated flow above a shallow water table aquifer drained by ditches. *J. Hydrol.* **250** 122-133.

KNUTSON JH and SELKER JS (1994) Unsaturated hydraulic conductivities of fibreglass wicks and designing capillary wick pore-water samplers. *Soil Sci. Soc. Am. J.* **58** 721-729.

KLUTE A (1952) Some theoretical aspects of the flow of water in unsaturated soils. *Soil Sci. Soc. Proc.* **16** 144-148.

KLUTE A (1965) Laboratory measurement of hydraulic conductivity of saturated soil. In: Black, C.A. (ed.) Methods of soil analysis. Part1: 210-221pp.

LENTZ RD and KINCAID DC (2003) An automated vacuum extraction control system for soil water percolation samplers. *Soil Sci. Soc. Am. J.* **67** 100-106.

LORENTZ S, GOBA P and PRETORIUS J (2001) Hydrological processes research: Experiments and measurements of soil hydraulic characteristics. WRC Report no: K5/744, Pretoria, South Africa.

LOUIE MJ, SHELBY PM, SEMSRUD JS, GATCHELL LO and SELKER JS (2000) Field evaluation of passive capillary samplers for estimating groundwater recharge. *Water Resour. Res.* **36** 2407-2416.

MANJUNATHA MV, OOSTERBAAN RJ, GUPTA SK, RAJKUMAR H and JANSEN H (2004) Performance of subsurface drains for reclaiming waterlogged saline lands under rolling topography in Tungabhadra irrigation project in India. *Agric. Water Manage.* **69** 69-82.

MASARIK KC, NORMAN JM, BRYE KR and BAKER JM (2004) Improvements to measuring water flux in the vadose zone. *J. Environ.Qual.* **33** 1152-1158.

MERTENS J, DIELS J and FEYEN J (2007) Numerical analysis of passive capillary wick samplers prior to field installation. *Soil Sci. Soc. Am. J.* **71** 35-42.

MUALEM Y (1976) A new model for predicting the hydraulic conductivity of unsaturated porous media. *Water Resource. Res.* **12** 513-520.

NACHABE M, MASEK C and OBEYSEJERA J (2004) Observations and modelling of profile soil water storage above a shallow water table. *Soil Sci. Soc. Am. J.* **68** 719-724.

NANDAGIRI L and PRASAD R (1996) Field evaluation of unsaturated hydraulic conductivity models and parameter estimation from retention data. *J. Hydrol*. **179** 197-205.

NICHOL CF, ROWLETT DK and BARBOUR SL (2008) A new standpipe lysimeter design for measurement of soil matric Suction. *J. Vadose Zone* **7** 919-929.

PAYERO JO and IRMAK S (2008) Construction, installation and performance of the re-packed lysimeter. *Irrig Sci.* **26** 191-202.

POULSEN TG, MOLDRUP P, IVERSEN BV and JACOBSEN OH (2002) Three-region Campbell model for unsaturated hydraulic conductivity in undisturbed soils. *Soil Sci. Soc. Am. J.* **66** 744-752.

PREVEDELLO CL, LOYOLA JMT, REICHARDT K and NIELSEN DR (2008) New analytical solution of Boltzmann transform for horizontal water infiltration into sand. *J.Vadose Zone* **7** 1170-1177.

QIU GY, YANU T and MOMII K (1998) An improved methodology to measure evaporation from a bare soil based on comparison of surface temperature with a dry soil surface. *J. Hydrol.* **210** 93-105.

RATLIFF LF, RITCHIE JT and CASSEL DK (1983) Field measured limits of soil water availability as related to laboratory measured properties. *Soil Sci. Soc. Am. J.* **47**: 770-775.

REICHARDT K, PORTETAN-FILHO O, LIBARDI PL, BACCHI OOS, MORAES, SO, OLIVERIA JCM and FALLERIOS MC (1998) Critical analysis of the field determination of soil hydraulic conductivity functions using the flux-gradient approach. *Soil Tillage Res.* **48** 81-89.

REYNOLDS WD and ELRICK DE (2002) Principles and Parameter Definitions. *In Dane JH and Top GC (ed.) Methods of soil analysis.* Part 4: Physical methods. 2nd ed. SSSA, Madison, WI, pp 797-801.

RICHARDS LA (1950) Laws of soil moisture. *Transactions of American Geophysics Union.* **31** 750-756.

RIMMER A, STEENHUIS TS and SELKER JS (1995) One-dimensional model to evaluate the performance of wick samplers in soils. *Soil Sci. Soc. Am. J.* **59** 88-92.

RITCHIE JT (1972) Model for predicting evaporation from a row crop with incomplete cover. *Water Resour*. **8** 1204-1213.

ROMANO N and SANTINI A (2002) Field test. *In Dane JH and Topp GC (Eds.). Methods of soil analysis*. Part 4, Physical methods, p 725-727.

RUPP H, MEISSNER R, LEINWEBER P, LENNARTZ B and SEYFARTH M (2007) Design and operability of large weighable fen lysimeter. *Water Air Soil Pollut.* **186** 323-335.

SARAVANAPAVAN T and SALVUCCI GD (2000) Analysis of rate limiting processes in soil evaporation with implications for soil resistance model. *Advances in water resour*. **23** 493-502.

SAS INSTITUTE. 1999-2001. SAS user's guide: Statistics.8th ed. SAS Ins., Cary, NC.

SCHAAP MG, LEIJ FJ and VAN GENUCHTEN MTH (1998) Neural network analysis for hierarchical prediction of soil water retention and saturated hydraulic conductivity. *Soil Sci. Soc. Am. J.* **62** 847-855.

SCHAAP MG, LEIJ FJ and VAN GENUCHTEN MTH (2001) Rosetta: A computer program for estimating soil hydraulic parameters with hierarchical pedotransfer functions. *Soil Sci. Soc. Am. J.* **251** 352-361.

SENTEK PTY LTD (2003) Sentek Diviner 2000 User Guide version 1.2. Australia Sentek Pty Ltd, Stepney, South Australia.

SHEARER MN and VOMCIL J (1981) Twenty-five years of modern irrigation scheduling promotional efforts. In: *Irrigation scheduling for water and energy conservation in the 80's: Proceedings of the ASAE irrigation scheduling conference,* American Society of Agricultural Engineers, St. Joseph, MI, 23-81 pp.

ŠIMŮNEK J, SEJNA M and VAN GENUCTHEN MTH (1999) The Hydrus-2D software package for simulating two-dimensional movement of water, heat and multiple solutes in variably saturated media. Version 2.0. IGWMC-TPS-53. Colorado School of Mines, Golden, CO.

ŠIMŮNEK J, VAN GENUCHTEN MT, and ŠEJNA M (2008) Development and applications of the HYDRUS and STANMOD software packages and related codes. *Vadose Zone J* **7**:5870600.

SISSON JB, GEE GW, HUBBELL JM, BRATON WL, RITTER JC, WARD AL and CALDWELL TG (2002) Advances in tensiometry for long-term monitoring of soil water pressures. *J. Vadose Zone.* **1** 310-315.

SOIL CLASSIFICATION WORKING GROUP (1991) Soil Classification: A taxonomic System for South Africa. The Department of Agricultural Development, Pretoria.

SOIL SCIENCE SOCIETY OF AMERICA (1997) Glossary of soil science terms. *SSSA*, Madison, WI.

STEGMAN EC, MUSICK JT and STEWART JL (1980) Irrigation water management, p763-816, *In ME Jensen (ed.) Design and operation of farm irrigation system*. *ASAE*, st. Joseph, MI.

STEPHENS DB, HSU KC, PRIEKSAT MA, ANKEY MD, BLANDFORD N, ROTH TL, KELSEY JA and WHITWORTH JR (1998) A comparison of estimated and calculated effective porosity. *Hydrogeology Journal*. **6** 156-165.

STEVENS JB, DÜVEL GH, STEYN GJ, and MAROBANE W (2005) The range, distribution and implementation of irrigation scheduling models and methods in South Africa. WRC Report no: 1137/1/05, Pretoria, South Africa.

STIRZAKER RJ (2003) When to turn the water off: Scheduling micro-irrigation with a wetting front detector. *Irrig. Sci.* **22** 177-185.

STIRZAKER RJ (2006) Soil moisture monitoring: state of play and barriers to adoption. Irrigation Matters Series No. 01/06 CRC for irrigation futures.

STIRZAKER RJ (2008) Factors affecting sensitivity of wetting front detectors. *In proceedings of the fifth International Symposium on Irrigation of Horticultural Crops*, Goodwin I, O'Connell MG (eds.). *Acta Holticulturae* **792** 647-654.

STIRZAKER RJ and Hutchinson PA (2005) Irrigation controlled by a wetting front detector: field evaluation under sprinkler irrigation. *Aust. J. Soil Res.* **43** 935-943.

STIRZAKER RJ, MAEKO TC, ANNANDALE JG, STEYN JM, ADHANOM GT, and MPUISANG T (2012). Can irrigation be objectively scheduled from wetting front depth? Unpublished manuscript.

STIRZAKER RJ, STEVENS JB, ANNANDALE JG, and STEYN JM (2008) The Wetting Front Detector: A Tool to Help Irrigators Learn. In 'Water Saving in Agriculture: Innovative Technologies and Management for Water Saving in Irrigated Agriculture,' *International Commission on Irrigation and Drainage (ICID) Special publication No 95: 1-14*

STIRZAKER RJ, STEVENS JB, ANNANDALE JG and STEYN JM (2009) Stages in the adoption of a wetting front detector. *Irrig. Drain.* **59** 367-376**.**

STRIZAKER RJ, STEVENS JB, ANNANDALE JG, MAEKO T, MPANDELI S, MAUROBANE W, NKGAPELE J and JOVANOVIC NZ (2004a) Building capacity in irrigation management with wetting front detectors. WRC Report no: TT 230/04, Pretoria, South Africa.

STIRZAKER RJ, STEYN JM, ANNANDALE JG, ADHANOM GT, VAN DER LAAN M and M'MARETE CM (2010) Adapting the wetting front detector to small scale furrow irrigation and providing a basis for the interpretation of salt and nutrient measurements from the water sample. WRC Report No.1574/1/10, Pretoria, South Africa.

SUMNER DM (2007) Effects of capillarity and microtopography on wetland specific yield. *Wetlands* **27** 693-701.

TESFAMARIAM EH, ANNANDALE JG, STEYN JM and STIRZAKER RJ (2010) Exporting large volumes of municipal sewage sludge through turfgrass sod production. *J. Environ. Qual.* **38** 1320-1328.

TYNER JS and BROWN GO (2004) Improvements to estimating unsaturated soil properties from horizontal infiltration. *Soil Sci. Soc. Am. J* **68** 1-6.

VAN BAVEL CHM (1961) Lysimetric measurements of evaporation rates in the eastern United States. *Proc. SSSA.* **25** 138-141.

VAN DER LAAN M, STIRZAKER RJ, ANNANDALE JG, BRISTOW KL and DU PREEZ CC (2010) Monitoring and modelling draining and resident soil water nitrate concentrations to estimate leaching losses. *Agric. Water Manage.* **97** 1779-1786.

VAN DER VELDE M, GREEN SR, GEE GW, VANCLOOSTER M and CLOTHIER BE (2005) Evaluation of drainage from passive suction and non-suction flux meters in volcanic clay soil under tropical conditions. *J.Vadose Zone.* **4** 1201-1209.

VAN GENUCHTEN MTH (1980) A Closed–form equation for predicting the hydraulic conductivity of unsaturated soils. *Soil Sci. Soc. Am. J.* **44** 892-898.

WARD A and GEE G (1997) Performance evaluation of field-scale surface barrier. *J. Environ. Qual.* **26** 694-705.

WATSON K (1966) An instantaneous profile method for determining the hydraulic conductivity of unsaturated porous materials. *Water Resour. Res.* **2** 709-715.

WEIHERMÜLLER L, SIEMENS J, DEURER M, KNOBLAUCH S, RUPP H, GÖTTLEIN A and PŸTZ T (2007) *In situ* soil water extraction: A review. *J. Environ. Qual.* **36** 1735-1748.

YANFUL EK and MOUSAVI SM (2003) Estimating falling rate evaporation from finite soil tubes. *The Science of the Total Environment*. **313** 141-152.

ZHANG ZF, ANDY L and GEE GW (2003) Estimating soil hydraulic parameters of a field drainage experiment using inverse techniques. *Vadose Zone J.* **2** 201-211.

ZHU Y, FOX RH and TOTH JD (2002) Leachate collection efficiency of zero-tension pan and passive capillary fibreglass wick lysimeter. *Soil Sci. Soc. Am. J.* **66** 37-43.

ZUR B, BEN-HANAN U and YARDENI A (1994) Control of irrigation amounts using velocity and position of wetting front. *Irrig.Sci.* **14** 207-212.

APPENDIX

APPENDIX 1

Boundary conditions and analytical solutions at the wick-soil contact:

$$h_{z=L} \begin{cases} \geq h_{cr}; hL^* \geq h_{cr}, \\ = h; hL^* < h_{cr} \end{cases} \quad (2.2)$$

(Eq. 2.2) can be explained as:

- Pressure head at the soil-wick contact ($h_{z=L}$) $\geq$ h_{cr}; if the pressure head above L in the soil profile $\geq$ h_{cr}
- Pressure head at the soil-wick contact ($h_{z=L}$) = h; if the pressure head above L in the soil profile < h_{cr}

where L* = $\lim L_{\Delta z \to 0} + \Delta z$, L represents the length of the Tube filled with wick material. The length of the Tube is limited to the condition where $|h_{cr}| <$ L.

Ben-Gal and Shani (2002) used the one-dimensional Darcy equation for $0 \geq h \geq h_{cr}$ to yield (Eq. 2.3), which shows that the drainage water in the soil and the wick at the contact should be equal to meet the requirements (Eq. 2.2). This relationship can be applied to Figure 2.2b, with cross sectional areas A1 at the contact in the soil assuming a homogenous and isotropic soil, and A2 for a homogenous and isotropic wick of a drain at the bottom of the design:

$$Q^{soil} = Q^{wick}$$
$$-A^{soil} * K^{soil}(h) * \left[\frac{dh}{dz} - 1\right] = -A^{wick} * K^{wick}(h) * \left[\frac{dh}{dz} - 1\right] \quad (2.3)$$

For known soil hydraulic properties and lysimeter dimensions, the hydraulic conductivity, length and cross-sectional area of the wick needs to be determined to meet the conditions (Eq. 2.2). The lower boundary condition specified at the soil-wick contact therefore remains valid when the drainage water (Q) in the soil and the wick are equal (Eq. 2.3).

The pressure head at the soil-wick contact varies between h = L for the no flow condition and h = 0 for saturated flow. As the pressure head at the drain media (A2) shown in Figure 2.2b becomes zero, the drainage water through the wick material can be estimated using:

$$Q^{wick} \cong -A^{wick} * K_{eff} * \left[-\frac{h}{L} - 1 \right] \qquad (2.4)$$

where K_{eff} is the effective hydraulic conductivity of the wick.

Ben-Gal and Shani (2002) used the Gardner hydraulic model to estimate K_{eff} :

$$K_{eff} = K_s * e^{\alpha h} \qquad (2.5)$$

Assuming a unit hydraulic gradient in the soil at length L, a non-limiting flow condition can be established at the soil-wick contact (Eq. 2.2), when the following condition is satisfied (Rimmer *et al*., 1995):

$$A^{wick} \geq \frac{A^{soil} * K^{soil}(h) * L}{K_{eff} * (L - h)}; \quad 0 \geq h \geq h_{cr} \qquad (2.6)$$

The boundary conditions considered in the soil above the wick, at the bottom of the wick and at the soil-wick contact are:

$$\begin{aligned} K_s(z) &= -q_s \qquad for \quad z = \infty \\ K_w(z) &= K_s w \qquad for \quad z = 0 \end{aligned} \qquad (2.7)$$

$$\begin{aligned} q_s(z) &= q_w(z) \qquad for \quad z = L_w \\ h_s(z) &= h_w(z) \qquad for \quad z = L_w \end{aligned} \qquad (2.8)$$

The boundary conditions (Eq. 2.7) show that hydraulic conductivity in the soil above the wick is equal to the flux; and the hydraulic conductivity at the lower end of the wick equals the saturated conductivity of the wick. Eq. (2.8) shows that the flux and pressure heads are continuous at the wick-soil contact (Rimmer *et al*., 1995).

APPENDIX 2

True positive response (+), false negative responses (circle), mean bulk soil tensions of each event with error bars, and tension sensitivity (dotted line) in response to irrigation (a to o).

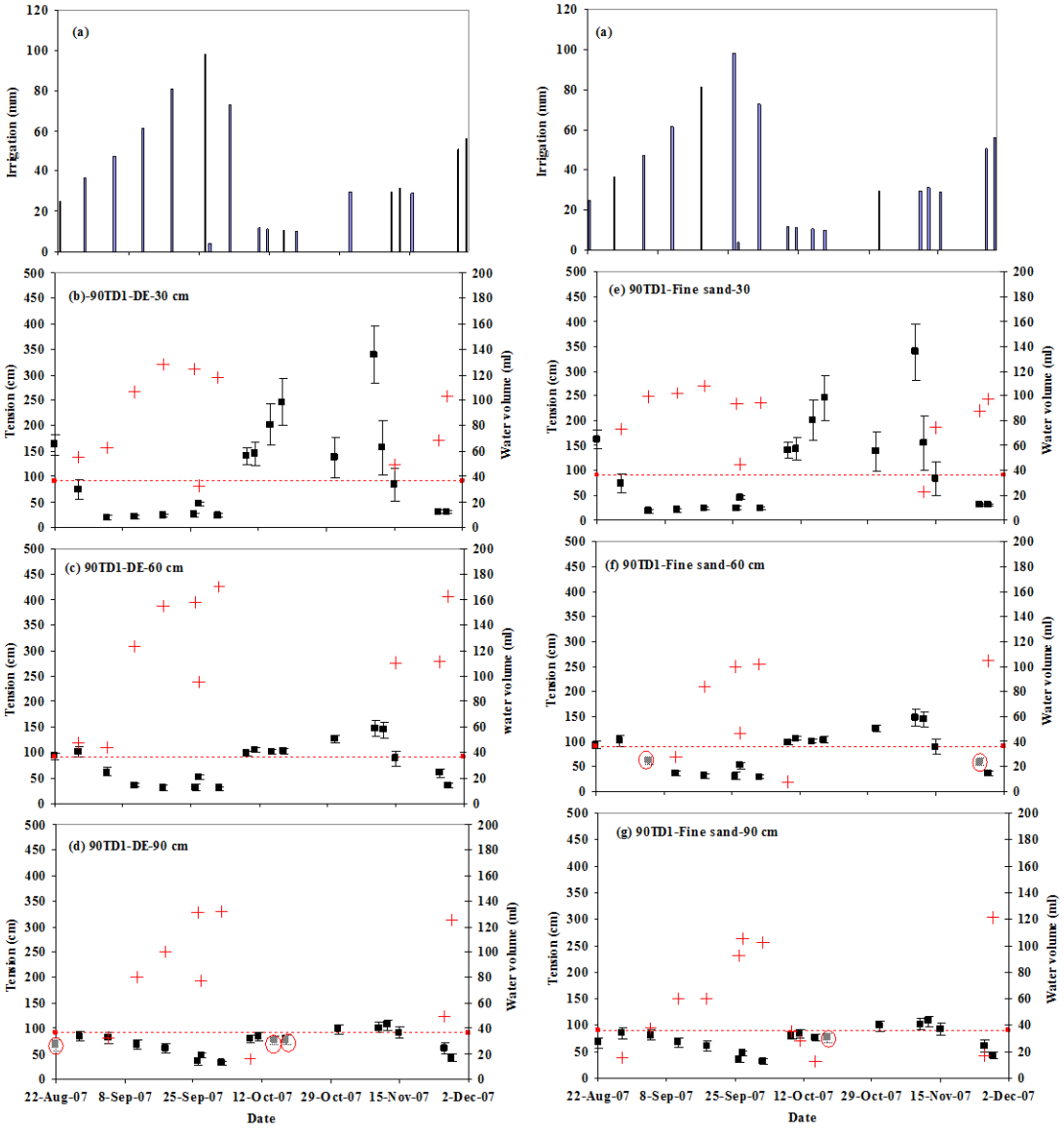

(a)

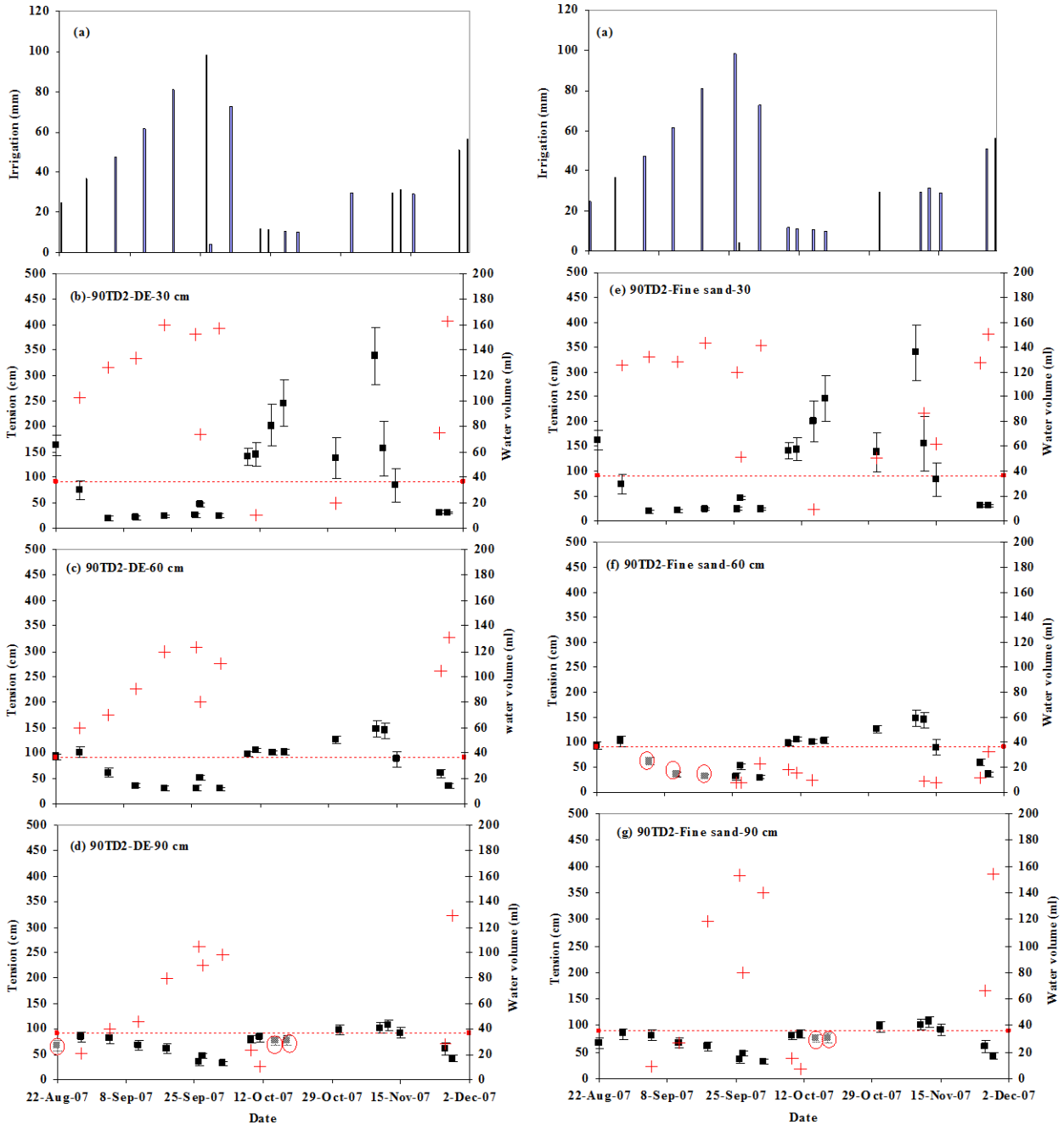

(b)

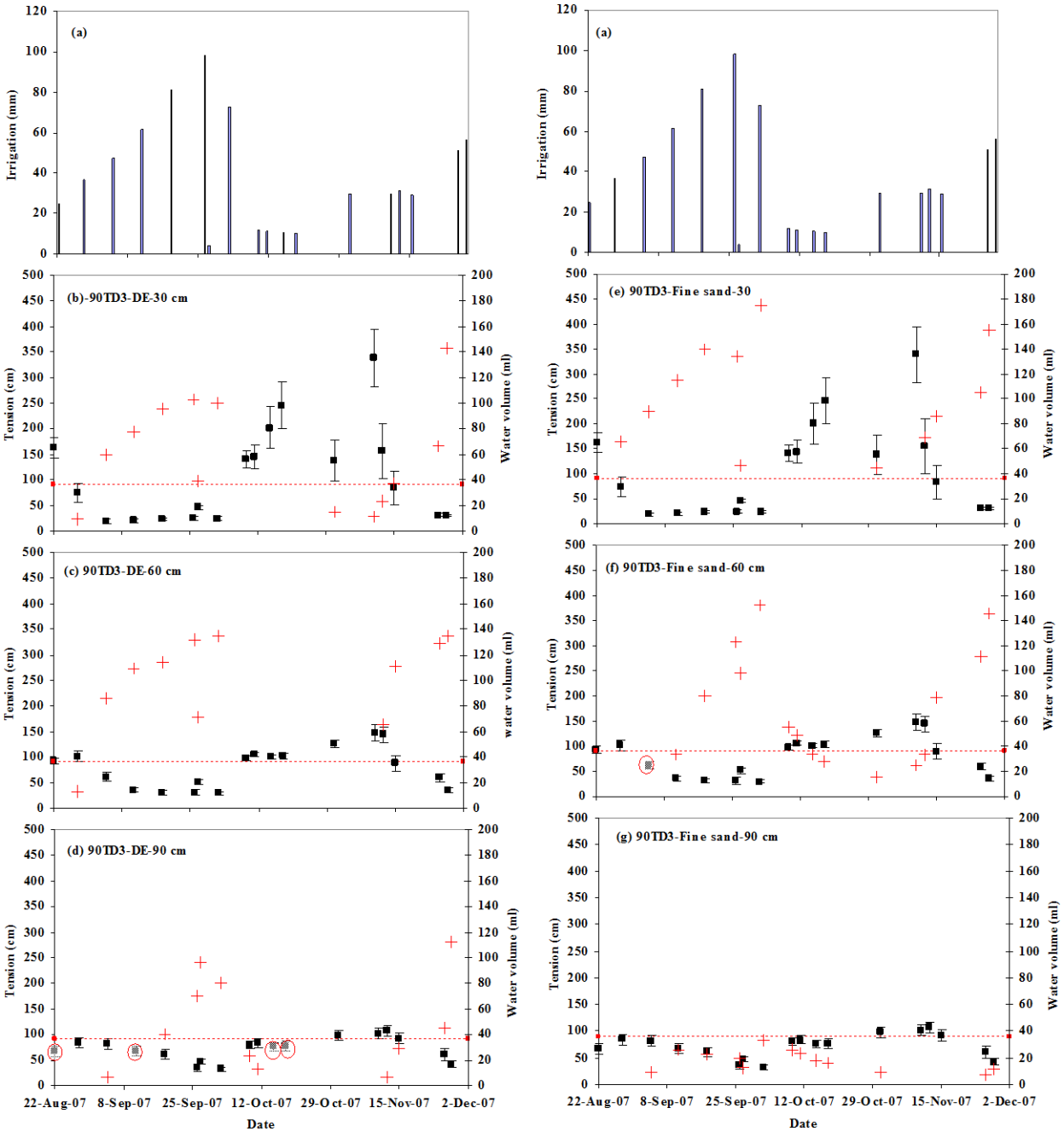

(c)

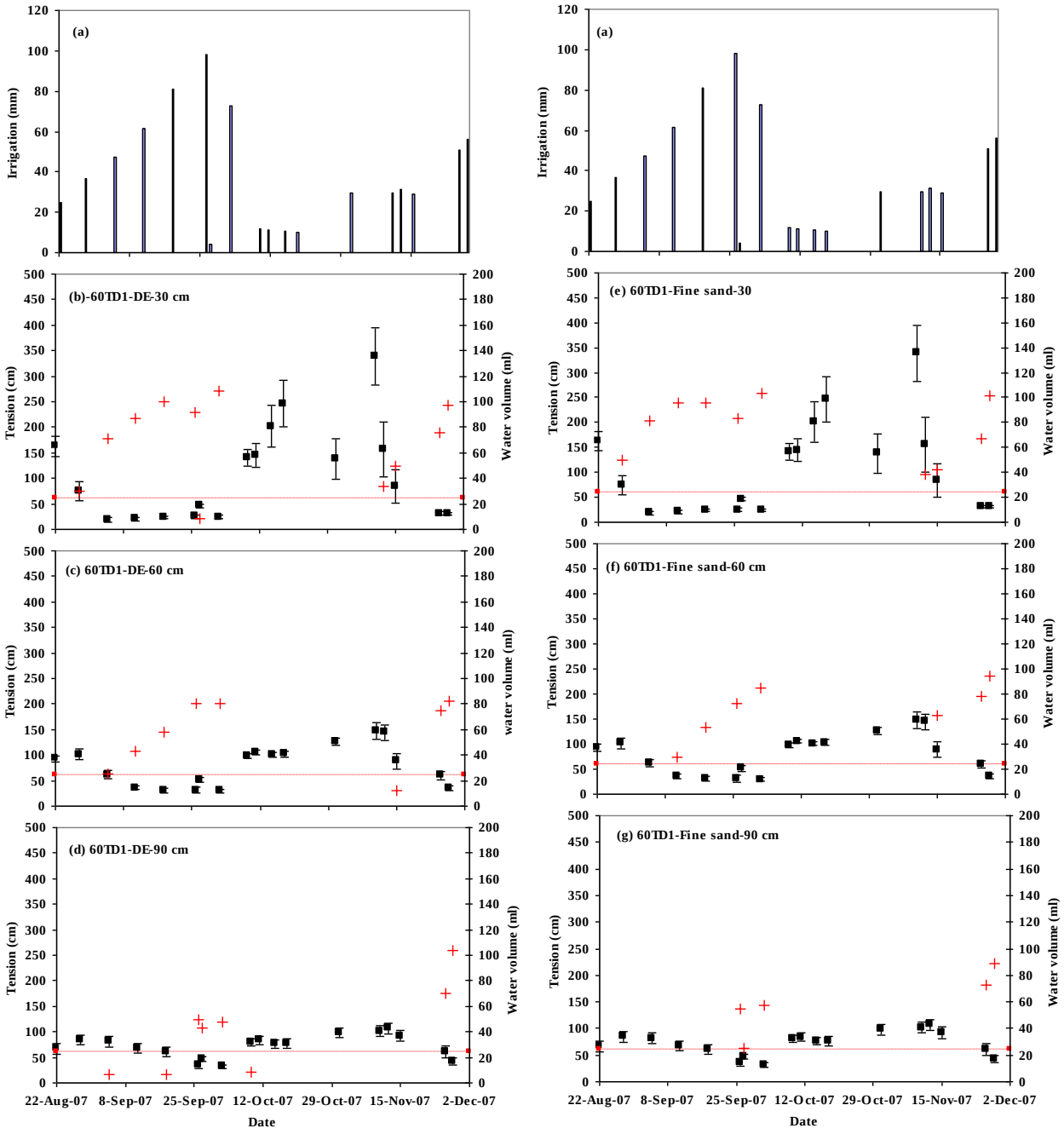

(d)

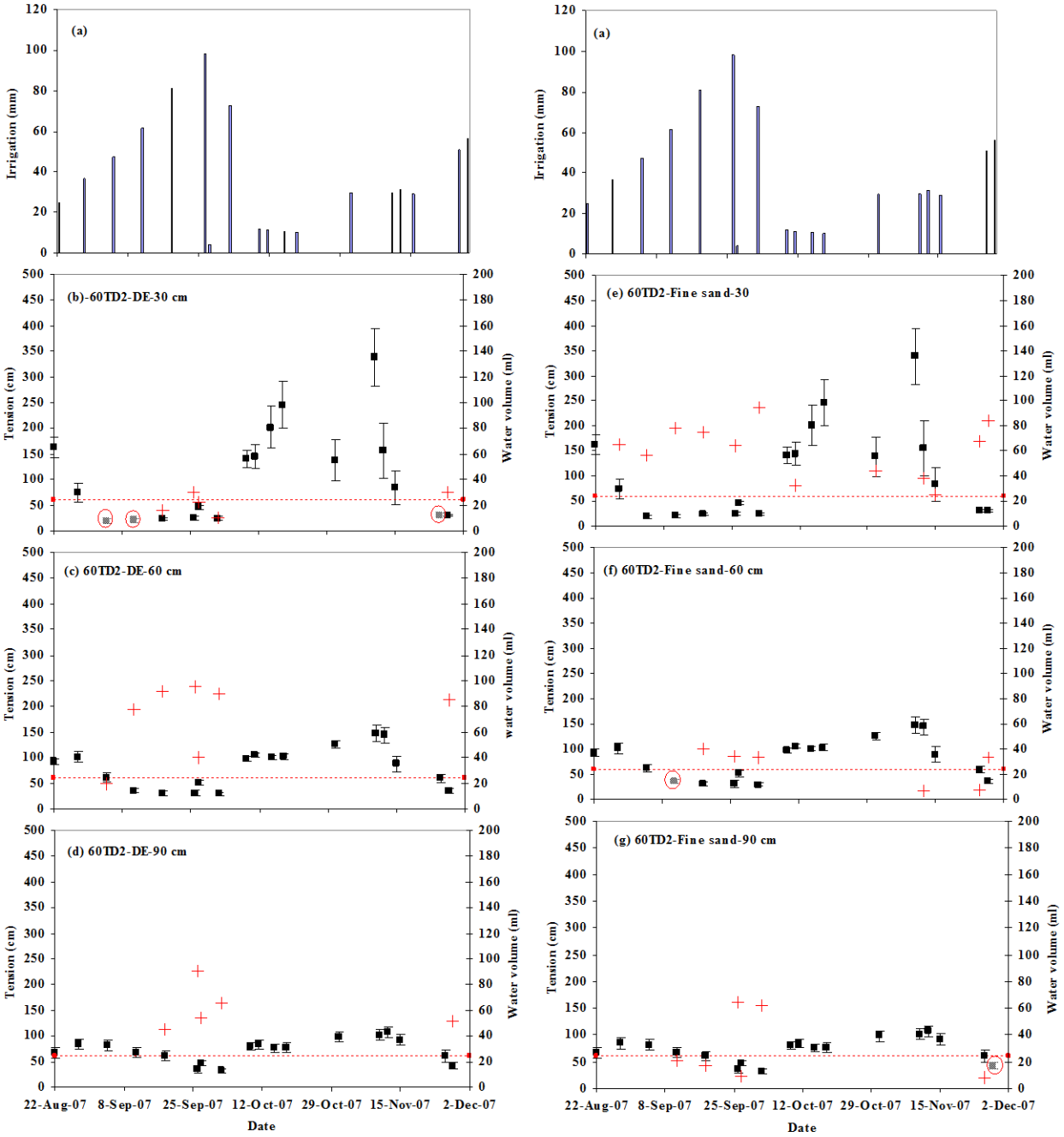

(e)

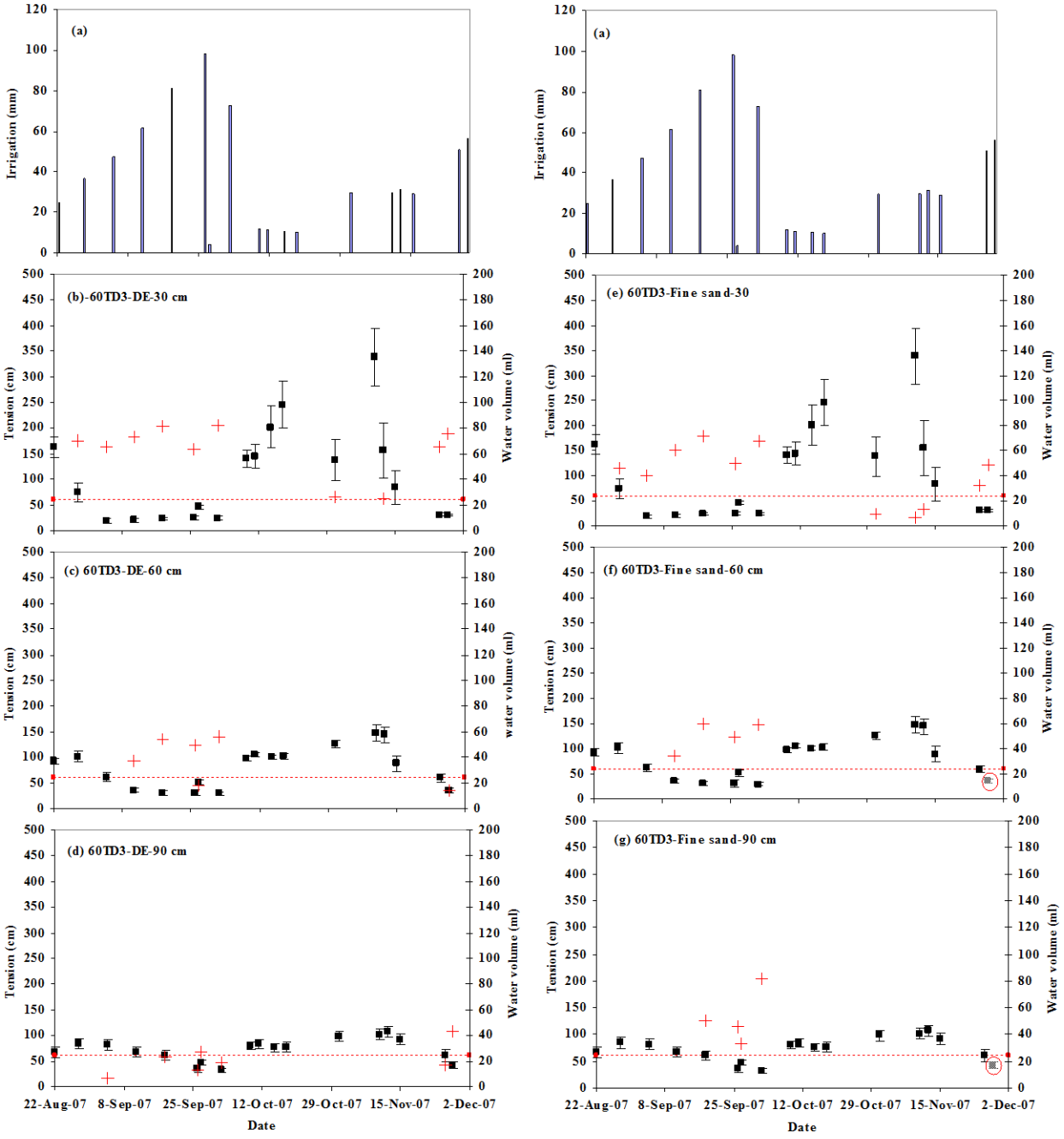

(f)

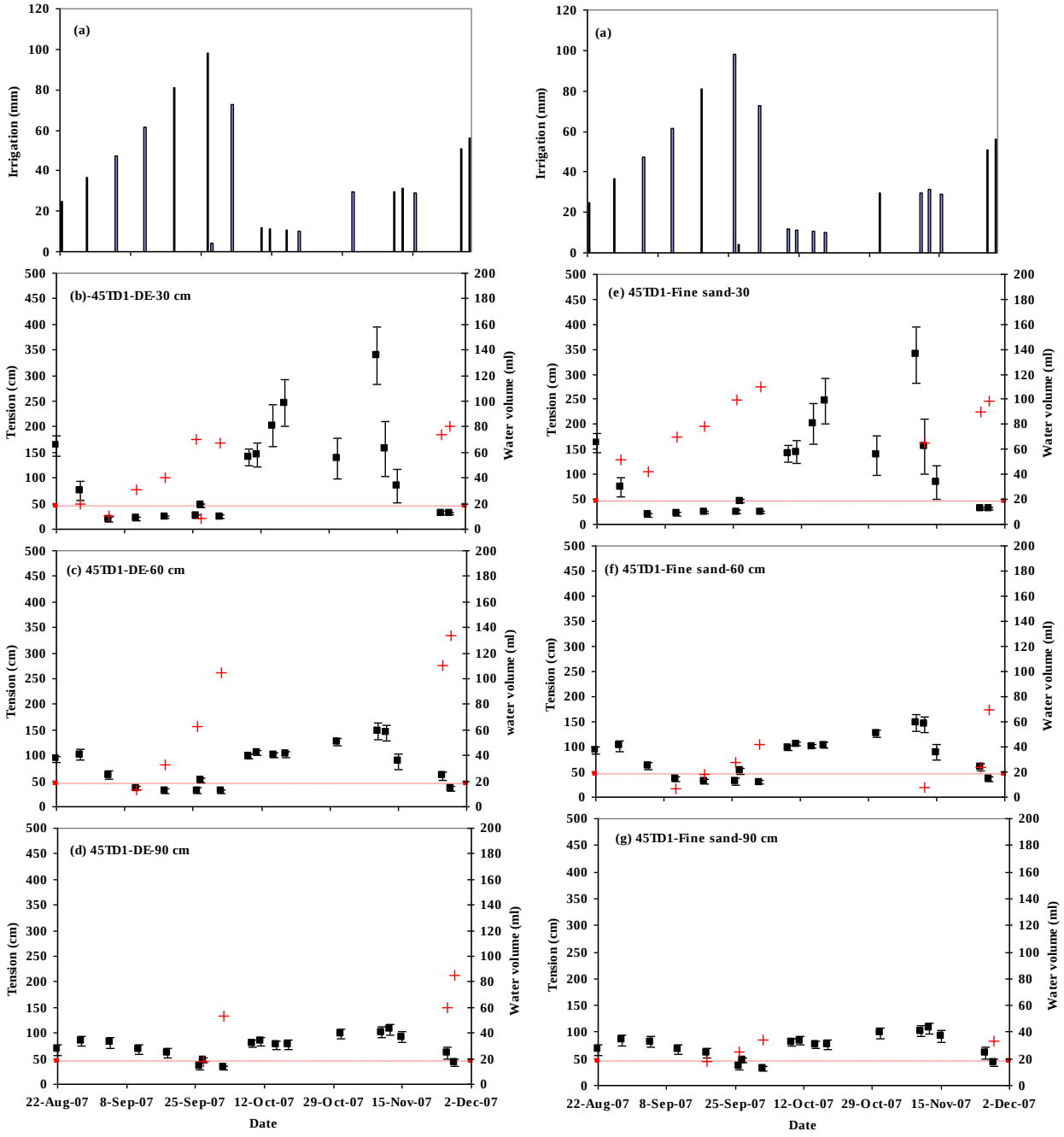

(g)

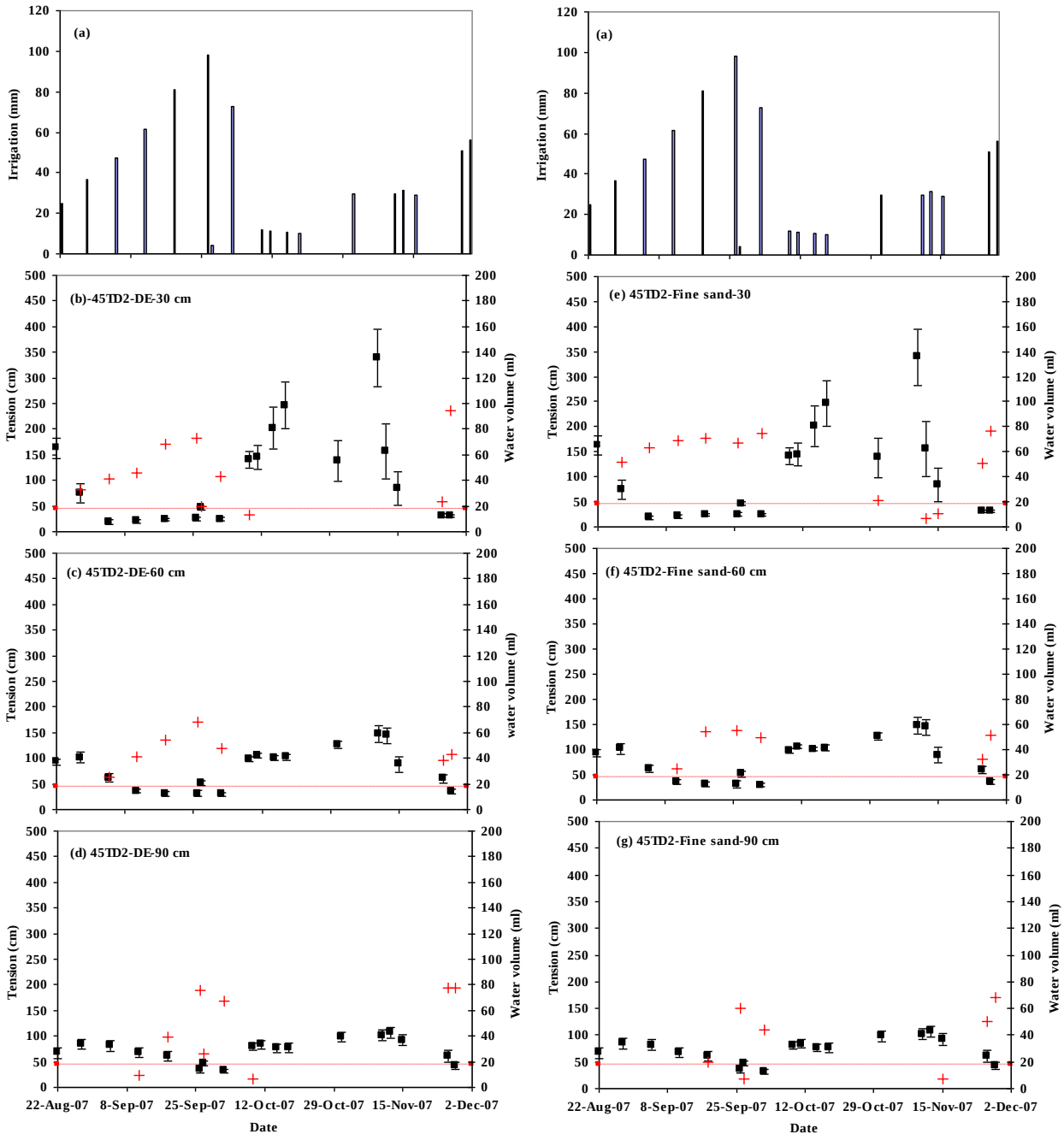

(h)

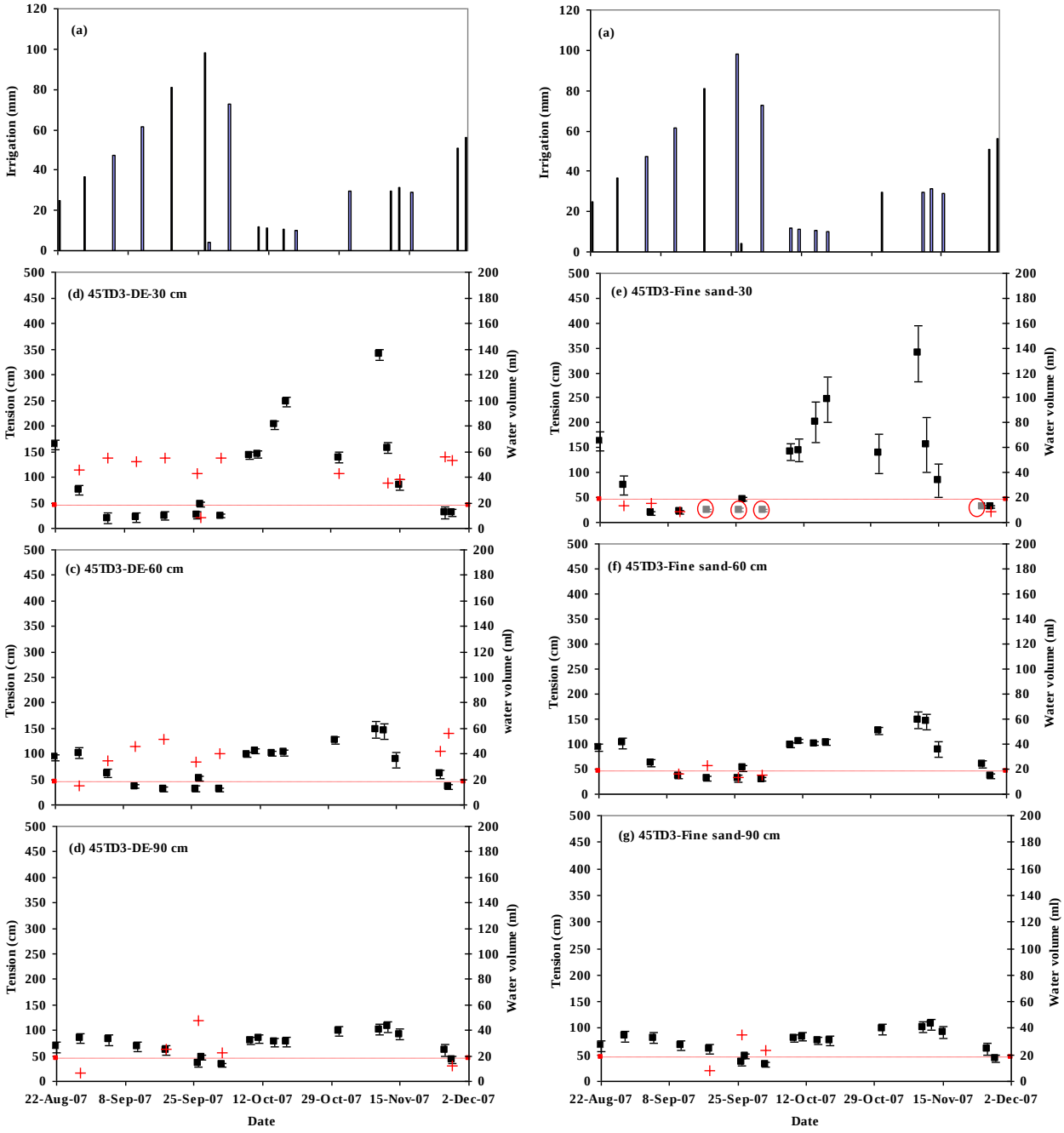

(i)

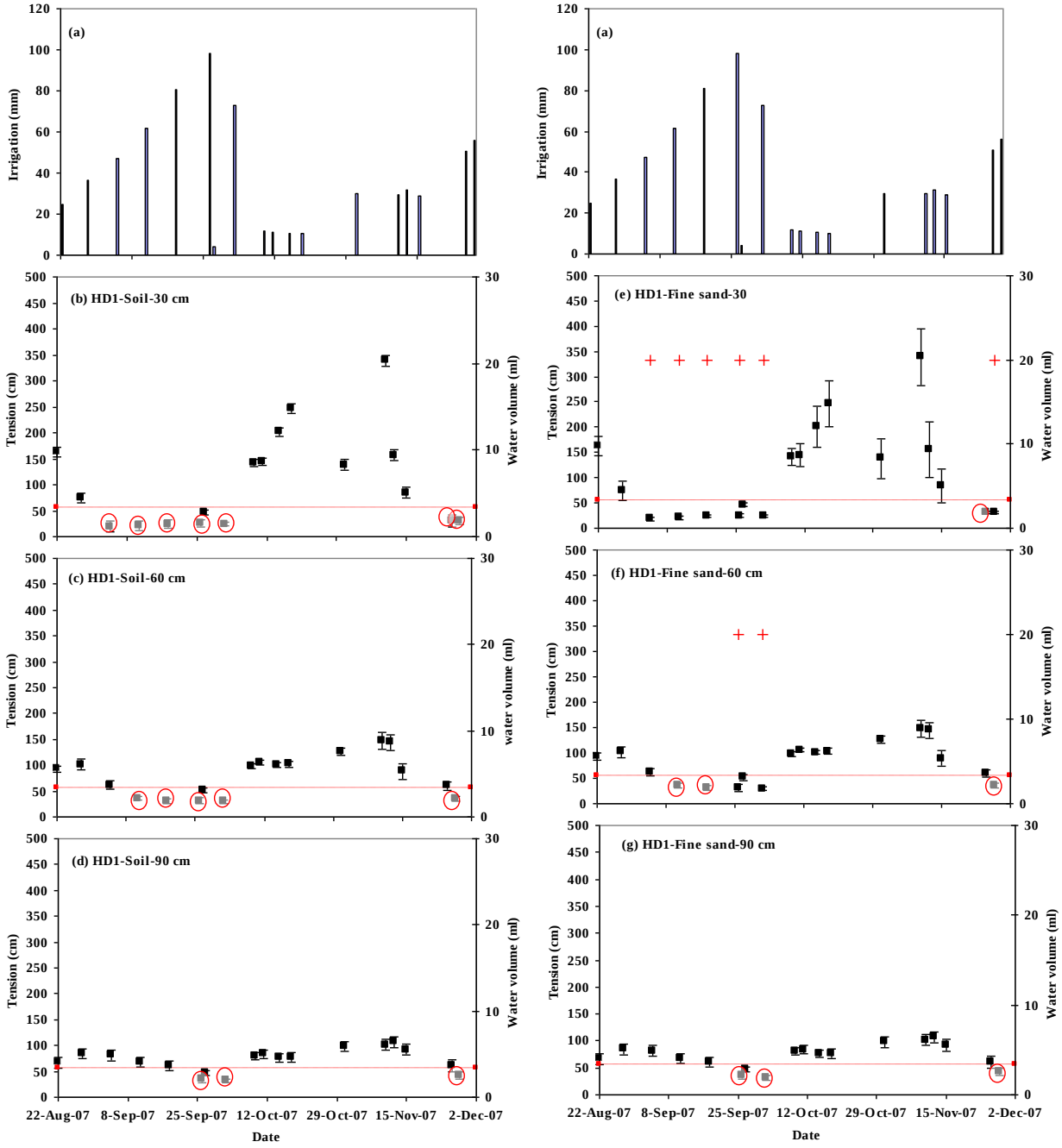

(j)

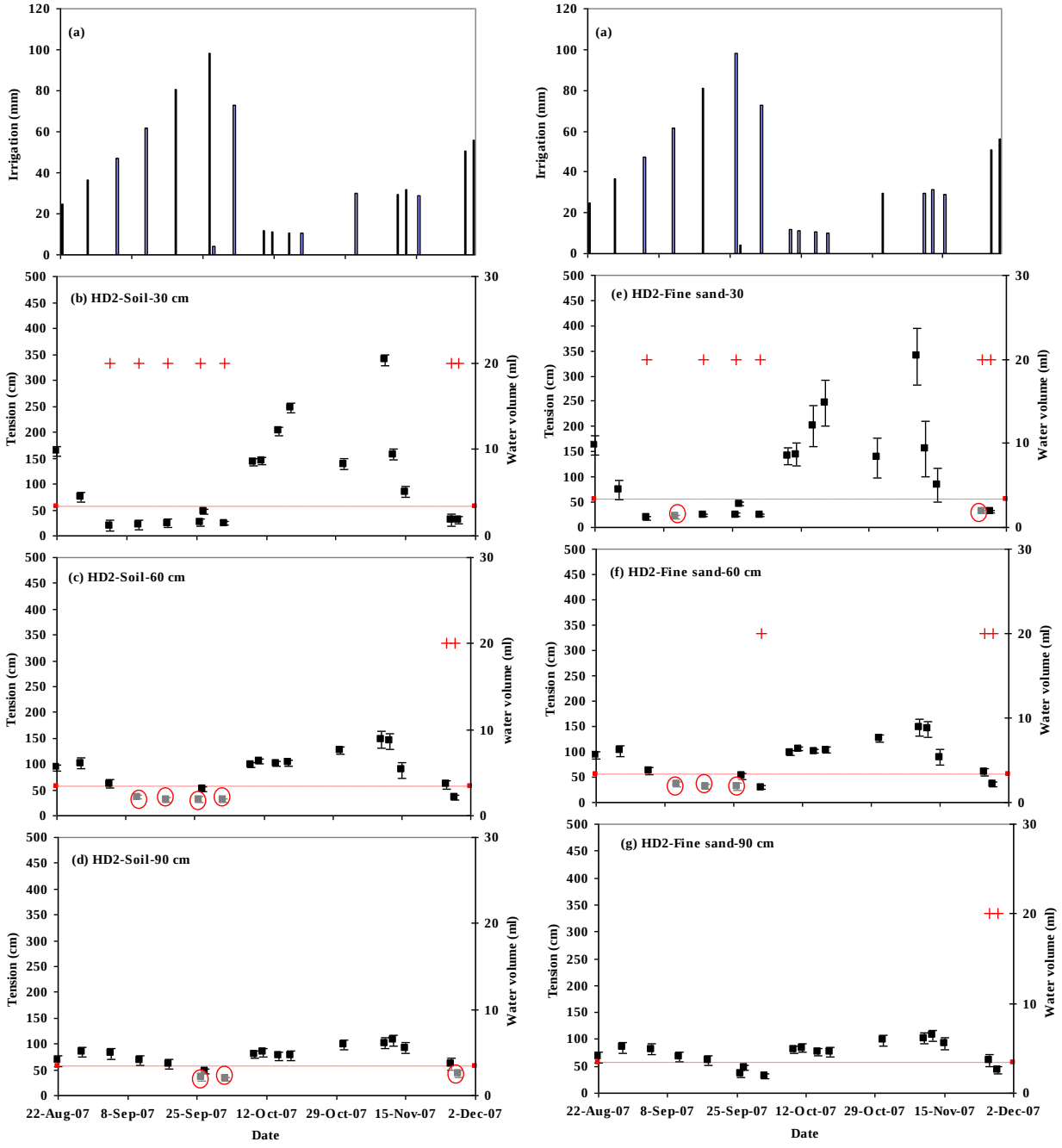

(k)

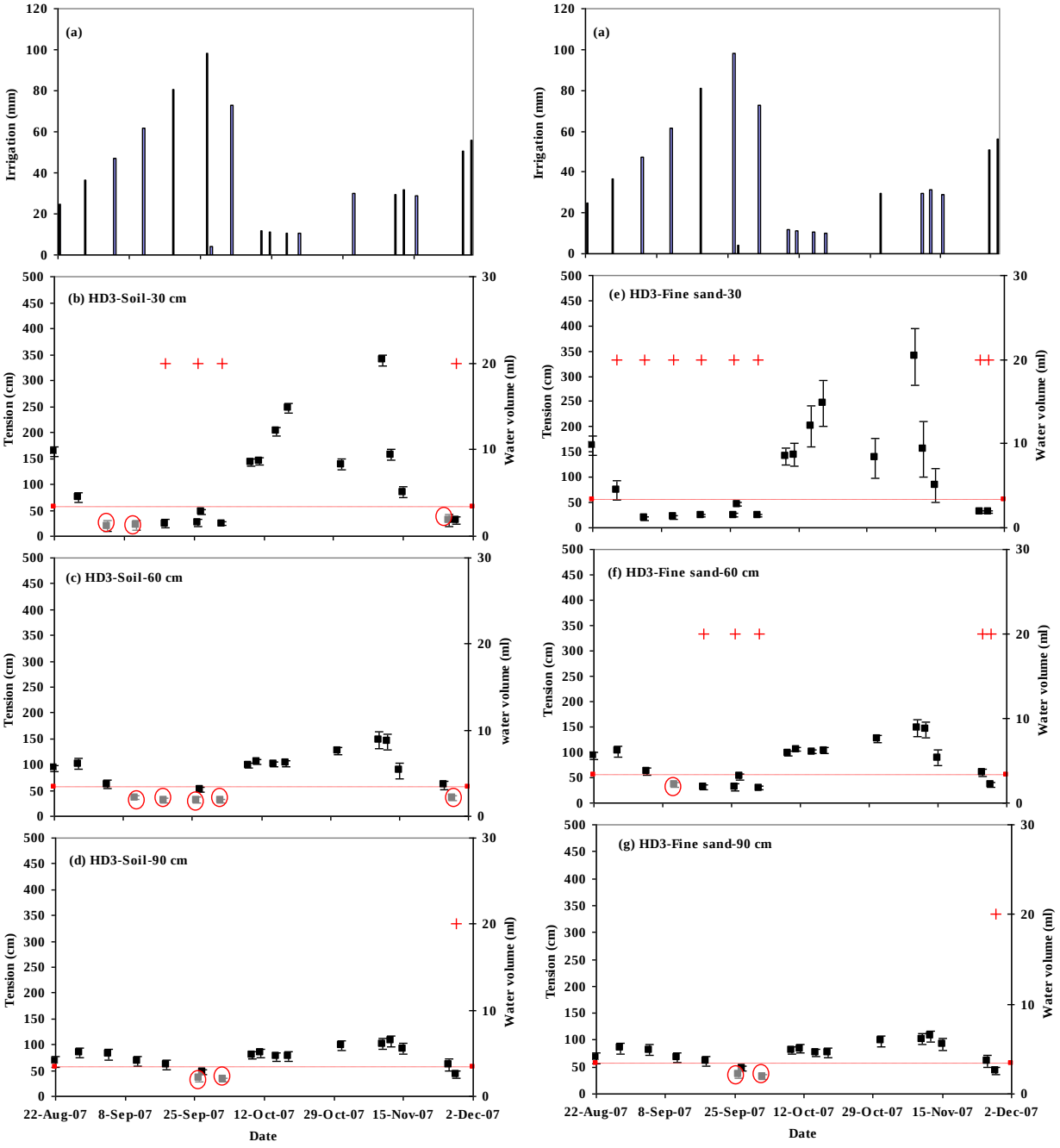

(l)

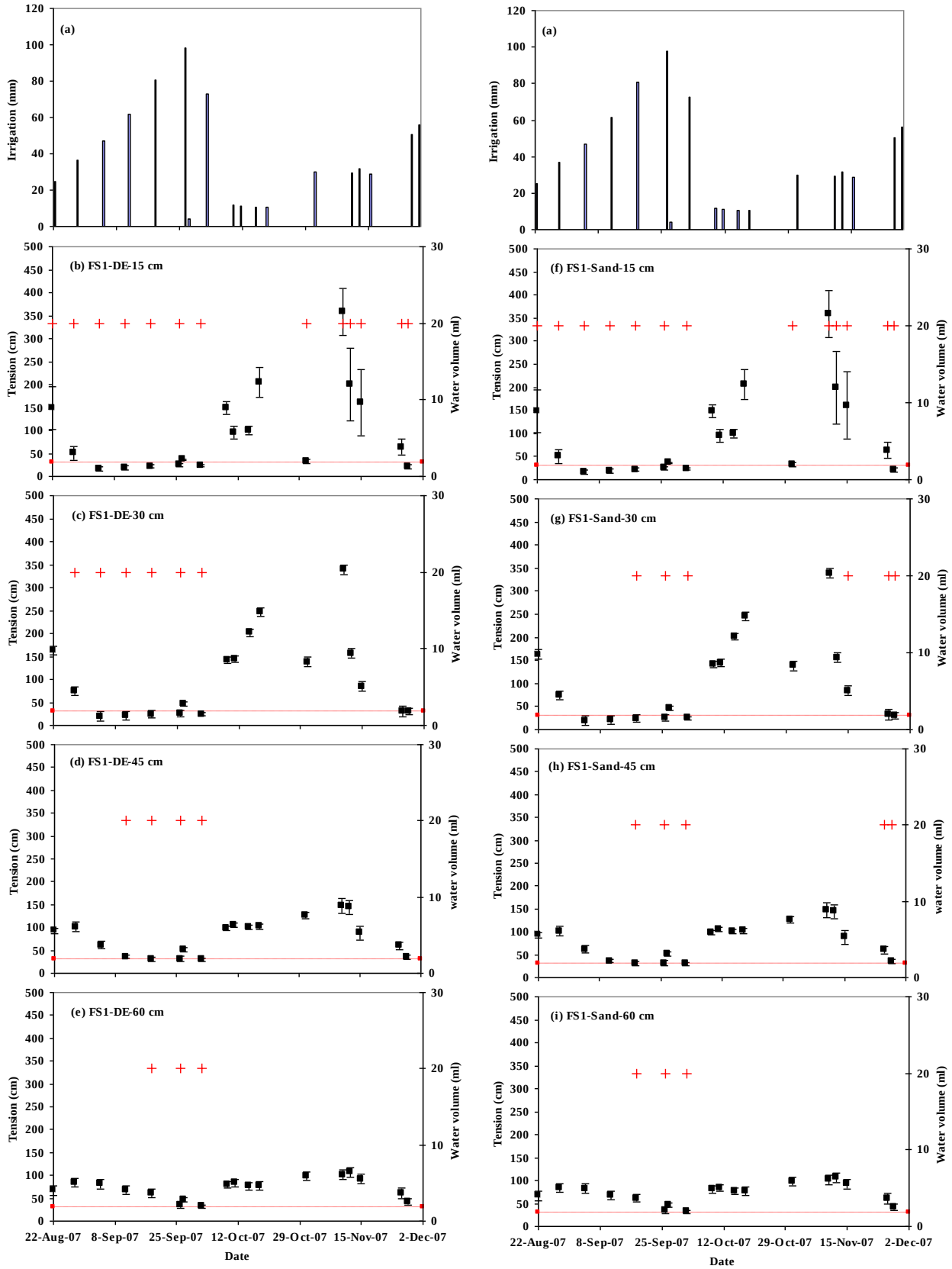

(m)

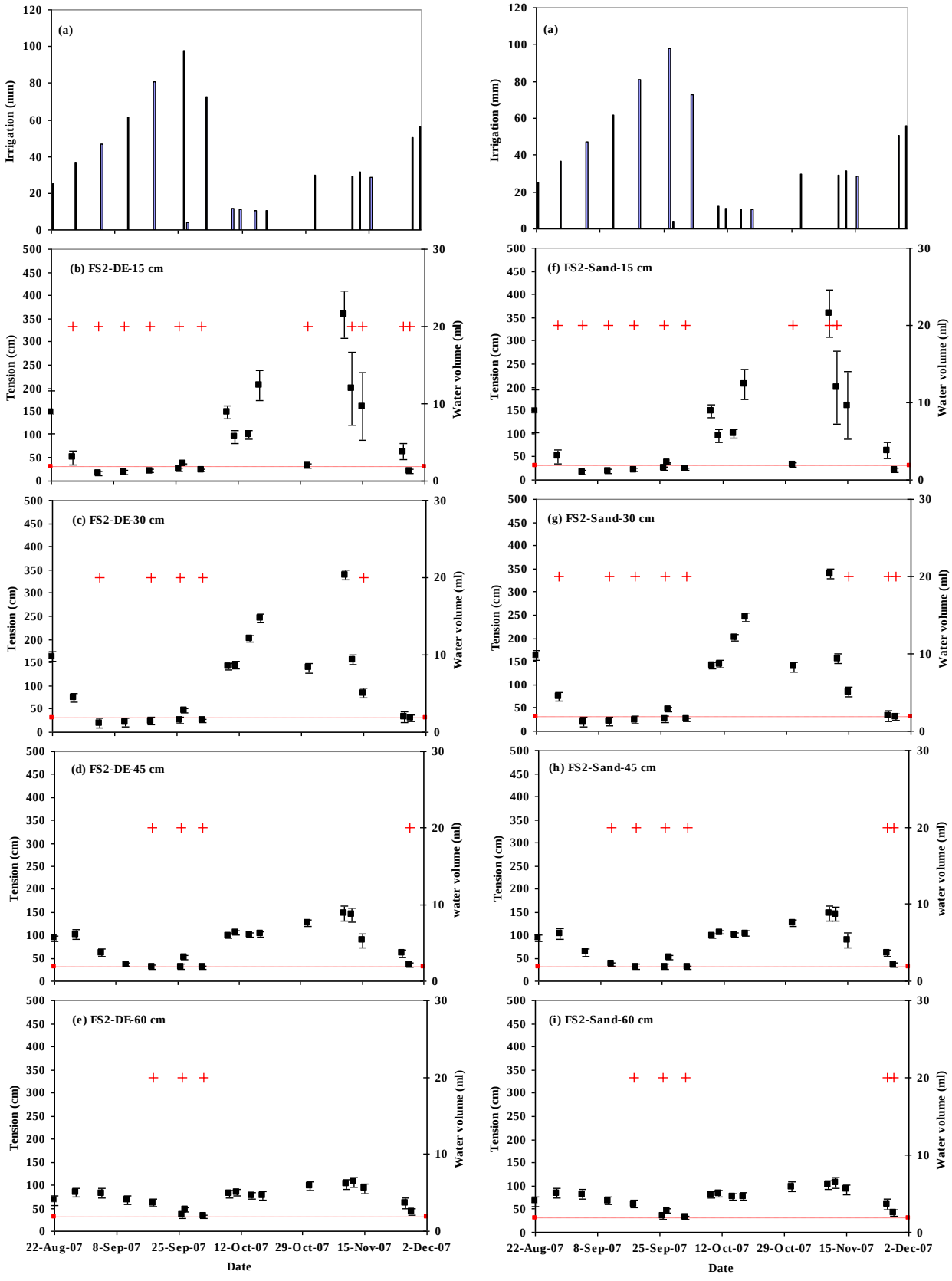

(n)

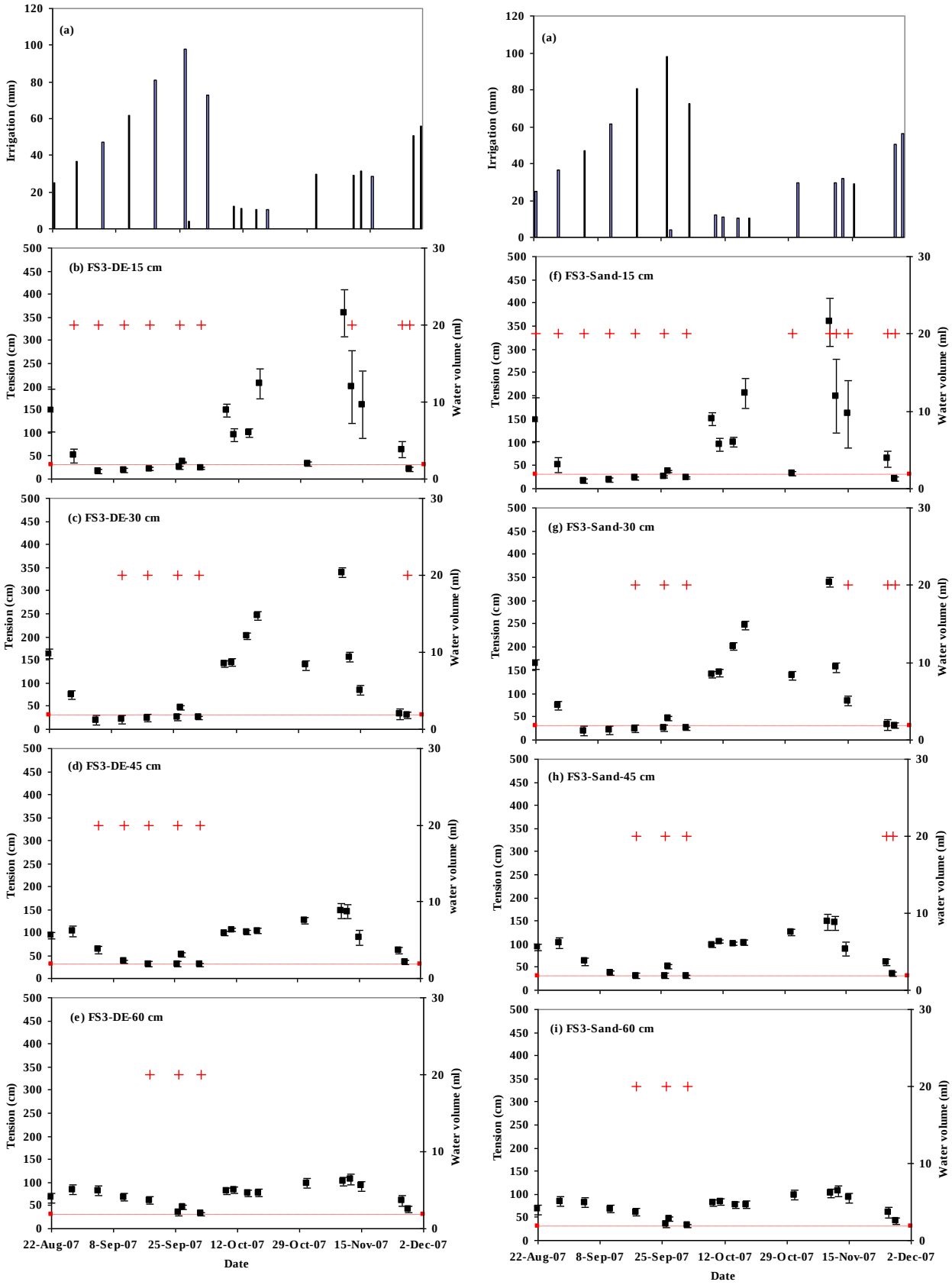

(o)

APPENDIX 3

True positive response (+), false negative responses (circle), mean bulk soil tensions of each event with error bars, and tension sensitivity (dotted line) of WFD types in response to rainfall (a to o).

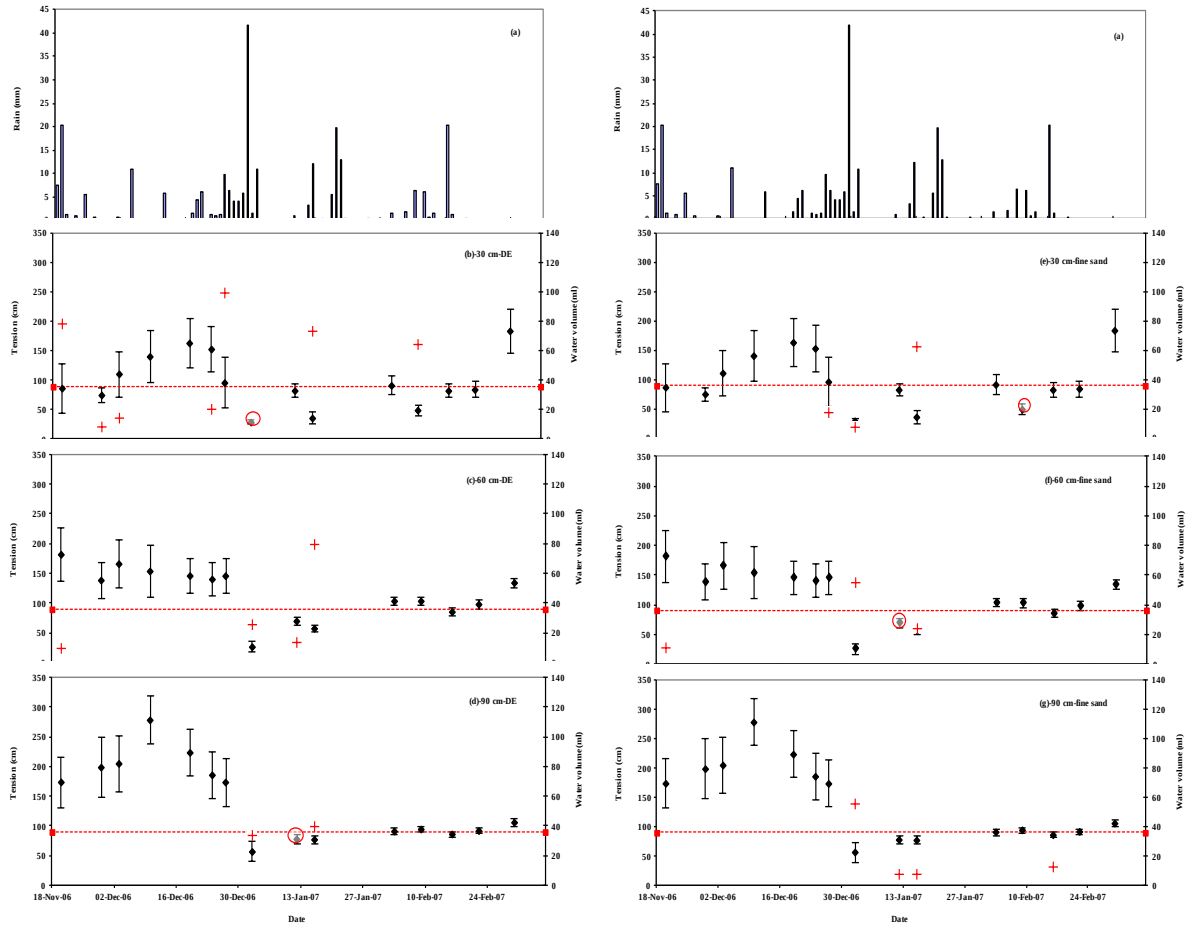

(a)

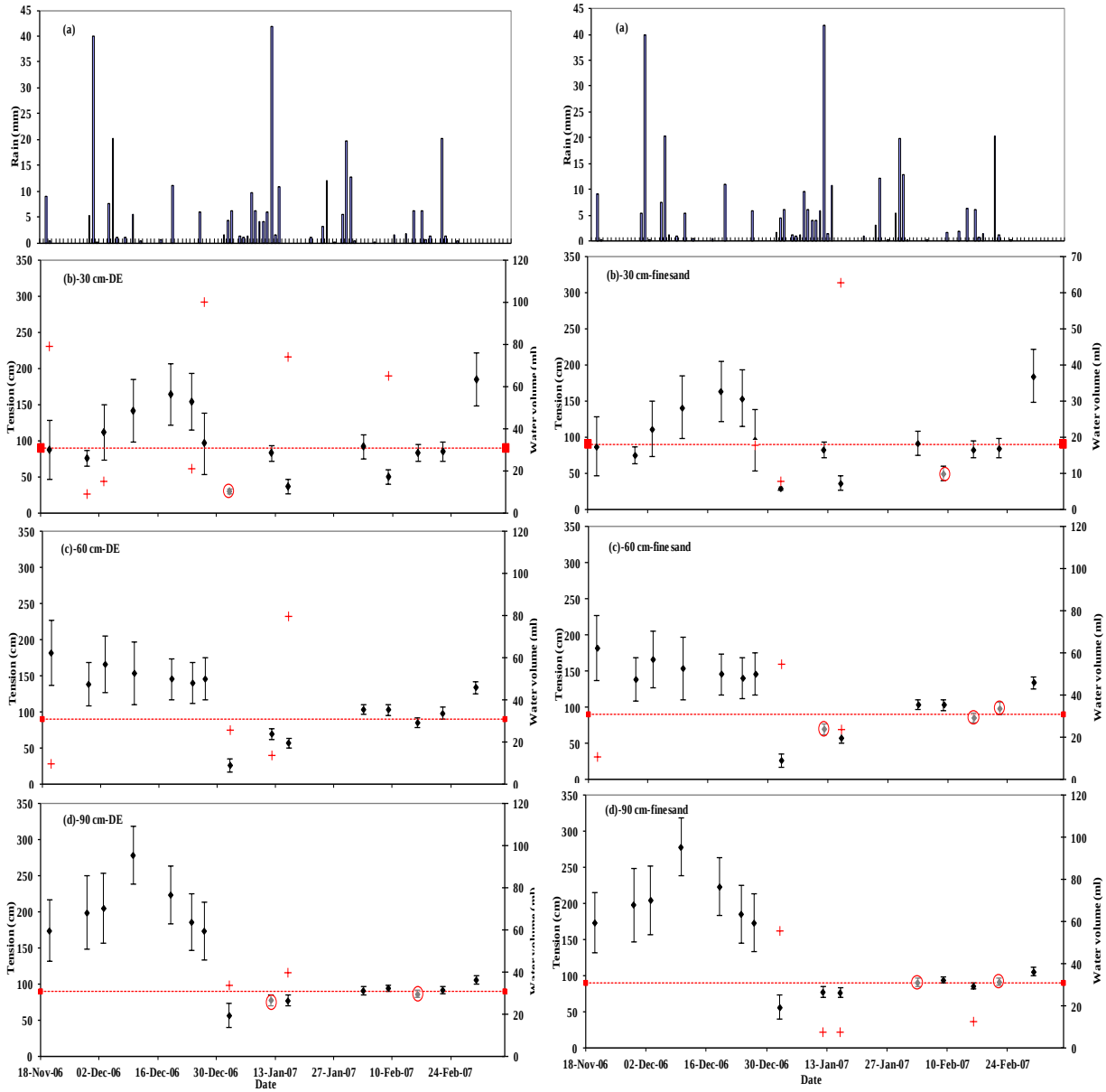

(b)

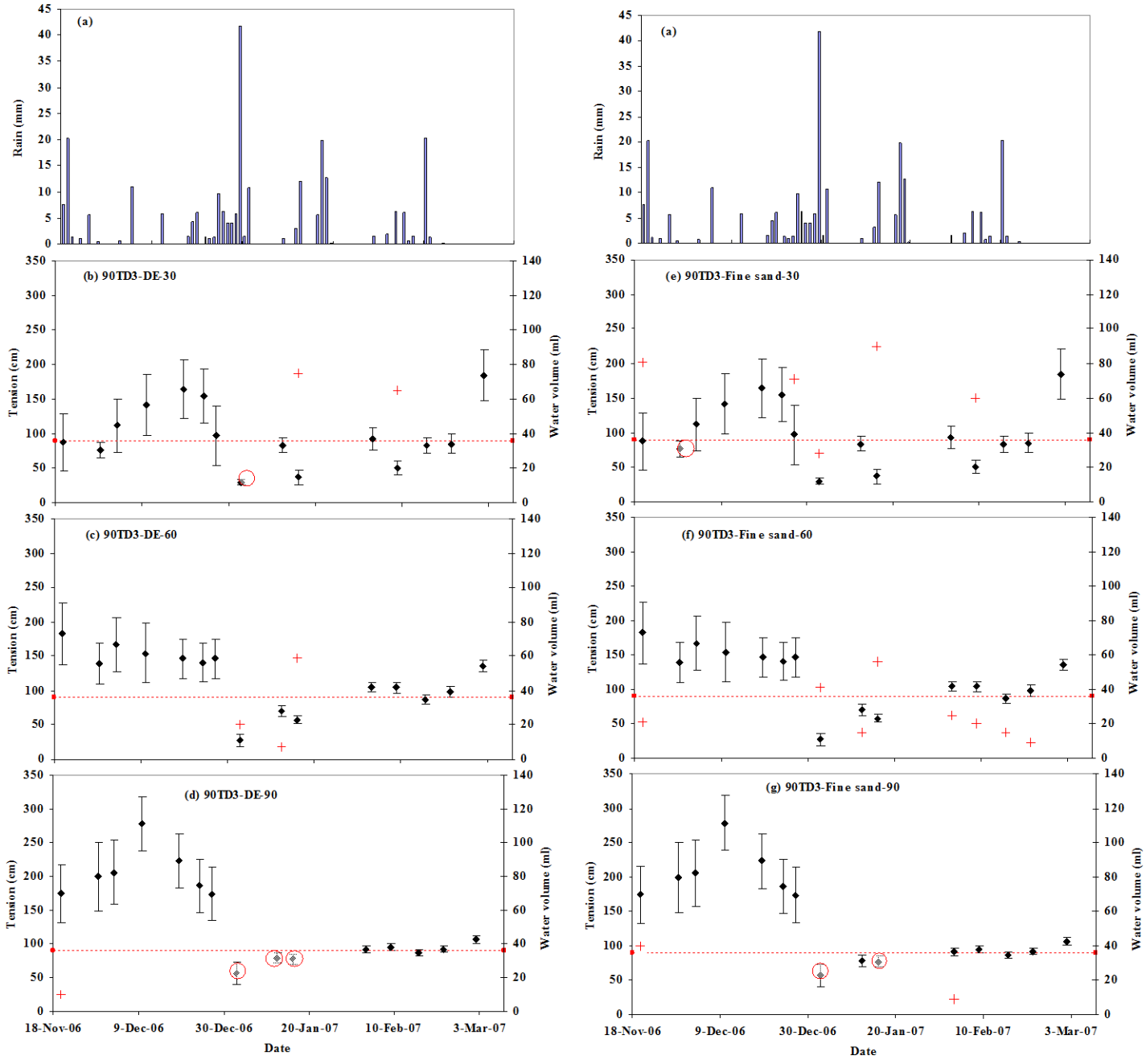

(c)

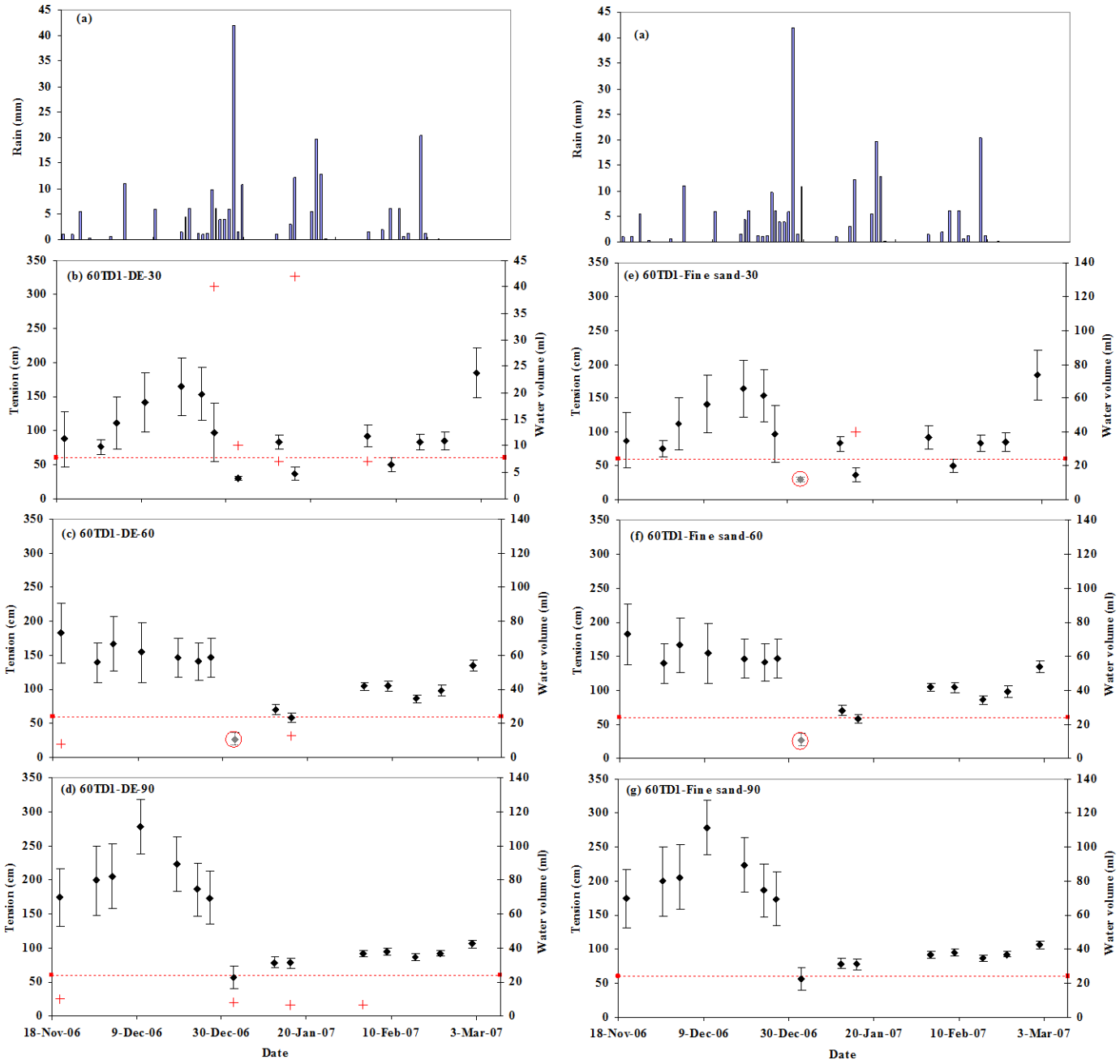

(d)

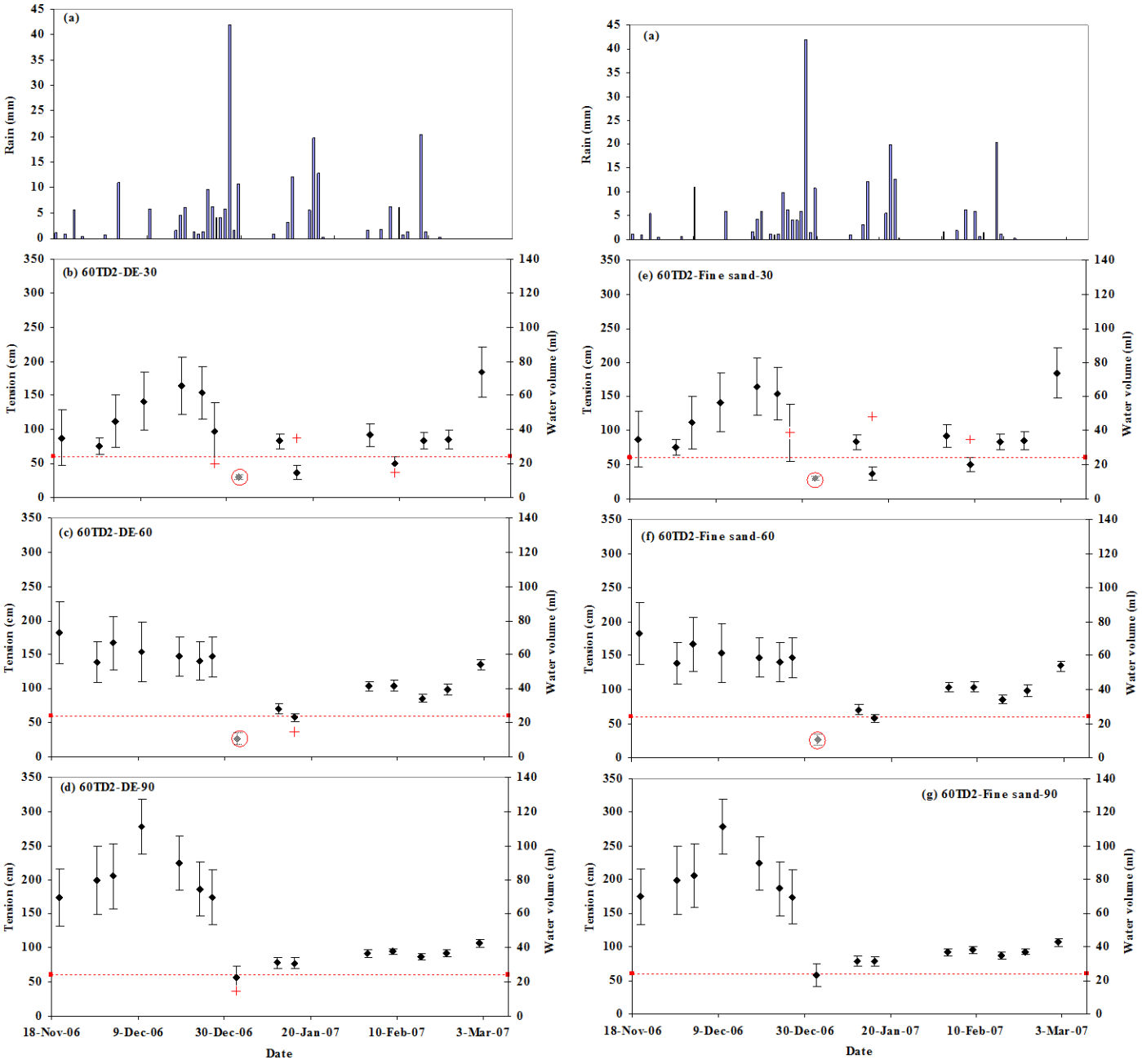

(e)

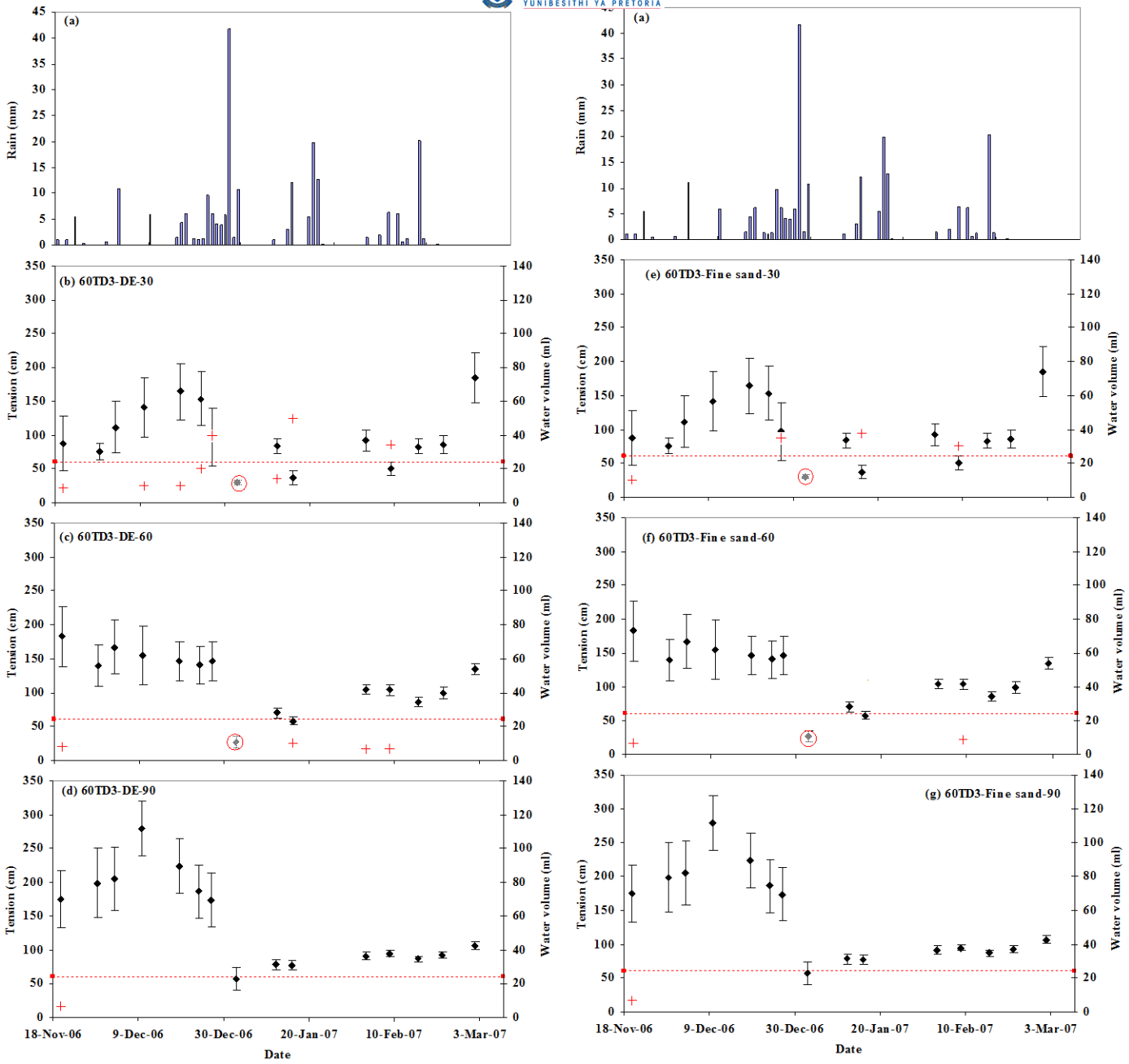

(f)

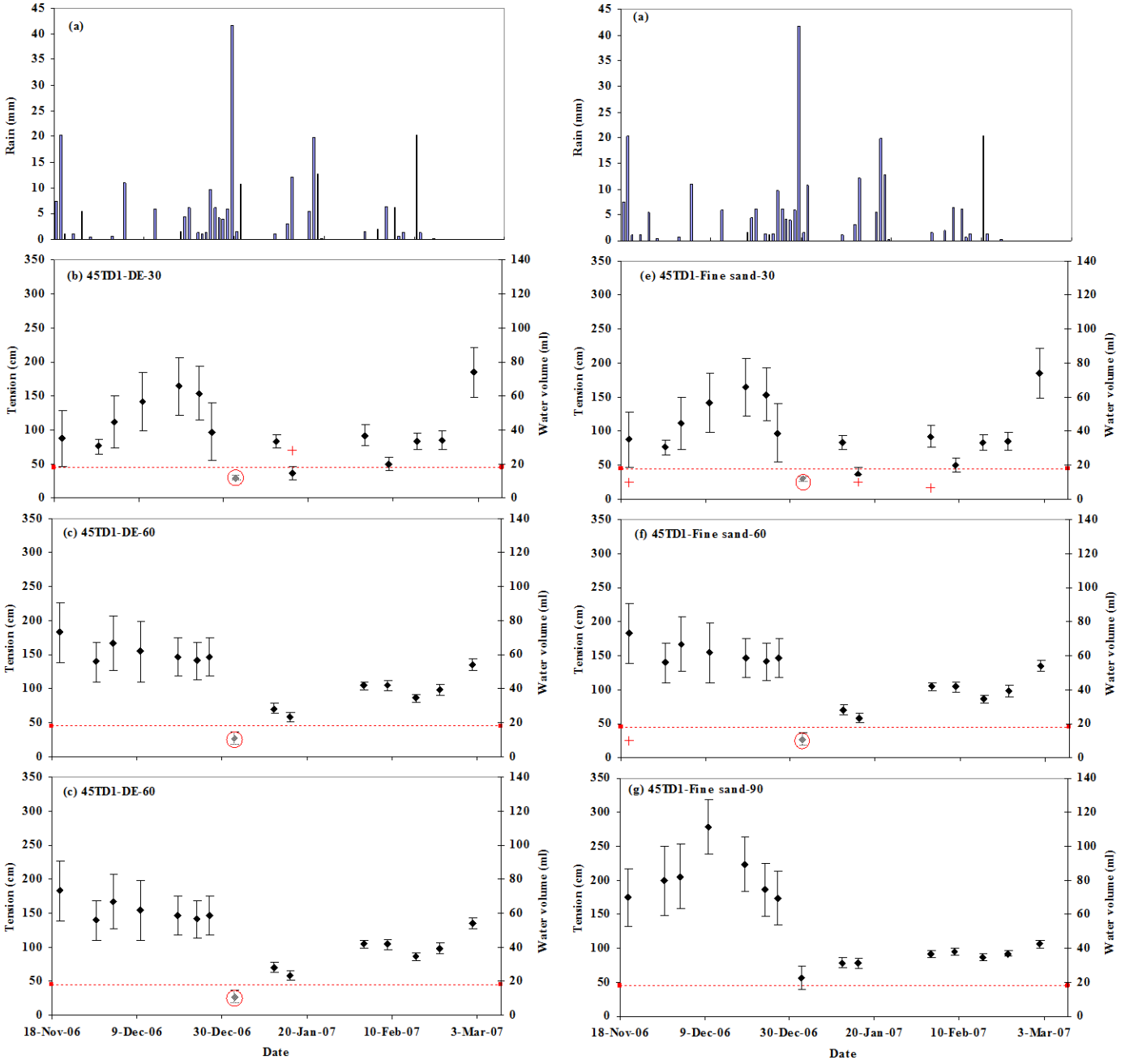

(g)

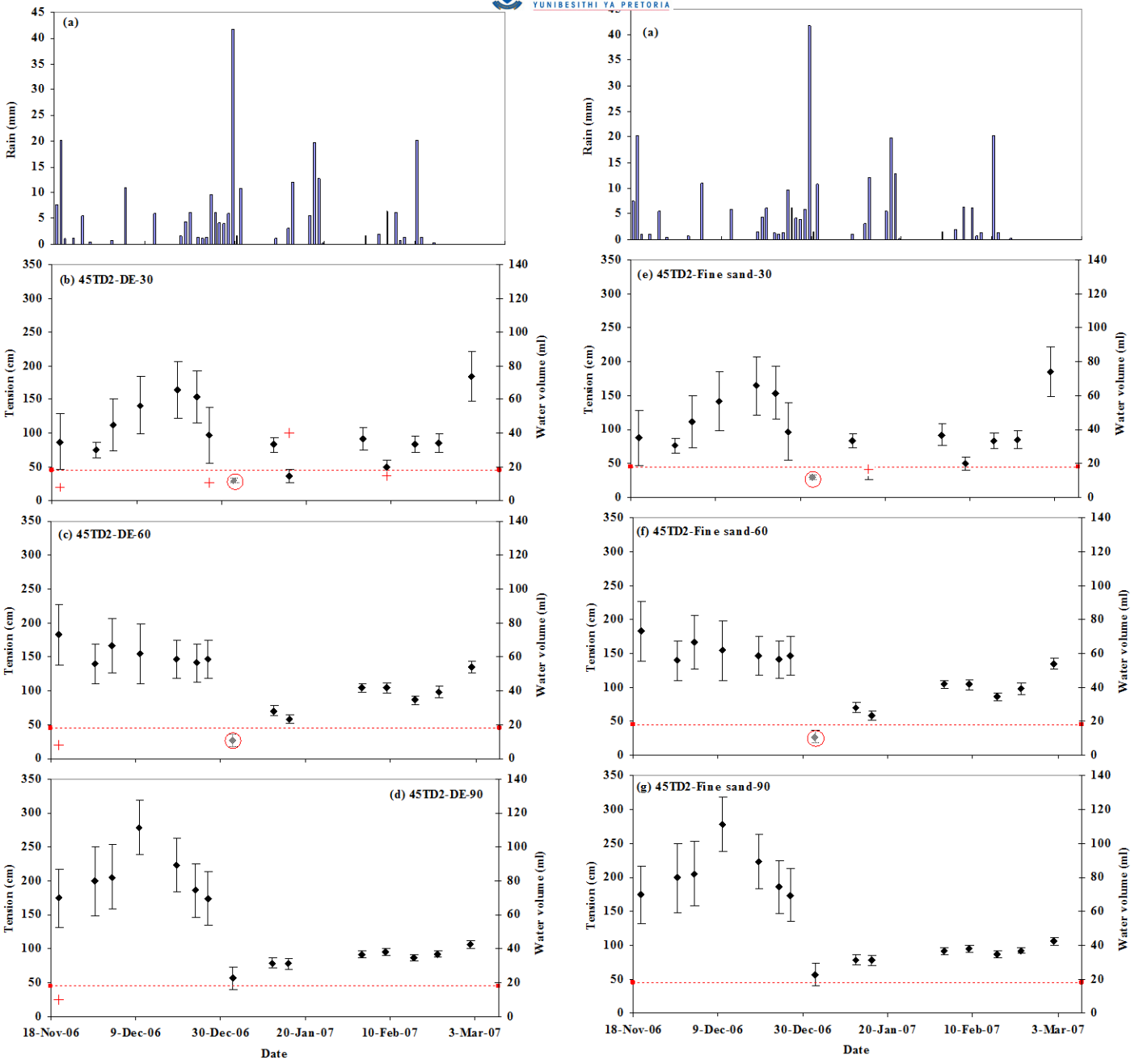

(h)

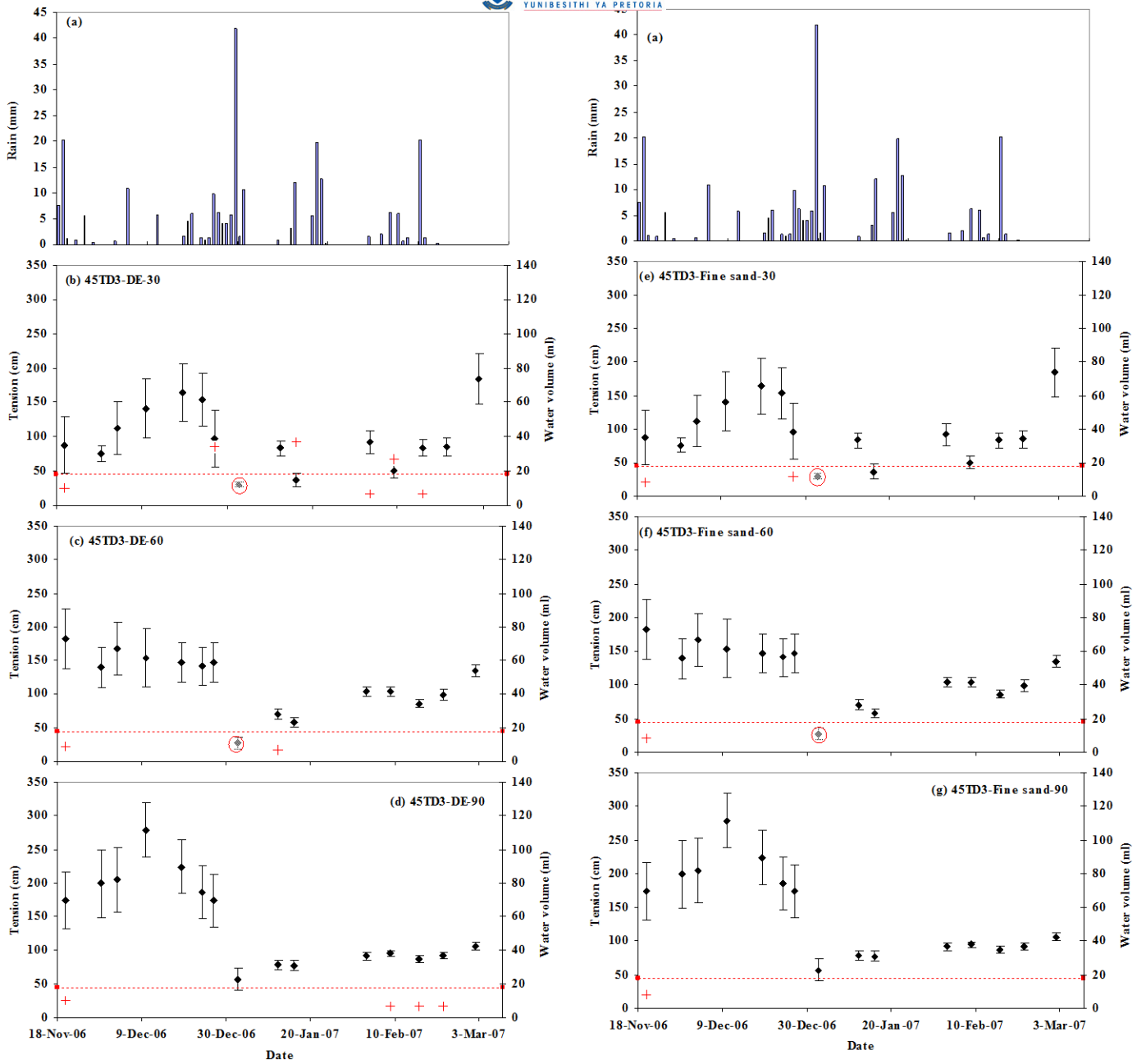

(i)

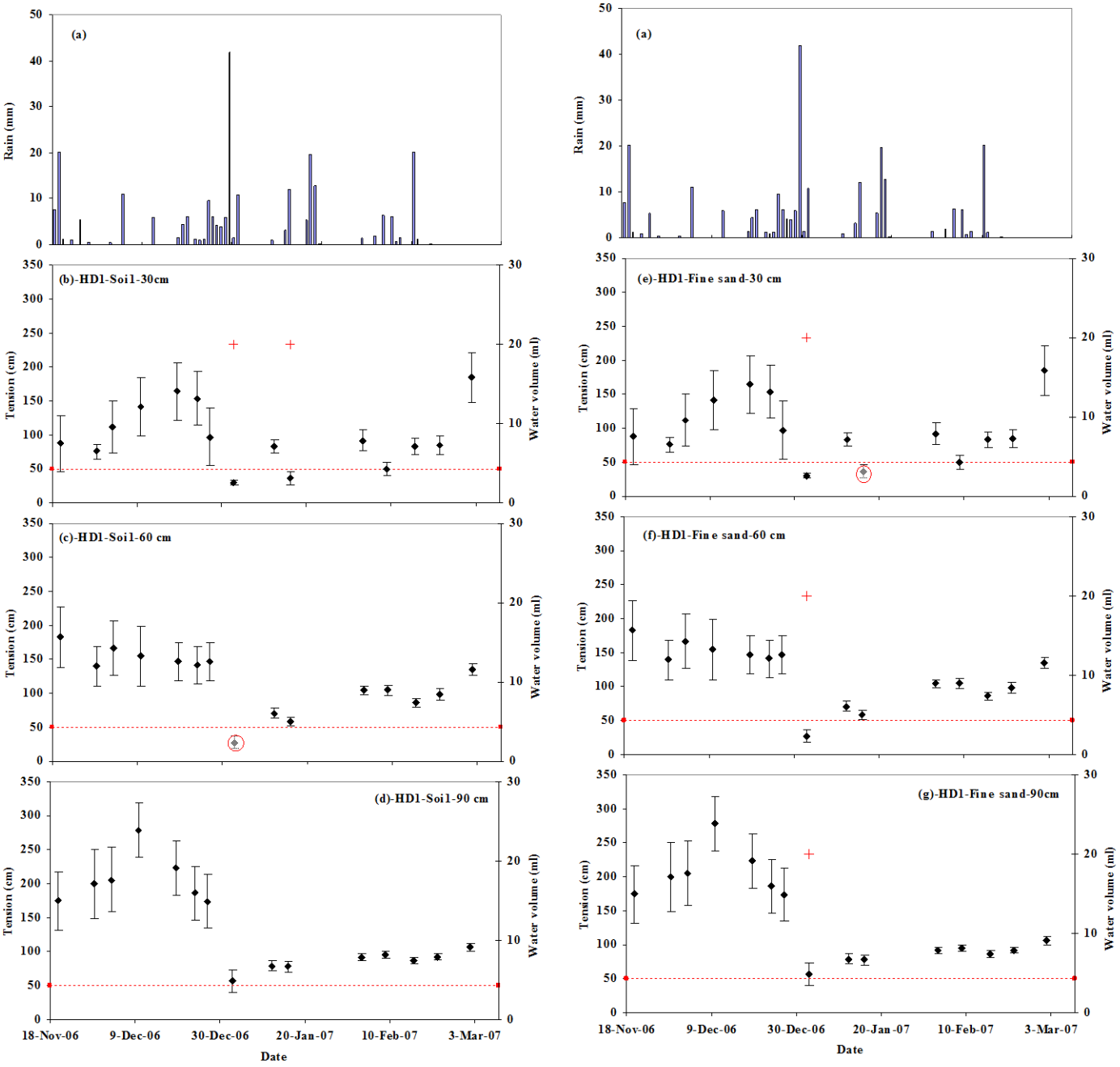

(j)

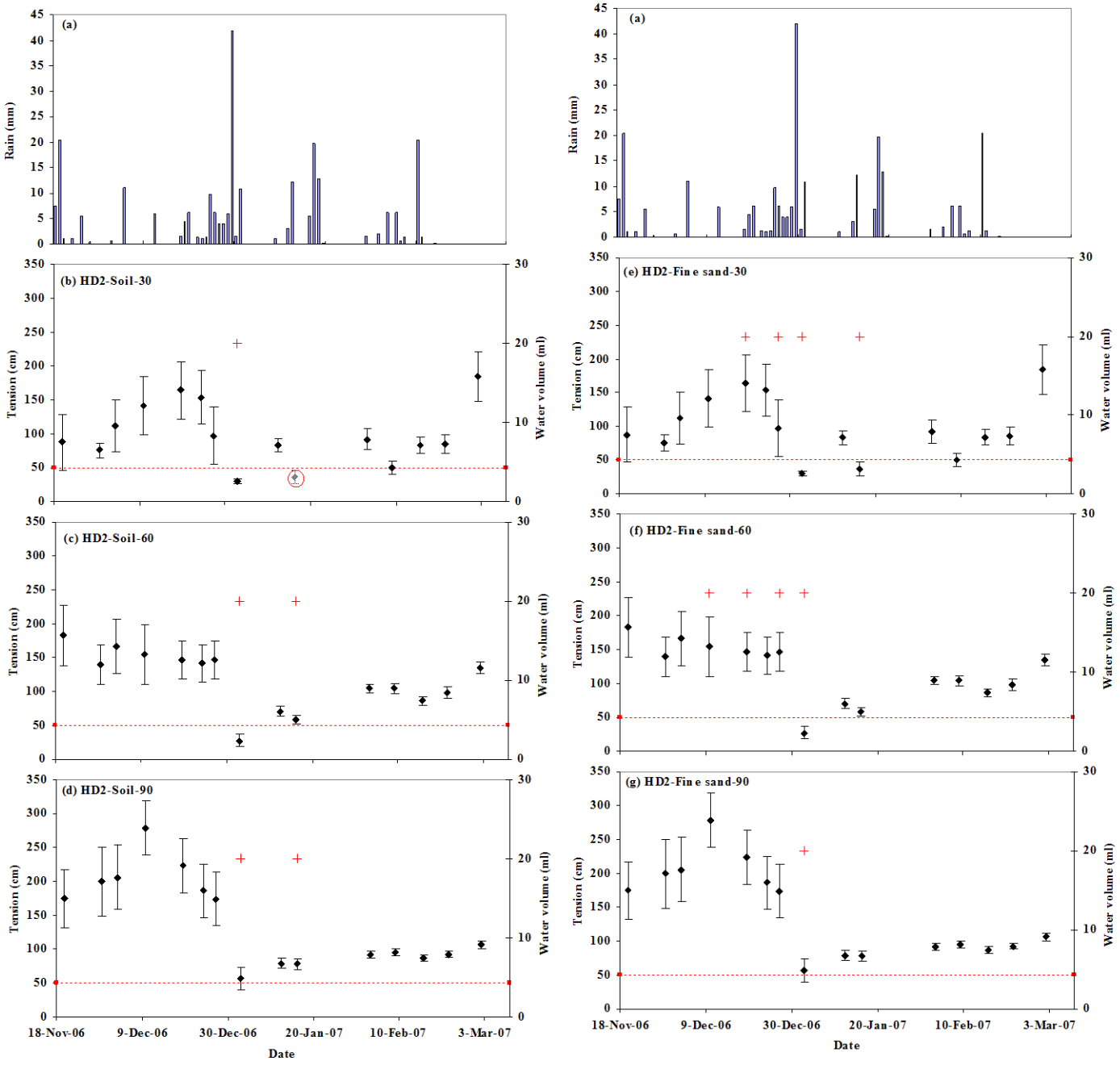

(k)

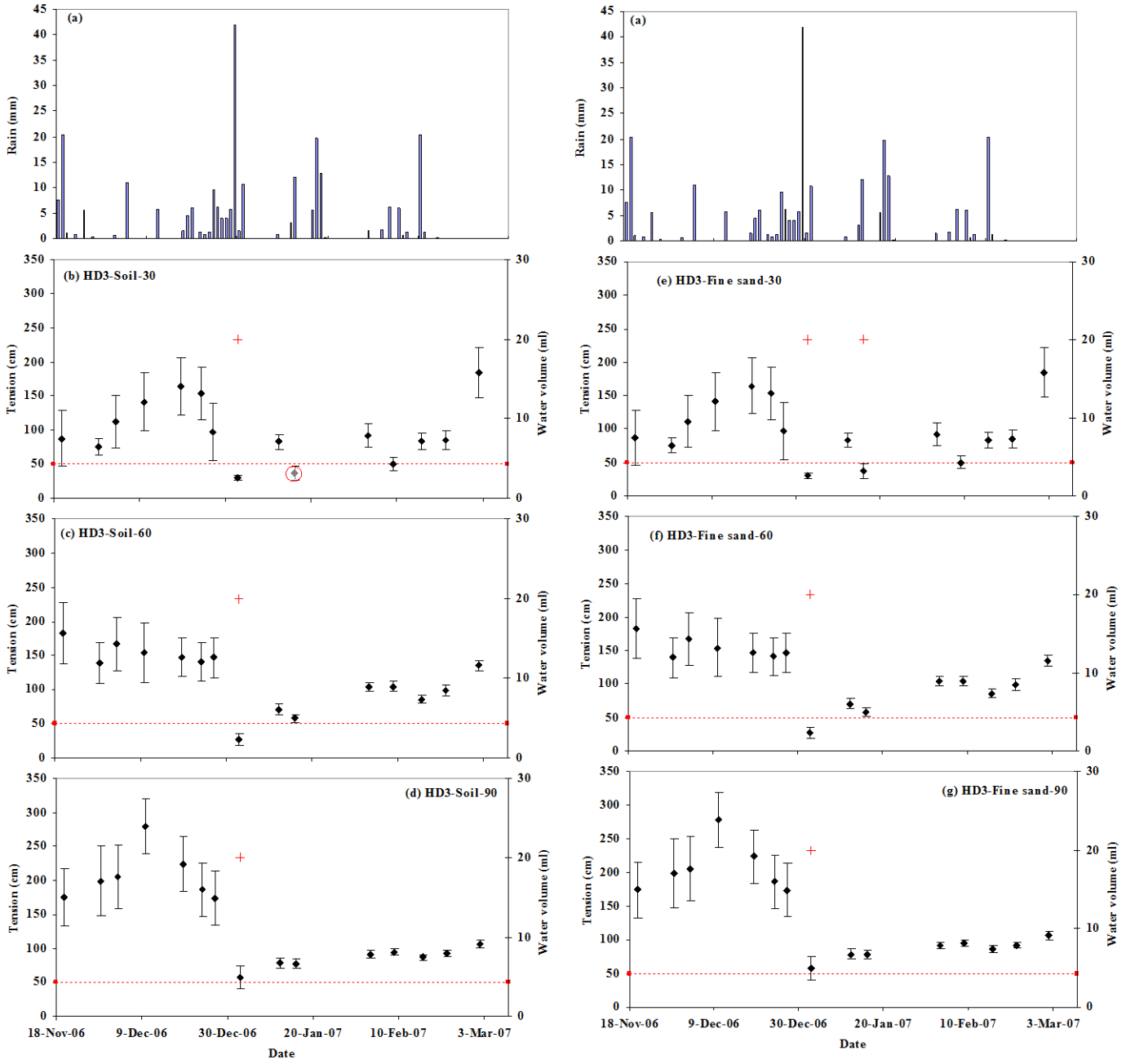

(l)

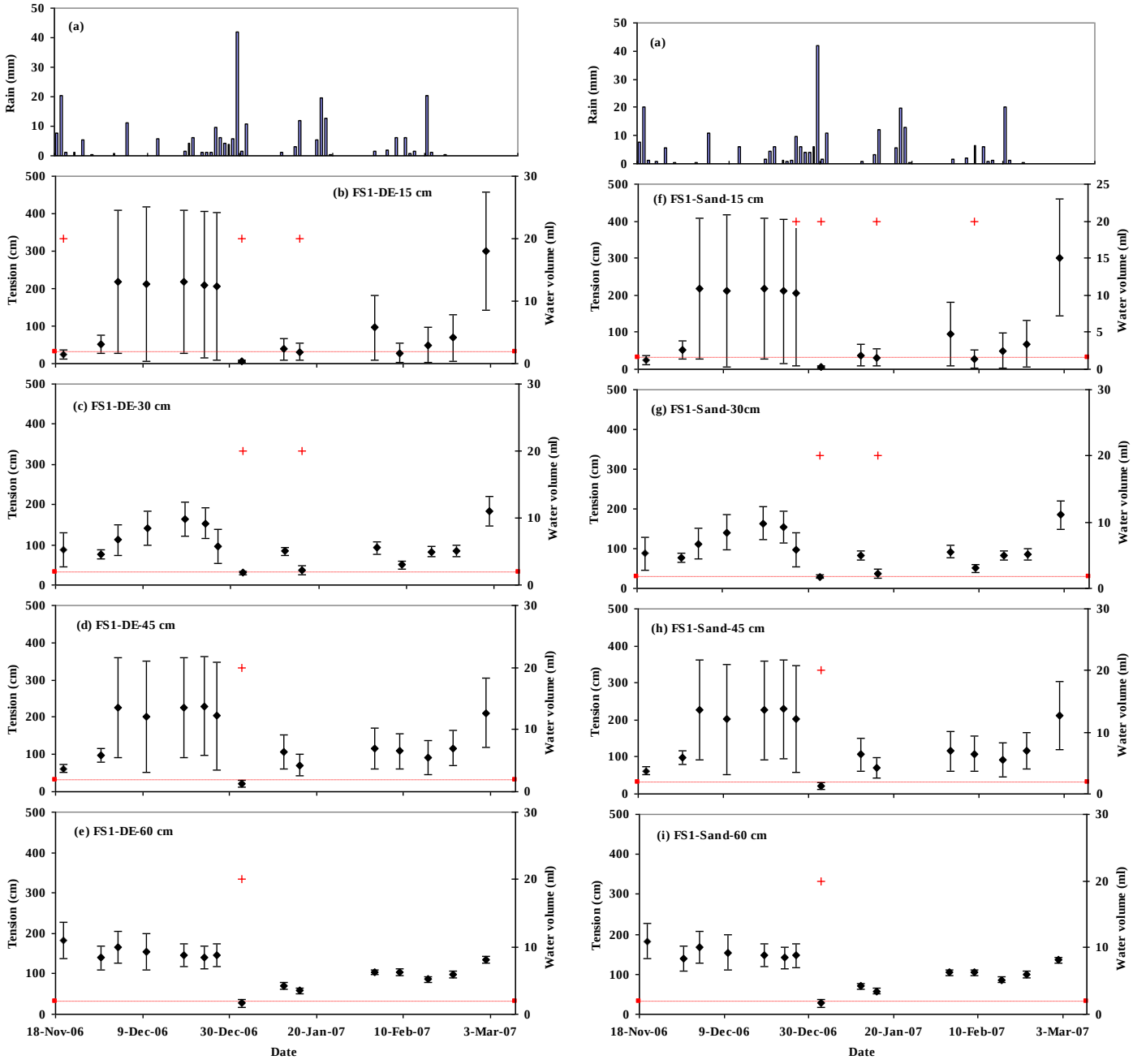

(m)

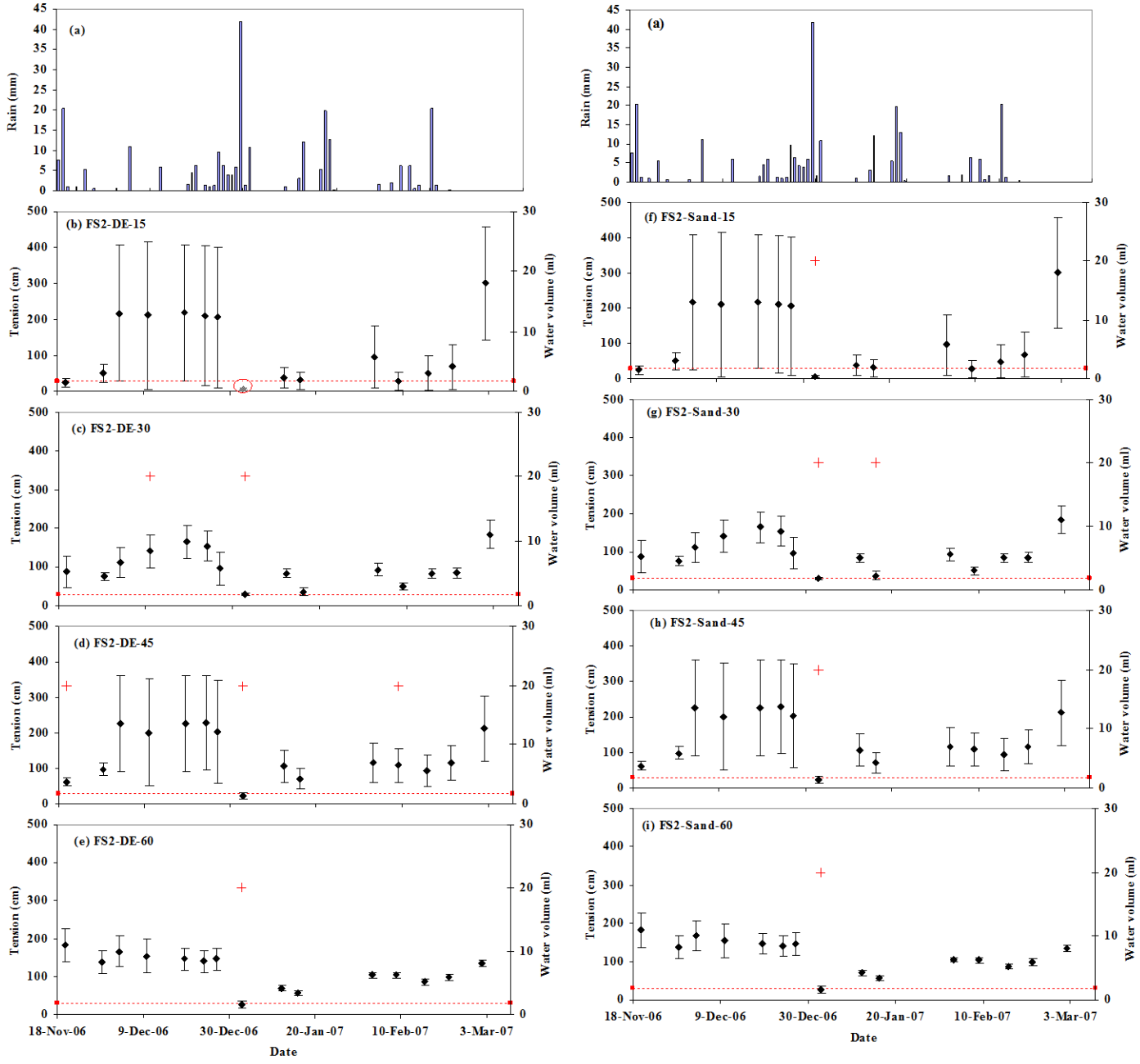

(n)

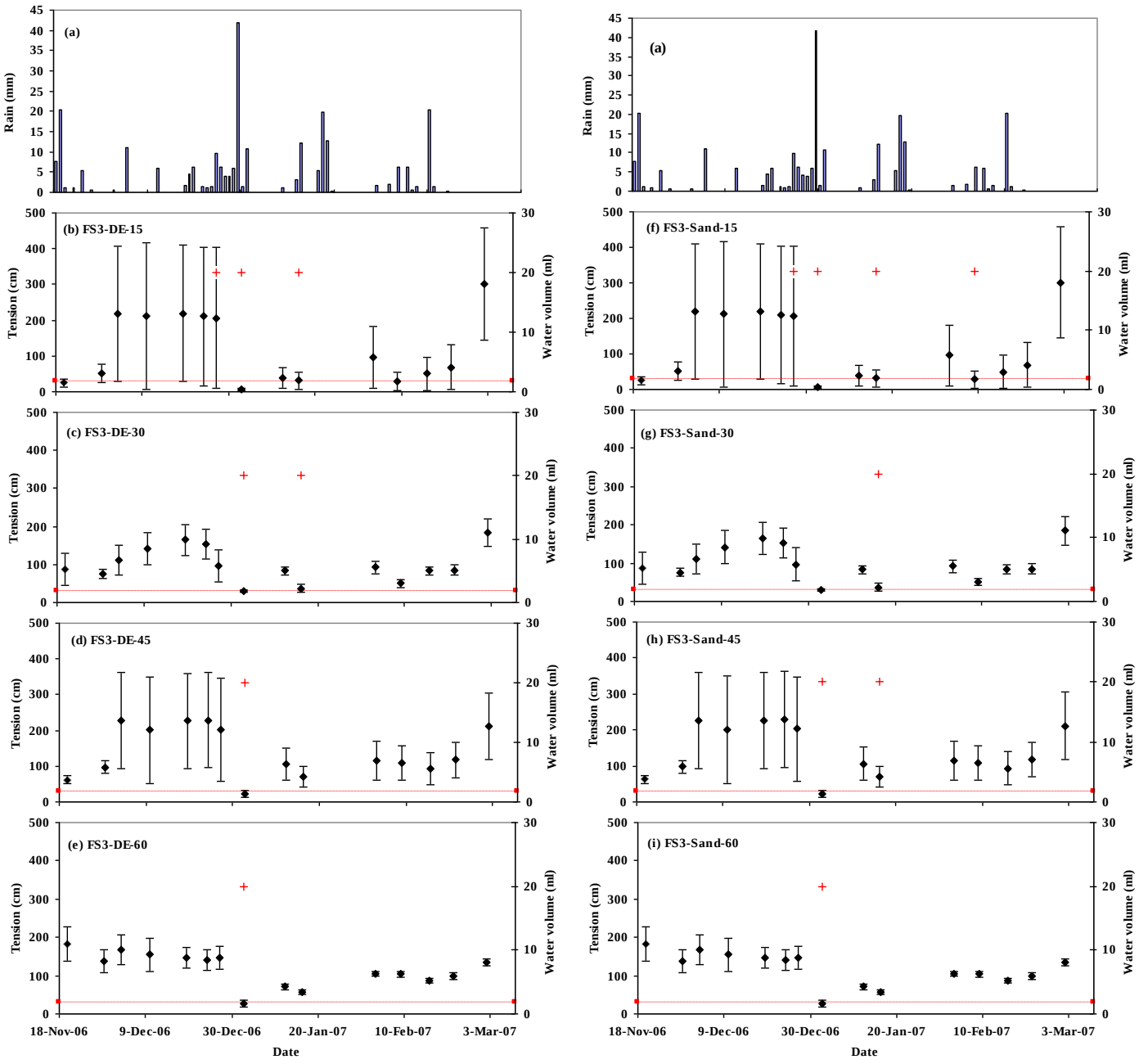

(o)

APPENDIX 4

Table 1. FS response evaluated for the three soils and three depths (30, 45 and 50 cm) using surface drip irrigation. The response type '0' means FS is not activated, '1' and '1*'represent triggered FS during infiltration and redistribution respectively.

(a) Irrigated at a deficit of 50% of plant available water within the root zone.

Irrigation amount Litres (L)	Loam			Clay			Sand		
	FS-Response (0 or 1)			FS-Response (0 or 1)			FS-Response (0 or 1)		
	30	45	50	30	45	50	30	45	50
2	0	0	0	0	0	0	0	0	0
4	0	0	0	0	0	0	0	0	0
8	0	0	0	0	0	0	1	0	0
16	1	0	0	0	0	0	1	1	1
64	1	1	1	1	1	1	1	1	1

(b) Irrigated at a deficit of 25% of plant available water within the root zone.

Irrigation amount Litres (L)	Loam			Clay			Sand		
	FS-Response (0 or 1)			FS-Response (0 or 1)			FS-Response (0 or 1)		
	30	45	50	30	45	50	30	45	50
2	0	0	0	0	0	0	0	0	0
4	0	0	0	0	0	0	0	0	0
8	1	0	0	0	0	0	1	0	0
16	1	1	0	1	0	0	1	1	1
64	1	1	1	1	1	1	1	1	1

Table 2. FS response evaluated for three soils and three depths of placements (15, 20 and 30 cm) using sprinkler irrigation:

(a) Irrigated at a deficit of 50% of plant available water within the root zone.

Irrigation amount (mm)	Loam			Clay			Sand		
	FS-Response (0 or 1)			FS-Response (0 or 1)			FS-Response (0 or 1)		
	15	20	30	15	20	30	15	20	30
10	0	0	0	1	0	0	1	0	0
15	0	0	0	1	0	0	1	1	0
30	1	1	0	1	1	1	1	1	1
45	1	1	0	1	1	1	1	1	1

(b) Irrigated at a deficit of 25% of plant available water within the root zone.

Irrigation amount (mm)	Loam			Clay			Sand		
	FS-Response (0 or 1)			FS-Response (0 or 1)			FS-Response (0 or 1)		
	15	20	30	15	20	30	15	20	30
10	0	0	0	1	1	0	1	1	0
15	1	0	0	1	1	1	1	1	1
30	1	1	1	1	1	1	1	1	1
45	1	1	1	1	1	1	1	1	1

Table 3. FS response evaluated for three soils at three depths (20, 40 and 60 cm) using furrow irrigation:

(a) Irrigated at a deficit of 50% of plant available water within the root zone.

Irrigation amount (mm)	Loam			Clay			Sand		
	FS-Response (0 or 1)			FS-Response (0 or 1)			FS-Response (0 or 1)		
	20	40	60	20	40	60	20	40	60
25	1	1	0	1	1	0	1	1*	1*
50	1	1	1	1	1	1	1	1	1
75	1	1	1	1	1	1	1	1	1

* triggered during redistribution

(b) Irrigated at a deficit of 25% of plant available water within the root zone.

Irrigation amount (mm)	Loam			Clay			Sand		
	FS-Response (0 or 1)			FS-Response (0 or 1)			FS-Response (0 or 1)		
	20	40	60	20	40	60	20	40	60
25	1	1	1	1	1	1	1	1	1*
50	1	1	1	1	1	1	1	1	1
75	1	1	1	1	1	1	1	1	1

* triggered during redistribution

Table 4. Wetted depth, soil tension at a wetting front and placement depth to wetted depth ratio determined during FS evaluations for five different soils and three initial conditions under drip irrigation.

	Surface drip irrigation						
		Daily plant water use = 9 Litres/plant/day				Zur-eq.7	Hydrus model
Placement depth-Zp	FC-2days (cm)	wetted depth (inflection)-cm Zr'	wetted depth (FC-2days)-cm Zr	wetting front tension at the inflection point-cm	tension (cm) at depletion -initial condition	Zp/Zr	Zp/Zr'
30-loamsand-10%		71	75	-28	-27	0.4	0.42
30-loamsand-25%		67	50	-32	-32	0.6	0.45
30-loamsand-50%	-27.4	56	0	-45	-45		0.54
50-loamsand-10%		111	42	-27	-27	1.2	0.45
50-loamsand-25%		106	30	-31	-31	1.7	0.47
50-loamsand-50%	-26	87	0	-44	-44		0.57
30-loam-10%		87	0	-44	-44		0.34
30-loam-25%		70	0	-67	-67		0.43
30-loam-50%	-40	52	0	-145	-144		0.58
50-loam-10%		111	0	-47	-48		0.45
50-loam-25%		94	0	-70	-71		0.53
50-loam-50%	-37	79	0	-150	-151		0.63
30-clayloam-10%		79	0	-52	-52		0.38
30-clayloam-25%		66	0	-108	-108		0.45
30-clayloam-50%	-37	48	0	-330	-333		0.63
50-clayloam-10%		100	0	-57	-58		0.50
50-clayloam-25%		85	0	-118	-117		0.59
50-clayloam-50%	-33	72	0	-350	-351		0.69
30-sandyloam-10%		90	0	-88	-88		0.33
30-sandyloam-25%		70	0	-200	-201		0.43
30-sandyloam-50%	-70	49	0	-1100	-1096		0.61
50-sandyloam-10%		115	0	-113	-113		0.43
50-sandyloam-25%		95	0	-240	-245		0.53
50-sandyloam-50%	-55	78	0	-1350	-1350		0.64
30-sandyclayloam-10%		96	0	-60	-62		0.31
30-sandyclayloam-25%		84	0	-105	-104		0.36
30-sandyclayloam-50%	-54	65	0	-230	-232		0.46
50-sandyclayloam-10%		121	0	-72	-72		0.41
50-sandyclayloam-25%		106	0	-115	-115		0.47
50-sandyclayloam-50%	-48	89	0	-250	-250		0.56

Table 5. Wetted depth, soil tension at a wetting front and placement depth to wetted depth ratio determined during FS evaluations for five different soils and three initial conditions under sprinkler irrigation.

Sprinkler irrigation							
		Eto = 6 mm/day	wetted depth (FC-2days)-cm			Zur-eq.7	Hydrus model
Placement depth-Zp	FC-2days (cm)	wetted depth (inflection)-cm Zr'	Zr	wetting front tension at the inflection point-cm	tension (cm) at depletion -initial condition	Zp/Zr	Zp/Zr'
15-loamsand-10%		63	54	-33	-33	0.28	0.24
15-loamsand-25%		59	47	-38	-38	0.32	0.25
15-loamsand-50%	-30	42	0	-53	-53		0.36
30-loamsand-10%		105	101	-27	-27	0.30	0.29
30-loamsand-25%		99	91	-32	-32	0.33	0.30
30-loamsand-50%	-27.4	87	0	-44	-45		0.34
15-loam-10%		60	0	-61	-61		0.25
15-loam-25%		52	0	-88	-88		0.29
15-loam-50%	-44	43	0	-180	-183		0.35
30-loam-10%		104	55	-43	-44	0.55	0.29
30-loam-25%		87	46	-67	-67	0.65	0.34
30-loam-50%	-40	65	0	-145	-144		0.46
15-clayloam-10%		59	19	-48	-48	0.79	0.25
15-clayloam-25%		48	0	-95	-96		0.31
15-clayloam-50%	-42	37	0	-250	-258		0.41
30-clayloam-10%		81	40	-52	-52	0.75	0.37
30-clayloam-25%		66	0	-108	-108		0.45
30-clayloam-50%	-37	50	0	-330	-333		0.60
15-sandyloam-10%		67	0	-147	-148		0.22
15-sandyloam-25%		54	0	-310	-311		0.28
15-sandyloam-50%	-79	42	0	-1800	-1804		0.36
30-sandyloam-10%		112	50	-87	-88	0.60	0.27
30-sandyloam-25%		95	0	-198	-201		0.32
30-sandyloam-50%	-70	68	0	-1100	-1096		0.44
15-sandyclayloam-10%		60	0	-89	-89		0.25
15-sandyclayloam-25%		53	0	-135	-136		0.28
15-sandyclayloam-50%	-59	40	0	-280	-286		0.38
30-sandyclayloam-10%		96	46	-62	-62	0.65	0.31
30-sandyclayloam-25%		85	0	-104	-104		0.35
30-sandyclayloam-50%	-54	69	0	-230	-232		0.43